Malarial retinopathy and neurovascular injury in paediatric cerebral malaria

Thesis submitted in accordance with the requirements of the University of Liverpool

for

The degree of Doctor in Philosophy

by

Ian James Callum MacCormick

Date of submission

January 2016

Declaration

I declare that this thesis was written by me and that the work contained herein is my own, except where explicitly stated otherwise in the text.

The work within this thesis has not been submitted for any other degree or professional qualification.

Ian James Callum MacCormick

Blantyre, Malawi, 2015

Dedication

To Dad:

Thanks for your example.

Ephesians 5:1-2

Outputs related to this thesis

Publications directly related to the results presented in this thesis

MacCormick IJ, Maude RJ, Beare NA, Borooah S, Glover S, Parry D, Leach S, Molyneux ME, Dhillon B, Lewallen S, et al. Grading fluorescein angiograms in malarial retinopathy. Malar J. 2015 Sep 24;14(1):367. doi: 10.1186/s12936-015-0897-7. PubMed PMID: 26403288; PubMed Central PMCID: PMC4583163.

MacCormick IJ, Czanner G, Faragher B. Developing retinal biomarkers of neurological disease: an analytical perspective. Biomark Med. 2015;9(7):691-701. PubMed PMID: 26174843.

MacCormick IJ, Beare NA, Taylor TE, Barrera V, White VA, et al. Cerebral malaria in children: using the retina to study the brain. Brain. 2014 Aug;137(Pt 8):2119-42. PubMed PMID: 24578549; PubMed Central PMCID: PMC4107732.

MacCormick IJ, Beare NA, Taylor TE, Barrera V, White VA, et al. Reply: Retinopathy, histidine-rich protein-2 and perfusion pressure in cerebral malaria. Brain. 2014 Sep;137(Pt 9):e299. PubMed PMID: 24919966; PubMed Central PMCID: PMC4132643.

Publications arising from work done during my Clinical Research Fellowship, where the results are not directly reported in this thesis

Moxon CA, Chisala NV, Mzikamanda R, MacCormick I, Harding S, Downey C, Molyneux M, Seydel KB, Taylor TE, Heyderman RS, et al. Laboratory evidence of disseminated intravascular coagulation is associated with a fatal outcome in children with cerebral malaria despite an absence of clinically evident thrombosis or bleeding. J Thromb Haemost. 2015 Sep;13(9):1653-64. doi: 10.1111/jth.13060. Epub 2015 Aug 27. PubMed PMID: 26186686; PubMed Central PMCID: PMC4605993.

Zhao Y, MacCormick IJ, Parry DG, Beare NA, Harding SP, et al. Automated Detection of Vessel Abnormalities on Fluorescein Angiogram in Malarial Retinopathy. Sci Rep. 2015 Jun 8;5:11154. PubMed PMID: 26053690.

Zhao Y, MacCormick IJC, Parry DG, Leach S, Beare NAV, et al. Automated detection of leakage in fluorescein angiography images with application to malarial retinopathy. Sci Rep. 2015 Jun 1;5:10425. PubMed PMID: 26030010.

Barrera V, Hiscott PS, Craig AG, White VA, Milner DA, et al. Severity of retinopathy parallels the degree of parasite sequestration in the eyes and brains of Malawian children with fatal cerebral malaria. J Infect Dis. 2015 Jun 15;211(12):1977-86. PubMed PMID: 25351204; PubMed Central PMCID: PMC4442623.

Zheng Y, Kwong MT, MacCormick IJ, Beare NA, Harding SP. A comprehensive texture segmentation framework for segmentation of capillary non-perfusion regions in fundus fluorescein angiograms. PLoS One. 2014;9(4):e93624. PubMed PMID: 24747681; PubMed Central PMCID: PMC3991579.

Piddock K, Beare N, MacCormick I. Malarial retinopathy affecting visual function in a Malawian adult with cerebral malaria. IDCases. 2014; 1(4):82.

MacCormick IJ, Beare NA, Harding SP. Imaging of retinal whitening in retinal vein occlusion may shed light on malarial retinopathy. Eur J Ophthalmol. 2012 Sep-Oct;22(5):868; author reply 869. PubMed PMID: 22467585.

Manuscripts submitted and in preparation

MacCormick I, Seydel K, Czanner G, Beare N, Molyneux M, Taylor T, Harding S, Neurovascular barrier breakdown is associated with clinical outcomes in retinopathy positive paediatric cerebral malaria [in preparation]

Acknowledgements

I am grateful to the patients who participated in this research, to patients' families for giving consent to take part, and also to the clinicians and other staff on the Paediatric Research Ward in Blantyre, Malawi, where this work was carried out.

This thesis would not have been written if it had not been for the encouragement of my primary supervisor Prof Simon Harding, and I have been glad for support from him and my other supervisors – Prof Terrie Taylor, Dr Macpherson Mallewa, and Mr Nicholas Beare. Prof Taylor in particular has given much of her time to providing helpful advice during my stay in Blantyre. Likewise Dr Karl Seydel and Prof Malcolm Molyneux have patiently endured my questions and helped me in the course of many stimulating discussions. The MRI data would not have been available for analysis but for the hard work of Dr Sam Kampondeni, Dr Mike Potchen, and Dr Gretchen Birbeck. I'm grateful to colleagues and seniors at the University of Liverpool and the Liverpool School of Tropical Medicine and Hygiene for their support and input, including Dr Gabriela Czanner, Dr Valentina Barrera, Prof Brian Faragher, and Dr Paul Knox. The fluorescein angiograms could not have been captured without the generous support of Topcon, and in particular the work of Leigh Mahler. Prof Baljean Dhillon and Prof Susan Lewallen also provided helpful advice at various points.

As well as working on the Paediatric Research Ward, I have spent much time at the Malawi-Liverpool-Wellcome Trust in Blantyre, and am grateful to the many support staff here, and at the University of Liverpool, who helped to manage many aspects of working in Malawi.

Final thanks go to my family, and in particular my wife Hazel for her encouragement, patience, and support during our time in Malawi.

Abstract

Background

Diseases of the brain are difficult to study because this organ is relatively inaccessible. Only one part of the central nervous system is available to direct, non-invasive observation – the retina. The concept of the retina as a window to the brain has created much interest in the retina as a source of potential markers of brain disease. Paediatric cerebral malaria is a severe neurological complication of infection with the parasite Plasmodium falciparum, which is responsible for death and disability in a significant number of children in sub-Saharan Africa. As with many neurological diseases, the precise mechanisms by which this infection causes damage to the brain remain unclear, and this hampers efforts to develop effective treatments. It may be that studying the retina in paediatric cerebral malaria could both illuminate pathogenesis specific to this disease, and also provide an illustration of how to approach retinal biomarkers in a new, and potentially more effective way.

Methods

I approached the aim of developing retinal features as markers of brain disease in paediatric cerebral malaria via several objectives. I made use of an existing clinical study to collect new retinal data from ophthalmoscopic examinations and fundus fluorescein angiograms from patients over three successive malaria seasons in Malawi, and added these to historical data obtained previously at the same site. I devised a new method for grading retinal images. I reviewed the biological plausibility of associations between retina and brain in cerebral malaria, and then considered analytical methods to interpret my retinal data effectively. Finally I estimated associations between retinal features, outcomes, and a radiological measure of brain swelling using combinations of regression models.

Results

My review of retinal and cerebral histopathology, vascular anatomy and physiology indicated that certain retinal and brain regions may be similarly prone to damage from sequestration as a result of interactions between aberrant rheology and microvascular geometry, such as branching patterns and arteriole to venule ratios. My review of evaluations of analogy and surrogacy suggested that biological similarities between retina and brain could be used to justify statistical evaluation of the amount of information the subject and object of the inference share about a common outcome, as used to assess surrogate end points for clinical trials. This kind of approach is able to address questions about whether a particular retinal feature is effectively equivalent to an analogous disease manifestation in the brain. I report analyses on three overlapping groups of subjects, all of whom had retinopathy positive cerebral malaria: children with admission ophthalmoscopy (n=817), children with admission fluorescein angiography (n=260), and children with admission angiography and MRI of the brain (n=134). Several retinal features are associated with death and longer time to recover consciousness in paediatric cerebral malaria. Broadly speaking, these features appear to reflect two processes: neurovascular sequestration (e.g. orange vessel discolouration and death), and neurovascular leakage (e.g. >5 sites of punctate leak and death). Respective adjusted odds ratios and 95% confidence intervals for these particular associations are: 2.88 (1.64-5.05); and 6.90 (1.52-31.3). Other related processes may also be important, such as ischaemia, which can be extensive. Associations between retina and brain are less clear, in part because of selection bias in the samples.

Conclusions

Neurovascular leak is important in fatal paediatric cerebral malaria, suggesting that fatal brain swelling may occur primarily as a result of vasogenic oedema. Other processes are also likely to be involved, particularly neurovascular sequestration, which is visible on retinal imaging as orange vessels or intravascular filling defects. Sequestration may plausibly cause leak through direct damage to tight junctions and by increasing transmural pressure secondary

to venous congestion. Several types of retinal leakage are seen and some of these may represent re-perfusion rather than acute injury. Future work to investigate temporal changes in retinal signs may find clearer associations with radiological and clinical outcomes. The steps taken to evaluate retinal markers in cerebral malaria illustrate a more rigorous approach to retinal biomarkers in general, which can be applied to other neurological diseases

List of abbreviations

20D = 20 dioptre

A = Exposure to treatment, or to a disease that causes manifestations in the source and target domains (e.g. surrogate and true endpoint; retina and brain)

AA = Adjusted association

AIC = Akaike information criterion

Ang = Angiopoietin

BCS = Blantyre Coma Scale

BIC = Bayesian information criterion

BMP = Blantyre Malaria Project

CG = Cannot grade

CI = Confidence interval

CM = Cerebral malaria

CMRgluc = Cerebral metabolic rate (glucose)

$CMRO_2$ = Cerebral metabolic rate (oxygen)

CNP = Capillary non-perfusion

CNS = Central nervous system

Coef. = Coefficient

CRAE = Central retinal artery equivalent

CRVE = Central retinal vein equivalent

CSF = Cerebrospinal fluid

DA = Disc area

DD = Disc diameter

df = Degrees of freedom

ENT = Ear, nose, and throat

EPCR = Endothelial protein C receptor

ETDRS = Early Treatment Diabetic Retinopathy Study research group (1985)

FA = Fluorescein angiography / angiogram / angiographic

FAZ = Foveal avascular zone

fMRI = Functional magnetic resonance imaging

HRP2 = Plasmodium falciparum histidine rich protein 2

ICAM-1 = Intercellular adhesion molecule 1

IJCM = Ian MacCormick

IQR = Inter-quartile range

IVFD = Intravascular filling defects

JAM = Junction adhesion molecule

LDR = length to diameter ratio

LED = Light emitting diode

LL = Log likelihood

logit = Logistic regression

LR = Likelihood ratio

LRF = Likelihood reduction factorial

MLW = Malawi Liverpool Wellcome Trust Clinical Research Programme

MMP = Matrix metalloprotease

Mret = The retinal microvasculature in cerebral malaria in African children programme grant

MRI = Magnetic resonance imaging

MRP = Malaria research project

MRS = Magnetic resonance spectroscopy

NO = Nitric oxide

Obs = Number of observations

OCT = optical coherence tomography

ologit = Ordered logistic regression

OR = Odds ratio

P. falciparum = Plasmodium falciparum

P. vivax = Plasmodium vivax

PAR1 = Protease activated receptor 1

PDGF = Platelet derived growth factor

PE = Proportion explained

PEDF = Pigment epithelium derived growth factor

PET = Positron emission tomography

PfEMP-1 = Plasmodium falciparum erythrocyte membrane protein 1

PIG = Proportion of information gain

PRW = Paediatric Research Ward

QECH = Queen Elizabeth Central Hospital

RCT = Randomised controlled trial

RE = Relative effect

regress = Linear regression

RPE = Retinal pigment epithelium

RSS = Residual sum of squares

S = Source domain (e.g. surrogate endpoint; retina)

SD = Standard deviation

SEM = Structural equation modelling

SMA = Severe malarial anaemia

SPH = Simon Harding

Std. Err. = Standard error

T = Target domain (e.g. true endpoint, brain)

VEGF = Vascular endothelial growth factor

WHO = World Health Organization

Z = Outcome of disease

ZO = Zonula occludens

Table of Contents

Index of Tables

Index of Figures

Chapter 1 – Introduction and aims of thesis

1.1 Aim of chapter

State the aim and objectives of the thesis. Provide relevant background information so that subsequent chapters can be understood in terms of current knowledge about malarial retinopathy, and within the broader context of neuroscientific research involving models and biomarkers.

1.2 Thesis aims and objectives

Aim: Develop retinal features as markers of brain disease in paediatric cerebral malaria

O1: Review the biological plausibility of associations between retina and brain

O2: Review methods for evaluating surrogate-like relationships between retina and brain

O3: Design a grading system for fluorescein angiography images in severe malaria

O4: Estimate associations between admission retinal features and death

O5: Estimate associations between admission retinal features and MRI features

These objectives were achieved in large part through conducting a cohort study to collect original retinal data within an existing program of research. I performed dilated indirect ophthalmoscopy and fundus fluorescein angiography on subjects over the course of three malaria seasons in 2012, 2013, and 2014 and added these data to pre-existing data collected within the same parent study between 1999 and 2011.

1.3 Introduction to the chapter

In this chapter I will introduce ideas and themes that I think are essential for understanding the rest of the thesis. As with a map, it is helpful to begin by orientating oneself to broad contours before looking more closely at a particular feature. In this thesis, the "feature" is malarial retinopathy, in children with

cerebral malaria (CM), and the related question: “does malarial retinopathy tell us anything about the brain?”.

However in my view this particular question sits within a large scale context. Much as the features of a town can only be understood properly within the context of the local topography, so questions about malarial retinopathy are understood best when they are framed by broader questions about the nature of scientific inference in neuroscience. As I go on to describe, issues with using the retina to understand the brain in paediatric CM are very similar to problems faced by scientists trying to learn about *any* cerebral disease process. It follows that techniques and resources from other areas of science may be usefully applied in the specific case of paediatric CM; and *vice versa*, if I can make some small advance in tackling inferences about CM from retinal observations, then these may be equally useful to researchers working in other fields.

So much for the broad context. Most of this thesis consists of fine detail on particular areas of the map. As well as a description of the bigger picture, the reader will need a guidebook to lead them through the nooks and crannies of paediatric CM.

Therefore this chapter consists of several sections. The first discusses problems with studying the brain in general, and why biomarkers and models are so appealing. I then describe why the retina is seen as an attractive source of biomarkers, and even by some as a “window” to the brain, before going on to touch on what this might mean in analytical terms. In these sections I am dealing with the “map”.

In the next sections I begin to introduce the reader to details about the particular case in which I intend to apply my analysis. This begins with a description of paediatric CM – including definitions, epidemiology, and an outline of a typical case. I then provide more detail by discussing the place of paediatric CM within severe malaria in general. This includes a range of severe malarial syndromes, of which CM is only one.

From here I describe malarial retinopathy, and discuss its features and frequency in paediatric CM and other (non-comatose) paediatric severe malarial syndromes. Next there is a review of clinical associations with malarial retinopathy. Finally I give a short account of the history of ocular complications of malaria, both real and assumed. This raises a caution for current investigators, like me.

Subsequent chapters deal with the specific objectives necessary to approach the aim of developing retinal markers of brain disease in paediatric CM. I hope that this introduction will have equipped the reader to approach the following chapters with an adequate sense of the broad context of biomarkers in neuroscience, and the detail relevant to the particular syndrome being studied in this case – retinopathy positive paediatric CM.

1.4 The problem of studying the brain: the appeal of biomarkers and disease models

The human brain is relatively inaccessible, and this poses a problem for research into many neurological conditions. Scientists have traditionally responded by developing models of, and biomarkers for, brain physiology and disease. Many important inferences about human neurological physiology and pathogenesis have been made from models. Famous examples include the Aplysia sea slug, and the Squid giant axon. Work on both of these models led to Nobel Prizes: Eric Kandel gained insights into the mechanisms of learning and memory through his experiments on Aplysia; and Alan Hodgkin, Andrew Huxley and John Eccles studied the Squid giant axon to elucidate the ionic basis for the action potential. Many other neuroscientific models exist (Dowling, 2012). Although it may seem like there are major differences between biomarkers and animal models, in reality the basis of scientific inference is similar since both rest on an argument from analogy. Insights about what makes conclusions based on an animal model or biomarker valid can be applied to considerations of the retina as a model of, or source of biomarkers about, the brain. This idea is central to this thesis and is discussed further below and in Chapter 3.

Models are attractive because, in the best cases, they allow valid and useful conclusions to be drawn about the inaccessible human brain through the study of a more accessible substitute. In these cases the model is immensely valuable because without it such conclusions simply could not be drawn – or at least, not within the limits of contemporary science and ethical norms. However, models also have inherent limitations.

Scientific models are only helpful in so far as they are similar to the real object of interest. In the case of neurological diseases, this object is the human nervous system as it responds to a certain pathogen or disease process. By definition, a model will never be identical to the objective it simulates, and the limits of proper inference are delineated by the extent to which the model and the object share similarities that are relevant to the disease in question.

Such relevant similarities can (and should) be described before drawing conclusions from a scientific model. This is the basis for the evaluation of model animals in scientific research (Belzung and Lemoine, 2011; van der Staay *et al.*, 2009; Willner, 1986). But describing known similarities and differences can be difficult, and will not necessarily produce consensus about the validity of inferences drawn from the model. For example, the mouse model of CM remains controversial in spite of much research on malaria infection in humans and mice (Craig *et al.*, 2012).

More fundamentally, there are limits to the extent one can describe the important similarities. Besides the practical limits to time and effort, it is impossible to compare and contrast aspects of a model with corresponding features of the human if these features (which may be highly relevant to a particular disease) are simply not yet known. Future scientific developments are likely to change our appreciation of human and animal biology in ways that are not easily predictable. Consequently even the most sincere attempt to validate a model by comparing it with the object of interest is missing something. This omission may, or may not, be scientifically significant. The famous quote from George Box, which he made about statistical models, is relevant to inferences from models in general:

> "Remember that all models are wrong; the practical question is how wrong do they have to be to not be useful." (Box and Draper, 1987) (p74).

I mentioned that scientific models are valuable when conclusions could not otherwise be drawn within the limits of contemporary science. Perhaps advances in scientific methodology can offer solutions that make models of neurological disease redundant. For example, several imaging modalities now provide opportunities to visualise the human brain in great detail. Magnetic Resonance Imaging (MRI), Functional MRI (fMRI), Magnetic Resonance Spectroscopy (MRS), and Positron Emission Tomography (PET) are perhaps the main techniques currently used for imaging the human brain.

However all imaging techniques rest on assumptions about the biological meaning of the signals they detect. For example the Blood Oxygen Level Dependant (BOLD) signal in fMRI is related to local blood flow, but an interpretation in terms of neurological activity relies on assuming a theoretical model involving complex interactions between blood flow, oxygen extraction, and neurovascular coupling (Buxton, 2010; Buxton *et al.*, 2014; Kim and Ogawa, 2012; Yablonskiy *et al.*, 2013). The spatial resolution of many imaging techniques is also comparatively limited. There is no doubt that radiological imaging of the human brain has revolutionised neuroscience, but it is not without limitations of its own.

Another traditional approach is to study the human brain *post mortem*. This allows microscopic effects of neurological disease to be directly examined, and has led to important advances in medical science generally, and the field of CM research in particular (reviewed in World Health Organization, 2014b). However, while this method allows detailed observations of fixed tissue from one point in time, it provides much less information about the dynamic disease processes that led there (Baskurt and Meiselman, 2003); and, with the exception of local biopsy, histopathology can only be applied to a specific set of (fatal) cases.

1.5 The retina as a possible “window to the brain”

The human retina, in contrast to the rest of the central nervous system (CNS), is accessible to visual observation. Compared to MRI of the brain, non-invasive imaging of the retina is relatively straightforward – and with capillary level resolution. Functional imaging of the retinal neurovasculature is possible (Harris, 2010) using techniques ranging from fluorescein angiography (FA) (Dithmar and Holz, 2008) to variations of optical coherence tomography (OCT) (Leitgeb *et al.*, 2014). The neuronal activity of specific cell layers can be measured using visual electrophysiology (Lochhead *et al.*, 2003, 2010; Southern *et al.*, 2008; Yospaiboon *et al.*, 1984). Direct optical access to the retina gives potential for improvements in resolution beyond the limits of diffraction, using super-resolution fluorescence microscopy – the subject of the 2014 Nobel Prize in chemistry (Van Noorden, 2014).

The retina is also very similar to the brain. The retina is an extension of the CNS with similar embryology to the brain. Like the brain the retina is composed of nervous tissue that has similar behaviour and metabolic demands to cerebral neuronal networks. The blood retina barrier appears to be approximately similar to the blood brain barrier (Patton *et al.*, 2005). Furthermore, the retina seems to sustain similar damage to the brain in paediatric CM (MacCormick *et al.*, 2014), and other neurological conditions (London *et al.*, 2013). I go into more detail about similarities between retina and brain that are relevant to paediatric CM in Chapter 2.

The combination of direct, non-invasive visual access, and extensive similarities to the human brain gives the retina considerable appeal as a neuro-scientific research tool. There is a great temptation to describe the retina as a “window to the brain”, and in this context several associations between retina and brain have been reported (reviewed in (London *et al.*, 2013; MacCormick *et al.*, 2014; MacGillivray *et al.*, 2014; Patton *et al.*, 2005)). However, the literature does not appear to recognise that the concept of the retina as a “window to the brain” involves more than just direct associations. Rather it is similar to treating a retinal feature as a surrogate marker of a corresponding brain feature.

Consequently, I propose a new approach for empirically evaluating retinal features in the context of paediatric CM, which borrows from statistical methods to assess surrogate endpoints in randomised controlled trials (RCT). The statistical literature on this subject is voluminous, but some broad principles for assessing surrogate endpoints are outlined briefly in the International Conference on Harmonisation document E9 (International Conference on Harmonisation, 1998). In general, the strength of evidence for surrogacy depends on:

1) The biological plausibility of associations between the surrogate and the true endpoint
2) Demonstration that the surrogate can predict the true endpoint
3) Demonstration that the surrogate and true endpoint respond similarly to treatment

In this thesis I adapt these principles for observational studies of paediatric CM by describing:

1) The biological plausibility of associations between the retina and brain in paediatric CM (Chapter 2)
2) Associations between retinal variables and relevant outcomes
    a) Death and time to coma resolution (Chapter 6 and 7)
    b) Brain swelling (Chapter 8)

The value of a surrogate endpoint usually lies in its ability to replace an impractical true endpoint in a clinical trial. Rather than aiming to develop malarial retinopathy as a surrogate endpoint for future clinical trials in paediatric CM, in this thesis I attempt instead to provide evidence for vascular disease mechanisms underlying important clinical outcomes. This is by showing that one or more retinal features contain a large amount of the same information as that contained in a measurement of the brain.

In summary, the study of neurological disease is limited by lack of direct access to the brain. Solutions to this problem include the use of animal models,

radiological imaging, and histopathology. Each has the potential to provide important and complimentary information. Additional insights may be gained by studying the retina as an *in vivo* model of the brain, and if so this approach may be a worthwhile addition to the scientific repertoire. The retina appears to have great potential as a tool for studying certain cerebral disease processes, including those involved in paediatric CM. However, foundational assumptions inherent in the interpretation of all types of model (animal, theoretical – in the case of MRI, or retina) may be easily overlooked. These must be addressed for the full potential of the retina as a model of the brain to be realised, and to prevent unjustified conclusions from being drawn. I hope that ideas developed in the context of paediatric CM will be applicable to a broader range of neurological diseases that manifest in the retina.

Paediatric CM appears to be a good test case in which to evaluate retinal biomarkers according to my new approach. The next sections introduce this disease and discuss definitions, epidemiology, and related characteristics of paediatric CM.

1.6 Paediatric cerebral malaria

1.6.1 Definition

Paediatric CM is one of several severe malarial syndromes caused by the parasite *P. falciparum*. According to the World Health Organization (WHO), CM is diagnosed when three criteria are met: peripheral *P. falciparum* parasitaemia, impaired consciousness (Blantyre Coma Scale ≤ 2), and the absence of another identifiable cause of coma (World Health Organization, 2014b). Definitions of severe malarial syndromes are shown in Table 1. Parasitaemia is assessed with microscopy, and coma with the Blantyre Coma Scale (BCS, a six point (0-5) modification of the Glasgow Coma Scale) (Molyneux *et al.*, 1989). It should be possible to rule out hypoglycaemia and meningitis (Taylor, 2009), but tests for alternative causes of coma are not available throughout much of sub-Saharan Africa. This means that the clinical definition of paediatric CM over-diagnoses approximately 22% of cases, compared to a reference test of cerebral histopathology. However, in the context of clinically defined paediatric CM, the

presence of malarial retinopathy is highly sensitive and specific for cerebral sequestration in fatal cases (Taylor *et al.*, 2004). This has led to modified definitions of paediatric CM, which can be considered either "retinopathy positive" (implying the presence of cerebral sequestration) or "retinopathy negative" (implying a lack of cerebral sequestration, and an alternative cause of coma or death [1]).

This has important implications for research on paediatric CM, since an inaccurate case definition will inevitably produce errors in estimates of incidence, and also of clinical associations that could otherwise indicate relevant disease mechanisms.

1 The comparison of retinopathy against cerebral histopathology used a cut-off of 23.3% vessels parasitised to define cerebral sequestration as "present" or "absent". In other words, subjects with "no sequestration" actually had <23.3% vessels parasitised (see Figure 2 in (Taylor *et al.*, 2004)), Subjects with non-malarial coma (group 4) had higher % vessels parasitised than some subjects with clinically defined CM (group 3). Consequently, the absence of malarial retinopathy implies *little or no* cerebral sequestration (*and* an alternative cause of death), rather than the absolute absence of any neurovascular parasites at all. More recent research has shown significant direct associations between the severity of malarial retinopathy, and the severity of sequestration in both retinal and cerebral vessels (Barrera *et al.*, 2015). This is consistent with the notion of a spectrum of neurovascular pathology in paediatric malaria of all severities. It is helpful that retinopathy visible on ophthalmoscopy happens to distinguish a clinically useful break-point in this spectrum.

Table 1: Features of severe malaria syndromes.

The presence of *P. falciparum* in peripheral blood, and the absence of any other cause of the severity feature, is assumed for all definitions. For example, paediatric CM is defined as Blantyre coma score <3 in the presence of peripheral *P. falciparum* parasitaemia, and the absence of another identifiable cause of coma. Adapted from Table 4 in (World Health Organization, 2014b).

Feature of severe *falciparum* malaria	Definition
Impaired consciousness	A Glasgow Coma Score <11 in adults or a Blantyre coma score <3 in children
Acidosis	A base deficit of >8 meq/l or, if unavailable, a plasma bicarbonate of <15 mM or venous plasma lactate >5 mM. Severe acidosis manifests clinically as respiratory distress – rapid, deep and laboured breathing
Hypoglycaemia	Blood or plasma glucose <2.2 mM (<40 mg/dl)
Severe malarial anaemia	A haemoglobin concentration <5 g/dl or a haematocrit of <15% in children <12 years of age (<7 g/dl and <20%, respectively, in adults) together with a parasite count >10 000/μl
Renal impairment	Plasma or serum creatinine >265 μM (3 mg/dl) or blood urea >20 mM
Jaundice	Plasma or serum bilirubin >50 μM (3 mg/dl) together with a parasite count >100 000/μl
Pulmonary oedema	Radiologically confirmed, or oxygen saturation <92% on room air with a respiratory rate >30/min, often with chest in drawing and crepitations on auscultation
Significant bleeding	Including recurrent or prolonged bleeding from nose gums or venepuncture sites; haematemesis or melaena
Shock	Compensated shock is defined as capillary refill ≥3 s or temperature gradient on leg (mid to proximal limb), but no hypotension. Decompensated shock is defined as systolic blood pressure <70 mm Hg in children or <80 mm Hg in adults with evidence of impaired perfusion (cool peripheries or prolonged capillary refill)
Hyperparasitaemia	*P. falciparum* parasitaemia >10%

1.6.2 A typical case of paediatric cerebral malaria

The typical history of paediatric CM involves a young child who rapidly develops coma after a short prodrome of fever and generalized illness. The coma may be preceded or accompanied by convulsions, from which the child does not wake.

On examination the child is usually febrile, and may have deep or rapid breathing. Coma is distinguished from prolonged post-ictal state by duration of at least 30 minutes after seizure. Convulsions or posturing, including opisthotonus, may be present (Molyneux et al., 1989; World Health Organization, 2014b).

Ophthalmoscopy through dilated pupils often reveals signs of malarial retinopathy: white patchy discolouration of the macula and/or peripheral retina; orange or white discolouration of retinal vessels; and/or retinal haemorrhages, typically with white centres. Papilloedema may be seen, but in isolation does not distinguish CM from other causes of coma (Beare *et al.*, 2006; Harding *et al.*, 2006; Lewallen *et al.*, 1999, 2008).

Investigation may reveal concomitant metabolic acidosis and/or severe anaemia. Peripheral *P. falciparum* asexual parasitaemia on microscopy is present by definition. Other treatable causes of coma in this setting must be ruled out and include malaria-associated hypoglycaemia and meningitis. Bacteraemia may be found, especially in infants and in the presence of severe anaemia (Bronzan *et al.*, 2007).

The duration of illness is usually short, and most patients recover or die within 48 hours (Figure 1). Death is typically by respiratory arrest, and case fatality with treatment is approximately 15%. Children who recover are at risk of neurodisability (Molyneux *et al.*, 1989) and epilepsy (Birbeck, Molyneux, *et al.*, 2010). Guidelines for treatment have been published (World Health Organization, 2014b).

Figure 1: Time from admission to recovery or death.
Histograms illustrating the distribution of time between admission to the paediatric research ward and recovery of Blantyre Coma Score = 3/5 (left); and time between admission and death (right). These data are from retinopathy positive subjects recruited between 1999 and 2014 (n=909; n=200, respectively). Note the differences in time scale.

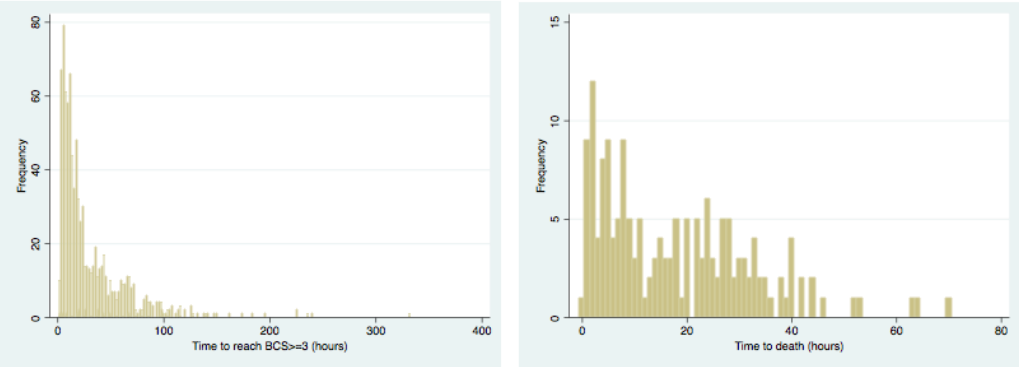

1.6.3 Epidemiology of paediatric CM

The incidence of paediatric CM in central Africa has been estimated at 2.5 (0.4-4.2) cases per 1000 child years (median cases (IQR) for the year 2000) (Roca-Feltrer *et al.*, 2008). This is similar to a previous estimate of isolated CM incidence in children under 5, which ranged from 0.9-3.5 cases per 1000 child years. "Isolated" CM refers to cases without characteristics of other severe malaria syndromes, such as severe malarial anaemia or respiratory distress/acidosis, which commonly occur along with impaired consciousness. The "total" incidence of CM estimated in the same study was 6.1 cases per 1000 child years (Murphy and Breman, 2001).

Cases of paediatric CM make up a relatively small proportion of all severe malaria in children. A review of data from 13 hospitals across East and West Africa found CM in 4% of paediatric admissions with malaria (Okiro *et al.*, 2009). A study in Tanzania found the overall frequency of CM relative to other severe malarial syndromes was 7% (Reyburn *et al.*, 2004).

The proportion of CM to other types of severe malaria appears to depend on transmission intensity. The frequency of CM was related to altitude (a marker of transmission intensity) and age, and ranged from 2.9% for altitudes <600m, to 12.7% for altitudes 600-1200m, and 22.1% for altitudes >1200m. The median age of children affected by CM increased from 1 year, to 6 years, to 26 years for the same locations (Reyburn *et al.*, 2005). The association between age of CM onset and transmission intensity is consistent with data from several studies (Okiro *et al.*, 2009; Snow *et al.*, 1994, 1997). Since CM has a relatively high mortality rate (14% to 47% in (Reyburn *et al.*, 2005); and approximately 15% on the research ward in Blantyre (Seydel *et al.*, 2015)), death from severe malaria can be more frequent in low transmission areas than in high transmission areas (Reyburn *et al.*, 2005). This has led to concerns that efforts to reduce malarial transmission may lead to a paradoxical rise in absolute numbers of CM cases (Snow *et al.*, 1994).

1.7 Paediatric cerebral malaria in the context of severe malaria in general

1.7.1 Definitions of severe malaria

Plasmodium falciparum is the major cause of a group of overlapping syndromes which collectively are termed “severe malaria”. Severe *P. falciparum* malaria is diagnosed when one or more of the features listed in Table 1 are present, in the absence of an alternative cause. The most common manifestations in children are severe malarial anaemia, impaired consciousness (i.e. CM), and acidosis. In adults the most common syndromes are jaundice, acidosis, impaired consciousness, and renal failure.

1.7.2 Epidemiology of severe malaria

The global annual incidence of severe malaria is estimated at approximately 2 million cases, with ~90% occurring in children under 5 years in sub-Saharan Africa (World Health Organization, 2014a, 2014b). Estimated worldwide mortality from severe malaria has fallen from 985,000 in 2000 to 627,000 in 2012.

In many countries falling death rates are associated with the roll out of interventions against mosquitos and improved anti-malarial treatment (World Health Organization, 2014b). No decline in severe or fatal malaria had been reported in Malawi up to 2010 (Roca-Feltrer *et al.*, 2012), however the number of children being admitted to the Paediatric Research Ward appears to have started dropping since then.

1.7.3 Severe malaria in children and adults

Manifestations of severe malaria are different in children and adults (Figure 1). Since severe malaria largely affects children in sub-Saharan Africa, and adults in South and South-East Asia, the extent to which clinical presentation is influenced by age independently of host and parasite factors related to geography is unclear (MacCormick et al., 2014; World Health Organization, 2014b). A small number of reviews have compared paediatric and adult CM histopathology (Hawkes *et al.*, 2013; MacCormick *et al.*, 2014), and development of the brain and blood-brain-barrier relevant to CM (Hawkes *et al.*, 2013). The specific severe malaria syndrome of CM may be different in adults and children. For example, blood brain barrier dysfunction appears to be common in fatal paediatric cases, and atypical in adults (Brown *et al.*, 1999, 2000, 2001).

Even within the paediatric population the proportion of particular severe malaria syndromes varies with transmission intensity and age. For example, severe malarial anaemia is dominant in young children (median age 1 year) in high transmission settings, while CM predominates in slightly older children (median age 3 years) in areas where transmission is less intense (Carneiro et al., 2010; Reyburn et al., 2005; Roca-Feltrer et al., 2010; World Health Organization, 2014b). The developmental rate of different physiological systems during childhood growth may be relevant to this phenomenon (Billig *et al.*, 2012). Neonatal infection is rare, possibly because of maternal immunity or the presence of foetal haemoglobin (Pasvol *et al.*, 1977).

Depth of coma and severity of acidosis appear to be particularly important predictors of death in both children and adults (World Health Organization,

2014b). This has been found in several studies (Hanson *et al.*, 2010; Helbok *et al.*, 2009; Jallow *et al.*, 2012; Marsh *et al.*, 1995; Mishra *et al.*, 2007; Molyneux *et al.*, 1989; Newton *et al.*, 2013; von Seidlein *et al.*, 2012). Other signs that appear to indicate worse prognosis in severe paediatric malaria include papilloedema, retinal haemorrhages (Beare et al., 2004), respiratory distress (Marsh *et al.*, 1995) (thought to be a marker of metabolic acidosis), jaundice, raised blood white cell count, witnessed convulsions at admission, and severity of peripheral parasitaemia (Molyneux *et al.*, 1989). Histidine rich protein 2 (HRP2) is a protein produced by the *P. falciparum* parasite, and plasma levels have been linked to mortality in paediatric cases of severe *P. falciparum* malaria (Hendriksen *et al.*, 2012), and are able to both diagnose retinopathy status (Seydel *et al.*, 2012) and predict later development of retinopathy positive CM in children (Fox *et al.*, 2013).

1.8 Description of the *P. falciparum* parasite life cycle

The human phase of the *P. falciparum* life cycle begins when an infected female Anopheles mosquito introduces sporozoites into a human host. These invade liver cells and multiply to produce primary tissue schizonts. Rupture of tissue schizonts releases large numbers of merozoites into the circulation, which then invade erythrocytes to develop into trophozoites. These multiply through asexual division into schizonts which rupture to release erythrocytic merozoites, which immediately invade more erythrocytes to produce more trophozoites. A small number of merozoites develop into gametocytes, which can be taken up again from the circulation by a feeding mosquito. In the mosquito midgut gametocytes begin a process involving sexual and asexual multiplication that eventually leads to the production of new sporozoites, which are ready for transmission to new human hosts (Bradley and Warrell, 2003).

1.9 Malarial retinopathy in severe malaria

1.9.1 Features of malarial retinopathy

Malarial retinopathy has been described most often on the basis of dilated fundus examination in paediatric CM, using direct or indirect ophthalmoscopy. The signs of malarial retinopathy visible on ophthalmoscopy of the paediatric retina are retinal haemorrhages, retinal whitening, and vessel discolouration. Malarial retinopathy is present if one or more of these features are seen (Beare *et al.*, 2006; Harding *et al.*, 2006; Lewallen *et al.*, 1999). Papilloedema is often present, but isolated papilloedema does not indicate malarial retinopathy (Harding *et al.*, 2006; Lewallen *et al.*, 1999). Since ophthalmoscopic examination of conscious young children is challenging, most observations of malarial retinopathy are from children with CM. However, malarial retinopathy does occur in paediatric severe malarial anaemia, and may occur in uncomplicated malaria as well (Beare et al., 2004; Lewallen et al., 1999).

Fluorescein angiography (FA) is a standard procedure for investigating the structure and function of ocular vessels, and particularly those of the retina (Dithmar and Holz, 2008). Since damage to neural parenchyma caused by sequestration is likely to result from blockage or leakage from microvessels, FA can potentially provide important information about cerebral malaria pathogenesis beyond that gained from ophthalmoscopy or colour retinal images. So far only a small number of papers have reported FA abnormalities in severe malaria, and so analysis of FA images forms a major part of this thesis (see Chapters 5 and 7 for more details).

Malarial retinopathy is also seen in adults with severe *P. falciparum* malaria. The frequency appears to be different from that in children, and not all of the features seen in children have been reported in adults (Abu Sayeed *et al.*, 2011; Maude *et al.*, 2009). Ocular signs have also been reported in cases of infection with *P. vivax* (Biswas *et al.*, 1996).

The clinical appearance of malarial retinopathy is described here. The pathological implications of retinopathy features, and their possible correlates in the brain, are discussed in Chapter 2.

1.9.2 Retinal whitening

Retinal whitening is a patchy opacification, in contrast to reflection from the internal limiting membrane which has a more glossy appearance (Figure 2 and 3). Retinal whitening is often visible around the fovea and patches of whitening may appear to radiate temporally from the fovea out along the horizontal raphe.

The centre of the fovea is never affected by whitening, and the typically dark foveal appearance provides a useful contrast for detecting subtle foveal whitening around its edge. Patches of retinal whitening range in size from small discrete lesions to large confluent areas. Areas of retinal whitening can be associated with white vessels (Figure 4) or capillaries (Figure 5). Retinal whitening often occurs in the same locations as capillary non-perfusion (CNP) (see below), but in contrast to CNP whitening may become more obvious over successive days while CNP improves (Figure 6).

Figure 2: a) Normal retinal anatomy; b) Severe whitening in the macula and peripheral retina.

2a) Retinal vessels enter and leave through the optic disc, which is always nasal to the macula. The macula and fovea are centred on the foveola. Vessels branch to form four arcades. The superotemporal and inferotemporal arcades roughly bracket the macula. The horizontal (or temporal) raphe is the region between the two temporal arcades. Peripheral retina includes everything out with the macula. See Chapter 5 for more details.

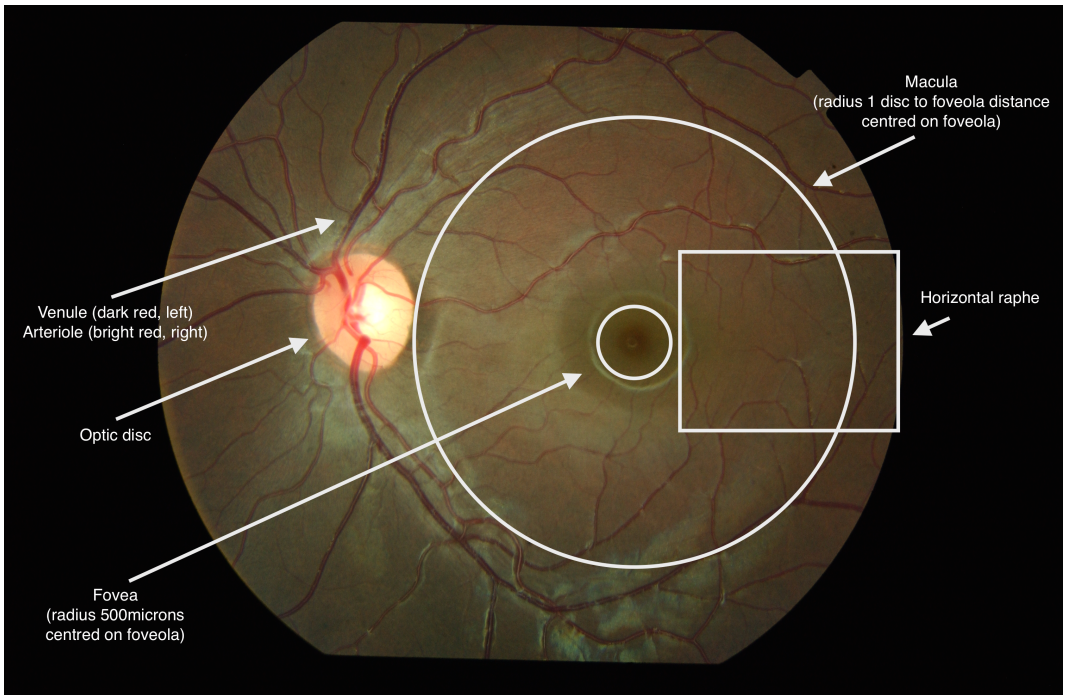

2b) Cotton wool spots are also visible (for example about 1 disc diameter from the disc at 11 o'clock), and there is a single blot haemorrhage inferior to the disc.

Figure 3: Severe foveal whitening and orange vessels.

Foveal whitening (single white arrow), and a large number of orange vessels (double white arrows) can be seen. Note that whitening tends to have geographical boundaries and a matt texture, while in contrast reflection from the internal limiting membrane has a more glossy appearance, and may seem to lie in sheets along the arcades or around the macula (single black arrow).

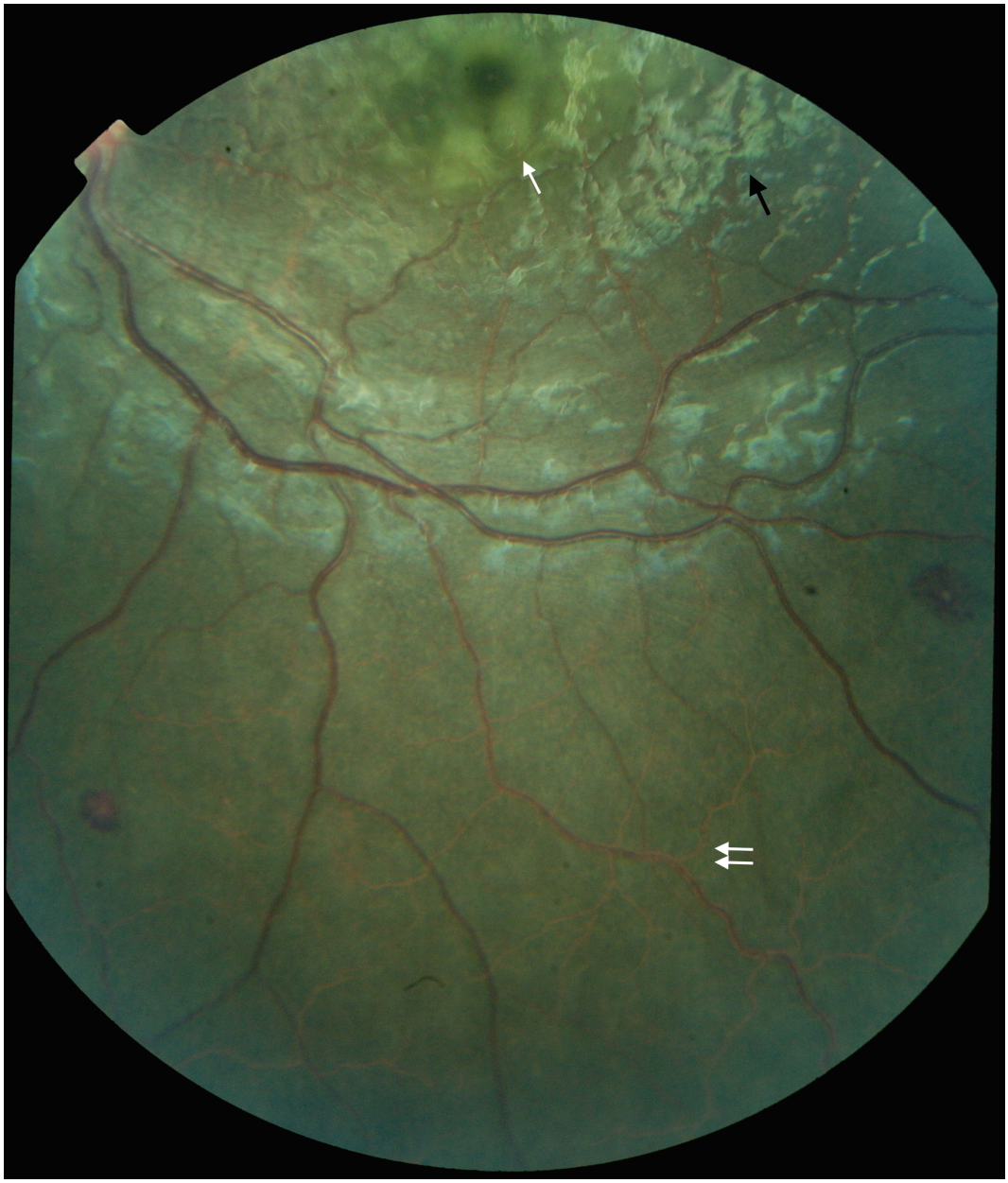

Figure 4: Large area of peripheral whitening with white vessels in the same territory.

White vessels begin abruptly at the edge of the peripheral whitening, which in this case looks like a tide mark. Smaller patches of whitening are concentrated in the raphe between the fovea and temporal periphery.

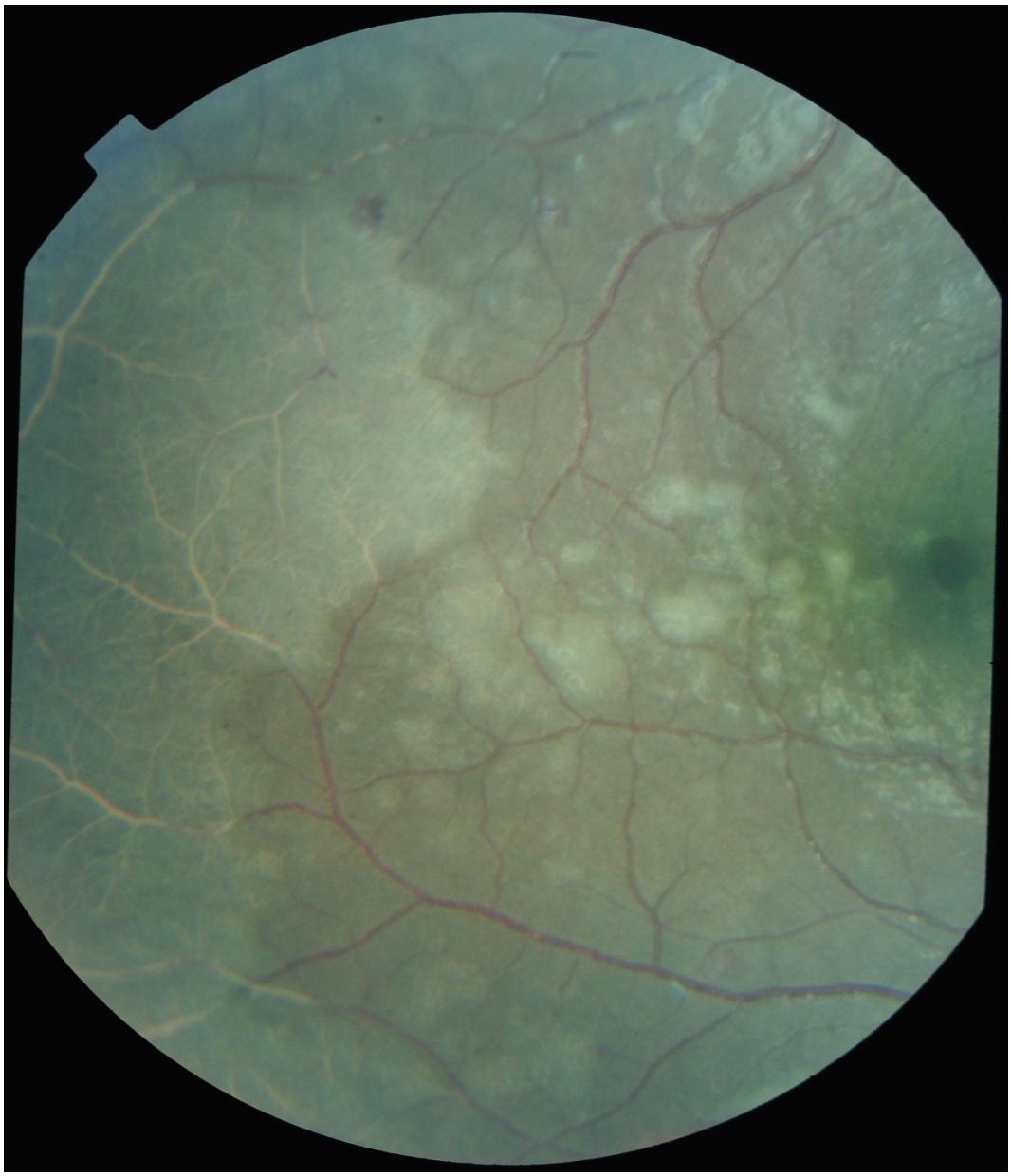

Figure 5: White capillaries.

White capillaries (single white arrow) typically overlie areas of peripheral whitening, and appear similar to frost. White centred retinal haemorrhages are also visible.

Figure 6: Appearance of retinal whitening over several days.
Colour and angiographic images taken from the same eye over successive days show resolution of capillary non-perfusion within one day, but relatively little improvement in macular whitening over five days. In the final set of images (from 18/02/2014) post-capillary venule leak has developed in the area of whitening. All angiographic images were taken at approximately the same time after injection (5 to 6 minutes). This late leakage may represent angiogenesis (see Chapter 9).

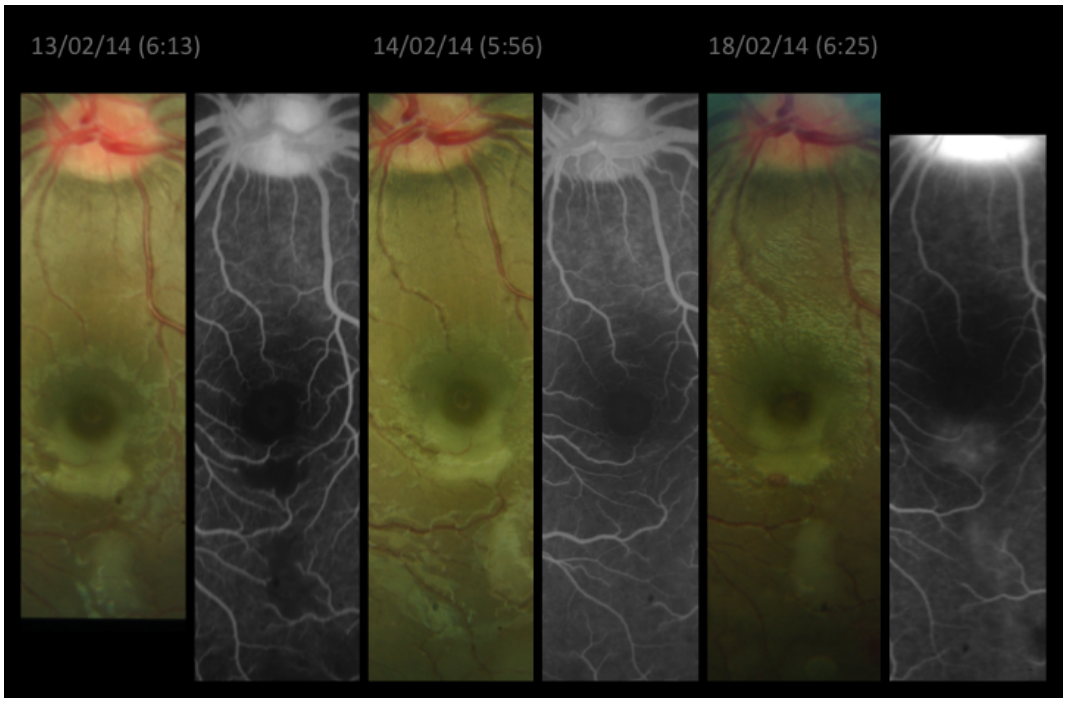

1.9.3 Retinal haemorrhage

Retinal haemorrhages seen in malarial retinopathy are often white-centred, and may be blot or flame shaped. They can occur anywhere in the retina and have no obvious spatial distribution in connection with vascular structures. The number of haemorrhages can range from one to well over 50, and in very severe cases they can obscure a large proportion of the posterior pole (Figure 7). Haemorrhages appear to be closely related to large focal leak seen on FA, since colour images of specific retinal areas before and after large focal leak consistently show the new development of haemorrhage at the same location as the leak (Figure 8).

Figure 7: Extensive white centred retinal haemorrhages.
Severe macular whitening is also visible. See figures 2, 3, and 5 for examples of less severe haemorrhage.

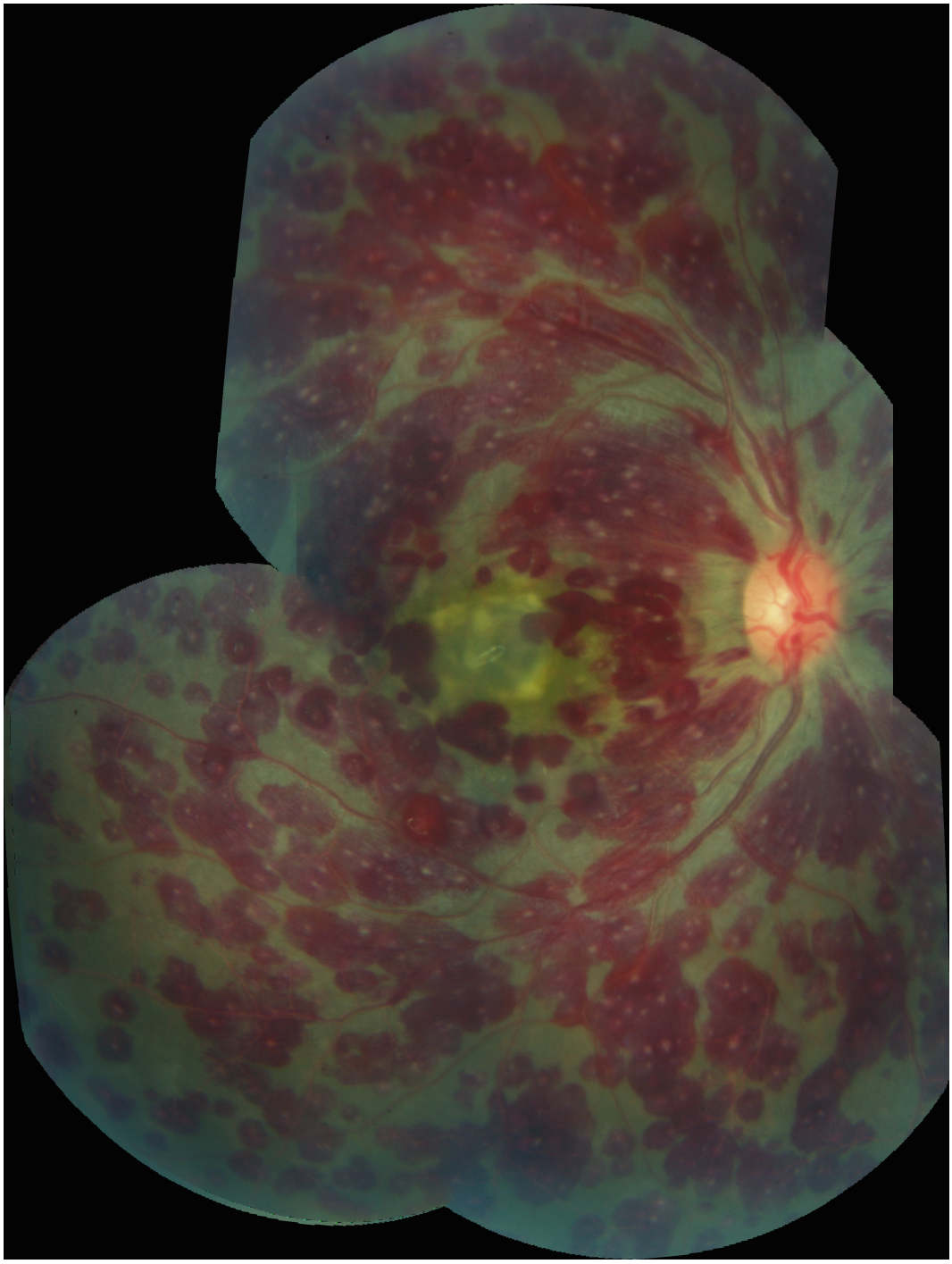

Figure 8: Haemorrhage and large focal leak.
Series of images taken before, during, and immediately after angiogram show the development of large focal leak by nine minutes. After the angiogram a new haemorrhage is present at the exact site of leak, surrounded by a halo of fluorescein.

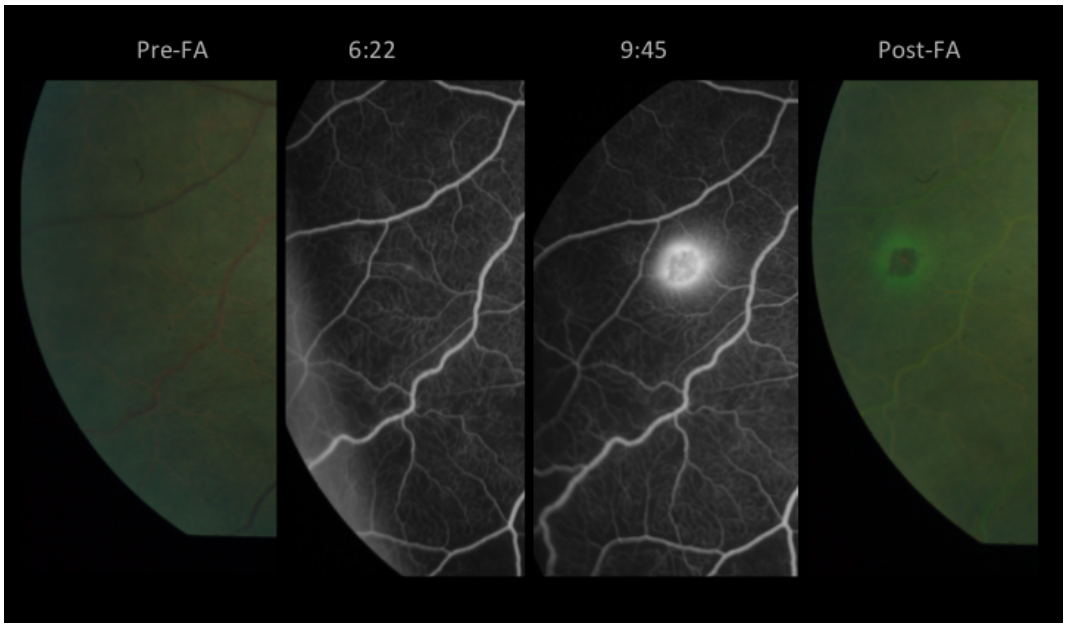

1.9.4 Vessel discolouration

Retinal vessels may appear orange or white (Figure 3 and 4). Orange vessels can be seen in the macula and the periphery. Larger vessels may have patches of orange discolouration along their length while small branching vessels appear completely orange. Patches of orange can be co-localised to individual intravascular filling defects (IVFD) seen on FA (Figure 9). White vessels and capillaries are usually seen in areas of retinal whitening. For example, a vessel may become white abruptly at the edge of a large patch of peripheral whitening (Figure 4). Vessel discolouration and IVFD are thought to represent sequestration (Beare *et al.*, 2009; Lewallen *et al.*, 2000). Retinal haemorrhage and whitening have been described in adults with malaria, but vessel discolouration has only been reported in children (Abu Sayeed *et al.*, 2011; Maude *et al.*, 2009).

Figure 9: Orange vessels and matching intravascular filling defects.
Matching colour and fluorescein angiogram images of a venule with orange discolouration. Sites of orange discolouration appear to correspond to intravascular filling defects (arrows).

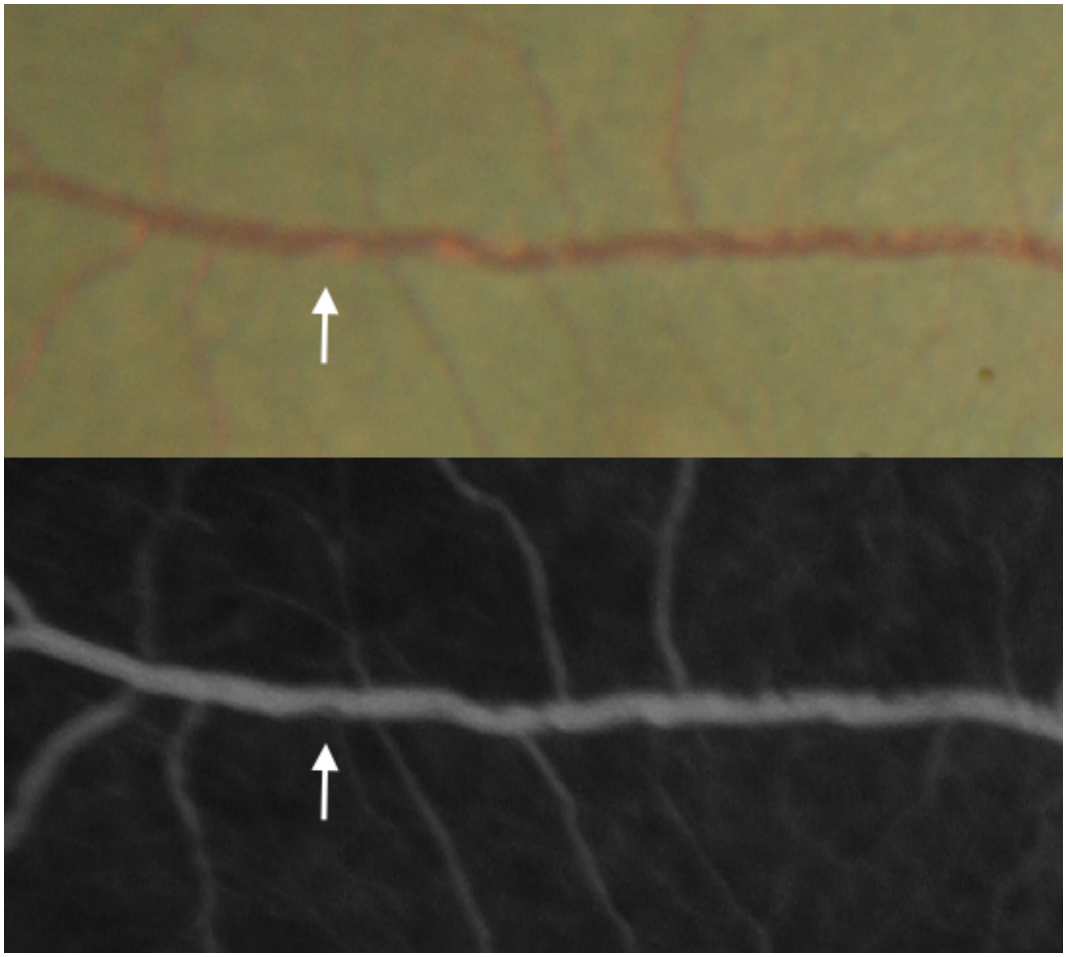

1.9.5 Additional features of malarial retinopathy

FA in children with CM reveals several features in addition to those visible on ophthalmoscopy. These include capillary non-perfusion (CNP), intravascular filling defects (IVFD), and various types of leakage (Beare *et al.*, 2009). Angiographic changes have been reported in adults (Davis *et al.*, 1992; Maude *et al.*, 2011), but it is not yet clear how similar angiographic features of malarial retinopathy in adults are to those in children. This is one of the reasons for developing a grading scheme for FA features in malaria (see Chapter 5).

Other retinal imaging modalities have been applied to malarial retinopathy. Electroretinography measures the retinal response to visual stimuli. In children with malarial retinopathy there is a significant association between retinal whitening and b-wave reduction indicating depressed function of cone second order neurone of the inner retina (Lochhead *et al.*, 2010). Ultrasonic measurement of optic nerve sheath diameter has been performed (Beare *et al.*, 2008), and associated directly with raised opening pressure and frequency of neurological sequelae in children surviving CM (Beare *et al.*, 2012).

1.10 Frequency of malarial retinopathy in children

The frequency of retinopathy is likely to depend on the patient group being studied, the technique used to examine the retina, and the experience of the examiner. Malarial retinopathy has been studied most extensively in paediatric CM, and less often in other severe malarial syndromes, or in adults. After reviewing the literature I selected the following studies of paediatric CM (Table 2) as the most likely to give reliable estimates of the frequency of malarial retinopathy in children with clinically defined CM (WHO criteria) (World Health Organization, 2014b).

In each study, an ophthalmologist used dilated indirect ophthalmoscopy to examine the retina of consecutive admissions, and a high proportion of eligible subjects were examined (74% to 100%) within 24 hours of admission. Other studies also exist, but refer to non-standard criteria for CM, use methods other than dilated indirect ophthalmoscopy, or do not report clearly interpretable proportions of subjects with retinopathy (Burton et al., 2004; Haslett, 1991; Hero et al., 1997; Kariuki et al., 2014; Lewallen et al., 1996; Mohammed et al., 2010; Molyneux et al., 1989; Newton et al., 1991; Olumese et al., 1997; Oluwayemi et al., 2013; Schémann et al., 2002).

Table 2: Studies reporting the frequency of malarial retinopathy in paediatric cerebral malaria

Study	Country and year	Any retinopathy	Haemorrhage	Macular whitening	Peripheral whitening	Vessel discolouration
(Lewallen *et al.*, 1993)	Malawi 1992	Not reported	20/56 (36%)	19/56 (34%)	10/56 (18%)	11/56 (20%) (vessel obstructions)
(Lewallen *et al.*, 2008)	Malawi 1999-2005	525/879 (59.7%)	Not reported	Not reported	Not reported	Not reported
(Beare et al., 2004)	Malawi 1999-2000	170/278 (61%) (may include isolated papilloedema)	129/278 (46%)	127/278 (46%)	123/278 (44%)	90/278 (32%)
Notes: Lewallen et al. (2008) includes subjects from Beare et al. (2004). Both studies are included in the table since Lewallen et al. (2008) may give a more accurate estimate of the overall frequency of malarial retinopathy than Beare et al. (2004)						

In contrast to observations by ophthalmologists in Malawi, one study involving dilated indirect ophthalmoscopy by an ophthalmologist in Ghana found any retinopathy in 19/26 (73%) paediatric CM cases. This study used a non-standard definition of CM (Essuman *et al.*, 2010). In contrast a non-ophthalmologist (using dilated indirect ophthalmoscopy) found retinopathy in 43/140 (30.7%) of children with CM (WHO criteria) in Kenya (Kariuki *et al.*, 2014). In both reports sampling was consecutive, but the proportion of eligible subjects studied is unclear, and the definition of "any retinopathy" included isolated papilloedema.

In addition to the studies reporting retinopathy in clinically defined CM, one study reported malarial retinopathy in histopathologically confirmed CM – a more stringent definition than the WHO clinical criteria (Taylor *et al.*, 2004). Taylor et al. found malarial retinopathy (excluding isolated papilloedema) in 19/20 (95%) of histopathologically confirmed CM cases, compared to 1/10 (10%) cases of coma of other cause. The latter group included subjects with apparent clinical CM, but no cerebral sequestration and another identifiable cause of death at autopsy (Taylor *et al.*, 2004). This is greater than the frequency of malarial retinopathy in approximately 60% in clinically defined cases (Beare et al., 2004; Lewallen et al., 2008).

Malarial retinopathy appears to be less common in paediatric severe malarial syndromes other than CM. In the following studies an ophthalmologist performed indirect ophthalmoscopy on admission on consecutive children with severe malaria. The definition of "any retinopathy" may include isolated papilloedema (Table 3).

Table 3: Studies reporting the frequency of malarial retinopathy in different paediatric severe malarial syndromes

Study	Country and year	Severe malaria syndrome	Any retinopathy	Haemorrhage	Macular whitening	Peripheral whitening	Vessel discolouration
(Essuman *et al.*, 2010)	Ghana 2002	Cerebral malaria	19/26 (73%)	Peripheral haemorrhage 11/26 (42%) Macular haemorrhage 1/26 (4%)	10/26 (39%)	11/26 (42%)	9/26 (35%)
		Severe malarial anaemia	14/26 (54%)	Peripheral haemorrhage 7/26 (27%) Macular haemorrhage 2/26 (7%)	7/26 (27%)	2/26 (8%)	6/26 (22%)
		Respiratory distress	3/6 (50%)	Peripheral haemorrhage 2/6 (33%)	1/6 (17%)	0/6 (0%)	1/6 (17%)
(Beare et al., 2004)	Malawi 1999-2000	Cerebral malaria	170/278 (61%)	129/278 (46%)	127/278 (46%)	123/278 (44%)	90/278 (32%)
		Severe malarial anaemia	25/47 (53%)	14/47 (30%)	11/47 (23%)	21/47 (45%)	10/47 (21%)

Notes:
In Essuman et al. (2010) the proportion of the sample studied with reference to the number of eligible subjects is not clear. The definition of "any retinopathy" may include isolated papilloedema or cotton wool spots. The definition of cerebral malaria is non-standard (BCS≤3 instead of BCS≤2). No orange vessels were observed – in this study vessel discolouration refers only to white vessels. In Beare et al. (2004) the definition of "any retinopathy" may include isolated papilloedema. The number of subjects examined as a proportion of eligible was 82%.

The studies listed above suggest that the frequency of malarial retinopathy in African children with clinically defined CM (WHO criteria) is approximately 60%, when examined by an ophthalmologist using dilated indirect ophthalmoscopy. Haemorrhages and macular whitening are seen in approximately 30-40%. Vessel discolouration appears to be less frequent than other retinal signs (approximately 20-30%) (Beare et al., 2004; Lewallen et al., 1993).

This is greater than a reported frequency of approximately 50% in children with severe malarial anaemia (Beare et al., 2004; Essuman et al., 2010), and consistent with otherwise unpublished data in a review showing a trend towards much lower frequency in moderate or uncomplicated malaria (Lewallen *et al.*, 1999).

It seems clear that none of the three retinal features characteristic of malarial retinopathy (haemorrhage, whitening, orange or white vessels) are specific to CM. All have been reported in children with severe malarial anaemia (Beare et al., 2004; Essuman et al., 2010), and also in respiratory distress/metabolic acidosis (although in small numbers in only one study) (Essuman *et al.*, 2010).

However it does appear that, within a specific population of children with clinically defined CM, retinopathy does reflect the nature and severity of brain histopathology (Barrera *et al.*, 2015; Taylor *et al.*, 2004; White *et al.*, 2001). These observations raise questions about how often retinal signs occur in uncomplicated paediatric malaria, or in paediatric systemic illness in general, and what associations (if any) retinal signs might have with the brain in these other conditions.

Whether in children or in adults, in general the frequency of retinopathy appears to be lower in studies where examination was performed by a non-ophthalmologist clinician (Abu Sayeed *et al.*, 2011; Kariuki *et al.*, 2014), or when methods other than dilated indirect ophthalmoscopy or fundus photography are used. Although high sensitivity and specificity for dilated direct ophthalmoscopy compared to dilated indirect ophthalmoscopy has been reported (Abu Sayeed *et al.*, 2011), estimated retinopathy frequency is less in studies that used direct

ophthalmoscopy. For example, Looareesuwan et al., (1983) found haemorrhage in 14.6% of adult CM (dilated direct ophthalmoscopy) compared to 55% in Maude et al., (2009) (dilated retinal photography), and 40% in Abu Sayeed et al., (2011) (dilated indirect ophthalmoscopy by a non-ophthalmologist).

It is possible that retinopathy frequency within paediatric CM also varies between geographical regions in sub-Saharan Africa. Reported frequency of 30% in Kenya (Kariuki *et al.*, 2014) is lower than Malawi (60%) (Beare et al., 2004), which in turn is lower than in Ghana (73%) (Essuman *et al.*, 2010). This could reflect differences in transmission intensity, or variation in the interaction of host and parasite factors. However this interpretation is difficult to substantiate on the basis of existing evidence. Differences in methodology, and definition of retinopathy and CM used in these studies are likely to influence retinopathy frequency in addition to any underlying biological causes.

1.11 Associations with malarial retinopathy in children

Investigators have approached questions about associations with paediatric malarial retinopathy in different ways, and interpretation of results depends on study design. Studies can be divided into four groups:

1) Studies comparing variables between children with retinopathy-positive or retinopathy-negative CM (Conroy et al., 2010, 2012; Lewallen et al., 2008; Milner et al., 2012; Phiri et al., 2011; Postels et al., 2014; Postels, Taylor, et al., 2012; Potchen et al., 2012)

2) Studies comparing retinopathy-positive (or histopathologically confirmed) CM with a control group defined by non-malarial diagnosis (Birbeck, Molyneux, *et al.*, 2010; Taylor *et al.*, 2004).

3) Studies testing associations within a sample of exclusive retinopathy-positive (or histopathologically confirmed) CM cases (Kampondeni *et al.*, 2013; White *et al.*, 2001).

4) Studies testing associations within in a mixed sample consisting of both retinopathy-positive and retinopathy-negative CM cases (Beare et al., 2004; Beare et al., 2004; Lewallen, 1998; Lewallen et al., 1993; Lochhead et al., 2010; Postels, Birbeck, et al., 2012; Seydel et al., 2012).

It seems that malarial retinopathy has several associations, at least in the Malawian paediatric population. For example, retinopathy appears to be associated with death. Papilloedema is an important prognostic factor in multivariate models on separate cohorts of mixed retinopathy positive and negative CM patients (Beare et al., 2004; Lewallen et al., 1993). "Any retinopathy" is associated with death in a study comparing subjects with retinopathy (including papilloedema) with subjects who have completely normal fundi (i.e. no papilloedema) (Lewallen *et al.*, 2008).

This choice of control group may bias the analysis towards risk of death with retinopathy, since papilloedema will only be present in one group. It is less clear if any specific features besides papilloedema have clear prognostic significance. Associations between death and peripheral whitening (Lewallen *et al.*, 1993), and retinal haemorrhages (Beare et al., 2004) have been reported but not reproduced. In addition these results are relevant to clinically defined CM, but not necessarily retinopathy-positive CM.

Retinopathy has been associated with several histopathological features. In histopathologically confirmed fatal CM the number of retinal haemorrhages is correlated with the number of brain haemorrhages (White *et al.*, 2001), and the presence of any retinopathy pre-mortem is has high positive and negative predictive value for cerebral sequestration in fatal coma (Taylor *et al.*, 2004).

This latter study has been highly influential. However, there is potential for bias favouring sensitivity and specificity of retinopathy to predict sequestration.

Retinal exam was performed on 83% of CM cases, but only 56% of controls. Retinal exam data is minimal in the control group, but extensive for the cases, suggesting a possible further systematic difference in data collection. The control group consisted of subjects with retinopathy negative CM, and also patients diagnosed with non-malarial coma. This may raise the chances of finding significant cerebral sequestration in patients with retinopathy, in contrast to the control group, since a proportion of controls have a non-malarial diagnosis.

Having made these points, it should be remembered that, as with other influential contributions to the literature (Beare et al., 2004), this study was designed before the diagnostic importance of malarial retinopathy was recognised (World Health Organization, 2014b). The composition and investigation of the control group are features of the state of knowledge at the time of the study, rather than an intentional effort to bias the results.

Furthermore, the conclusions of (Taylor *et al.*, 2004) are consistent with more recent work from the same autopsy series showing that the severity of retinopathy is correlated to both sequestration in the retina and brain in children with retinopathy positive CM (Barrera *et al.*, 2015). Efforts to replicate these findings in an independent sample are warranted.

Clinically defined paediatric CM cases can be distinguished into retinopathy positive and negative groups by a specific HRP2 threshold (Seydel *et al.*, 2012). This suggests that quantitive HRP2 may be a useful diagnostic tool in patients with suspected CM instead, or in addition to, ophthalmoscopy. It also suggests that parasite burden may be important in CM pathogenesis.

Children with retinopathy positive CM appear to have different MRI brain features from those with retinopathy negative CM. Features most strongly associated with retinopathy include basal ganglia abnormalities, high cerebral cortical T2 signal, and high T2 signal in the corpus callosum (Postels *et al.*, 2014; Potchen *et al.*, 2012). Similar results have been reported by two studies, but the large degree of overlap in patient samples means that the findings should probably not be regarded as having been independently replicated. It is not yet clear why

these specific MRI features should be associated with retinopathy. This question is discussed further in Chapter 2.

Several other associations have been reported, which largely suggest hypotheses, rather than confirm them. Retinopathy is more frequent earlier, compared to later, in the Malawian malaria season (Postels, Birbeck, *et al.*, 2012). Endothelial damage (Conroy *et al.*, 2010, 2012), low Vitamin A (Lewallen, 1998), parasite diversity (Milner *et al.*, 2012), and anaemia may have important roles in the pathogenesis of malarial retinopathy. Retinal whitening may reflect dysfunction of the inner retina (Lochhead *et al.*, 2010), consistent with blockage of visible retinal vessels in the same territory as whitening (Beare *et al.*, 2009).

Although survivors of retinopathy positive CM are more likely to develop epilepsy than similar children admitted with non-malaria non-comatose diagnoses (Birbeck, Molyneux, *et al.*, 2010), children surviving retinopathy positive CM appear to have a similar risk of neurological complications to children with malaria-associated coma but no retinopathy (Postels, Taylor, *et al.*, 2012).

1.12 History of malarial retinopathy

Reports of retinal complications of malaria exist from only a few decades after the invention of the direct ophthalmoscope by von Helmholtz in 1851, and before the earliest identification of malarial parasites in peripheral blood by Laveran in 1880, or the observation by Marchiafava and Bignami of cerebral sequestration in 1894.

For example, in 1877 Mackenzie described white centred retinal haemorrhages in patients with ague and included drawings of lesions that appear very similar to those in modern day colour images (Figure 10). He also cited two earlier reports of retinal signs in malaria in 1875 and 1876 (Mackenzie, 1877). Testalin (1866), cited by (Warlomont, 1866), appears to describe blindness in a child with malaria. Poncet, (1879) has been widely cited as reporting retinal haemorrhages in a significant proportion of malaria cases. Several other case reports and case series of ocular complications of malaria exist from before 1950, many in languages other than english, reflecting the widespread prevalence of malaria within Europe,

the Americas, and colonised territories during this period (de Andrade, 1937; Blatt, 1928; Carlotti, 1918; Chastang, 1918; Davis, 1909; Dedimos, 1932; Fialho, 1927; Finnoff, 1929; Fisher, 1921; Goldfeder *et al.*, 1935; Gubergrits, 1934; Kiep, 1922; Kirk, 1918; Laveran, 1880; Lombardo, 1945; Manson, 1920; Migliorini, 1917; Morano, 1909; Motegi *et al.*, 1934; Pagliari, 1933; Pereyra, 1922; Sedan, 1929; Sulzer, 1890; Toulant, 1938; Villard, 1930; Werner, 1911).

Figure 10: Early drawing of malarial retinopathy
A drawing of the posterior pole of the retina, showing white-centred retinal haemorrhages in an adult with ague (from (Mackenzie, 1877)).

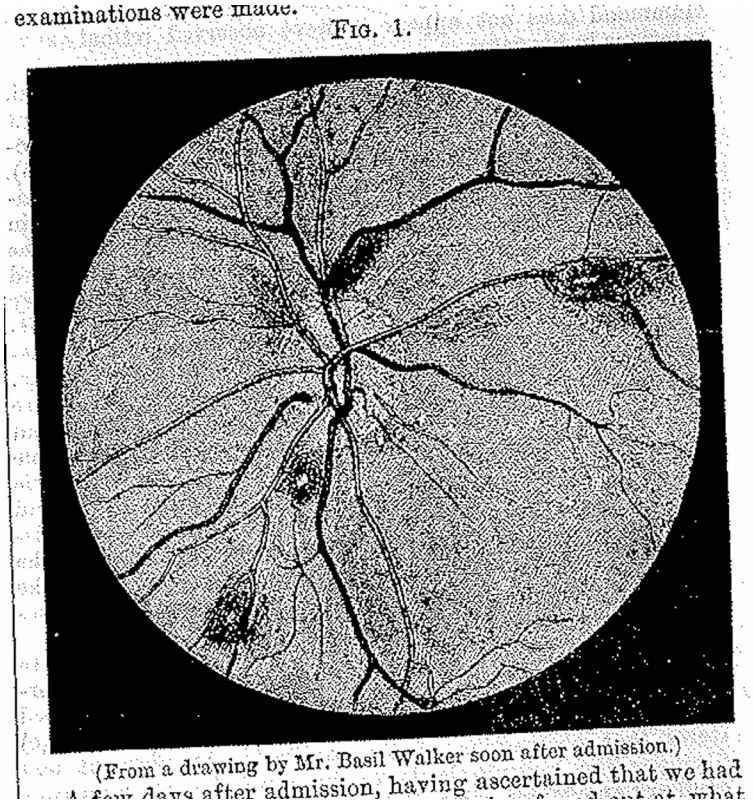
examinations were made.

FIG. 1.

(From a drawing by Mr. Basil Walker soon after admission.)

A few days after admission, having ascertained that we had

By 1920 there was enough literature on malaria and the eye for a thesis to be written on the subject (Lavagnac, 1920), and several ocular complications of malaria are described in what is probably the first textbook on tropical ophthalmology, published the same year (Elliott, 1920). The earliest report of retinal histopathology in CM may be Dudgeon (1921) in a journal section by Fisher, who published paintings of parasitised erythrocytes in the central retinal and choroidal vessels (Fisher, 1921) (Figure 11).

Figure 11: Early paintings of retinal histology in fatal adult cerebral malaria. From (Fisher, 1921). The image on the left shows a vessel in the optic nerve, the image on the right shows vessels in the retina (Prof Paul Hiscott, personal communication)

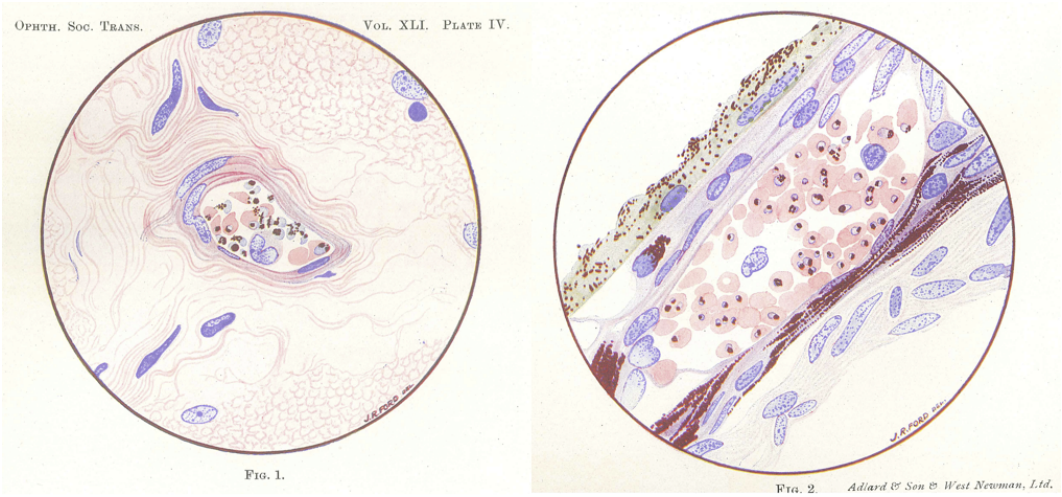

A wide range of ocular symptoms and signs were attributed to malaria, which before the mid 1900s was endemic in much of Europe as well as the United States. These include keratitis, uveitis, optic neuritits, and paralysis of the extraocular muscles. Few if any of these are now regarded as specific complications of malaria.

In his discussion of this list Elliott recognised that not all ocular associations with malaria were equally likely to be caused by malaria, and complained that

> "Some observers appear to have fallen into the error of ascribing to malaria every morbid condition... without a sufficiently careful examination of the facts and circumstances of each case." (p445) (Elliott, 1920).

However, herpetic keratitis seems to have had particularly strong associations with malarial fever. One report even describes the dramatic onset of herpetic keratitis just after therapeutic inoculation with tertian malaria (i.e. *P. falciparum*) to treat neurosyphilis (Finnoff, 1929).

So perhaps it is not unreasonable that although Elliot recognised that keratitis could occur in a range of febrile illnesses, and also that malaria parasites had never been isolated from corneal scrapings, he decided that herpetic keratitis was

> "so widely described as a malarial manifestation that we may probably accept it with but little hesitation" (p452) (Elliott, 1920).

Historical conclusions like this are interesting in their own right, but they also prompt a renewed awareness that association does not prove causation. The retinal manifestations currently blamed on malaria are implicated by a much greater amount of evidence – particularly retinal and cerebral histopathology (Barrera *et al.*, 2015; Taylor *et al.*, 2004; White *et al.*, 2001). But clinicians and scientists have been mislead in the past, and may easily be mislead again (Kuhn, 1984). We still need to apply "a sufficiently careful examination of the facts".

Other than isolated case reports (Bell, 1975), it seems that after 1950 relatively little was published on ocular complications of malaria until the 1980s, when two studies of retinal haemorrhages in adults with severe malaria were published from work in Asia (Davis *et al.*, 1982; Looareesuwan *et al.*, 1983).

Retinal haemorrhages were first described in paediatric CM in Malawi 1989 (Molyneux *et al.*, 1989), and Kenya in 1991 (Newton et al., 1991). Lewallen and others provided the first description of malarial retinopathy as a constellation of retinal features, including haemorrhage but also retinal whitening ("oedema") and vessel discolouration ("vessel obstructions"). They also reported associations between retinal features and death (Lewallen *et al.*, 1993, 1996).

These features then became the subject of more extensive investigations, particularly in Malawian children with CM, but also paediatric cases from other regions of sub-Saharan Africa (Lewallen *et al.*, 1999) and adults in South and South-East Asia (Abu Sayeed *et al.*, 2011; Maude *et al.*, 2009). Malarial retinopathy was again the subject of a thesis in 2005 (Beare, 2005).

FA was performed in a case of malaria as early as 1984 (Yospaiboon et al., 1984). Later studies evaluated retinal vessel leak more systematically in adult (Davis *et al.*, 1992) and paediatric severe malaria (Hero *et al.*, 1997). A broader range of angiographic features were described in paediatric CM 2009 (Beare *et al.*, 2009).

1.13 Conclusions

Retinal biomarkers are currently being sought for a range of neurological diseases. This search is justified by the simplicity of examining the retina compared to the brain, but also in part by somewhat casual references to similarities between these two organs, and the idea that the retina might provide a "window". However, successful development of retinal biomarkers depends on understanding, and exploiting, the nature of analogy between these two regions of the central nervous system in ways that are specific to the disease in question. The syndrome of paediatric CM appears to be a good case study for this process, because many associations between retina and brain have already been mapped out.

Paediatric CM is one of several severe malarial syndromes caused by *P. falciparum*, which involves malarial retinopathy in approximately 60% of cases. The presence of sequestered parasites in the cerebral circulation is reckoned to be central to a disease process which is still poorly understood. Work over several decades has led to the presence of malarial retinopathy defining a new diagnostic category: "retinopathy positive CM". This group has different characteristics from cases of CM without retinopathy, including a greater chance of cerebral sequestration, particular features on MRI brain, and higher levels of plasma HRP2. Furthermore, the severity of malarial retinopathy is directly proportional to the degree of sequestration in both retina and brain.

The current literature suggests that visible manifestations of neurovascular damage in the retina may approximate similar mechanisms in the brain, in retinopathy positive paediatric CM. If this is true, retinal imaging may provide useful insights into cerebral disease processes that are otherwise inaccessible. However, developing retinal signs as biomarkers of evolving cerebral pathology will require several steps beyond what has been done previously.

The biological plausibility of associations between retina and brain in paediatric CM needs to be established. I attempt this in Chapter 2. Statistical methodology to evaluate the supposed analogy between retina and brain must be found. It may be possible to adapt existing techniques originally designed to validate surrogate end points, and I examine this approach in Chapter 3. Although associations have been reported between ophthalmoscopic exam and cerebral disease features, this has not been done for FA. I describe a method for reliably quantifying angiographic signs in severe malaria (Chapter 5), and go on to test associations between these retinal features and clinical outcomes (Chapter 7) and features of MRI brain scans (Chapter 8).

These steps may lead to insights about CM disease mechanisms, and, insofar as retinal features might reflect brain diseases more generally, may also test a new approach for developing and evaluating retinal markers for a range of neurological disorders.

Chapter 2 – Is it reasonable to draw conclusions about the brain from the retina in paediatric cerebral malaria?

2.1 Aim of chapter

Determine the plausibility of associations between retina and brain in paediatric cerebral malaria by reviewing the literature and comparing retina and brain in terms of cerebral malaria histopathology, vascular anatomy and physiology.

2.2 Summary of chapter

2.2.1 What is known already

Cerebral malaria is a dangerous complication of infection which takes a devastating toll on children in sub-Saharan Africa. Although autopsy studies have improved understanding of cerebral malaria pathology in fatal cases, information about *in vivo* neurovascular pathogenesis is scarce because brain tissue is inaccessible in life. Biomarkers may provide insight into pathogenesis and thereby facilitate clinical studies with the ultimate aim of improving the treatment and prognosis of cerebral malaria. The retina is an attractive source of potential biomarkers for paediatric cerebral malaria because, in this condition, the retina seems to sustain microvascular damage similar to that of the brain. In paediatric cerebral malaria a combination of retinal signs correlates, in fatal cases, with the severity of brain pathology, and has diagnostic and prognostic significance. Unlike the brain, the retina is accessible to high-resolution, non-invasive imaging.

2.2.2 What this chapter involved

I reviewed the literature on retinal and cerebral manifestations of retinopathy-positive paediatric cerebral malaria. I then compared retina and brain in terms of anatomical and physiological features that could help to account for similarities and differences in vascular pathology.

2.2.3 What this chapter adds to current knowledge

These comparisons address the question of whether it is biologically plausible to draw conclusions about unseen cerebral vascular pathogenesis from the visible retinal vasculature in retinopathy-positive paediatric cerebral malaria. In the process I develop new hypotheses about why these vascular beds are susceptible to sequestration of parasitised erythrocytes. In later chapters I go on to use these hypotheses to inform my analysis of data from retina and brain in paediatric cerebral malaria.

2.3 Introduction

Paediatric cerebral malaria (CM) is a clinical syndrome that kills and disables children through mechanisms that remain incompletely understood. Adhesion of parasitised erythrocytes to the microvascular endothelium, leading to their sequestration in the brain, is the pathological signature of both adult and paediatric CM, and is thought to be the chief cause of injury (Ponsford *et al.*, 2012; Taylor *et al.*, 2004). Several hypothetical mechanisms linking sequestration, which is entirely intravascular, to extravascular parenchymal damage have been proposed (van der Heyde *et al.*, 2006) but questions remain about which of these mechanisms are most important, how they might interact, and ultimately where new therapies should be directed. One of the reasons why such questions remain over 100 years after sequestration was first identified is because *in vivo* access to the brain is difficult, and advances in knowledge have relied on postmortem and *in vitro* studies. Improved understanding of *in vivo* neurovascular pathogenesis and the development of better treatments will be facilitated by disease models or surrogate markers.

The retina may be a good source of biomarkers of cerebrovascular injury because paediatric CM is associated with a retinopathy (“malarial retinopathy”) that accurately predicts cerebral sequestration (Taylor *et al.*, 2004), correlates with severity of brain involvement (Barrera *et al.*, 2015; White *et al.*, 2001), and may be associated with mortality (Beare et al., 2004). Unlike the brain, the eye allows non-invasive access for structural and functional imaging of the microcirculation, which is thought to be the major site of sequestration.

The concept that neurovascular injury observed in the retina resembles neurovascular injury lying unseen in the brain is based on the assumption that the two circulations are analogous in ways that are relevant to the pathogenesis of paediatric CM. Such assumptions should be supported by a biologically plausible rationale before specific retinal vascular features are considered as bio- or surrogate markers of cerebrovascular damage (International Conference on Harmonisation, 1998).

Is such a rationale likely? It is well known that the retina and brain have many similarities. Both are part of the CNS, with common embryological origins, vascular structure and metabolic demands. The relevance of these similarities for potential surrogate markers has been recognized (Patton *et al.*, 2005, 2006), especially for stroke (Doubal, 2010; Doubal *et al.*, 2009). Despite this, detailed comparisons of the microvasculature of the two organs are rare (Cogan and Kuwabara, 1984; Patton *et al.*, 2005).

My objective in this chapter is to discover how likely it is that the retinal vascular damage responsible for malarial retinopathy reflects analogous cerebrovascular damage in retinopathy-positive paediatric CM. To do this I compare the manifestations of paediatric CM in retina and brain, and then compare retina and brain in terms of vascular features likely to be important for CM pathogenesis. Concluding that retina and brain are analogous in ways relevant to this disease would justify further investigation to see whether specific retinal signs predict both brain damage detectable by MRI and the patient's response to treatment. The results of such investigations would address further criteria of surrogacy (International Conference on Harmonisation, 1998) (see Chapter 3)), and in the context of a strong biological rationale could shed light on the dynamics of CM neurovascular pathogenesis in the period between coma onset and recovery or death.

Malarial retinopathy can occur in parasitaemic children without CM (Beare et al., 2004), and indeed, some features of malarial retinopathy occur in conditions that don't involve malaria at all. For example, white-centred haemorrhages occur in

bacterial endocarditis. It is not clear if retinopathy predicts cerebral sequestration in malarial syndromes besides paediatric CM, or how often retinopathy might occur in severely ill children in general.

I therefore discuss retinopathy in the specific clinical context of paediatric CM. In this particular population malarial retinopathy has high positive and negative predictive values to distinguish between the presence and absence of cerebral sequestration in fatal cases (Taylor *et al.*, 2004). Until associations between retinopathy and cerebral sequestration are known for malaria in general, extrapolation from this chapter to severe malaria syndromes other than paediatric CM is not appropriate.

This chapter is divided into four sections. In the first section I describe manifestations of CM in the paediatric brain and retina. The neurovascular effects of CM on retina and brain are then compared.

In the second section I introduce the concept that patterns of neurovascular pathology in retina and brain may be understood in terms of haemorheological dysfunction involving microvascular haematocrit, blood viscosity and shear stress. These factors depend on interactions between intrinsic properties of blood and structural properties of microvascular networks, and this suggests that microvascular architecture may be a useful point of comparison for a CM-specific analogy between retina and brain.

The third section describes microvascular architecture in the human retina and brain, and compares features that may be relevant to the pathogenesis of CM.

I end by discussing how my comparison of retina and brain provides a biologically plausible rationale for considering retinal signs as potential biomarkers or surrogates of brain damage in retinopathy-positive paediatric CM. I consider how observations of retinal vessel structure and function might allow inference of *in vivo* cerebrovascular pathogenesis.

2.4 Manifestations of retinopathy-positive cerebral malaria in the paediatric brain

2.4.1 Sequestration

Sequestration is the histopathological hallmark of paediatric CM (Taylor *et al.*, 2004). Sequestration results from the binding of parasitised erythrocytes to vascular endothelium. Parasitised erythrocytes also bind in vitro to other erythrocytes (rosetting), and to platelets (clumping, or auto-agglutination). Sequestration is mediated by adhesion between malarial antigens on the surface of the infected erythrocyte and several host receptors on the vascular endothelium. The *P. falciparum* surface antigen most studied is *P. falciparum* erythrocyte membrane protein 1 (PfEMP1), which is encoded by a family of var genes (reviewed in Craig and Scherf, 2001; Miller et al., 2013; Rowe et al., 2009). PfEMP1 undergoes antigenic variation, associated with differential sequestration between organs in children (Montgomery *et al.*, 2007). Of several host receptors, intercellular adhesion molecule 1 (ICAM1) has received the most attention. ICAM1 is a cytokine-inducible endothelial receptor normally involved in leucocyte rolling before firm endothelial adhesion, and is up regulated in brain vessels in fatal paediatric CM (Armah *et al.*, 2005; Brown *et al.*, 2001). Because it results from adhesion between antigens and receptors, sequestration is likely to be influenced by shear stress (Fedosov, Caswell and Karniadakis, 2011; Fedosov, Caswell, Suresh, *et al.*, 2011; Kaul *et al.*, 1991).

In fatal paediatric CM, sequestration is seen in most microvessels of both grey and white matter of the cerebral hemispheres. Sequestration occurs on the margins of larger pial and subarachnoid vessels (Dorovini-Zis *et al.*, 2011), but a calibre threshold above which sequestration does not occur has not been described. Sequestration is thought to be most severe in capillaries and post capillary venules — although only one study, in adults, has compared sequestration between vessel types (MacPherson *et al.*, 1985).

Sequestration seems to be a fundamental component of CM pathogenesis, but the exact mechanisms linking it to tissue injury in CM are unclear. Microvascular obstruction from sequestration leads to impaired perfusion, but also endothelial

activation associated with apoptosis, reduced dilatory capacity, and a procoagulant state (Moxon *et al.*, 2009; Rowe *et al.*, 2009). Parasitised erythrocytes bind to endothelial protein C receptor (Turner *et al.*, 2013). The associated loss of protein C receptor in cerebral vessels is likely to result in unmodified signalling through several molecular cascades leading to inflammation, loss of vascular barrier function, activation of platelets and production of fibrin (Moxon *et al.*, 2013).

Endothelial dysfunction may also result from *P. falciparum*-associated reductions in nitric oxide (NO) synthesis and bioavailability (reviewed in Miller et al., 2013), and increased oxidative stress (Griffiths *et al.*, 2001; Narsaria *et al.*, 2011), which can reduce erythrocyte deformability (Dondorp *et al.*, 1997, 2003) and impair neurovascular coupling as well as control of vascular tone (reviewed in Faraci, 2011).

These points illustrate how tissue damage associated with sequestration may be caused through synergistic mechanisms, including (and probably not limited to) inflammation and coagulation, in addition to congestion of blood flow secondary to reductions in lumen diameter. Local coagulopathy and loss of endothelial barrier function are consistent with haemorrhage and brain swelling seen in the paediatric brain, and with quantifiable manifestations of malarial retinopathy.

2.4.2 Haemorrhage

Histopathology reveals subtypes of CM within fatal retinopathy-positive paediatric CM. In Malawi 75% of cases coming to autopsy have sequestration with associated perivascular haemorrhages and intravascular micro thrombi, whereas 25% have sequestration but no haemorrhages or other perivascular pathology visible on routine haematoxylin and eosin-stained sections (Dorovini-Zis *et al.*, 2011).

Petechial haemorrhages on the cut surface of fresh brain correspond to microscopic ring haemorrhages. Ring haemorrhages occur frequently in the white matter of the cerebral hemispheres, and extend to the grey–white border. They are rare in cortical and subcortical grey matter, but occur throughout the cerebellum

and brainstem (White *et al.*, 2001). Diffuse axonal injury follows the same distribution (Dorovini-Zis *et al.*, 2011).

In general, ring haemorrhages in paediatric CM consist of extravasated uninfected erythrocytes; each haemorrhage is centred on a distended capillary containing infected erythrocytes and commonly a micro thrombus (Dorovini-Zis *et al.*, 2011).

2.4.3 Brain swelling and vessel leakage

Studies of paediatric CM where retinopathy status was either unknown or a combination of retinopathy-positive and retinopathy-negative cases, have found raised opening pressure at lumbar puncture (Newton et al., 1991), clinical signs consistent with brain herniation (12/12 fatal cases, 17/49 survivors) (Newton *et al.*, 1994), papilloedema (Beare et al., 2004), and enlarged optic nerve sheath diameter (Beare *et al.*, 2012).

Raised brain weight and extravasation of fibrinogen from microvessels occurs in histopathologically confirmed paediatric CM, although these do not distinguish CM from fatal coma of other cause. Leakage is most often associated with vascular pathology such as haemorrhage, but fibrinogen is also seen in cerebral grey matter where haemorrhages are absent (Dorovini-Zis *et al.*, 2011). Focal loss of blood–brain barrier cell junction proteins (ZO1, occludin, vinculin) occurs adjacent to sequestration. The distribution of fibrinogen, IgG and C5b-9 in these cases did not indicate widespread leakage into brain tissue (Brown *et al.*, 2001).

2.4.4 Brain imaging

Consistent with reports of raised intracranial pressure in clinically defined paediatric CM, MRI in retinopathy-positive paediatric CM reveals moderate to severe brain swelling in 47% (57/120) of cases. This is significantly more common than in paediatric CM without retinopathy (7/32 cases, OR 3.2, 95% CI 1.3–8) (Potchen *et al.*, 2012).

Discrete lesions are seen in basal ganglia, thalamus, corpus callosum, and cerebral grey and white matter. All are significantly more frequent in retinopathy-positive CM than retinopathy-negative cases. Cortical abnormalities can be predominantly

frontal or posterior. Lesions do not respect arterial watersheds (Potchen *et al.*, 2012), but may reflect territories of venous drainage (Andeweg, 1996; Meder et al., 1994). Distribution of lesions according to venous territories is consistent with sequestration occurring primarily on the venous side of the microvasculature.

2.5 Manifestations of cerebral malaria in the paediatric retina

Several clinical (Lewallen *et al.*, 1999) and FA features of malarial retinopathy (Beare *et al.*, 2009) are illustrated in Figure 12. Standard images of all features are available in Harding et al., (2006).

Figure 12: The features of paediatric malarial retinopathy.
(A) Colour retinal image showing white-centred haemorrhages and retinal whitening extending from the macula into the temporal periphery (horizontal raphe). (B) A fluorescein angiogram shows severe capillary non-perfusion in the retinal periphery (marked in yellow). Capillary non-perfusion typically coincides with retinal whitening. (C) Leakage of fluorescein from retinal venules. (D) Vessel mottling can be seen on a magnified fluorescein angiogram image. Images are from different subjects.

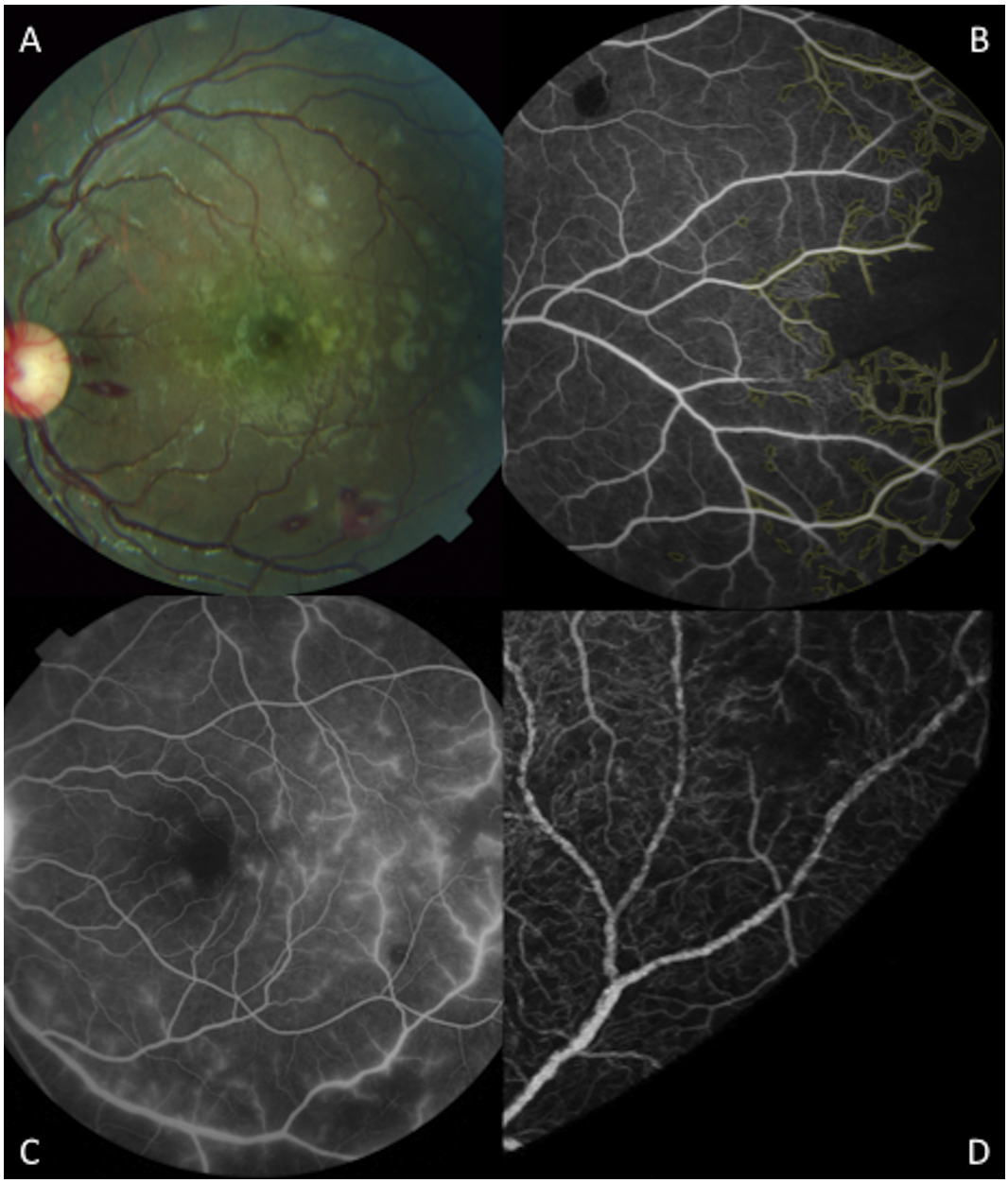

2.5.1 Sequestration in retinal vessels

Sequestration is distributed unevenly in capillaries and the margins of larger retinal vessels. Sequestration and vessel discolouration tend to occur at vascular branch points (Lewallen *et al.*, 2000), where greater turbulence exists to disrupt laminar flow (Nagaoka and Yoshida, 2006). It has been proposed that de-haemoglobinization of parasitised erythrocytes is responsible for the clinically observed white or orange discolouration of retinal vessels seen in paediatric cerebral malaria (Lewallen *et al.*, 2000). Haemozoin could also contribute to orange discolouration. Retinal vessels, particularly venules, can have a mottled appearance on FA, which may represent sequestration (Beare *et al.*, 2009). The discolouration and mottled appearance of retinal vessels in malarial retinopathy appears to be pathognomonic for paediatric severe malaria, but is reported in severe malarial anaemia as well as CM (Beare et al., 2004).

2.5.2 Retinal vessel leakage

Fluorescein leakage is seen in ~40% of cases with malarial retinopathy and indicates blood–retinal barrier disruption. It does not co-localize with vessel mottling (Beare *et al.*, 2009). White et al. (2009) reported leakage of fibrinogen from retinal vessels in 31% (11/35) of cases with CM versus 7% (2/29) coma of other cause. Leakage was not reported in terms of vessel type, but FA imaging suggests that leaking is predominantly from venules (Beare *et al.*, 2009) (Figure 12). Again, this is consistent with CM pathogenesis centring on capillaries and post-capillary venules.

2.5.3 Retinal whitening

Retinal whitening appears as discrete areas of pale discolouration of the retina (Figure 12A), which correspond approximately to areas of CNP seen on FA. Retinal whitening and CNP seem to occur earliest and most severely in watershed regions such as the margin of the foveal avascular zone, horizontal raphe and retinal peripheries. In contrast to the scattered geometric lesions seen in the macula, whitening and CNP in the retinal periphery can occur in large tide-mark

distributions that cut across arterioles and venules of varying sizes (Beare *et al.*, 2009) (Figure 12B).

Whitening is likely to be caused by oncotic cell swelling in response to reduced perfusion (Beare *et al.*, 2009). Other possible mechanisms include metabolic steal by large numbers of parasites (Hero *et al.*, 1997), and occlusion caused by micro thrombi (White *et al.*, 2009). These theories are not mutually exclusive.

Areas of pale retinal discolouration are seen in other retinal conditions including arterial occlusion, venous occlusion (Browning, 2004), and Purtscher's retinopathy (Agrawal and McKibbin, 2006). Mild whitening has also been reported in paediatric severe malaria without coma (Beare et al., 2004; Burton et al., 2004). The severity and pattern of whitening seen in malarial retinopathy—around the fovea and extending into the horizontal raphe—appears to be specific to CM. Whitening in retinal vein occlusion is associated with swelling of the inner nuclear and outer plexiform layers of the retina (Sarda *et al.*, 2011). In paediatric CM there is a significant inverse correlation between electroretinographic cone b-wave amplitude and severity of retinal whitening (Lochhead *et al.*, 2010), indicating dysfunction of bipolar cells in the inner nuclear layer. The inner nuclear and outer plexiform layers are supplied by the deep capillary plexus, which forms the superficial half of a watershed with the underlying choriocapillaris (McLeod, 2010). This suggests that patterns of retinal whitening in CM may correspond to venous congestion in areas with limited collateral drainage as well as high metabolic demand.

2.5.4 Retinal haemorrhages

The haemorrhages of malarial retinopathy are often white-centred. Retinal vessel thrombi are more common in fatal paediatric CM than in coma of other cause. Micro thrombi are sometimes associated with haemorrhage, but often occur independently (White *et al.*, 2009). White-centred haemorrhages also occur in bacterial endocarditis, leukaemia, and a range of other conditions in which capillary fragility and elevated venous pressure seem to be common factors (Duane *et al.*, 1980; Ling and James, 1998; Zehetner and Bechrakis, 2011). Retinal haemorrhages have also been observed in children with severe malarial

anaemia without profound coma, and severity seems to increase with decreasing consciousness (Beare et al., 2004). In paediatric CM, the number of retinal haemorrhages at autopsy correlates significantly with the number of brain haemorrhages (White *et al.*, 2001). Retinal haemorrhages usually involve the inner retinal layers, but can extend to all layers. Different locations within the retina give rise to the appearance of blot or flame haemorrhages. Sub retinal haemorrhage with secondary retinal detachment is seen with unusually large retinal haemorrhages (White *et al.*, 2009).

2.6 Manifestations of cerebral malaria: paediatric retina and brain compared

Several similarities exist between paediatric retina and brain vascular pathology (Table 4).

Microvascular sequestration is a defining histopathological feature of paediatric CM in both retina and brain, and is thought to be the principal cause of tissue injury in both sites. Whenever brain and retinal histology has been compared in cases of fatal paediatric CM, brain sequestration is always associated with retinal sequestration (Lewallen *et al.*, 2000; White *et al.*, 2009). On the other hand retinal vessel discolouration is not seen in fatal coma of other cause, implying absence of retinal sequestration in these cases (White *et al.*, 2009). Recent work found a significant association between the intensity of sequestration in retina and brain, and between the severity of retinopathy and retinal sequestration (Barrera *et al.*, 2015). Sequestration appears to be patchy within microvascular networks of each organ, but is more widespread in brain than retina.

Table 4: Manifestations of cerebral malaria in the retina and brain

Feature	Characteristic	Paediatric retina	Paediatric brain	Adult brain
Sequestration	Frequency	Always present in fatal cerebral malaria (Lewallen *et al.*, 2000). Unclear if absent in fatal coma of other cause or severe malarial anaemia	Always present in fatal cerebral malaria, and absent in fatal coma of other cause (Dorovini-Zis *et al.*, 2011; Taylor *et al.*, 2004) Commonly associated with sequestered leukocytes (Armah *et al.*, 2005; Brown *et al.*, 2001)	Always present in fatal cerebral malaria (MacPherson *et al.*, 1985; Oo *et al.*, 1987; Pongponratn *et al.*, 1991; Sein *et al.*, 1993) In cerebral malaria density is greater in brain than other organs (MacPherson *et al.*, 1985; Pongponratn *et al.*, 1991) Significant sequestration may be present in fatal non-cerebral malaria (MacPherson *et al.*, 1985; Silamut *et al.*, 1999) The percentage of vessels with sequestration is greater in cerebral malaria than non-cerebral malaria (Ponsford *et al.*, 2012)
	Location	Patchy distribution within capillary network (Lewallen *et al.*, 2000) Variation between retinal regions not yet defined	Most microvessels, and the margins of pial and larger vessels (Dorovini-Zis *et al.*, 2011) Grey and white matter of cerebrum, subcortex, brainstem and cerebellum (Armah *et al.*, 2005; Dorovini-Zis *et al.*, 2011)	Occurs in capillaries, venules, and very occasional arterioles (MacPherson *et al.*, 1985) Occurs in grey and white matter, but most dense in cerebral white matter (Nagatake *et al.*, 1992) Density reduces from cerebrum to cerebellum to brainstem (Pongponratn *et*

Feature	Characteristic	Paediatric retina	Paediatric brain	Adult brain
				al., 2003) Density greater in cerebellum than cerebrum (Sein *et al.*, 1993)
	Vessels involved	Capillaries and margins of larger vessels (Lewallen *et al.*, 2000) Vessel discolouration affects capillaries, venules, and arterioles (personal observation)	Occurs in brain microvessels, pial and larger vessels (Dorovini-Zis *et al.*, 2011)	Predominant site is the capillary bed, but also occurs in larger pial and subarachnoid vessels (Spitz, 1946) Uncommon in arterioles (MacPherson *et al.*, 1985)
Haemorrhages	Type	White-centred, blot (White *et al.*, 2001) Parasitised erythrocytes rarely seen outside vessel (White *et al.*, 2001)	Ring (Dorovini-Zis *et al.*, 2011) Parasitised erythrocytes rarely seen outside vessel (Dorovini-Zis *et al.*, 2011; White *et al.*, 2001)	Ring, perivascular (Nagatake *et al.*, 1992; Sein *et al.*, 1993; Spitz, 1946; Turner, 1997) Parasitised erythrocytes are seen outside vessel (Sein *et al.*, 1993; Turner, 1997)
	Frequency	Gross haemorrhages present in 78% fatal cerebral malaria, 7% fatal coma of other cause (White *et al.*, 2009)	Any type present in 80% fatal cerebral malaria (Dorovini-Zis *et al.*, 2011)	Ring haemorrhages present in up to 30% of cases of fatal cerebral malaria (Spitz, 1946) No significant difference in haemorrhage frequency between cerebral malaria (~60% of cases) and non-cerebral malaria (~40% of cases) (Medana *et al.*, 2011)
	Location	All retinal quadrants. Usually restricted to inner retinal layers, with extension to subretinal haemorrhage in severe cases (White *et al.*, 2009)	Common in white matter, rare in grey matter except in the cerebellum (Dorovini-Zis *et al.*, 2011; White *et al.*, 2001)	Usually occur in cerebral white matter; also reported in pons, medulla, cerebellum, and cortical grey matter (Nagatake *et al.*, 1992; Sein *et al.*, 1993; Spitz, 1946; Turner, 1997)

Feature	Characteristic	Paediatric retina	Paediatric brain	Adult brain
				No difference in haemorrhage frequency between cortex, diencephalon, and brainstem (Medana *et al.*, 2011)
Vessel leakage	Type	Fibrinogen leakage along vessels with and without associated haemorrhage (White *et al.*, 2009)	Fibrinogen leakage often associated with haemorrhage, can be independent of haemorrhage (Dorovini-Zis *et al.*, 2011)	Rarefaction of the perivascular space, perivascular pools of proteinaceous material, vacuolar parenchymal oedema, oedema between fibres of white matter tracts, fluid-filled spaces between myelin fibres. No difference between fatal cerebral and non-cerebral malaria (Medana *et al.*, 2011)
	Frequency	Fibrinogen leakage in 31 % cases fatal cerebral malaria, 7% fatal coma of other cause (White *et al.*, 2009) Average (standard deviation) number of foci is 1.2 (2.6) in fatal cerebral malaria and 0.21 (1.1) in coma of other cause (White *et al.*, 2009)	Unclear how many cases of fatal cerebral malaria have leakage of any type Leakage greater in white than grey matter (associated with haemorrhages) (Dorovini-Zis *et al.*, 2011)	At least one type of oedema present in all cases of both cerebral and non cerebral malaria (Medana *et al.*, 2011) Oedema between white matter tract fibres is most common in: brainstem > diencephalon > cortex (Medana *et al.*, 2011)
	Location/ vessels involved	Associated with vessels but not defined in terms of retinal quadrants or vessel type (White *et al.*, 2009) Angiographic fluorescein leakage predominantly affects venules (Beare *et al.*, 2009)	Cerebral white and grey matter, subcortex, brainstem and cerebellum (Dorovini-Zis *et al.*, 2011)	Brainstem, diencephalon, cerebral cortex (Medana *et al.*, 2011)
Regions vulnerable to presumed ischaemia on		Retinal whitening and capillary non-perfusion appears to be especially	Regions where MRI brain signal changes distinguish between retinopathy-positive and	Regions reported to be involved: Brain stem, thalamus, cerebellum, corpus

Feature	Characteristic	Paediatric retina	Paediatric brain	Adult brain
imaging		prominent at the foveal avascular zone, horizontal raphe, and retinal periphery. All are watershed regions (Beare *et al.*, 2009)	negative CM (highest to lowest OR): Basal ganglia, corpus callosum, cerebral cortex, thalamus, cerebral white matter, posterior fossa (Potchen *et al.*, 2012)	callosum, cerebral white matter (Rasalkar *et al.*, 2011; Yadav *et al.*, 2008)

Whereas the density of sequestration in paediatric CM appears to be roughly equal between cerebral white and grey matter, cerebellum and brainstem (Armah *et al.*, 2005), the distribution and density of sequestration in the eye as a whole has not yet been formally evaluated. Both the percentage of parasitised vessels and the intensity of sequestration are higher in the retina than in the adjacent choroid (Barrera *et al.*, 2015).

The intensity of tissue specific sequestration within the eye might be explained by the distribution of endothelial receptors in different vascular beds. ICAM1 is constitutively expressed by retinal vascular and choroidal endothelium at low levels (Duguid *et al.*, 1992), and in the choriocapillaris expression is greatest at the macula (Mullins *et al.*, 2006). Expression of retinal endothelial ICAM1 increases in infectious (Toxoplasma gondii) (Smith *et al.*, 2007) and non-communicable diseases (Funatsu *et al.*, 2005), and in response to vascular endothelial growth factor (Lu *et al.*, 1999).

Physiological differences between retinal and choroidal vascular beds may also influence sequestration, as they differ significantly in terms of capillary width, blood flow volume and oxygen extraction. In isolated rat microvessels sequestration density is inversely related to venule diameter, suggesting flow velocity and shear rate may be important (Kaul *et al.*, 1991). Several authors suggest that microvascular architecture may contribute to differential sequestration rates in various organs (Nagatake *et al.*, 1992; Sein *et al.*, 1993; Spitz, 1946).

White-centred and ring haemorrhages are common in the retina and brain, respectively. Presumably ring haemorrhages are spherical before histopathological sectioning, which like retinal imaging, provides a two dimensional view of the observed tissue. The haemorrhages of paediatric CM generally affect inner retinal layers and cerebral white matter. In both sites long vessel segments are present, and these may be important in determining the localization of haemorrhages (Spitz, 1946). Clinically, haemorrhages in malarial retinopathy may occur without white centres (i.e. blot haemorrhages), or may develop white centres over time. At histopathology retinal haemorrhages often appear similar to ring haemorrhages—

centred on a small thrombosed vessel with a halo of non-parasitised erythrocytes (White *et al.*, 2009). Variations in appearance result from the histological section and differences between retinal and cerebral cellular architecture.

Some areas of retina and brain appear to be affected more frequently by perfusion abnormalities than others. In the retina, FA imaging suggests that watershed regions such as the horizontal raphe and margin of the foveal avascular zone are especially susceptible to CNP (Beare *et al.*, 2009). In the brain, patterns of T2 and diffusion-weighted imaging signal changes on MRI (Potchen *et al.*, 2012) could represent boundaries of venous territories. Analysis of venous watershed regions in retina and brain may identify vessel properties that are important for the microvascular pathogenesis of CM.

2.7 Haemorheology and neurovascular manifestations of cerebral malaria

Blood flow characteristics such as viscosity, haematocrit, and shear stress are relevant to paediatric CM because they are likely to influence both the delivery of parasitised erythrocytes to organ regions and the propensity for adherence to the endothelium and other erythrocytes. Shear stress strongly influences endothelial binding, for both leucocytes (Crane and Liversidge, 2008; Xu *et al.*, 2002) and parasitised erythrocytes (Fedosov, Caswell and Karniadakis, 2011), and is related to the deformability of parasitised and uninfected erythrocytes in severe adult falciparum malaria. Admission erythrocyte deformability is reduced in adult severe malaria compared with uncomplicated cases, and is associated with mortality (Dondorp *et al.*, 1997). Platelet mediated auto-agglutination (clumping) of erythrocytes is also associated with severity of malaria in adults (Chotivanich *et al.*, 2004; Pain *et al.*, 2001).

The movement of blood in small vessels is complex and depends on the character of blood and the vascular network it flows through. Unlike water (a Newtonian fluid), blood is a suspension of cells in plasma, and is an example of a shear thinning non-Newtonian fluid. The movement of blood in small vessels therefore varies with viscosity, haematocrit, blood cell deformability, aggregation and

interaction with the endothelium (reviewed in: Baskurt and Meiselman, 2003; Lipowsky, 2005; Popel and Johnson, 2005; Schmid-Schönbein, 1999).

Blood viscosity decreases with increasing shear rate (Figure 13), and as shear rate is related to blood velocity and vessel width, blood moves more easily at greater velocities and in vessels with narrower calibre (Baskurt and Meiselman, 2003). Erythrocyte aggregation and deformation are major determinants of shear thinning (Popel and Johnson, 2005), and both are altered in *P. falciparum* infection (Chotivanich *et al.*, 2004; Dondorp *et al.*, 1997; Fedosov, Caswell and Karniadakis, 2011; Pain *et al.*, 2001). Erythrocyte stiffness is particularly important under high shear conditions, whereas non-streamlined aggregates increase resistance at low shear rates that are insufficient to break bonds between erythrocytes (Baskurt and Meiselman, 2003). Consistent with this, experimentally induced rosetting of *P. falciparum* infected erythrocytes is seen in venules, but not arterioles where shear rates are likely to be higher (Kaul *et al.*, 1991). Besides shear rate, viscosity depends on the volume fraction of erythrocytes in plasma (i.e. haematocrit). Rising haematocrit is associated with an exponential increase in viscosity.

Figure 13: Flow characteristics of blood.
(A) Illustration of shear rate in parabolic (laminar) flow. Shear rate is a function (dy / dr) of flow velocity (y) and vessel width (r). At a given velocity shear rate is greater in narrow vessels than wide vessels. Blood is a shear thinning fluid, meaning that blood viscosity decreases with increasing shear rate. Shear stress is the product of viscosity and shear rate. (B) Phase separation with heterogeneous haematocrit in vessel branches. Variable haematocrit arises when erythrocytes are distributed unevenly as a result of phase separation. Erythrocytes flow in a central column surrounded by a cuff of plasma. The proportion of erythrocytes to plasma in vessel branches depends on branching angle, daughter vessel width, and daughter vessel flow rate. Daughter vessels branching at near 90° have a relatively high proportion of plasma and therefore lower haematocrit than the parent vessel.

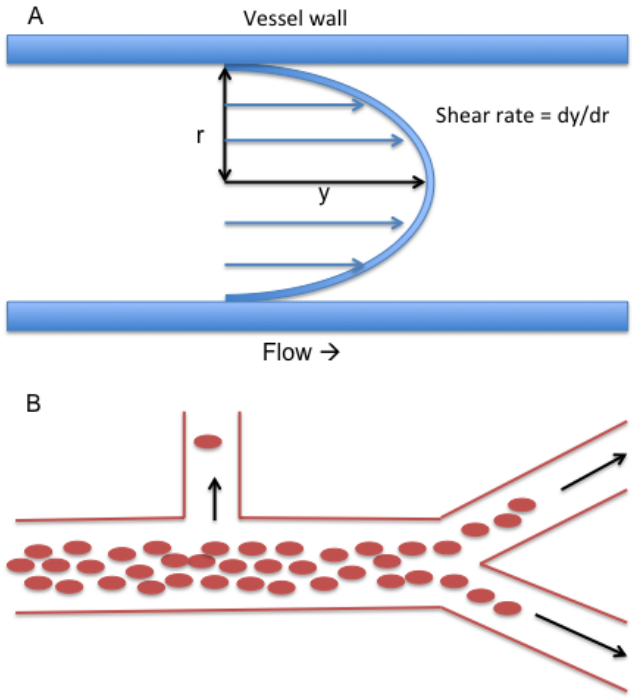

2.7.1 Variable viscosity

Under normal conditions blood viscosity decreases as vessel width reduces. This phenomenon is known as the Fåhræus-Lindqvist effect, and is thought to result from migration of erythrocytes away from the vessel wall and into a central column—reducing resistance to flow by creating a lubricating cell-depleted layer next to the endothelium. Apparent viscosity reaches a minimum at an internal diameter of 5–7 μm (close to erythrocyte dimensions: ~6–8 μm diameter, 2 μm thick) after which it rises steeply (Popel and Johnson, 2005). Apparent viscosity is greater *in vivo* than in equivalent glass tubes of the same internal diameter, and this is thought to result from resistance to flow produced by an endothelial lining (the endothelial surface layer or glycocalyx) (Popel and Johnson, 2005; Pries *et al.*, 2000). Protrusion of endothelial cell pseudopods into the vessel lumen during endothelial activation can almost double capillary resistance to flow (Schmid-Schönbein, 1999), and sequestered erythrocytes, or associated inflammation, may produce a similar effect.

Erythrocytes are by far the most common suspended component of blood, and so under physiological conditions local haematocrit and shear rate are the major determinants of apparent viscosity in microvessels (Lipowsky, 2005). Leucocytes make up a relatively small fraction of total blood volume (~1/600). Nonetheless, as a typical inactivated neutrophil is ~8 μm wide, temporary obstruction of capillaries (internal diameter 4–8 μm) is common, and leucocytes can increase resistance to blood flow within an organ even without binding to endothelium, depending on leucocyte count, haematocrit and the capillary length of the organ involved. The effect is greater in organs with long capillary segments than in those with short segments such as the pulmonary circulation, and probably results from reductions in capillary erythrocyte velocity to match that of the slower leucocytes (Schmid-Schönbein, 1999). Leukocytes, which are relatively large and stiff, also strip the endothelial surface layer from capillary endothelium as they pass. This effect may persist into post-capillary venules and result in increased exposure of endothelial receptors such as ICAM1 (Popel and Johnson, 2005), presumably facilitating endothelial binding and subsequent migration through the vessel wall. Parasitised erythrocytes are similar to leucocytes in that they are relatively stiff and bind to ICAM1 (Fedosov, Caswell, Suresh, *et al.*, 2011; Moxon *et al.*, 2011),

and this may contribute to microvascular congestion, while exposure of capillary and post-capillary endothelial receptors as a result of stripping of the endothelial surface layer may be an important step in sequestration. Post-capillary venules may favour sequestration because shear stress is lower than in arterioles (Nagaoka and Yoshida, 2006). Microvascular resistance is likely to be raised by high proportions of inflexible erythrocytes, sequestration and auto-agglutination, leading to reduced velocity, increased viscosity, and lower shear stress. Increased viscosity can have a dramatic effect on the retinal circulation, and ultimately lead to venous stasis or occlusion (Pournaras *et al.*, 2008). Congestion and blockage of venules and capillaries secondary to high blood viscosity is therefore consistent with clinical signs of malarial retinopathy such as haemorrhage and capillary non-perfusion.

2.7.2 Variable haematocrit

Local microvascular haematocrit is not the same as systemic haematocrit. The haematocrit of blood flowing into a small tube is significantly less than that measured in the static effluent exiting the tube. This is known as the Fåhræus effect, and—as with the Fåhraeus–Lindqvist effect—is thought to result from the tendency of flowing erythrocytes to migrate axially to form a central column (Lipowsky, 2005; Popel and Johnson, 2005).

Microvessel haematocrit is not distributed evenly between vessels. When blood meets a bifurcation there is unequal division of erythrocytes into the daughter vessels. Distribution depends on parent vessel haematocrit, branching angle and daughter vessel flow rates. Flow rate is especially influential. This effect is known as phase separation and, again, is thought to result from the axial position of erythrocytes (Figure 13). As a result microvessel haematocrit is heterogeneous across a network (Hirsch *et al.*, 2012; Popel and Johnson, 2005), and can show great variation (Ganesan *et al.*, 2010; Guibert *et al.*, 2010). As haematocrit is a major determinant of blood viscosity, the concept of phase separation and heterogeneous haematocrit within microvascular networks is crucial to understanding the possible role of haemorheological factors in the retinal and cerebral manifestations of retinopathy-positive paediatric CM.

2.7.3 Computational models of blood flow

The close relationship between haemorheology and microvascular architecture means that computational models of flow parameters can be extended from single vessels to entire networks. Models exist for mouse retina (Ganesan *et al.*, 2010) and primate cerebral cortex (Guibert *et al.*, 2010). The mouse model predicts high regional haematocrit in the retinal periphery, but varying up to a factor of four, likely owing to phase separation. Predicted viscosity is greatest in capillaries and peri-capillary vessels, but can also vary significantly (by a factor of three) owing to heterogeneous local haematocrit. Shear stress is lower in venules than arterioles of the same size, and again reduces towards the peripheral retina for vessels of a given width (Ganesan *et al.*, 2010). Distribution of more erythrocytes to the retinal periphery than to the posterior pole may be important physiologically, because oxygen delivery depends on blood viscosity as well as on haematocrit (Cho and Cho, 2011). It may be that the macula benefits from greater oxygen transfer as a result of lower regional viscosity compared to the retinal periphery.

Estimations from the mouse are unlikely to correspond exactly to the human retina. However, the haemorheological principles behind the model may help to explain some features of malarial retinopathy. For example the peripheral retina may develop large zones of CNP that cut across arterioles and venules, while macular CNP tends to affect smaller patches of capillaries (Beare *et al.*, 2009) (Figure 12B). This may be because greater parasite delivery to the periphery promotes occlusion of wider vessels, compared to the macula, which has higher metabolic demands but lower microvascular haematocrit.

2.7.4 The relationship between flow and microvascular networks in paediatric cerebral malaria

In summary, haemorheological factors may both influence and be influenced by *P. falciparum*. For example, organ regions with physiologically high microvascular viscosity and low shear stress may be especially susceptible to sequestration, while *P. falciparum*-associated erythrocyte stiffness, auto-agglutination and

sequestration are likely to increase viscosity. As well as factors arising from blood itself, predisposition of microvascular regions to high or low haematocrit and viscosity depends on vessel network architecture. The combination of physiological heterogeneity within microvascular networks, which is influenced by network architecture, and pathological derangements of blood movement caused by *P. falciparum*, may help to explain manifestations of CM in retina and brain. If so, common neurovascular network architecture could contribute to a biologically plausible rationale for inferring unseen cerebrovascular pathogenesis from the visible retina. Therefore I now compare retinal and cerebral microvasculature geometry and topology (Table 5).

Table 5: Vascular features that are likely to be important in CM pathogenesis

Area of comparison	Similarities / differences	Discussion
Vascular geometry	Similarities	First and second generation retinal arterioles are ~100μm wide (Nagaoka and Yoshida, 2006), deep white matter arterioles are 100 to 170μm wide (Nonaka *et al.*, 2003b), arterioles in the putamen are ~100 to 150μm wide (Nonaka et al., 1998). Retinal perifoveal capillaries are ~5.4μm wide (Wang *et al.*, 2011), cerebral grey matter capillaries are ~6.5μm wide (Lauwers *et al.*, 2008), capillaries in the putamen ~5 to 7μm wide (Wolfram-Gabel and Maillot, 1994). The largest retinal venules are 130μm to 150μm wide (Nagaoka and Yoshida, 2006), cerebral grey and white matter venules range up to 125μm (Duvernoy et al., 1981). Retina (Pournaras *et al.*, 2008), cerebral grey (Cassot *et al.*, 2010) and white matter (Nonaka *et al.*, 2003a) all have near 90° branches from relatively long straight trunks. Caudate and putamen have retrograde arteriolar branching. Basal ganglia venous branches join at right angles (Nonaka *et al.*, 1998).
	Differences	First generation retinal arterioles are ~100μm wide (Nagaoka and Yoshida, 2006), cerebral grey matter penetrating arterioles are 20 to 65μm wide (Duvernoy et al., 1981; Reina-de La Torre et al., 1998). The largest retinal venules are 130mm to 150mm wide (Nagaoka and Yoshida, 2006) (Nagaoka and Yoshida, 2006), principal veins in the putamen can be up to ~500μm wide (Wolfram-Gabel and Maillot, 1994). Retinal arteriolar and venular length between bifurcations is similar to the length of entire penetrating arterioles or venules in grey matter
Vascular topology	Similarities	Strahler order in the macula is ~3.5, in cerebral grey matter it is 3 to 5 (Cassot *et al.*, 2010; Yu *et al.*, 2010). Capillary density immediately around the human foveal avascular zone is similar to primate cortex (Tam *et al.*, 2010)
	Differences	Human macular superficial and deep plexus have density 40% and 20% per unit *area*, while human grey matter has density ~1.5 to 2% brain *volume* (Cassot *et al.*, 2006; Lauwers *et al.*, 2008; Mendis *et al.*, 2010).

Area of comparison	Similarities / differences	Discussion
		Arteriole/venule ratio in retina is 1:1, in cerebral grey matter it is 2:1, in basal ganglia it is up to 5:1 (Cassot *et al.*, 2010; Wolfram-Gabel and Maillot, 1994)
Watershed regions	Similarities	Both brain and retina have arterial and venous watershed regions. Insufficient venous outflow can cause oedema, haemorrhage, and ischaemia in brain (Teksam *et al.*, 2008) and retina (Browning, 2004)
	Differences	Retinal arteriolar and venular watersheds tend to have the same distribution, e.g. the edge of the foveal avascular zone, and horizontal raphe. In the brain arteriolar and venular watersheds cover different anatomical territories (Miyawaki and Statland, 2003a, 2003b). In the retina venous drainage almost always follows arterioles. Variation in cerebral venous drainage is common in children (Widjaja and Griffiths, 2004)
Metabolic demand	Similarities	Metabolic demand per unit tissue for retina and brain is comparable, and higher than any other organ (Wong-Riley, 2010). Both retina and brain depend on a constant supply of oxygen and glucose (Mckenna *et al.*, 2006). Both inner retina and brain vessels have an arterio-venous O_2 difference of ~40-50% (McLeod, 2010; Seifert and Secher, 2011). Retinal metabolism is greatest around the fovea and in retinal layers rich in synapses (Birol *et al.*, 2007; Yu and Cringle, 2001). Cerebral metabolism is greater in grey matter than white matter (Sokoloff, 2003)
	Differences	Cerebral metabolic demand peaks in childhood. $CMRO_2$ is 4.3 to 6.2ml O_2/100g/min (3 to 6 years, whole brain) (Kennedy and Sokoloff, 1957). CMRgluc is >30mmol/100g/min (1 to 2 years, calcarine cortex, transverse temporal cortex, lenticular nuclei) (Chugani *et al.*, 1987). It is not clear if retinal metabolic demand changes significantly after birth
Blood flow	Similarities	Both retina and brain receive high blood flow volume per unit tissue

Area of comparison	Similarities / differences	Discussion
	Differences	Inner retinal blood flow volume is roughly half that of the adult brain (25:50 ml/100g/min, inner retinal circulation to total brain) (Kety and Schmidt, 1948; Madsen *et al.*, 1993; Pournaras *et al.*, 2008; Sokoloff, 2003). Cerebral blood flow is much higher in early childhood compared to adulthood (130ml/100g/min, age 2 to 4 years) (Wintermark et al., 2004). It is not clear if retinal blood flow undergoes similar changes in childhood. Paediatric peak systolic cerebral blood flow velocity is ~95cm/sec in the middle cerebral artery and ~4.5cm/sec in the central retinal artery (Geeraerts *et al.*, 2005)

$CMRO_2$ = Cerebral metabolic rate for oxygen

CMRgluc = Cerebral metabolic rate for glucose

2.8 The retina

2.8.1 Retinal microvasculature

The retina has a dual blood supply. The inner retinal circulation supplies the visible inner surface of the retina. The choroidal circulation, lying between the retinal pigment epithelium and sclera, supplies the outer retina, including the photoreceptors (Hayreh, 2010a; McLeod, 2010). Retinal and choroidal circulations have major differences in anatomy and physiology. The choroid is made up of an outer layer of large vessels (Haller's layer), a middle layer of smaller vessels (Satler's layer), and an innermost layer of capillaries (the choriocapillaris). The range of capillary width in the choriocapillaris is large compared to inner retina (3–50 μm versus 3.5–6 μm) (Anand-Apte and Hollyfield, 2010). Although anatomical studies classically suggested that the choroid has multiple anastomoses, *in vivo* functional imaging reveals end-arterial segmental perfusion with associated watershed regions (Hayreh, 1990, 2010a). In the macaque, choroidal blood flow volume is roughly 20 times greater than in the retina, and nine times greater than cerebral grey matter, per weight of tissue (Alm and Bill, 1973; Hayreh, 2010a). Wide capillaries and high volumetric flow rate may help to explain why the choriocapillaris is apparently less susceptible to sequestration than inner retinal vessels in fatal paediatric CM (Barrera *et al.*, 2015).

2.8.2 Geometry of the inner retinal circulation

The central retinal artery usually divides to produce four branches that extend from the optic disc into the four quadrants of the retina (Figure 14). Further branching is either at right angles to the main trunk or dichotomous (i.e. two daughter branches at approximately right angles to each other) (Berntson, 1995; Pournaras *et al.*, 2008).

Figure 14: Retinal vascular anatomy.
Seen on fluorescein angiography during venous filling, and showing arteriole and venule segments from the optic disc, the foveal avascular zone at the centre of the macula, and the horizontal raphe.

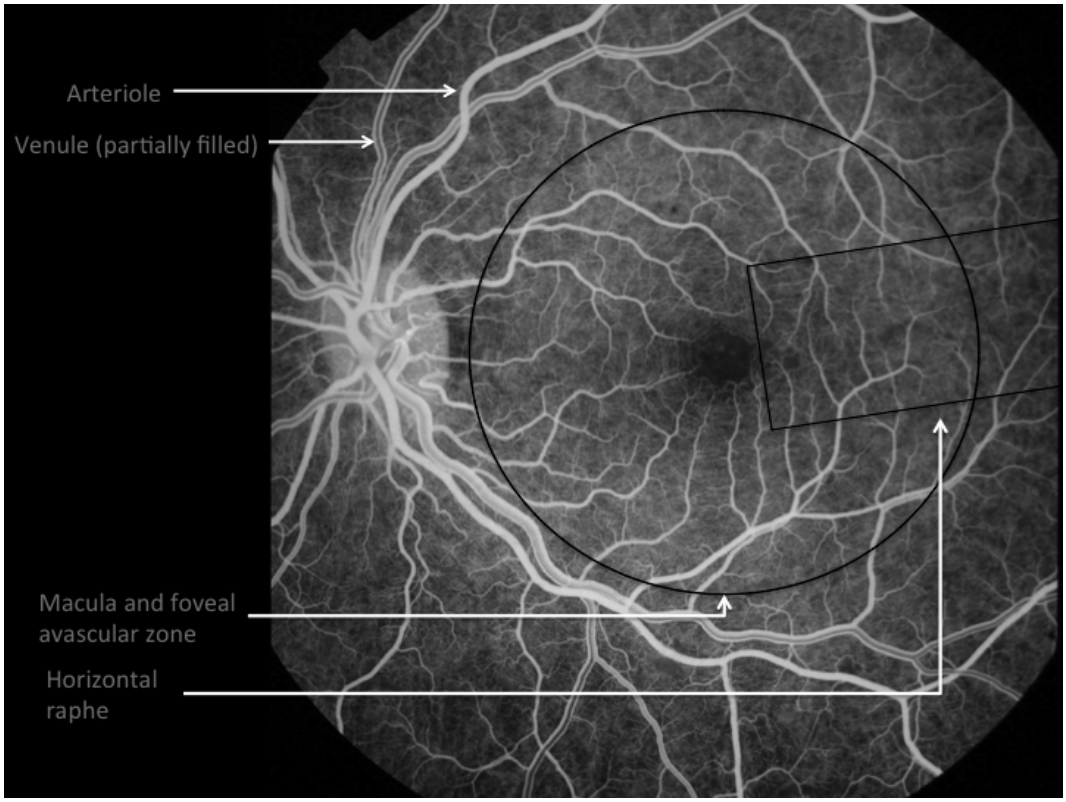

In healthy adults the central retinal artery is ~160 µm wide (Dorner *et al.*, 2002). First and second generation arterioles are ~100 µm wide, whereas first and second-generation venules are ~150 and 130 µm, respectively (Nagaoka and Yoshida, 2006). Retinal arteriolar cross sectional profiles tend to be circular, whereas venule lumens may be circular but tend to collapse (Feke *et al.*, 1989).

Vascular segments extend close to the anterior limit of the retina, leaving a peripheral avascular zone ~1.5 mm wide. Each terminal arteriole gives rise to a network of 10 to 20 interconnected capillaries (Hayreh, 2010b). Capillary arrangement varies between retinal locations. In general there are two layers: a superficial plexus between the nerve fibre layer and ganglion cell layer, and a deep plexus between the inner nuclear and outer plexiform layers (McLeod, 2010). Only one layer exists adjacent to the fovea and at the far periphery. The

peripheral network is also relatively sparse. In the peripapillary region a third capillary layer extends radially from the optic disc for a distance of up to several millimetres (Hayreh, 2010b).

Capillaries are absent at the foveal avascular zone, and adjacent to retinal arterioles (Figure 14). The foveal avascular zone is supplied by diffusion from the underlying choriocapillaris and in adults is ~400 μm wide and 350 μm high (Yu *et al.*, 2010). Periarteriolar capillary free zones are between 50 and 120 μm wide (Kuwabara and Cogan, 1960). They reflect the combined radius of oxygen diffusion from both artery segment and adjacent capillaries. Capillary-free zones are narrower next to venules, reflecting the high oxygen extraction (~50%) of the retinal circulation and reducing oxygen diffusion radius from post-capillary venules (McLeod, 2010).

Draining venules rise obliquely from the capillary plexuses to the nerve fibre layer and combine to form vascular patterns similar to retinal arterioles. Venules are generally slightly wider than arterioles, with shorter distances between bifurcations, narrower branching angles and less tortuosity (Hughes *et al.*, 2009). Postcapillary venules interdigitate with precapillary arterioles in an alternating pattern (Bek and Jensen, 1993); this can become strikingly apparent in malarial retinopathy when leakage affects venules more than arterioles (Beare *et al.*, 2009) (Figure 12C). Venules follow arterioles to converge at the optic disc, where they drain into the central retinal vein. Venous blood from the inner retina then flows into the cavernous sinus, either directly or by way of the superior ophthalmic vein. There are no valves (Hayreh, 2010b; Semmer *et al.*, 2010).

Some information exists about vessel geometry in children (Table 6). Paediatric central retinal artery equivalent (CRAE) and central retinal vein equivalent (CRVE) are calculated values based on the widths of first generation retinal vessels, and seem to be similar to adult values. Arteriolar bifurcation angle (the angle subtended between two branches from a parent arteriole) seems to be greater in children than adults, as does arteriolar length to diameter ratio. It is not clear how these differences might affect sequestration.

Table 6: Retinal vessel geometry in children and adults

Measurement	Children				Adults			
	Age	n	Value	Reference	Age	n	Value	Reference
CRAE 0.5-1.0 DD from optic disc margin	7-9y	760	156.4 (155.4–157.3)µm; mean (95%CI)	(Cheung *et al.*, 2007)	43-86y	4231	165.29 (15.42) (98.1-223.4)µm; mean (SD) (range)	(Lee *et al.*, 2004)
	9y	266	168.41 (14.82)µm; mean (SD)	(Sun *et al.*, 2009)				
	4-6y	385	159.08µm (mean of groups)	(Li *et al.*, 2011)				
	6y	1612	163.2 (14.0)µm; mean (SD)	(Rochtchina *et al.*, 2008)				
	6y	1608	163.3-166.9µm (range)	(Taylor *et al.*, 2007)				
CRVE 0.5-1.0 DD from optic disc margin	7-9y	760	225.4 (224.1-226.8)µm; mean (95%CI)	(Cheung *et al.*, 2007)	43-86y	4231	242.08 (22.86) (165.1-352.9)µm; mean (SD) (range)	(Lee *et al.*, 2004)
	9y	266	247.48 (18.99)µm; mean (SD)	(Sun *et al.*, 2009)				
	4-6y	385	222.12µm (mean of groups)	(Li *et al.*, 2011)				
	6y	1612	227.3 (18.3)µm; mean (SD)	(Rochtchina *et al.*, 2008)				
	6y	1608	228.8-234.8µm (range)	(Taylor *et al.*, 2007)				
Arteriolar bifurcation angle	12y	263	78.63° (mean of groups)	(Tapp *et al.*, 2007)	45-75y	167	69.5° (64.5-78.3); median (range)	(Hughes *et al.*, 2009)
Arteriolar simple tortuosity	12y	263	0.025 (mean of groups)	(Tapp *et al.*, 2007)	45-75y	167	0.004 (0.0002-0.11); median (range)	(Hughes *et al.*, 2009)
Arteriolar LDR	12y	263	13.1 (mean of groups)	(Tapp *et al.*, 2007)	45-75y	167	9.8 (3.5); mean (SD)	(Hughes *et al.*, 2009)

2.8.3 The macula

The macula is a unique region within the CNS situated temporally to the optic disc and specialised for fine resolution colour vision. Several subregions exist within the macula, for which adult vessel topology has been described (Yu *et al.*, 2010). Macular arterioles and venules are paired, with an average of nine pairs converging radially towards the fovea. Only three pairs enter the fovea itself to supply the terminal capillary ring marking the edge of the foveal avascular zone. Macular capillaries arise at right angles from parent arterioles and venules (Yu *et al.*, 2010) — an arrangement consistent with significant phase separation and variation in viscosity. Mean perifoveal capillary width has been measured at 5.4 µm using ultra-high resolution optical coherence tomography (Wang *et al.*, 2011). This is slightly narrower than capillaries in post-mortem sections of human temporal cortex (6.5 µm) (Lauwers *et al.*, 2008).

2.8.4 The retinal periphery

At the far periphery arterioles form looping arcades with adjacent venules, which may also be traversed by bridging vessels. Trypsin digest reveals peripheral loops with a diameter greater than capillaries at the posterior pole (up to 30 µm versus 5 µm). This arrangement varies between quadrants within eyes, and between individuals (Spitznas and Bornfeld, 1977). If retinal haematocrit is indeed concentrated towards the periphery, these vessels may facilitate flow of blood with relatively higher viscosity than found at the macula. These vascular features are visible in FA images in paediatric subjects (Penman *et al.*, 1994), though the optical properties of the eye mean that appearances on FA are likely to be magnified compared to histopathology. In malarial retinopathy normal arteriovenous loops should not be confused with CNP in the far periphery.

2.8.5 Topology of inner retinal vessels

Topological measurements exist for the human macula and fovea. Using the generation number and Strahler taxonomy schemes, average macular branching generation for both arterioles and venules is ~11.5, and average Strahler vessel order is ~3.5. This indicates a high number of bifurcations from each arteriole and

venule within a relatively short vessel segment length (Yu *et al.*, 2010). Strahler order in human cerebral grey matter is 3 to 5 (Cassot *et al.*, 2010).

Macular capillary density 1500 μm from the centre of the foveal avascular zone is ~40% in the superficial capillary network and 20% in the deep network, calculated as percentage of sample area filled by vessel segments (Mendis *et al.*, 2010).

The relatively sparse capillary network encircling the foveal avascular zone has been quantified as total capillary length/sample area. Average density ranges from 30 to 34 mm/mm^2 (Tam *et al.*, 2010). Direct comparison of two dimensional retinal area with three dimensional brain volume is difficult, but capillary density in the human brain has been measured at ~250 mm/mm^3 (visual cortex) (Bell and Ball, 1985).

2.8.6 Watershed regions

Excepting arteriovenous loops in the far periphery, the absence of arterial, venous, and arteriovenous anastomoses means that there are several watershed zones in the inner retinal circulation (Figure 14). These exist between:

i. Terminal vessels of each of the four arcades, most notably the superior and inferior temporal branches where they form the horizontal raphe;
ii. Vessels of the retina and vessels of the ciliary body at the anterior limit of the retina; and
iii. The deep capillary plexus and choriocapillaris throughout the retina, because there is no communication between the inner retina and the choriocapillaris. As the foveal avascular zone is supplied solely by the choriocapillaris this watershed is demarcated clinically in central retinal artery occlusion as the edge of the classic ‘cherry red spot’.

It is important to note that arterial and venous watersheds in the retina are identical, because of pairing of arterioles and venules. This is not the case in the brain, where arterial and venous territories are different.

2.8.7 Retinal metabolism and blood flow

The retina is considered by many to be the most metabolically active tissue in the body (Kur *et al.*, 2012; Wong-Riley, 2010). High demands may put it at greater risk of ischaemia in CM. Perifoveal oxygen consumption in the dark-adapted macaque is 4.9 ml/100 g/min (Birol *et al.*, 2007). Retinal oxygen consumption in man is estimated at 9.7 ml O_2/100 ml retina/min (Anderson and Saltzman, 1964) or ~10 ml O_2/100 g retina/min (assuming retinal specific gravity of 1.0425) (Stefánsson *et al.*, 1987), compared with ~3 ml/100 g/min for brain (Kety and Schmidt, 1948; Madsen *et al.*, 1993; Sokoloff, 2003). In the macaque, retinal glucose consumption is amongst the highest in the CNS (Sperber and Bill, 1985). Estimates of energy expenditure based on ATP used per neuron suggest the human retina may consume ~11.75 mW/g, and the human brain ~10.5 mW/g (assuming retinal weight = 0.4 g, retinal energy = 4.7 mW; brain weight = 1400 g, brain energy = 14.6 W) (Sarpeshkar, 2010).

Only a small proportion of blood from the ophthalmic artery goes to the inner retinal circulation. The value often reported is ~4% (Pournaras *et al.*, 2008; Williamson and Harris, 1994). It is not clear if this figure is from human or animal studies, but for comparison Alm and Bill (1973) found that retinal flow in the macaque makes up ~3.3% of blood to the retina and uvea combined (~27/811 mg/min). Consequently, inner retinal blood flow volume is a small fraction of ocular flow, which is itself a small fraction of blood flow in the internal carotid artery.

In non-human mammals, the retinal layers with highest metabolic rate are the inner segments of the photoreceptors, the outer plexiform layer, and the deeper region of the inner plexiform layer (Yu and Cringle, 2001). Oxygen reaches these layers by diffusion from the choriocapillaris (photoreceptor inner segments), and deep capillary plexus (outer plexiform and deep inner plexiform layers) (McLeod, 2010). In the macaque, demand for oxygen is highest at the perifovea (Birol *et al.*, 2007), and is likely to decrease towards the periphery where photoreceptor density is substantially lower (Jonas *et al.*, 1992). Patterns of metabolic demand may influence the susceptibility of neuronal tissue to the effects of sequestration, and

resulting manifestations of malarial retinopathy. Retinal whitening is common in the highly metabolically active perifovea.

Measurements of human mean blood flow volume in the inner retinal circulation have been made using laser Doppler flowmetry, and vary between studies from ~30 to 80 µl/min/retina (reviewed in Pournaras et al., 2008), which is ~9 to 25 µl/100 mg/min, assuming a human retinal weight of 326 mg (Feke *et al.*, 1989). The wide range may result from methodological differences. For comparison, inner retinal blood flow in the macaque, measured by radioactive microspheres, is ~18 µl/100 mg/min (assuming specific gravity of blood = 1.06 and macaque retinal weight of 128 mg) (Alm and Bill, 1973; Feke *et al.*, 1989).

In humans retinal blood flow volume is likely to be approximately half that of the brain, by tissue weight (i.e. 25:50 ml/100 g/min, inner retinal circulation to total brain) (Pournaras *et al.*, 2008; Sokoloff, 2003).

Mean perifoveal capillary flow velocity ranges from 1.37 to 3.3 mm/s. Leucocyte movement is pulsatile, and velocity in perifoveal vessels 7–11 µm wide is ~1.4 mm/s (Pournaras *et al.*, 2008). Rather than passing equally through all capillary segments perifoveal leucocytes seem to follow preferred pathways (Tam *et al.*, 2011). Similar patterns may exist for the movement of parasitised erythrocytes.

Estimated shear stress in healthy adults is highest in first generation arterioles (mean 54.0 dyne/cm2), 20% lower in second-generation arterioles, and 50% lower in both first and second-generation venules (Nagaoka and Yoshida, 2006; Nagaoka *et al.*, 2009).

2.9 The brain

The circulation of the brain is substantially more complex than that of the retina. I give a brief overview before focusing in more detail on three brain areas typically involved in acute paediatric retinopathy-positive CM: the basal ganglia, cerebral grey matter and cerebral white matter. All are affected significantly more often in children with retinopathy-positive CM than in paediatric patients with CM without retinopathy (Potchen *et al.*, 2012). Retinopathy could therefore reasonably be associated with vascular disease processes in these areas, if microvascular characteristics are similar in both organs.

2.9.1 Cerebral vasculature architecture and watershed regions

Carotid and basilar arteries supply the variably anastomotic Circle of Willis, which sends off branches including the anterior, middle and posterior cerebral arteries. Arterial territories are exclusive and vary between individuals (Miyawaki and Statland, 2003a). As in the retina, arterial territories become apparent clinically in thrombo-embolic arterial occlusion when infarction occurs up to the watershed of that arterial territory.

Unlike the retina where arterioles and venules cover identical territories, cerebral venous drainage does not parallel the arterial supply. Several classifications exist (reviewed by Nowinski, 2012), but essentially venous drainage can be understood in terms of superficial and deep venous systems (Oka *et al.*, 1985; Ono *et al.*, 1984). Although venous anastomoses exist within each system, there is no physiological anastomosis between superficial and deep systems (Andeweg, 1996, 1999). They join at the torcula (confluens sinuum), where the straight sinus (draining the deep system) meets the superior sagittal sinus and transverse sinus (draining the superficial system) (Miyawaki, 2003). Anatomy is variable but the superficial venous system includes several cortical veins and sinuses that drain the exterior cortex, ranging in average width from ~0.5 to 5.0 mm (Oka *et al.*, 1985). The deep system drains subcortical and periventricular structures such as the insular cortex and basal ganglia. The watershed between the superficial and deep venous systems lies between the periventricular and subcortical white matter

(Andeweg, 1996). Ultimately venous blood leaves the cranial vault through the internal jugular or spinal veins, and a small number of emissary veins.

Major venous channels show significant variation (Miyawaki, 2003). In a magnetic resonance venography series of healthy children the inferior sagittal sinus was not seen in 54%. The right or left of the following were absent in many cases (% cases absent): vein of Trolard (~80%), vein of Labbe (~50%), superficial petrosal sinus (66%), and inferior petrosal sinus (~33%) (Widjaja and Griffiths, 2004). Lack of major collateral channels would make associated brain regions more vulnerable to venous congestion in paediatric CM. Variation in venous drainage could help to explain patterns of MRI signal changes in acute retinopathy-positive paediatric CM in the same way that venous territories within the superficial system appear to influence the distribution of radiographic lesions in paediatric cerebral venous thrombosis (Meder *et al.*, 1994; Teksam *et al.*, 2008).

2.9.2 Vascular anatomy of the basal ganglia

The basal ganglia comprise several interrelated nuclei with different neuronal structures, vascular architectures, and embryological origins. The arterial supply of the basal ganglia arises mainly from the middle cerebral artery with some contributions from the anterior cerebral artery and anterior choroidal artery. Branches from the anterior cerebral and anterior choroidal arteries supply the head of the caudate nucleus and globus pallidus (Akima, 1993). Ten to 20 lenticulostriate arteries from the middle cerebral artery enter the putamen, where they spread out in a fan shape and divide into two to three branches, each ~100 to 150 μm wide. These form capillary networks within the putamen and cross the internal capsule to supply the caudate nucleus (Nonaka *et al.*, 1998).

The vasculature of the putamen and caudate nucleus is distinct from that of the globus pallidus, internal and external capsules. Branching arterioles (~50 μm wide) of the putamen may reflect back and coil around the parent vessel before branching further. Precapillary arterioles of the putamen are ~20 μm wide (Wolfram-Gabel and Maillot, 1994). Retrograde arteriolar branching is seen but it is not clear if this is a feature of old age or is universally present (Nonaka *et al.*,

1998). If the latter they could produce heterogeneous viscosity from phase separation in children. In the globus pallidus, arterioles tend to be fewer and straighter, with no coiling. The end arteriolar branches (~40 µm wide) form arteriolar anastomoses as well as a capillary net (Wolfram-Gabel and Maillot, 1994).

The capillary networks of the putamen and caudate nucleus have a similar density to the cerebral grey matter (600–650 capillaries per mm^2 in a 30 to 40 µm mesh), whereas the capillary density of the internal capsule approximates that of the cerebral white matter. The globus pallidus has capillary density between these extremes (200–350 per mm^2 in a 60–80 µm mesh) (Nonaka *et al.*, 1998; Wolfram-Gabel and Maillot, 1994). Capillary density seems to be proportional to the density of synapses (Akima, 1993). Capillaries of the putamen are ~5–7 µm wide (Wolfram-Gabel and Maillot, 1994).

Venules and veins throughout the basal ganglia are generally wider than the arterial vessels, and smaller veins meet larger vessels at right angles (Nonaka *et al.*, 1998). In the putamen, five arterioles are typically arranged around a single central ‘principal’ vein, which together form a vascular unit. These veins can be large (~500 µm wide) (Wolfram-Gabel and Maillot, 1994). The high ratio of arterioles to veins suggests a similarity to cerebral cortical vessels, and an important difference with the retina where arterioles and venules are paired. Congestion of a principal vein is likely to have a disproportionate impact on perfusion. This may be relevant to CM since sequestration is thought to occur in venules to a greater extent than arterioles, although it is not clear how often congestion occurs in venules up to 500 µm wide.

2.9.3 Vascular anatomy of the cerebral grey matter

Branches from the anterior, middle, and posterior cerebral arteries produce a network of pial arterioles on the cerebral surface. Cortical arterioles (~20 to 90 µm wide) branch from the pial vessels and travel on the brain surface for ~150 to 750 µm before turning 90° to penetrate the cortex (Reina-de La Torre *et al.*, 1998).

There are no capillaries on the brain surface, and the absence of artero-venous anastomoses at this point means that all arterial blood is forced into penetrating cortical arterioles and the capillaries of the cerebral cortex (Duvernoy *et al.*, 1981).

Penetrating cortical arterioles reach depths of 150 µm to ~3 mm and have widths between ~20 and 65 µm. They branch to form capillaries and pre-capillary arterioles at several levels parallel with the brain surface. Mean arteriolar branching angle is 112 to 126°, depending on daughter vessel diameter (Cassot *et al.*, 2010). Some pre-capillary branches are recurrent (Duvernoy *et al.*, 1981; Reina-de La Torre *et al.*, 1998).

The topology of cortical vessel segments can be thought of in terms of 'tree-like' penetrating vessels and 'net-like' capillaries (Lauwers *et al.*, 2008). The tree-like arteriolar and venular segments have a long parent vessel 'trunk' from which smaller branches emanate (Cassot *et al.*, 2010), and are suited to rapid movement of blood, whereas the capillary net is homogeneous and space-filling—suited to nutrient exchange (Lorthois and Cassot, 2010). Cortical penetrating arterioles and venules have a Strahler branching order from 3 to 5 between surface pial vessels and the capillary network (Cassot *et al.*, 2010). Unlike capillaries of the inner retina, it seems there are no boundaries between capillaries arising from different arterioles.

Average total vascular density in temporal cortex is ~500 mm/mm^3, of which capillaries contribute ~50% (Cassot *et al.*, 2006). This is consistent with human visual cortex, which has an average capillary density of ~250 mm/mm^3 (Bell and Ball, 1985). Narrow artero-venous anastomoses may exist at the capillary junction, but it is difficult to distinguish these from larger capillaries (Duvernoy *et al.*, 1981).

Ascending cortical venules have ~50% more branches than arterioles; mean branching angle is 118 to 129° (Cassot *et al.*, 2010). Ascending veins include principal veins (Group V5), which arise from subcortical white matter, and are 120–125 µm wide. The diameter of venules decreases as vessel origin becomes

more superficial, ranging from 65 µm (Group V4) to 20 µm (Group VI). Once ascending venules reach the cortical surface they make a 90° turn to converge on surface venules (~130 µm wide). The surface venous network is anastomotic with channels up to 180 µm wide, but has fewer anastomoses than the arteriolar network, and some lobules have no surface venous anastomoses. This drains into larger veins adherent to the arachnoid dura (Duvernoy *et al.*, 1981). The largest veins (1.3 to 3.3 mm) cross the subdural space to meet sinuses incorporated into the dura mater (Oka *et al.*, 1985). There are no venous anastomoses in the cerebral grey matter, and only rare reports of arteriovenous anastomoses (Duvernoy *et al.*, 1981).

2.9.4 Occlusion of cortical vessels

The absence of anastomoses between penetrating vessels means that penetrating cortical arterioles and ascending venules represent a physiological bottleneck. Experimental occlusion of penetrating arterioles in rat cortex leads to severe reduction in blood flow velocity in vessels at least seven branches downstream from the occlusion (Nishimura *et al.*, 2010).

In the rat, ascending venules are twice as prevalent as penetrating arterioles, and this is likely to explain the relatively low extent of flow disruption after ascending venule occlusion (Nguyen *et al.*, 2011). In contrast human grey matter penetrating arterioles outnumber venules on average by 2:1 (Cassot *et al.*, 2010), and principal veins are sometimes surrounded by several rings of arterioles. The tissue volume of such vascular units is variable (Duvernoy *et al.*, 1981). The general implication is that, as in the basal ganglia, a low ratio of venules to arterioles in human cortex may mean venous congestion in CM disrupts flow to disproportionately large areas of tissue.

2.9.5 Vascular anatomy of the cerebral white matter

The cerebral white matter is supplied by penetrating arterioles from the pial arteriolar network, which remain unbranched within the cerebral grey matter until its deepest layer. These arterioles enter the subcortical white matter perpendicular to the brain surface. Vessels express branches at ~90° from the main trunk—five to ten, depending on trunk length. Only a proportion of arterioles reach the

periventricular zone, where they arborize. A few form arteriolar anastomoses (Nonaka *et al.*, 2003a, 2003b). Penetrating arterioles have an internal diameter of 30 to 40 µm in subcortical white matter, compared to 40 to 60 µm in the grey matter (Nonaka *et al.*, 2003a), and 100 to 170 µm in deep white matter (Nonaka *et al.*, 2003b).

There has been disagreement about whether the deep white matter also receives arterioles from ventricular sources (Van den Bergh and Van der Eecken, 1968). Moody et al., (1990), Nelson et al., (1991) and Nonaka et al., (2003b) found no evidence of periventricular arterioles directed towards the brain surface.

Cerebral white matter is drained by superficial medullary veins and deep medullary veins. The former drain subcortical white matter into superficial cerebral veins on the brain surface, and the latter drain periventricular white matter into subependymal veins at the lateral ventricle (Andeweg, 1996; Hassler, 1966; Meder *et al.*, 1994; Nonaka *et al.*, 2003b). Superficial medullary veins are thought to drain the external 1–2 cm of white matter (Meder *et al.*, 1994), and the deep medullary veins the remainder (Hassler, 1966; Hooshmand *et al.*, 1974). Trans-cerebral veins connecting superficial and deep venous systems have been reported (Hassler, 1966; Huang and Wolf, 1964; Meder *et al.*, 1994; Nakamura *et al.*, 1994; Schaller, 2004), but may be artefactual as functional anastomoses between superficial and deep venous systems are not consistent with patterns of injury seen after deep venous system obstruction (Andeweg, 1999; Hassler, 1966). The predominance of haemorrhages in white matter is consistent with relatively long venous drainage pathways (Spitz, 1946), suggesting that haemorrhages arise from increased transmural pressure within congested venules.

2.9.6 Cerebral blood flow and metabolism

Like the retina the brain is highly metabolically active (reviewed in Wong-Riley, (2010), and depends on a constant supply of oxygen and glucose (Mckenna *et al.*, 2006).

Normal cerebral blood flow characteristics vary with age and between brain regions (Ide and Secher, 2000; Kety, 1950). Abnormal cerebral blood flow in the

middle cerebral arteries has been reported in cases of paediatric CM with seizure or raised intracranial pressure (Newton *et al.*, 1996).

Total cerebral blood flow and metabolism changes dramatically during childhood (Kennedy and Sokoloff, 1957; Kety, 1956; Kinnala *et al.*, 1996; Mckenna *et al.*, 2006; Takahashi *et al.*, 1999; Wintermark *et al.*, 2004). Cerebral blood flow increases rapidly during the first year of life (Varela *et al.*, 2012) and flow volume peaks at 55% cardiac output between age 2 to 4 (~130 ml/100 g/min) before declining to adult values (Wintermark *et al.*, 2004). In comparison the brain of a resting adult receives ~16.5% cardiac output (Kety, 1950), or ~50 ml/100 g/min (Kety and Schmidt, 1948; Madsen *et al.*, 1993; Sokoloff, 2003).

Cerebral metabolic rate for oxygen is also highest from 3 to 6 years, ranging from 4.3 to 6.2 ml O_2/100 g/min (Kennedy and Sokoloff, 1957). The average of 5.25 ml would be >50% total body oxygen (Mckenna *et al.*, 2006). Adult resting cerebral metabolic rate for O_2 is ~3 ml/100 g/min (Kety and Schmidt, 1948; Madsen *et al.*, 1993; Sokoloff, 2003), and accounts for ~20% of total body oxygen consumption (Kety, 1950). Cerebral arteriovenous oxygen difference is ~40% in adults (Seifert and Secher, 2011), comparable to retinal oxygen extraction of ~50% (McLeod, 2010). The developmental curve for cerebral metabolic rate for glucose follows a similar trajectory to cerebral blood flow, though with a more gradual decline to adult values at around age 17 (Chugani, 1998; Chugani *et al.*, 1987; Kinnala *et al.*, 1996).

The highest regional peak in cerebral blood flow is in the calcarine cortex (area V1, 155 ml/100 g/min, 29 months). Basal ganglia, temporal, frontal, and occipital cortices have lower peaks (~125 to 140 ml/100 g/min) (Wintermark *et al.*, 2004). The highest regional peak in the cerebral metabolic rate for glucose at this age is in the calcarine cortex, transverse temporal cortex, and lenticular nuclei (all >30 µmol/100 g/min between 1 and 2 years) (Chugani *et al.*, 1987).

2.9.7 Flow in cerebral microvessels

Data on capillary flow dynamics in human brain are scarce, although many studies on animal models exist (Hudetz *et al.*, 1996; Jespersen and Ostergaard, 2011;

Vovenko, 1999). Capillary flow velocity is between 0.6 and 2.4 mm/s in rat cortex (Hudetz *et al.*, 1996), which overlaps the lower range of velocities in human perifoveal vessels (Pournaras *et al.*, 2008).

Guibert et al. (2010) have modelled blood flow in primate cortex, which has a ratio of arterioles to venules similar to human brain. They found that local haematocrit could vary by approximately a factor of two owing to phase separation. Brain haematocrit measured by dual tracer single-photon emission computed tomography in adult humans is ~76% systemic haematocrit (Sakai *et al.*, 1985). Blood is thought to make up ~3–5% of brain volume, and three quarters of this is venous (An and Lin, 2002). Blood volume is greater in grey (~5 ml/100 g) than white matter (~2 ml/100 g) (Kuppusamy *et al.*, 1996) consistent with greater capillary density in grey matter.

2.10 Retina and brain compared: implications for studying neurovascular pathogenesis

Retina and brain microvasculature have much in common, including circulation-tissue barriers and local control over blood flow (Patton *et al.*, 2005). After reviewing microvascular haemorheology and the microvasculature of retina and brain regions, it seems that sequestration-induced injury could be influenced by several characteristics (Table 5).

2.10.1 Vessel branching

Retinal vessels are relatively long and straight, with right-angled or dichotomous branches. This is also true of cerebral grey matter, white matter and basal ganglia —although brain-specific features are also present. Haemodynamic models suggest near 90° arteriolar branching produces significant variation in haematocrit and viscosity (Ganesan *et al.*, 2010; Guibert *et al.*, 2010) and therefore may be important in distributing parasitised erythrocytes and fostering sequestration. Right-angled venular confluences may also provide opportunities for sequestration since cells may continue to roll along the endothelium when moving from a smaller to larger vessel before joining the axial flow stream, potentially stripping the endothelial surface layer and exposing ICAM1 (Popel and Johnson,

2005; Schmid-Schönbein, 1999). Local variation in haematocrit and viscosity associated with branching architecture may explain why retinal vessels full of parasitised erythrocytes can be found immediately adjacent to vessels unaffected by sequestration (Lewallen *et al.*, 2000).

2.10.2 Arteriole to venule ratio

Both basal ganglia and cerebral grey matter have more arterioles than venules, whereas in the retina, arterioles and venules are paired. A high ratio of arterioles to venules in the absence of anastomoses may make these brain regions more vulnerable than the retina to the effects of post-capillary venous congestion with parasitised erythrocytes.

2.10.3 Venous drainage and watershed regions

Retina and brain both have vascular watersheds that are amenable to imaging. Although retinal arterial and venous watersheds are identical, retinal arterioles and venules can be distinguished using FA. In the brain, arterial supply and venous drainage occur over different territories, and radiological changes to these anatomical regions can be assessed using MRI. Retinal CNP is most common in watershed regions, and brain lesions may also follow patterns of venous drainage into superficial and deep systems, especially those of the cerebral white matter. Sequestration is thought to mainly involve capillaries and post-capillary venules, and retinal white-centred haemorrhages occur in other conditions involving venous congestion (Duane *et al.*, 1980). These points suggest comparison of retinal and cerebral venous watersheds in CM is reasonable, and perhaps that the severity of non-perfusion in retinal watersheds might reflect the degree of T2 or diffusion-weighted imaging abnormalities in the cerebral white matter in acute CM (Figure 15). The consequences of venous congestion are much greater in brain than retina. For example, swelling of the splenium, or posterior cerebrum could compress the vein of Galen against the tentorium, potentially obstructing outflow from the deep venous system and rapidly raising intracranial pressure (Andeweg, 1999).

Figure 15: Comparison of retinal and cerebral venous watershed regions.
(A) Fluorescein angiogram showing capillary non-perfusion at the macula and horizontal raphe, which is an arteriolar and venular watershed between the supero-temporal and infero-temporal arcades. Axial (B) and coronal (C) MRI images show extensive high T2 signal in the subcortical white matter of a different child with cerebral malaria (white arrows). The cerebral white matter is the site of a venous watershed between superficial and deep venous systems.

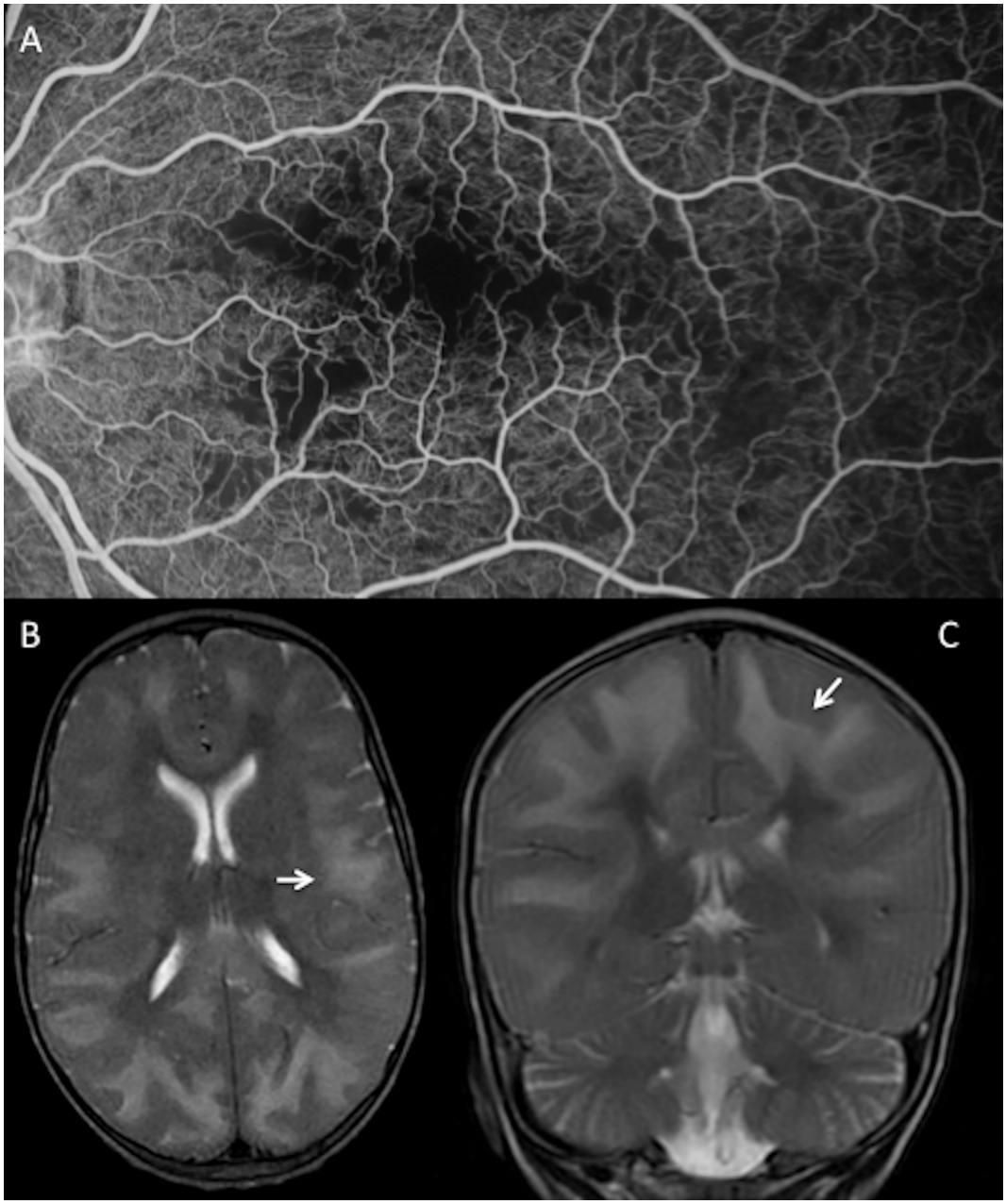

2.10.4 Blood flow and metabolism

Adult inner retinal blood flow is roughly half that of the brain. To my knowledge there are no data available on developmental changes to retinal blood flow during childhood. However, cerebral blood flow varies dramatically during childhood development, peaking within the age range typically admitted with paediatric CM in high transmission areas (Snow *et al.*, 1997; Wintermark *et al.*, 2004). The median age at admission with CM in high transmission areas appears to coincide with the childhood peak in total cerebral blood flow and metabolism. For example, the mean age of children admitted to the paediatric research ward in Blantyre, Malawi, ranged from ~3 to 4 years between 2001–10 (Roca-Feltrer *et al.*, 2012). Snow et al. (1997) found the median (IQR) age at admission with CM was low in high transmission areas and increased with falling endemicity—ranging from from 2 (1.5–6.5) years (hyperholoendemic), 4 (3–5) (mesoendemic), to 6.5 (4–7) years (hypoendemic). A similar pattern is found using residential altitude as a proxy for transmission intensity (Reyburn *et al.*, 2005). As suggested by others (Billig *et al.*, 2012) high metabolic demands may make the paediatric brain more vulnerable to the effects of sequestration than other paediatric organs, and in the context of high transmission predispose to early cerebral complications rather than the acute renal failure seen in adults (Thanachartwet *et al.*, 2013).

As in the brain, blood flow through the inner retinal circulation is subject to autoregulation, and remains stable in spite of changes to intraocular pressure and systemic blood pressure. The mechanisms behind this phenomenon are likely to include intrinsic myogenic and metabolic components. Inner retinal blood flow also responds to PaO2 and PCO2 in a similar way to cerebral blood flow (reviewed by Pournaras et al., 2008; Kur et al., 2012).

In addition, stimulation with flicker light produces a functional hyperaemia in the optic nerve head (Pournaras et al., 2008) and retinal areas corresponding to local illumination (Kur et al., 2012). Less data are available to describe this latter phenomenon, but the implication of current evidence is that the inner retina has a type of neurovascular coupling similar to that of the brain (reviewed by Filosa et al., 2015)

Retina and brain are comparable in that they both have very high metabolic demands, and in early childhood the brain may be more susceptible than the retina (and other organs) to the effects of dysfunctional microvascular flow. However CM is only one manifestation of severe malaria in children, and it is not clear how high paediatric cerebral metabolic rate for O_2 in isolation could influence which children develop CM, and which develop severe malarial anaemia or metabolic acidosis. Besides this, the frequency of coma in cases of severe malaria is similar in children and adults (World Health Organization, 2014b).

2.10.5 Complicating factors

The clinical picture of paediatric CM is complicated by the presence of multiple interrelated insults in addition to sequestration, including anaemia, hypoglycaemia, and metabolic acidosis (World Health Organization, 2014b). HIV is known to upregulate ICAM1 (Stins *et al.*, 2003) and infection may complicate CM pathogenesis (reviewed in Hochman and Kim, 2012). In addition to systemic insults, seizures are common (Birbeck, Molyneux, *et al.*, 2010) and could inflict brain injury without corresponding damage to the retina. Retinal signs could indicate a high tide mark of tissue injury common to particular regions of both retina and brain, which may or may not reach a threshold needed to induce coma, and thereafter trigger additional brain damage from other mechanisms, such as seizure. Alternatively, one or more co-insults may be necessary for development of the CM phenotype, as malarial retinopathy is also seen in children with severe malarial anaemia without coma, albeit less severely (Beare et al., 2004).

2.11 Conclusions

Description of the whole brain in terms of greater or lesser similarity to the whole retina is difficult, and probably inappropriate. Rather, analysis of data from retina and brain should take account of anatomical variation within both organs, as neither retina nor brain are homogeneous units. Both have regions where microvasculature may, or may not, be comparable in specific respects that are relevant to a given neurovascular disease.

Retina and brain are similar in ways relevant to paediatric CM. Similar vascular pathology suggests both organs experience similar disease processes. Similarities in terms of vessel network architecture, imaging abnormalities in venous watersheds, and high metabolic demand suggest that both organs may be vulnerable to sequestration for the same reasons. These factors may influence delivery of parasitised erythrocytes, the flow conditions necessary for sequestration, and the vulnerability of tissue to ischaemia associated with venous congestion or occlusion. The impact of congestion on common venous anatomy may explain the distribution of MRI brain and retinal FA lesions in paediatric CM.

The retina and brain also have differences. Arteriovenous ratios vary between brain regions, while in the retina arterioles and venules are paired. Cerebral arterial and venous watersheds are different, while retinal watersheds overlap. The paediatric brain has a metabolic peak in early childhood, which is likely to raise cerebral metabolic demands significantly above retinal demands in the age range typically affected by CM.

Considering these similarities and differences, a biologically plausible analogy can be made between the retinal periphery, or horizontal raphe, and the cerebral white matter, because these regions have similar vascular architecture. All receive blood from long vessels with near 90° branches, and so may contain blood with disproportionately high microvascular haematocrit and viscosity. The presence of venous watersheds gives little option for collateral drainage from these areas in the event of venous congestion. Given this background, similar degrees of coexistent injury to these retinal and brain areas in a population of children with retinopathy-positive CM would suggest that retinal CNP and leakage could be surrogates for brain ischaemia and swelling, and might provide a useful tool to understand cerebral vascular pathogenesis.

My review has limitations. Only three brain regions are compared with the retina, and comparable data are not available for all geometrical or topological variables at each site. I have resorted to measurements from adults where paediatric data are not available, and I have not attempted comparison of retinal or cerebral microvascular architecture with other organs in which sequestration is minimal or

absent (Milner *et al.*, 2014). I have not compared paediatric and adult malarial retinopathy—this deserves a separate review.

I have identified significant similarities and differences in retinal and cerebrovascular architecture, blood flow and metabolic demand. These comparisons inform new interpretations of retinal and cerebral data in retinopathy-positive paediatric CM by incorporating information on haemorheology and vascular architecture from multiple regions of the CNS. Increasingly comprehensive comparisons of human neurovasculature will provide greater insights into how far retinal vessel changes reflect neurovascular pathology. Mapping the contours of warranted analogy between retina and brain has the potential to strengthen the biological rationale of retinal imaging in neurology, inform interpretation of neurovascular data, and stimulate further hypotheses—for retinopathy-positive paediatric CM in particular, and for neurovascular disease in general.

Chapter 3 – Evaluating retinal markers of neurological disease

3.1 Aim of chapter

Describe an analytical approach to evaluating inferences about the brain from retinal data.

3.2 Summary of chapter

3.2.1 What is known already

The human brain is relatively inaccessible, and this poses a problem for research into many neurological conditions. Scientists have traditionally responded by developing models of, and biomarkers for, brain physiology and disease. The human retina is an attractive source of biomarkers since it shares many features with the brain. Some even describe the retina as a "window" to the brain, implying that retinal signs are analogous to brain disease features. If this is true the retina has the potential to be a powerful research model of neurological disease.

However, little attempt has been made to develop analytical methods to show whether or not retinal signs are equivalent to corresponding brain abnormalities. Such methods are essential for empirical assessment of the eye as a model of brain disease, and for advancing conclusions beyond simple inferences from straightforward associations between eye and brain.

3.2.2 What this chapter involved

I reviewed literature on statistical methods for evaluating surrogate end points in randomised clinical trials, and attempted to understand these within the structure of a valid argument from analogy.

3.2.3 What this chapter adds to current knowledge

I define what it means for a retinal marker to mirror a corresponding brain disease feature within a given biological paradigm, using cerebral malaria as a case study.

I then describe how existing statistical techniques can be adapted to evaluate the assumptions underlying this framework, and propose a more rigorous way to think about, and test, how clearly one might see the brain through the retinal "window". This approach is illustrated, using paediatric cerebral malaria as an example.

3.3 Introduction

3.3.1 The appeal of the retina as a research tool

There is a great temptation to describe the retina as a "window to the brain". For example, a recent review of neurological conditions was titled "The retina as a window to the brain – from eye research to CNS disorders" (London *et al.*, 2013). A popular textbook on retinal anatomy and physiology is called: "The retina – an approachable part of the brain" (Dowling, 2012). Similar language and concepts are present in recent literature on Alzheimer's disease (Cheung *et al.*, 2014), schizophrenia (Chu *et al.*, 2012), and stroke (Ong *et al.*, 2013).

The appeal of the retina as a neuro-scientific research tool arises from three points: firstly, it is difficult to directly observe the brain in living patients. This limits the amount and type of information that can be collected about the central nervous system (CNS) in health and disease. Secondly, the retina is thought to be very similar to the brain (MacCormick *et al.*, 2014; Patton *et al.*, 2005). The retina is part of the CNS, and has similar embryological origins, anatomy and physiology to other CNS regions. This leads to a related idea that retinal disease manifestations ought to be associated with brain disease manifestations – at least for certain conditions, where both organs are exposed to the same insults. Finally, unlike the brain, direct observation of the retina is relatively simple. Several non-invasive high resolution techniques to measure retinal structure and function are available (MacGillivray *et al.*, 2014), and technological advances are likely to increase the range and power of such modalities.

Given these points, it is not surprising that the retina has been the subject of a significant amount of biomarker research, leading to many reports of associations between retina and brain. Prominent associations include relationships between retinal parameters and outcomes from neurological conditions, such as stroke

(Doubal *et al.*, 2009), cognitive impairment (Cheung *et al.*, 2014; Ong *et al.*, 2014), multiple sclerosis (Green *et al.*, 2010), and others (reviewed in London et al., 2013; MacGillivray et al., 2014).

It is clear that associations between retina and brain exist for a range of neurological and neurovascular conditions of varying aetiologies. This is consistent with the hypothesis that the retina and brain are similar, and respond similarly to disease. However, although evidence of consistency with a hypothesis is valuable, associations between retina and brain cannot – on their own – justify the stronger conclusion that retinal markers mirror analogous brain features, or, in some sense, "provide a window to" the brain.

This chapter includes the following sections. Firstly, I describe epistemology[2] involved in treating retinal features as analogous to brain disease features. Similar logic is employed in statistical evaluation of surrogate end points. Secondly, I review of some major approaches to surrogate end point evaluation. These were designed for use on data from randomised controlled trials (RCT). Thirdly, I discuss whether these approaches can be applied to data from observational studies in general, and observational data on paediatric cerebral malaria (CM) in particular.

3.4 The retina as a window to the brain

3.4.1 Reasoning from an analogy between retina and brain

The phrase "window to the brain" suggests that some characteristic in the retina, or retinal manifestation of disease, is the same as an analogous characteristic or manifestation in the brain. It suggests that when one observes a retinal feature one is also observing, for all practical purposes, an equivalent or identical disease effect that is occurring in the brain. If this were true, one should certainly expect the given retinal and brain variables to be strongly positively correlated. But proof of equivalence requires evidence beyond direct association.

2 Epistemology is a branch of philosophy concerned with "the study of knowledge and justified belief" (Steup, 2005)

Consider two variables, S and T. If S and T are materially equivalent (symbolised S⇔T), then S is necessary and sufficient for T, and *vice versa*. If the retina is essentially a transparent window to the brain, this type of relationship ought to exist between retinal and brain variables. To the best of my knowledge, existing reports of retinal biomarkers of brain disease usually describe univariate or multivariate associations between retinal and brain variables, but this does not show that a retinal marker is necessary and sufficient for an analogous brain feature.

The point to take from this is not that authors describing the retina as a window are wrong – direct associations between retina and brain are important. On the contrary, this is a challenge. Considering the many biologically important characteristics shared by retina and brain, one ought to be able to describe retina-brain relationships in much stronger terms than those of simple associations.

What would this kind of description look like? The strict logic of material equivalence may not be appropriate for analysis of a biological system. Even if a retinal variable really was necessary and sufficient for an analogous brain variable, there are many reasons why this relationship might not be demonstrable. These include measurement error in key variables, and complexity introduced by other related factors such as confounders. Biology is a noisy science.

Therefore one can define equivalence (S⇔T) to mean: S contains the same information as T. The information contained in S (and also T) is necessarily relative to information outside itself. About *what* does S inform us? We are only interested in retinal variables because they might inform us about other variables. These might include:
1) A systemic disease process (A)
2) Analogous manifestation(s) of this disease process in the brain (T)
3) The ultimate outcome of the disease process (e.g. risk of death) (Z)

If S⇔T means S contains the same information as T, then this can be expressed as:
4) S and T contain the same information about each other

and, in addition
5) S and T both contain the same information about A and Z

However, since biology is noisy, one might want to define equivalence in even more pragmatic terms. Instead of defining equivalence on the basis of whether or not S and T contain *all* the same information about each other, A and Z, one can define it in terms of the *degree* to which S informs about T, with respect to A and Z.

In this case, a retinal feature could be considered equivalent to an analogous brain feature, if the retinal feature *contains a large amount of the information* about *disease exposure* (A), and/or *disease outcome* (Z), as that contained in an analogous brain feature (T). The retinal feature (S) and brain feature (T) should also *contain a large amount of information* about each other. These relationships are illustrated in Figure 16.

These considerations of what it might mean for the retina to be a window to the brain lead to a definition of equivalence that moves some way beyond existing analyses of prospective retinal biomarkers in terms of simple associations with brain variables or outcomes. However, they are not unique to questions about retina-brain associations.

Similar analogical reasoning is used when assessing the suitability of animal models, and in evaluating potential surrogate markers in RCTs. In each of these examples, the real object of interest is out of reach. This is the target (T) - for example the human subject, or the true clinical end point. What is available is an imperfect source of information (S) – a candidate model, or prospective surrogate marker. S may (or may not) provide useful information about the real object of interest (T). In both cases the biological plausibility of relationships between S, T, A and Z gives an essential *a priori* context to any empirical evaluation of S as a good source of information about T – whether S is an experimental model, surrogate marker, or “window” to another organ.

Figure 16: Structure of associations between retina and brain.

Equivalence between retina and brain variables can be thought of in terms of information contained in the retina (S) about the brain (T) with respect to disease exposures and effects (A and Z respectively). Arrows indicate hypothesized causal relationships; broken lines indicate direct associations that are assumed not to be causal. A = disease exposure or severity; S = source domain variable (e.g. a retinal variable); T = target domain variable (e.g. a brain variable); Z = clinical outcomes[3].

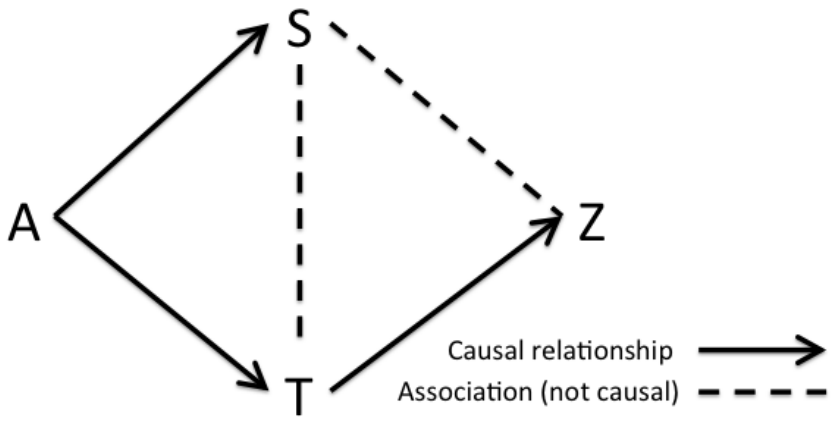

Recognizing that analogical reasoning is used in other areas of medical science suggests the possibility that existing statistical methods might be adapted for use in observational studies of retinal variables as potential biomarkers for brain disease. Taking statistical techniques developed to assess surrogacy in RCTs, and extending them to observational studies, could potentially allow important new inferences to be made about the pathogenesis and prognosis of neurological diseases from retinal data. Indeed, this methodology could be applied much more broadly. For example, a recent study used similar methods to simultaneously

3 If a retinal feature (S) is analogous to a brain feature, it ought to contain a large amount of information about the brain feature (T) both independently and with respect to the mechanism causing disease manifestations (A) and the clinical outcome (Z).

This figure also illustrates the biological paradigm relating disease exposure (A) to disease manifestations in retina (S) and brain (T), and finally to clinical outcome (Z) for paediatric CM. Note there is no direct path from A to Z. This implies that in CM, the disease (A) only causes death (Z) through manifestations in the brain (T). The paradigm can be modified to include different assumptions, and these pathways can be represented mathematically as a series of simultaneous equations in a structural equation model. S can be evaluated in terms of how much information it contains about A, or Z, compared to T (*cf* LRF, or PIG). It can also be evaluated in terms of the ratio of coefficients: $A \rightarrow S / A \rightarrow T$, or $S - Z / T \rightarrow Z$ (*cf.* the RE).

estimate the effect of bacteria strain on both biomarkers and mortality (Walker *et al.*, 2013).

However, questions about whether or not retinal observations reflect cerebral disease processes are different from questions about treatment effect in an RCT. Direct application of statistical methods from RCTs to observational studies are, in general terms, not usually appropriate. Analytical approaches that allow fuller exploration of potentially causal relationships are more suitable – for example, structural equation modelling (SEM). SEM has the advantage of allowing researchers to declare assumptions about relationships between exposures, outcomes, and potential confounders, and take account of these relationships when estimating coefficients (for more details see Beran and Violato, (2010); Kline, (2011)).

Even if one or more statistical methods for evaluating surrogacy in RCTs are appropriate for use in observational studies, certain theoretical misconceptions about surrogacy must be avoided. For example, Walker et al., (2013) discuss how, because their methodology is conceptually similar to the assessment of surrogate endpoints, they can conclude that the associations they describe represent causal relationships. This is incorrect. A surrogate marker may, or may not, be on the causal pathway between treatment (or disease) and true endpoint. Mediation is not a necessary condition of surrogacy (Joffe and Greene, 2009; VanderWeele, 2013).

This comment may seem esoteric, but it has very practical implications when considering the retina as a model of the brain. It does not make biological sense to think of the retina mediating the effect of a systemic process on the brain. If mediation is logically necessary for surrogacy, retinal manifestations might be better thought of as epiphenomena than glimpses of the brain through the supposed window of the eye[4].

4 Brain damage is rarely *caused* by a process that acts through (*is mediated by*) retinopathy, except perhaps in cases of trauma caused by blindness. Consider papilloedema and brain herniation. Papilloedema *does not* mediate the effect of raised intracranial pressure such that it causes brain herniation (i.e. intracranial pressure → papilloedema → brain herniation). Many writers consider mediation to be an important feature of a good biomarker. However in the case of papilloedema (and many retinal signs) ocular damage does not cause damage to the brain. Rather, retinal and brain damage result from common disease mechanisms.

A further caution about surrogate evaluation is relevant. Surrogate endpoints are attractive because they are easier, quicker, or cheaper to measure than the true clinical endpoint, while providing effectively the same information. New medicines can potentially reach the market more quickly and cheaply if licensing is based on surrogate outcomes rather than true clinical end points such as mortality. This was true of early anti-retroviral drugs, where CD4+ count was used as a surrogate for development of AIDS (discussed in Burzykowski et al., 2005). On the other hand, there is also a serious danger of being misled by a surrogate, because apparently good surrogate endpoints can produce paradoxical results. This occurred to disastrous effect when anti-arrhythmic drugs were licensed because they suppressed arrhythmia, but were later found to increase mortality (discussed in Biomarkers Definitions Working Group, 2001; Fleming and DeMets, 1996). If this type of paradox can occur in the context of RCTs, it can certainly cause problems for interpreting the meaning of retinal markers of brain disease.

3.5 Evaluation of analogical reasoning – surrogate endpoints

Evaluation of surrogate endpoints is an active area of statistical research, and several definitions and operational criteria have been proposed (reviewed in Burzykowski et al., 2005; Joffe and Greene, 2009; Lassere, 2007; VanderWeele, 2013; Weir and Walley, 2006). I summarize some of the more prominent approaches, with the aim of identifying statistical methods to investigate relationships between retina and brain within the context of a particular disease exposure and outcome. Key points about these methods are listed in Table 7 and described in the following subsections of this chapter.

Table 7: Definitions of valid surrogate endpoints.

Here I summarise some of the main statistical approaches to surrogacy, with operational criteria and comments.

Operational criteria or statistic	Definitions	Comments
Prentice's criteria (as expressed by (VanderWeele, 2013) $f(T\|S) \neq f(T)$ $f(T\|S,Z) = f(T\|S)$	A = treatment, S = surrogate endpoint, T = true outcome f(T) signifies the probability distribution of T f(TIS) signifies the probability distribution of T, given S f(TIA) ≠ f(T) means the probability distribution of T given A is not equal to the probability distribution of T alone. I.e. T is associated with Z f(T|S,A) = f(T|S) means the probability distribution of T given S and A is no different from the probability distribution of T given S. I.e. A has no effect on T after adjustment for S	A valid surrogate S should i) Be associated with the true outcome T ii) Completely capture the effect of treatment A on the true outcome T A candidate surrogate should be invalid if it fails to meet these criteria. Potentially more useful for excluding poor surrogates (given enough power) than validating good ones. The criteria (and related statistics) are not able to rule out the surrogate paradox (VanderWeele, 2013)
Proportion explained (PE) (Freedman *et al.*, 1992) $PE = 1 - \beta_s/\beta$	βs is the regression coefficient of a model of A on T, adjusted for S β is the regression coefficient of a model of A on T unadjusted S	A valid surrogate S should i) Have a PE close to 1 Reflects the degree of treatment effect captured by the surrogate, rather than ruling out candidate surrogates that do not capture the entire treatment effect. Can be applied to many types of data (Buyse and Molenberghs, 1998) The statistic is difficult to interpret, since it can lie outside 0-1, and will often have wide confidence intervals. As well as describing the association between A and T given S, the PE also depends on the association between A and S. It operates best

Operational criteria or statistic	Definitions	Comments
		when there is little or no association between A and S (Freedman *et al.*, 1992; Qu and Case, 2007; Weir and Walley, 2006)
Likelihood reduction factor (LRF) (Alonso *et al.*, 2004) as interpreted by (Qu and Case, 2007) LRF = 1 – exp(-LRT(A,S:A)/n) $LRF_{adj} = LRF/LRF_{max}$	LRT(A,S:A) is the likelihood ratio test statistic comparing a model of T given S and A, with a model of T given A n = number of subjects LRFmax is the LRF of the best possible fitted model	A valid surrogate (at the 'individual level') should i) Have an LRF close to 1 Reflects the degree of treatment effect captured by the surrogate, which is conceptually similar to the association between surrogate and true outcome, adjusted for treatment effect (both are expressed by f(T|S,A)) The LRF reduces to the meta-analytic statistic R^2_{indiv} for normally distributed endpoints (Alonso *et al.*, 2004) Can be applied to many types of data (Alonso *et al.*, 2004) As with the PE, a strong association between A and S will cause the LRF to approach 0. This is not the case for the LRF_{adj} in simulations (Qu and Case, 2007)
Proportion of information gain (PIG) (Qu and Case, 2007) PIG = LRT(*S* : 1)/LRT(*S*,*A* : 1)	LRT(S : 1) is the likelihood ratio test comparing a model of surrogate and intercept with a model including only the intercept LRT(S,A : 1) is the likelihood ratio test comparing a model of surrogate, treatment, and intercept with a model including only the intercept	A valid surrogate should i) Have a PIG close to 1 A more straightforward way of expressing the LRF_{adj} (Qu and Case, 2007)
Relative effect (RE) Adjusted association (AA) (Buyse and Molenberghs, 1998) RE = α/β AA = Aγ	β is the unadjusted estimate of the effect of A on T α is the unadjusted estimate of the effect of A on S β and α are estimated by separate logistic regression models γA is the effect of S on T adjusted for A, i.e. f(T|A,S)	A valid 'trial level' surrogate should i) Have RE = 1, or any precisely estimated value Accurate estimation is likely to require data from multiple trials, or multi-level analysis of a single large trial. The meta-analytic statistic is R^2_{trial}.

Operational criteria or statistic	Definitions	Comments
		A valid 'individual level' surrogate should i) Have AA = ∞ or 1 (depending on type of data) The AA is closely related to the LRF. The meta-analytic statistic is R^2_{indiv}. The RE and AA have the potential to give useful information in certain contexts. They cannot exclude the surrogate paradox (VanderWeele, 2013)

Notation is defined as follows:
Prentice's criteria
A = treatment, S = surrogate endpoint, T = true outcome
f(T) signifies the probability distribution of T
f(TIS) signifies the probability distribution of T, given S
f(TIA) ≠ f(T) means the probability distribution of T given A is not equal to the probability distribution of T alone. I.e. T is associated with Z
f(T|S,A) = f(T|S) means the probability distribution of T given S and A is no different from the probability distribution of T given S. I.e. A has no effect on T after adjustment for S

Proportion of treatment effect (PE)
βs is the regression coefficient of a model of A on T, adjusted for S
β is the regression coefficient of a model of A on T unadjusted for S

Likelihood reduction factor (LRF)
LRT(A,S:A) is the likelihood ratio test statistic comparing a model of T given S and A, with a model of T given A
n = number of subjects
LRFmax is the LRF of the best possible fitted model

Proportion of information gain (PIG)
LRT(S : 1) is the likelihood ratio test comparing a model of surrogate and intercept with a model including only the intercept
LRT(S,A : 1) is the likelihood ratio test comparing a model of surrogate, treatment, and intercept with a model including only the intercept

Operational criteria or statistic	Definitions	Comments
Relative effect, adjusted association (RE, AA) β is the unadjusted estimate of the effect of A on T α is the unadjusted estimate of the effect of A on S β and α are estimated by separate logistic regression models γA is the effect of S on T adjusted for A, i.e. f(T|A,S)		

3.5.1 Prentice's definition and criteria

In 1989 Prentice suggested a highly influential definition for surrogate endpoints, with operational criteria by which a variable could be tested statistically (Prentice, 1989) (Table 7). This became a fundamental reference point for many, if not all, subsequent authors on statistical evaluation of surrogate endpoints. His definition was based on the intuitive concepts that a good surrogate should:

1) Be associated with the true endpoint, and also
2) "Capture treatment differences as they affect the true endpoint" (Prentice, 1989; p433)

Prentice's definition and criteria formalized an important intuition about what it means for a surrogate outcome to be valid, and were foundational to later discussions about how to evaluate surrogate endpoints. However they also suffer from several major problems. The main requirement is that the surrogate acts as a perfect confounder for the relationship between treatment and true outcome. This is a very high, and probably unrealistic standard. Formulation in terms of hypothesis testing means that although the criteria may be suitable for invalidating poor surrogates (given adequate power), they can never truly verify a good surrogate, since this requires the null hypothesis be proved true instead of false (Freedman *et al.*, 1992). The criteria are only equivalent to Prentice's definition of validity for binary endpoints (Buyse and Molenberghs, 1998). They do not allow for confounders of the relationship between surrogate and true outcome, and do not exclude the type of surrogate paradox involved in the infamous arrhythmia trials (VanderWeele, 2013).

3.5.2 Proportion Explained (PE)

Several adaptations of Prentice's criteria have been proposed. Freedman et al., (1992) developed the Proportion Explained (PE) (Table 7). This uses Prentice's definition of a valid surrogate, but instead of testing whether or not the surrogate captures the entire effect of treatment on the true endpoint, the statistic measures the degree to which a surrogate endpoint captures treatment effect. It was

designed as a ratio of treatment effect on the true outcome, given the surrogate, to unadjusted treatment effect on the true outcome.

This addresses one of the main criticisms of Prentice's criteria. Unfortunately this statistic also suffers from several major problems. It is not a true ratio – it is larger than 1 if controlling for the surrogate changes the direction of treatment effect on the true outcome. Confidence intervals will be large unless the treatment effect on the true outcome is also very large (>4 standard errors). These issues make interpretation of the PE difficult (Buyse and Molenberghs, 1998). Furthermore, a close association between the treatment and surrogate leads to large variability in the numerator. Although one might expect a good surrogate outcome to be closely associated with the treatment, the PE functions best when there is no interaction between treatment and surrogate (Qu and Case, 2007; Weir and Walley, 2006).

3.5.3 Likelihood Reduction Factor (LRF) and Proportion of Information Gain (PIG)

Another approach to Prentice's criteria is the Likelihood Reduction Factor (LRF) (Alonso *et al.*, 2004) (Table 7). This was proposed within the context of a different concept of surrogacy, often referred to as the meta-analytic approach (discussed below) (VanderWeele, 2013). Alonso et al., (2004) suggested that the LRF could bridge these two concepts – on one hand, providing a statistic to evaluate Prentice's main criterion (treatment effect on the true outcome is captured by the surrogate), and on the other, an expression of "individual-level surrogacy" that could be applied to a range of data types from a single trial.

Like the PE, the LRF compares two models: a model of treatment effect on the true outcome (controlling for the surrogate), and an unadjusted model of treatment effect on the true outcome. The PE compares coefficients of the models; the LRF compares the fit of models. In some families of models (e.g. logistic) the LRF can only take a value between 0 and a number less than 1. An adjusted version of the LRF (LRF_{adj}) will always lie between 0 and 1. Unlike the PE and LRF, the LRF_{adj}

appears to be relatively unaffected by interaction between treatment and surrogate (Qu and Case, 2007).

Qu and Case, (2007) proposed a variation of the LRF_{adj}. This statistic, the 'proportion of information gain' (PIG), compares models using the likelihood ratio test (Table 7). Results from these tests are then used to produce a ratio. PIG is closely related to the LRF_{adj}. Like the LRF_{adj}, the PIG is unaffected by collinearity between treatment and surrogate (Qu and Case, 2007).

3.5.4 Meta-analytic approach: Relative Effect (RE) and Adjusted Association (AA)

Buyse and Molenberghs, (1998) proposed two separate statistics in place of the PE: the Relative Effect (RE) and the Adjusted Association (AA) (Table 7). In contrast to Prentice, they reasoned that a useful surrogate should allow investigators to predict the treatment effect on a true endpoint, given knowledge only of the treatment and surrogate. This is the concept behind the RE, which is the ratio of the effects, expressed as coefficients, of (treatment on true outcome) over (treatment on surrogate). An RE = 1 would indicate that the same magnitude of treatment effect operates on both the true outcome and surrogate endpoint, at a population, or trial, level. However, a value less than one would still allow prediction of treatment effects on the true outcome, provided the RE is estimated with little residual error. This may require large numbers of subjects. With this in mind, a similar statistic (R^2_{trial}) can be derived from multiple trials, or multilevel analysis of a single large trial (Molenberghs *et al.*, 2001). The RE relies on variability in the treatment effect on both surrogate and true endpoints. For an ideal trial level surrogate, α and β would have a monotonic relationship, with minimal residual error regardless of whether α and β are related linearly or non-linearly (Joffe and Greene, 2009).

Interestingly, the concept of an ideal trial level surrogate appears to be similar to that of nomic isomorphism. This is a special case of analogy, where source and target domains are interpretations of one physical theory. For example,

volumetric flow and electric current are not only analogous concepts, they are also both described by the same mathematical equation (Bartha, 2013).

Buyse and others also suggested that a useful surrogate should allow prediction of the true outcome for a particular individual, given knowledge of the treatment and surrogate. This is the idea behind the AA, which is the association between surrogate endpoint and true outcome, adjusted for the treatment. A perfect individual level surrogate endpoint has a value for AA indicating no effect of treatment on the relationship between surrogate and true endpoints (∞ for binary endpoints, 1 for continuous endpoints) (Buyse and Molenberghs, 1998). The corresponding meta-analytic statistic is R^2_{indiv} (Molenberghs *et al.*, 2001). As mentioned above, the AA is closely linked to the LRF (Alonso *et al.*, 2004). Both RE and AA (R^2_{trial} and R^2_{indiv}) can be applied to binary, ordinal, and continuous endpoints (Molenberghs *et al.*, 2001).

Relationships envisioned by Buyse & Molenberghs (1998) (Buyse and Molenberghs, 1998) between treatment, surrogate, and true endpoints can be illustrated (Figure 17).

The meta-analytic approach has the potential to give information about candidate surrogate endpoints that is more practical than hypothesis tests of Prentice's criteria, or the PE. However in practice evaluation of validity remains difficult (Buyse *et al.*, 2010), and although these statistics may give some useful information they do not rule out the surrogate paradox (VanderWeele, 2013).

Figure 17: Relationships between treatment (A), surrogate (S) and true endpoint (T).

A is assumed to influence T both directly, and also through S. The influence of unmeasured confounders is not included. α represents the association between A and S; β the association between A and T; and γ the association between S and T. β/α is the ratio of coefficients between A → S and A → T (the Relative Effect); γA is the association between S and T controlling for A (the Adjusted Association). Note that in an RCT the true end point (T) is usually the same as the clinical outcome (Z), and so there is only one 'triangle' (connecting A, S, and T) whereas in Figure 16 there are two (connecting A, S, T; and S, T, and Z). Observational studies of associations between retina and brain allow the relationship between S and T to be evaluated in terms of both A and Z, while in an RCT the S → T relationship is only evaluated in terms of A. Adapted from Figure 2 in (Buyse and Molenberghs, 1998).

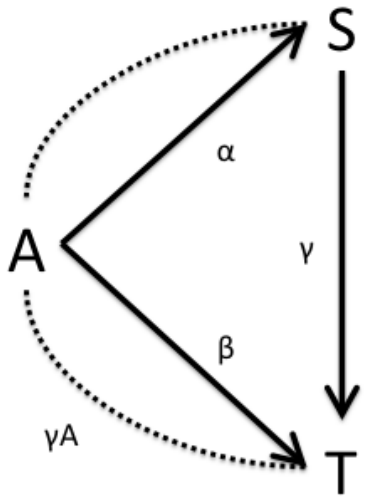

3.6 Qualitative evaluation of validity

Some authors recognize that it is not possible for a purely statistical definition of validity to fully evaluate whether or not a candidate surrogate endpoint is likely to be safe and effective (e.g. (Alonso *et al.*, 2004; VanderWeele, 2013)). At least two qualitative approaches have been proposed. These might be used instead of, or in addition to, attempts to measure statistical properties such as the LRF, PIG, AA, or RE.

Firstly, Wu et al., (2011) describe operational criteria to assess whether the direction of treatment effect on the surrogate is the same as that on the true endpoint. These are based on counterfactual terms, but can be assessed using procedures available in commercial statistical packages (e.g. generalized linear models).

Secondly, VanderWeele, (2013) discusses conditions that would be sufficient to ensure the surrogate paradox is avoided. He proposes three questions to assess the danger of being misled by a prospective surrogate (Figure 18):

1) Might there be a negative direct effect of treatment on the true endpoint, not through the surrogate?
2) Might the positive surrogate-true endpoint association be due to confounding?
3) Might treatment affect the surrogate for different people than for whom the surrogate affects the true endpoint (i.e. a lack of transitivity)?

If the answer to all three questions is “probably not”, one can have greater confidence that the surrogate endpoint does indeed reflect the true endpoint. This is a subjective assessment, based on *a priori* background information about relationships between treatment, surrogate, true endpoint, and potential confounders.

Figure 18: Relationships between treatment (A), surrogate (S), true endpoint (T), and unmeasured confounders (U).

Relationships between A and S, and A and T, are assumed to be estimated under conditions of experimental randomization, and therefore not subject to confounding in the same way as S → T. The surrogate paradox can arise through: (1) positive A → S → T effect, combined with a negative direct A → T effect; (2) confounding of S → T by U; (3) a lack of transitivity. In observational studies A is not randomized and so the relationships A → S and A → T are also subject to unmeasured confounders. These should be described, as far as possible, in a structural model on the basis of *a priori* information about the biological context. Adapted from Figure 2 in (VanderWeele, 2013)

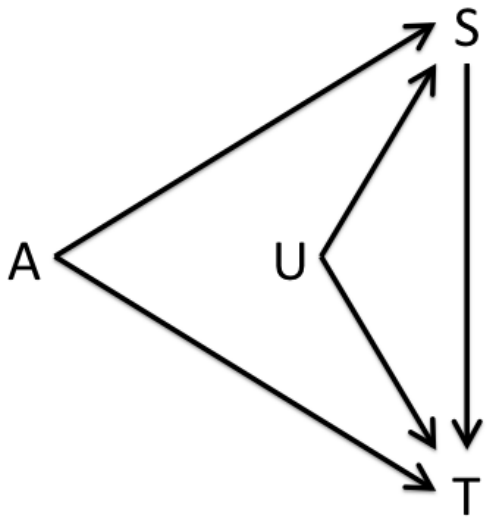

For both Wu et al., (2011) and VanderWeele, (2013), the conditions being assessed are sufficient, but not necessary. Failure to meet one (or more) does not prove a prospective surrogate is invalid. The criteria of Wu et al., (2011) make use of data from previous RCTs, while VanderWeele's questions rely on a *priori* knowledge of relationships between treatment, surrogate, and true outcome (VanderWeele, 2013).

This takes us back to considering the importance of the biological context, and the plausibility of analogy between what is measurable (e.g. the surrogate, the model

animal), and what one would like to know with certainty but can only infer (e.g. the true endpoint, human biology). Like judgements about the validity of analogical inferences in general (Bartha, 2013), when considering a surrogate endpoint the assessment of biological plausibility is ultimately subjective. The advantage of the questions proposed by VanderWeele is that they provide a systematic way to evaluate this context.

3.7 Adaptation of surrogate methodology to evaluate retinal biomarkers of brain disease

3.7.1 Strengths, weaknesses, and theoretical pitfalls

Thinking of retinal variables as "surrogate-like" entities (or proxy markers) and analysing them in terms of brain manifestation, disease exposure and outcome, has several potential advantages.

By forcing researchers to explicitly describe the biological paradigm being assumed, this approach incorporates information about disease specific biological context into analyses of retina-brain associations. There is no guarantee that the assumed biological paradigm is correct. But discovering that a well established retina-brain association does *not* hold when considered within the conventional biological context would be extremely useful, and could be investigated further by trying alternative frameworks that describe the data more accurately.

Showing that retinal variables are effectively equivalent to one or more brain variables ($S \Leftrightarrow T$), rather than just being directly associated, would allow investigators to reach much stronger conclusions about the meaning of retinal observations for a given disease. And even if a retinal variable (S) *did not* contain a large amount of the information in the brain variable (T), with respect to exposure (A) and clinical outcome (Z) - the assessment of these relationships would provide a more detailed view of the links between retina and brain than that provided by simple univariate tests of $S \rightarrow T$.

Having listed some strengths, several caveats should also be considered:

3.7.1.1 Imperfect measurement of disease exposure

An RCT has an unambiguous treatment variable. It is clear who had treatment or placebo, and information about treatment assignment is fully captured by the treatment variable. In contrast, an observational study of disease mechanisms may measure several variables that are somehow related to disease severity, but neither any single variable nor the combination of all available variables may capture all the important information about the disease exposure acting on observed manifestations of the disease, or on the clinical outcome. In other words, definition of A is simple for a clinical trial but might be very complex for an observational study. This has implications for estimating coefficients between A and S, T, or Z. A situation similar to the surrogate paradox could arise if A describes aspects of the disease that act to greater or lesser extent on S compared with T. For example, if A and S were positively associated, S and T were positively associated, but A and T were negatively associated (*cf.* VanderWeele's first question).

This could be addressed through thorough research of the disease in question before deciding what variables to measure for A, S, T, and Z. Investigators could consider using SEM to describe A as a latent variable, in order to summarize several observed variables that each describe part of a disease. They could also consider repeating the study in a separate validation cohort. In any case, publications arising from the analysis should clearly describe the rationale for choosing a particular variable to represent A, and explain the hazard of being misled if this variable doesn't fairly represent the disease in question with respect to S and T.

3.7.1.2 Incorrect paradigm relating disease, retina, brain, and outcome

VanderWeele's first question (VanderWeele, 2013) addresses the possibility of the surrogate paradox arising if there is a negative direct effect of A on T that is not mediated by S. In addition to imperfect disease exposure measurement, this

situation could also occur if the theoretical framework relating A, S, T and Z did not account for real direct effects of A on Z.

This could be addressed by assessing alternative frameworks that include or exclude direct paths from A to Z.

3.7.1.3 Lack of experimental randomization

In an RCT, the relationships A → S and A → T are estimated under experimental randomization, and the influence of confounders is controlled by design. Confounding could still occur for the relationship S → T, potentially resulting in the surrogate paradox (*cf.* VanderWeele's second question). However, in an observational study there is no experimental randomization, and all relationships are susceptible to confounding. Statistical control cannot substitute for a lack of experimental control (Joffe and Greene, 2009). With this in mind, note that the approach of Wu et al., (2011) involves inferences from pairwise measurements of association that can only be made under randomization, or by making untestable assumptions, and so is probably not suitable for observational data.

Again, this may be addressed by beginning with a thorough understanding of the biological context for the disease in question, and then designing a study to collect data on all known confounders of relationships between A, S, T, and Z, so that these can be included in the analysis. Investigators could consider repeating the study in a separate validation cohort. The increased risk of bias and confounding inherent in observational studies compared to RCTs (Vandenbroucke *et al.*, 2007), should be clearly described, and specifically that this particular analysis assumes there are no unmeasured confounders of relationships between A, S, T, and Z.

3.7.1.4 Lack of transitivity

The third route to the surrogate paradox involves a situation where the relationship A → S is positive for different people than for whom S → T is positive (a lack of transitivity) (VanderWeele, 2013). This situation ought to be avoided if paired data for A, S, T, and Z are collected on subjects in an observational study.

3.8 Proposed analytical framework

In this section I describe the application of these concepts to the data that I have collected in my clinical study of the retina in paediatric CM. However this approach is potentially relevant to any neurological disease with retinal manifestations.

3.8.1 Biological context of cerebral malaria

CM is a severe complication of infection with *P. falciparum*, characterized by coma, peripheral *P. falciparum* parasitaemia, and absence of any other identified cause of coma (World Health Organization, 2014b). It predominantly affects children in sub-Saharan Africa, and is an important contributor to the estimated 584,000 deaths worldwide from malaria in 2013 (World Health Organization, 2014a).

The mechanisms that allow the intravascular malaria parasite to cause coma and death remain unclear. However sequestration of parasitised erythrocytes in the microvasculature of the central nervous system is accepted as the chief pathological feature of the disease (Milner *et al.*, 2014; White *et al.*, 2013). It seems that, somehow, neurovascular sequestration causes injury to CNS parenchyma, which causes death. This constitutes a thumbnail sketch of a plausible biological paradigm for paediatric CM.

Measuring the severity of neurovascular sequestration in living patients is difficult. It may be possible to estimate total body parasite biomass by measuring a parasite-specific protein – Histidine rich protein 2 (HRP2) (Dondorp *et al.*, 2005). But although HRP2 does seem able to predict and diagnose CM (Fox *et al.*, 2013; Seydel *et al.*, 2012), plasma HRP2 cannot distinguish neurovascular sequestration from sequestration occurring in the rest of the body.

Several strong associations exist between retinal and brain manifestations of paediatric CM. For example, the presence of a characteristic malarial retinopathy accurately identifies true cases of paediatric CM from conditions with otherwise identical presentation (Taylor *et al.*, 2004), and the severity of retinal

haemorrhages is directly correlated with the severity of cerebral haemorrhages at autopsy (White *et al.*, 2001).

The severity of malarial retinopathy was recently shown to be directly associated with the severity of sequestration in both the retina and brain in fatal cases (Barrera *et al.*, 2015), suggesting that the retina may provide good biomarkers for cerebral sequestration and parenchymal injury in living patients. Furthermore, these associations are biologically plausible. They make sense in terms of anatomical and physiological similarities between discrete regions of retina and brain (MacCormick *et al.*, 2014).

Having considered the biological context of malarial retinopathy in paediatric CM, how might one test retina-brain associations to evaluate the equivalence of retinal and cerebral tissue damage in this disease?

3.8.2 Structure of disease paradigm and evaluation

Hypothetical relationships between disease severity (A), retina (S), brain (T) and outcome (Z) are illustrated in Figure 16. In this paradigm, both retina and brain are subject to proportional disease effects. Disease manifestations in retina and brain are directly associated, but cerebral disease manifestations alone cause death.

This framework can be evaluated in a number of ways, including simple tests of association between S and T that disregard other variables. Additional analyses could use surrogate-type statistics, such as the LRF or PIG, to estimate the degree to which S and T are interchangeable with regard to their relationship with A or Z. The ratio of coefficients for A → S and A → T could be calculated to derive a statistic similar in spirit to the RE. Importantly, both these specific coefficients as well as the global fit of the whole paradigm can be evaluated using SEM, and this can be compared to alternative frameworks (e.g. one with a direct A → Z path). The advantage of SEM is that it takes account of more complex (and realistic) relationships between variables than methods such as linear regression. Failure to include the correct confounding variables creates multivariate models that are

prone to bias (Greenland *et al.*, 1999). On the other hand, employing information about the biological context to specify a fuller model structure may provide a way to both limit bias and test the goodness of fit for the hypothetical biological paradigm.

3.9 Conclusion and future perspectives

My approach of treating retinal variables as proxy markers of brain disease has the potential to describe relationships between prospective retinal biomarkers and brain disease features much more richly than simple tests of association, or even multiple regression models. Careful attention must be given to the biological context within which retina-brain associations are being tested, since inadequate variable measurement, and the impact of unmeasured confounders, could lead to misleading results. However, this risk is arguably no greater than for conventional approaches. The risk may even be less, since the demand for an explicit description of the biological paradigm being hypothesized should at least help to clarify where assumptions might be less reliable.

Neurological biomarkers will be demanded with increasing urgency as industrialized populations continue to age, and growing numbers of people require investigations and treatments for neurodegenerative disease. So far, the retina has largely been investigated as a source of variables that are associated with brain dysfunction. If, as many authors seem to think, the retina truly is analogous to the brain, then the scientific community must develop methods to gain the clearest and most panoramic view through this biological window.

Chapter 4 – Setting, patients and methods

4.1 Aim of chapter

Describe where, when, and how the research described in this thesis was carried out

4.2 Introduction

The data analysed in this thesis were collected and processed in the context of a clinical research facility in a hospital serving a large, and growing city in sub-Saharan Africa. This imposed practical constraints on this work that most likely do not apply to similar projects being performed in Europe or the United States. This chapter begins with a brief description of where this project took place, and the research resources that were available, followed by details of how patients were recruited, and data collected and analysed. Detailed methods relevant to specific results are also described in relevant chapters.

4.3 Location

4.3.1 Malawi and Blantyre

This research took place in Malawi, a relatively small country in East Africa. Its surface area is roughly half that of the United Kingdom[5], and a significant proportion of this includes Lake Malawi, which along with Lake Victoria and Lake Tanganyika is one of the African Great Lakes of the East African Rift. Malawi is land locked and surrounded by Tanzania to the North, Zambia to the West, and Mozambique to the West, South and East (Figure 19). Lake Malawi contains more species of fish than any other lake on earth, and ophthalmologists may be interested to learn that cichlid colour vision appears to be an important factor in the development of such great species diversity (Pauers, 2011).

5 The surface area of Malawi is 118,484 Km^2, and that of the UK is 242,495 Km^2 (‘UNdata | Malawi’, ‘UNdata | United Kingdom’)

Figure 19: Location of Malawi and Blantyre.

The African continent (left) with Malawi in green, and the major cities within Malawi (right). Lilongwe, the capital, is shown with a star. Blantyre is shown by a green arrow. Images are from (‘CIA World Factbook | Malawi').

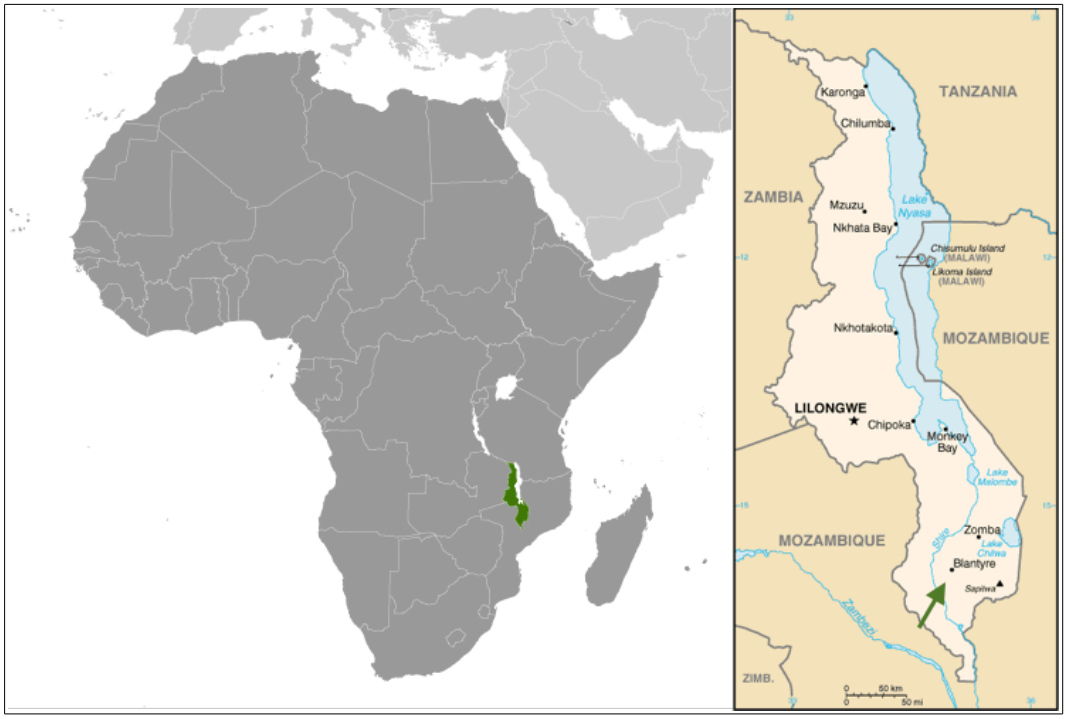

The population of Malawi is growing rapidly. The estimated population in 2014 was just over 17 million (‘CIA World Factbook | Malawi'), giving an estimated average population density of 196/ Km^2. Population growth is 3%, and there are an estimated 5 births per woman (‘The World Bank | Data’). A large proportion of the population are young. 45% were aged 0 to 14 years in 2013 (‘UNdata | country profile | Malawi’). A high proportion of children are enrolled in primary school, but a much smaller proportion go on to secondary school education (37%) (‘The World Bank | Data’). The prevalence of HIV in adults is roughly 10% (2013) and this has been declining steadily since 2000 (‘UNAIDS | Malawi’).

It is a poor country with an estimated gross national income per capita of $270 (in 2013). In the same year the Central African Republic had GNI per capita of $320, and the UK $41,680. Average life expectancy at birth is 55 years, and approximately 72% of the population live on less than $1.75 per day (data from 2010). The distribution of wealth is vastly unequal, with the wealthiest 10%

holding 37.5% of national income, and 2.2% in the hands of the poorest 10% (data from 2010). 90% of the workforce are employed in agriculture. The main exports are tobacco, sugar, and tea, but a large proportion of the economy is funded by international aid. In 2011 Malawi spent 8% of Gross Domestic Product on healthcare, and 5% on education ('The World Bank | Data'). Corruption is a significant problem, and Malawi is ranked 110/173 countries on the corruption perceptions index ('Transparency International'). Foreign aid was suspended in 2013 after a scandal about theft of government funds, known as "Cashgate" ('CIA World Factbook | Malawi').

Blantyre is the second largest city in Malawi after the political capital, Lilongwe, and is often referred to as the commercial capital. The population in 2015 is estimated at just over 1 million. It was founded in 1876 as a result of missionary work by the Church of Scotland, and was named after the birthplace of the Scottish explorer David Livingstone which is just south of Glasgow. It sits at a relatively high altitude of approximately 1000m in the Shire highlands above the Eastern edge of the East African Rift, and is surrounded by several hills ('Wikipedia | Blantyre'). Infrastructure is unstable, and shortages of electricity and water are common. Voltage surges occur when mains power is restored, resulting in damage to electrical equipment if it is not appropriately protected.

Malaria in Blantyre is seasonal, roughly following the start of the rainy season in November. Transmission within Blantyre is limited, consistent with its high altitude (Reyburn *et al.*, 2005), but nearby surrounding areas are lower and have much higher transmission (Figure 20) (Bennett *et al.*, 2013; Mathanga *et al.*, 2012; Wilson *et al.*, 2012).

Figure 20: The spatial distribution of estimated entomological inoculation rate in Malawi in 2010.

Blantyre has a low estimated rate of mosquito transmission in contrast to surrounding areas (‘Malaria atlas project’).

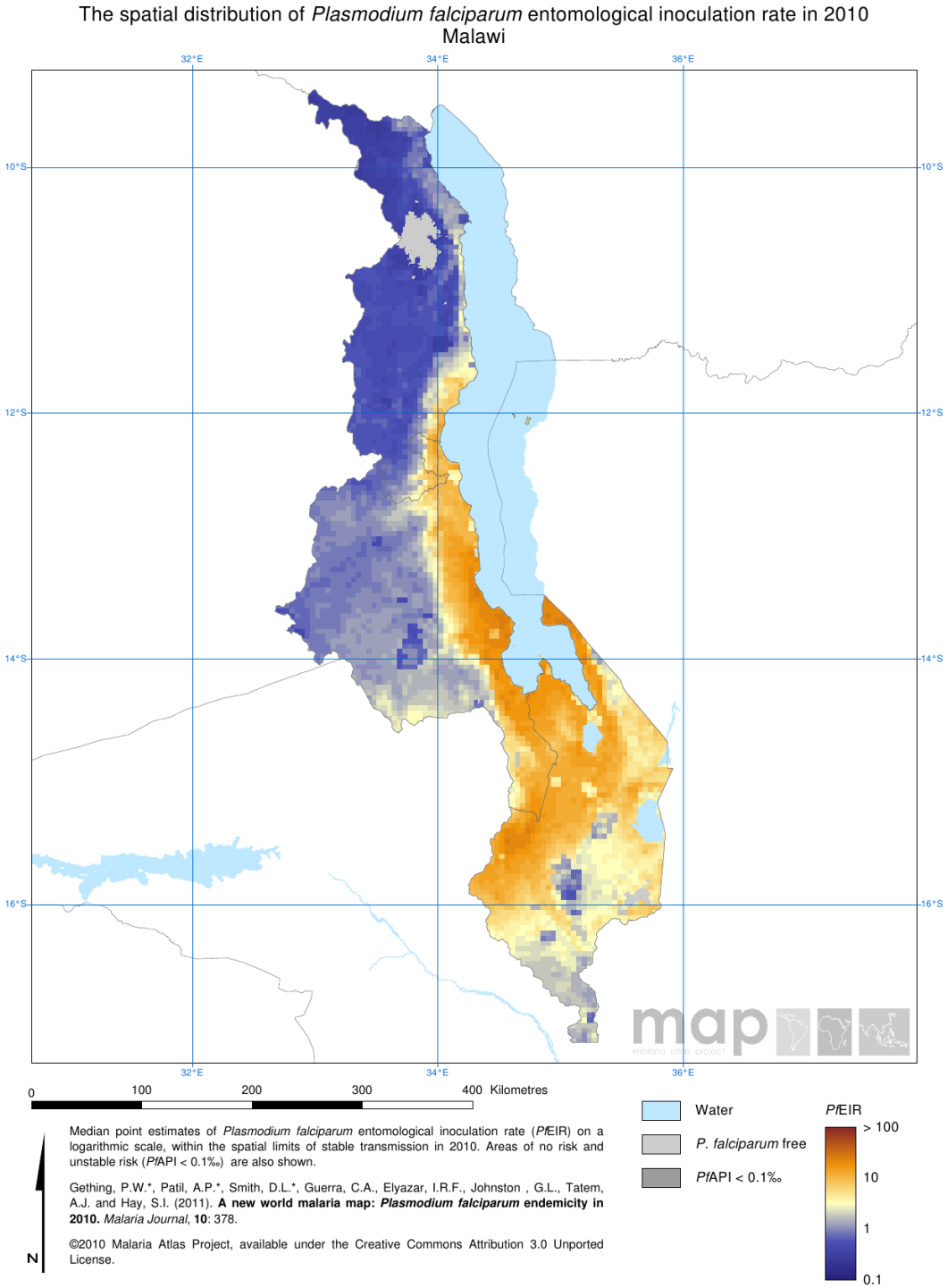

4.3.2 Queen Elizabeth Central Hospital

Queen Elizabeth Central Hospital (QECH) has approximately 1000 beds and functions as a secondary and tertiary referral centre for district hospitals and local heath centres throughout the Southern region of Malawi ('Wikipedia | Blantyre'). It has several departments, including Adult and Paediatric Medicine, various surgical specialities, Accident and Emergency, Dermatology, ENT, Obstetrics and Gynaecology, and Radiology. An Eye Hospital exists nearby in a separate building and functions autonomously from QECH. An MRI scanner was installed in 2008. However, in general resources are seriously inadequate and hospital wards are typically overcrowded and unsanitary. It is not unusual for the hospital to run out of essential medicines, and for patients to sleep on the floor due to a shortage of beds and space.

4.3.3 Paediatric research ward and Malaria Research Project

The Paediatric Research Ward (PRW) functions both as a clinical research facility and as a high-dependency unit for the Department of Paediatrics. It is much better staffed and equipped than other wards, and receives patients with cerebral malaria (CM) and other causes of coma. It also provides a space for paediatric research. The nurse to patient ratio is between 1:1 and 1:2. Traditionally the research emphasis has been on severe malaria, and the PRW is the site of a long running study on paediatric CM – the Malaria Research Project (MRP). This was started in 1986 by Terrie Taylor and Malcolm Molyneux, and has been jointly funded by National Institutes of Health, USA, and the Wellcome Trust, UK. Work in the PRW is largely continued by research affiliates within the University of Malawi College of Medicine (established in 1991): the Blantyre Malaria Project (BMP), and the Malawi-Liverpool-Wellcome Trust (MLW) Clinical Research Programme, established by Taylor and Molyneux, respectively[6]. The stability of the MRP over such a long period has resulted in the accumulation of a very large number of subjects, all recruited and treated according to consistent protocols (Taylor, 2009).

6 Malawi-Liverpool-Wellcome Trust Clinical Research Programme website: http://www.mlw.medcol.mw/

Although all subjects have had certain core investigations, involvement of various external collaborators and provision of research equipment at different times has led to groups of MRP subjects undergoing different types of additional investigation. For example, although the retina was being examined from 1993, collection of standardised retinal exam data began in 1999. Colour and FA images were taken from 2006. MRI brain scans were performed from 2009. A subgroup has data from all three imaging modalities.

Research output from the PRW has been diverse. Early influential work included the development of a standard way to assess the depth of paediatric coma (the Blantyre Coma Score) (Molyneux *et al.*, 1989), and the discovery that hypoglycaemia was a major cause of coma and death in children with severe malaria (Taylor *et al.*, 1988). A major theme has been the histopathology of fatal paediatric CM (Barrera *et al.*, 2015; Dorovini-Zis *et al.*, 2011; Milner *et al.*, 2005, 2013, 2014, 2015; Seydel *et al.*, 2006; Taylor *et al.*, 2004; Whitten *et al.*, 2011), and broadly speaking much work has been done on factors related to disease severity and death from this disease, including the role of malarial retinopathy.

The number of patients being admitted to the PRW with CM was stable until 2010 (Roca-Feltrer *et al.*, 2012) but has been declining since then. The number of admissions in 2014 was approximately half that in 2010 (when there were approximately n=160).

4.3.4 MRet Programme Grant

My PhD thesis is based on work carried out within a Programme Grant funded by the Wellcome Trust[7]. This programme (abbreviated title MRet) encompassed several work packages, relating to automated analysis of fluorescein images, associations between retinal features and MRI brain features, visual and visuomotor function in survivors of CM, and ocular histopathology. Of these, the work on retinal and MRI brain data is most directly relevant to this thesis, but my

7 Prof Simon P Harding, Prof Alister G Craig, Prof Malcolm E Molyneux, Prof Paul S Hiscott, Professor Robert Heyderman, Dr Paul C Knox, Dr Samuel D Kampondeni, Prof Terrie E Taylor, Dr Macpherson Mallewa. The retinal microvasculature in cerebral malaria in African children (MRet); grant number: 092668/Z/10/Z

role as Clinical Research Fellow for the programme meant I was involved in all work packages to some extent.

All MRet work packages depended on access to subjects initially recruited to the MRP. Retinal examination and imaging had previously been integrated into the admission study protocol in the course of prior studies (Beare, 2005), and this was continued for the duration of the MRet grant.

I carried out work for MRet from an office in MLW, which afforded internet access and support with finance, human resources, procurement and stores. I performed clinical examinations and retinal photography in the PRW, and liaised with colleagues and senior researchers in QECH and BMP.

4.4 Thesis methods

4.4.1 Ethical approval

The studies that provided data for the analyses in this thesis were approved by ethics committees of both local and collaborating institutions. The investigators involved in these studies adhered to the tenets of the Declaration of Helsinki.

4.4.2 Study design

The studies reported in chapters 6, 7, and 8 are all prospective cohort studies. Subjects with CM were recruited on admission to the PRW, retinal or MRI brain features were measured, and then subjects were followed over time so that clinical outcomes could be recorded.

4.4.3 Recruitment

Subjects analysed in this thesis were recruited to the MRP between 1999 and 2014. I personally examined subjects recruited between 2012 and 2014. Because the natural history of paediatric CM usually progresses to death or resolution of coma within a few days, follow up was completed while subjects were inpatients on the PRW.

Data from various imaging modalities is available from different years. This means that different, overlapping groups of subjects have data from particular combinations of these modalities.

Chapter 6 reports associations between ophthalmoscopic examination and clinical outcomes. Subjects with these data were recruited between 1999 and 2014 inclusive.

Chapter 7 reports associations between FA and clinical outcomes. Subjects with these data were recruited between 2006 and 2014 inclusive, but excluding 2011. No FA were performed in 2011.

Chapter 8 reports associations between retinal features and characteristics of MRI brain scans. Subjects with these data were recruited from 2009 to 2014 inclusive. Ophthalmoscopic examination *was* performed in 2011, but FA was not. This means that the group of subjects with both ophthalmoscopic and MRI data is larger than the group with both FA and MRI data.

4.4.4 Participants

Subjects were recruited to the MRP from consecutive admissions to the PRW. Comatose patients were transferred to the PRW from other wards at QECH. The long history of the PRW within the hospital has led to a good awareness of the importance of prompt referral – both for recruitment to various research projects and also so that patients can benefit from more intensive care. Criteria for recruitment to the MRP are shown in Table 8. In addition, subjects were only eligible for analyses reported in my thesis if they had paediatric CM and one or more signs of malarial retinopathy. Subjects were eligible for inclusion in analyses of admission parameters if they had retinal data collected within 48 hours of admission. This is a relatively long window, and was chosen to maximise sample size. The proportion of subjects with retinal data first recorded between 24 and 48 hours of admission tended to be smaller than those with data from <24 hours of admission.

Cerebral malaria was defined as:

- Peripheral *P. falciparum* parasitaemia, and
- Blantyre coma score ≤2, and
- No other identifiable cause of coma, after specifically ruling out hypoglycaemia, post-ictal state, and meningitis (World Health Organization, 2014b)

Malarial retinopathy was defined as the presence of one or more of the following signs, in the context of a clinical diagnosis of paediatric cerebral malaria:

- Retinal haemorrhage
- Retinal whitening
- Retinal vessel discolouration

In general most subjects have more than one sign. A detailed description of the retinal signs included in this definition in Chapter 1. Papilloedema is commonly seen in CM but does not, on its own, indicate the presence of malarial retinopathy (Taylor *et al.*, 2004). Subjects with severe papilloedema who also had peri-papillary haemorrhages in keeping with papilloedema were considered *not* to have malarial retinopathy if they had no other retinal signs.

Subjects were excluded from an analysis if:

- They did not have valid consent (i.e. it was withdrawn by the guardian)
- They had an admission coma score >2

Specific reasons for not imaging a subject were not recorded for every case. In general a subject would not undergo ophthalmoscopy or retinal imaging if the ophthalmologist was not available, or if the subject was either too unwell or recovering very rapidly. Similar reasons applied to MRI scans. Subjects were also not scanned if the MRI was being serviced.

Table 8: Recruitment criteria and treatment protocols for subjects in the Malaria Research Project from 1999 to 2014

Year	1999-2006	2007	2008 – 2013	2014
Admission criteria for unconscious patients	6 months ≤ Age BCS ≤ 2 MPs positive or negative CSF cloudy or clear	6 months ≤ Age BCS ≤ 2 MPs positive, CSF cloudy or clear MPs negative, CSF clear	6 months ≤ Age ≤ 12 years BCS ≤ 2 MPs positive CSF cloudy or clear	6 months ≤ Age ≤ 12 years BCS ≤ 2 MPs positive CSF cloudy or clear
Exclusion criteria	Grossly malnourished	Grossly malnourished	Grossly malnourished Obvious evidence of HIV infection	Grossly malnourished Obvious evidence of HIV infection
Treatment for malaria	IV quinine 20mg/kg over 4 hours, then: IV quinine 10mg/kg over 2 hours, every 12 hours (at least 3 doses), then: When able to swallow give a treatment dose of SP	IV quinine 20mg/kg over 4 hours, then: IV quinine 10mg/kg over 2 hours, every 12 hours (at least 3 doses), then: When able to swallow give a treatment dose of SP	IV quinine 20mg/kg over 4 hours, then: IV quinine 10mg/kg over 2 hours, every 12 hours (at least 3 doses), then: When able to swallow give a treatment dose of LA	IV artesunate 2.4mg/kg 12 hourly for 3 doses, then standard course of LA, through naso-gastric tube if necessary
BCS = Blantyre coma score; MPs = peripheral blood smear for *P. falciparum*; CSF = Cerebrospinal fluid; IV = Intravenous; Quinine = Quinine Dihydrochloride; SP = Sulfadoxine/Pyrimethamine; LA = Lumefantrine/Artemether				

4.4.5 Treatment

Patients admitted to the PRW with severe malaria were treated according to standard protocols and national guidelines (Table 8). Practical techniques for assessing and treating patients in this setting are described in (Taylor, 2009). Subjects did not undergo any research investigation that was deemed inappropriate by the PRW clinicians.

4.5 Variables

Outcome, exposure, and potentially confounding variables are listed in Table 9.

4.6 Sources of data

4.6.1 Standard history, examination and investigations

A range of variables were recorded from the standard admission history, examination and investigations.

This history included questions about subject age, sex, and duration of fever and coma pre-admission. The examination included assessment of features such as weight, height, rectal temperature, systolic blood pressure, signs of respiratory distress, presence of convulsions, and Blantyre coma score (Molyneux *et al.*, 1989).

Investigations included analysis of finger prick blood sample for blood glucose, packed cell volume (haematocrit) and density and species of peripheral parasitaemia. White cell count and platelet count were measured from a full blood count (Coulter Counter, Becton-Dickinson, Franklin Lakes, New Jersey). Blood lactate was measured using a finger prick blood sample (Lactate Pro point of care detector (Arkay Inc)). Plasma HRP2 was measured from stored samples using ELISA (Celabs). HIV status was determined using two different tests (Uni-Gold HIV1/2 – Trinity Biotech, Carlsbad, CA; Determine HIV1/2 – Inverness Medical, Orlando, Florida). A lumbar puncture was performed unless deemed inappropriate by the admitting clinician, and this was used to measure opening pressure and analyse cell count, Gram stain, and culture (Taylor, 2009).

The primary outcome was whether a patient recovered or died. Obvious neurological sequelae sometimes occurred in patients who survived, including focal neurological deficits, cortical blindness, and similar gross disabilities.

The secondary outcome was the time between admission and recovering from coma. This was defined as a Blantyre coma score of ≥3/5. Both were recorded in patient records on the basis of clinical examination.

4.6.2 Ophthalmoscopic examination

Retinal features were recorded by an ophthalmologist on a standard form (Harding *et al.*, 2006) (Appendix 1). The categories for grading severity of each feature were originally decided on the basis of clinical experience with malarial retinopathy, and consensus among experts. I have continued to use these gradings to maintain consistency with pre-existing data from Malawi and other sites. Tropicamide 1% and phenylephrine 2.5% eye drops were used to dilate both pupils, except in 2014 when only the left eye was dilated. Drops were repeated if necessary. Examination was performed using various makes and models of indirect and direct ophthalmoscope. From 2012 to 2014 a Keeler Digital Vantage Plus LED indirect ophthalmoscope and Volk 20D lens was used. The lids were opened manually, and indentation was not performed. Previous work indicates that grades for features of malarial retinopathy using this standard form to record findings from dilated indirect ophthalmoscopy are consistent between ophthalmologists (Beare *et al.*, 2002).

4.6.3 Retinal photography

Where possible retinal imaging was carried out immediately after indirect ophthalmoscopic examination. Pupils were dilated with tropicamide 1% and phenylephrine 2.5% if they were not already dilated. Comatose subjects were transferred to a special bed that was set at an appropriate height for the retinal camera. In almost all cases images were taken with the subject lying in the left lateral position (Figure 21). In some cases the right lateral position was used to prevent obstruction of a cannula in a scalp vein on the left side. A nurse was

present to monitor the patient during photography, and to assist with manual opening of the lids.

An ophthalmologist captured 50 degree retinal images using a Nikon D1-H digital camera attached to a Topcon 50-EX optical unit (Figure 21). The pupil lever was set to “small”. Flash was typically set to “36” for colour images and “75” to “100” for fluorescein images. Images were stored using Topcon Imagenet software on a desktop computer running Windows XP. Images were saved in JPEG format at various levels of compression from 2006 to 2010, and in TIF format from 2012 to 2014. Colour images were taken first, followed by FA. After checking the patency of the peripheral venous cannula, sodium fluorescein (10% or 20%) was injected. The dose was relative to subject weight[8], and given at approximately 1ml/sec. Images were taken throughout the fluorescein run in an attempt to capture as much of both retinas as possible at all stages of the angiogram. Images were typically not taken after 12min.

Figure 21: The author taking retinal photographs in the Paediatric Research Ward

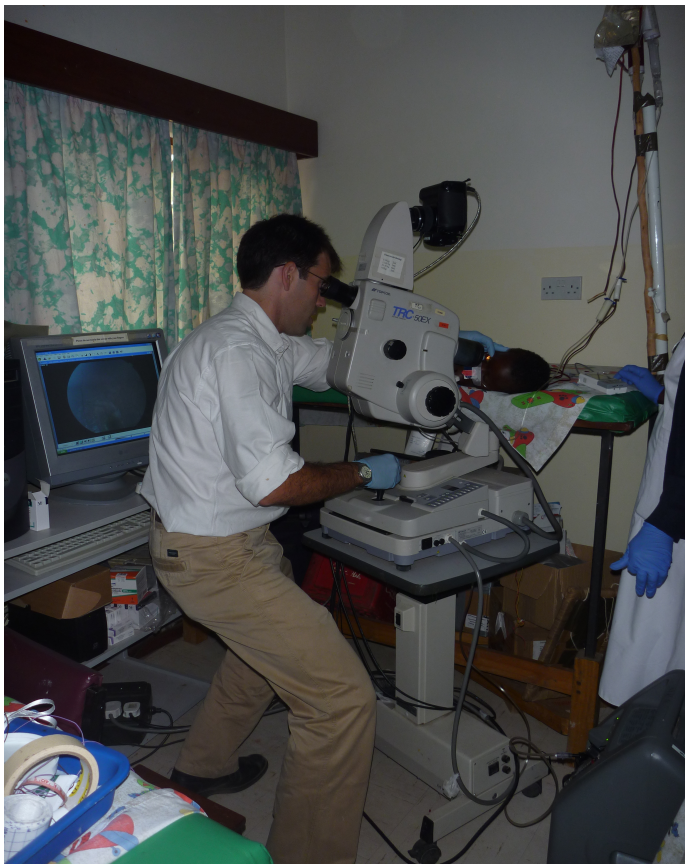

8 5-10Kg = 2ml; 11-20Kg = 3ml; 21-30Kg = 4ml; >30Kg = 5ml

4.6.4 MRI brain scans

All MRI scans were performed on a 0.35T Signa Ovation Excite scanner (GE Healthcare, Milwaukee, Wisconsin). Imaging protocols included sagittal T1 FLAIR, axial T2 FRFSE, axial T1, coronal T2 FRFSE, and EPI-DWI sequences. Detailed information about scan sequences can be found in Seydel et al., (2015) (supplementary information).

4.7 Data handling

4.7.1 Standard history, examination and investigations

Clinical data were recorded for each subject on paper charts at admission and during the hospital stay (Taylor, 2009). These was then double entered into a database by data entry clerks at the Blantyre Malaria Project and discrepancies were checked against the original records and corrected.

4.7.2 Ophthalmoscopic exam

Retinal exam data was entered into a database (REDCap) (Harris *et al.*, 2009). Data was entered once, by one individual (myself). I checked a random 10% sample of all forms and this revealed an average error rate of 0.5%.

4.7.3 Retinal photography

To generate quantitative data from FA sequences, I devised a grading scheme (Chapter 5; Appendix 2). To do this I reviewed angiographic features in Malawian children with CM and then presented representative images to an expert group with knowledge of severe malaria and malarial retinopathy. The consensus group then discussed and approved terminology, definitions of various levels of severity, and representative standard images. Where possible we attempted to maintain consistency with the pre-existing ophthalmoscopic grading scheme.

Grading of images was then performed by two professional graders in the Liverpool Ophthalmic Reading Centre, St Paul's Eye Unit, Liverpool, UK with 9.5 and 1.5 years experience in grading fluorescein angiogram (FA) images from other retinal diseases, such as age-related macular degeneration. Images were

viewed using Microsoft Office 2010 Picture Manager, on Dell P2412H screens with 1920×1020 resolution, and enhanced with standard tools as necessary (e.g. brightness, contrast). Montages were created using Imagenet IBase (Topcon, Japan), and a grid indicating retinal zones and quadrants was overlaid to facilitate grading and calibration (Chapter 5) (In house software, Matlab, Mathworks). Graders reviewed montages and original FA images, and were encouraged to check corresponding colour images.

Disagreement between graders was defined as ≥ two-level discrepancy for ordinal variables (i.e. variables with 3 or more levels), and any discrepancy in binary variables. Disagreement was adjudicated by one of two ophthalmologists with several years experience of FA in paediatric CM (myself, and Prof. Simon Harding). All observers were masked to subject identity and clinical characteristics, including outcome.

4.7.4 MRI brain scans

Two radiologists (Dr Sam Kampondeni and Dr Mike Potchen) graded MRI scans from 2009 to 2011, according to a scoring procedure they devised after subjectively examining images from 2009 and 2010 (Potchen *et al.*, 2013). Both graders were masked to retinopathy status and clinical outcome. Dr Kampondeni is based in Blantyre, Malawi, and has a fellowship in MRI; Dr Potchen is now based at the University of Rochester and has a fellowship in neuro-radiology. Inconsistencies between graders were resolved by discussion and mutual consensus. Agreement was formally checked for a sample of scans and found to be 71-96%, depending on the lesion (Seydel *et al.*, 2015). MRI scans from 2012 to 2014 were dual graded by a team of three neuro-radiologists at the University of Rochester, with adjudication by an independent observer (Dr Potchen). Data was entered directly into the NeuroInterp database (Potchen *et al.*, 2013).

4.7.5 Data processing

All data were exported to Microsoft Excel, and then imported to Stata (version 13, StataCorp, Texas). I then used Stata to clean and merge datasets, as well as create indicator variables for various subject groups, summary variables, and versions of ordinal variables with fewer categories than originally recorded. All FA variables

were collapsed to four levels (0 to 3) if the original variable had more levels than this. Commands were recorded in Stata do-files.

4.8 Statistical methods

Further details of specific statistical approaches used for a given analysis are described in the relevant chapter. All analyses were performed using Stata (version 13, StataCorp, Texas).

Individual variables were summarised using tables or histograms to check frequency and distribution. Summary tables were created to describe the characteristics of relevant subject groups, and where appropriate these were compared between groups using logistic regression to generate unadjusted odds ratios and 95% confidence intervals. In some cases where variables were highly skewed and the odds ratio seemed to be out of keeping with the difference in group medians I used the Kruskal-Wallis test to generate a p-value.

Potential selection bias was assessed by comparing subjects who did, or did not, have relevant investigations (e.g. ophthalmoscopic exam, FA, MRI brain).

Unadjusted associations with clinical outcomes were estimated in a similar way, by comparing groups of subjects who lived or died. Coma recovery time was not distributed normally and so analysis using linear regression would have been inappropriate. The distribution was truncated and highly skewed with over dispersion, and so truncated negative binomial regression was used to estimate unadjusted and adjusted associations with this outcome.

Variables were selected for multivariate regression models on the basis of these criteria:

- a plausible causal relationship is likely to exist with the outcome, based on expert opinion and evidence from the literature
- a statistically significant unadjusted association exists with the outcome, and this association is large enough to be clinically relevant

These criteria were selected because the aim of analysis was generally to develop a better understanding of disease mechanisms that might lead to the outcome. This aim is in contrast to the aim of predicting an outcome (Altman and Royston, 2000), and this distinction can be very important for interpreting results of statistical models.

For example, depth of coma and papilloedema are traditionally included in models of death in CM, because they are both significantly associated with death. However, recent evidence suggests that death occurs as a result of severe brain swelling (Seydel *et al.*, 2015). Note that, biologically speaking, papilloedema is likely to be *effects* of brain swelling rather than causes. Other variables (such as depth of coma on admission) are not clearly likely to be reasonable exposures that cause brain swelling or death, but may be related to brain processes in complex ways.

These variables do undoubtably contain information that is useful for *predicting* death from brain swelling. This is clear from their significant associations with this outcome. However, their inclusion as independent "exposures" in a model aimed at illuminating disease mechanisms leading to death does not make biological sense. As a result their inclusion could cause problems for biological interpretation of the model, as well as potentially affecting the coefficients of more plausible causes of death in unpredictable ways. These issues are helpfully discussed by Beyea and Greenland, (1999), and Greenland et al., (1999).

An arbitrary cut-off of $p<0.01$ was chosen for unadjusted associations, because it restricted the number of strata eligible for the multivariate models. However there were few, if any, cases where $0.01 < p < 0.05$ and a variable appeared to have a clinically significant effect size. I think it is reasonably likely that the threshold of $p<0.01$ did not exclude variables containing a clinically meaningful amount of information.

Table 9: List of variables used in this thesis, with description of each variable.

Suffixes indicate the eye from which data were obtained ("_r" or "_re" indicates the right eye; "_l" or "_le" indicates the left eye; "_w" indicates the worst affected eye)

Category	Variable	Abbreviation	Description	Measurement	Comments
Identification	ID number	pid	Unique four-digit number. Each number identifies a given subject	N/A	None
Clinical history	Age	age	Age of subject at admission (in months); .a = missing	History from parent/guardian, and/or health passport	Date of birth is notoriously unreliable in Malawi. Expect random error in this variable
	Sex	sex	Sex of a subject 0 = male; 1 = female; .a = missing	Admission history and examination	None
	Duration of fever pre-admission	feverdur	Time in hours; .a = missing	Admission history	None
	Duration of coma pre-admission	comadur	Time in hours; .a = missing	Admission history	None
	History of convulsions pre-admission	hxconv	0 = no; 1 = yes; .a = missing	Admission history	None
Clinical examination	Weight	wt	Kg; .a = missing	Admission exam	None
	Height	ht	Cm; .a = missing	Admission exam	None
	Mid-upper arm circumference (MUAC)	mac	Cm; .a = missing	Admission exam	None
	Rectal temperature	temp	Degrees C; .a = missing	Admission exam	None
	Systolic blood pressure	bp	MmHg; .a = missing	Admission exam	None
	Respiratory rate	resp	Breaths/sec; .a = missing	Admission exam	None
	Nasal flaring	nasflaring	0 = absent; 1 = present; .a = missing	Admission exam	None

Category	Variable	Abbreviation	Description	Measurement	Comments
	Chest indrawing	chstin	0 = absent; 1 = present; .a = missing	Admission exam	None
	Intercostal retraction	retraction	0 = absent; 1 = present; .a = missing	Admission exam	None
	Deep breathing	deepbr	0 = absent; 1 = present; .a = missing	Admission exam	None
	Grunting	grunt	0 = absent; 1 = present; .a = missing	Admission exam	None
	Respiratory distress	respdis	Any one of: nasal flaring, chest indrawing, retraction, deep breathing 0 = absent; 1 = present; .a = missing	Admission exam	none
	Witnessed convulsions during admission	admfits	0 = absent; 1 = present; .a = missing	Admission exam	None
	Blantyre coma score	comasc	0 = 0; 1 = 1; 2 = 2; 3 = 3; 4 = 4; 5 = 5; .a = missing	Admission exam	None
Clinical investigations	CSF opening pressure	opencsf	mmCSF; .a=,missing	Flexible manometer (Taylor et al., 2009)	None
	Peripheral parasitaemia	admpta	Cells; .a = missing	Microscopy of finger prick sample	None
	Peripheral white blood count	abldwbc	Cells; .a=missing	Venous full blood count (Coulter Counter, Becton-Dickinson, Franklin Lakes, New Jersey)	None
	Peripheral platelet count	platelet	Platelets; .a=missing	Venous full blood count (Coulter Counter, Becton-Dickinson, Franklin Lakes, New Jersey)	None
	Haematocrit	ahct	%; .a = missing	Finger prick sample and centrifuges microhaematocrit tube	None
	Venous lactate	admlact	mmol/L; .a=missing	Lactate Pro point of care detector (Arkray Inc)	None

Category	Variable	Abbreviation	Description	Measurement	Comments
	Histidine rich protein 2	hrp2	ng/ml; .a=missing	Celabs ELISA	None
	HIV	hiv	0 = negative; 1 = positive; .a = missing	Uni-Gold (Trinity Biotech, Carlsbad, CA) and Determine (Inverness Medical, Orlando, Florida)	Discrepant results were adjudicated by repeating one of the two tests
Outcomes	Clinical diagnosis	disdx	1 = cerebral malaria 2 = severe malarial anaemia 3 = cerebral malaria & severe malarial anaemia 4 = meningitis 5 = other malarial diagnosis 6 = non-malarial anaemia 7 = other non-malarial diagnosis .a = missing	Clinical assessment	None
	Clinical outcome	disoutcome	1 = full recovery 2 = recovery with neurological sequelae 3 = death 4 = withdrew .a = missing	Clinical assessment	None
	Time taken to reach BCS≥3	timetocs3	Time in hours; .a=missing or not applicable	Clinical assessment	Some subjects never woke up
	Fits after admission	fitsaftadm	0 = no; 1 = yes; .a = missing	Clinical assessment	None
Ophthalmoscopic examination	Retinal haemorrhages	ahaem_r ahaem_l ahaem_w	Severity of retinal haemorrhages 0 = none; 1 = 1-5; 2 = 5-20; 3 = 20-50; 4= >50; .a = missing; .c = can't grade	Dilated fundus examination using indirect ophthalmoscopy and standard grading form	See appendix for grading form

Category	Variable	Abbreviation	Description	Measurement	Comments
	Papilloedema	apap_r apap_l apap_w	Presence or absence of papilloedema 0 = absent; 1 = present; .a = missing; .b = not applicable; .c = can’t grade	Dilated fundus examination using indirect ophthalmoscopy and standard grading form	See appendix for grading form
	Severity of papilloedema	apaps_r apaps_l	Severity of papilloedema. Only graded if papilloedema was present. 2 = mild; 3 = moderate; 4 = severe; .a = missing; .b = not applicable; .c = can't grade	Dilated fundus examination using indirect ophthalmoscopy and standard grading form	Definitions from (Smith *et al.*, 2009)
	Disc hyperaemia	adiskhyp_r adiskhyp_l adiskhyp_w	Presence or absence of disc hyperaemia 0 = absent; 1 = present; .a = missing; .b = not applicable; .c = can’t grade	Dilated fundus examination using indirect ophthalmoscopy and standard grading form	See appendix for grading form
	Macular whitening	awhitcmac_r awhitcmac_l awhitcmac_w	Severity of macular whitening 0 = none; 1 = <1/3 disc area; 2 = 1/3 to 1 disc area; 3 = >1 disc area .a = missing; .b = not applicable; .c = can't grade	Dilated fundus examination using indirect ophthalmoscopy and standard grading form	See appendix for grading form
	Foveal whitening	acfa_r acfa_l acfa_w	Severity of foveal whitening 0 = none; 1 = <1/3 foveal area; 2 = 1/3 to 2/3 foveal area; 3 = >2/3 foveal area; .a = missing; .b = not applicable; .c = can't grade	Dilated fundus examination using indirect ophthalmoscopy and standard grading form	See appendix for grading form

Category	Variable	Abbreviation	Description	Measurement	Comments
	Peripheral whitening, temporal quadrant	awhitptemp_r awhitptemp_l awhitptemp_w	Severity of whitening in the temporal quadrant 0 = none; 1 = mild; 2 = moderate; 3 = severe; .a = missing; .b = not applicable; .c = can't grade		The temporal quadrant was seen more consistently than other quadrants. Therefore this quadrant was chosen to represent peripheral features
	Orange vessels, temporal quadrant	orvess_temp_r orvess_temp_l orvess_temp_w	Presence or absence of orange vessels in the temporal quadrant 0 = absent; 1 = present; .a = missing; .b = not applicable; .c = can't grade	Dilated fundus examination using indirect ophthalmoscopy and standard grading form	See appendix for grading form
	White vessels, temporal quadrant	wvess_temp_r wvess_temp_l wvess_temp_w	Presence or absence of white vessels in the temporal quadrant 0 = absent; 1 = present; .a = missing; .b = not applicable; .c = can't grade	Dilated fundus examination using indirect ophthalmoscopy and standard grading form	See appendix for grading form
	White capillaries, temporal quadrant	wcap_temp_r wcap_temp_l wcap_temp_w	Presence or absence of white capillaries in the temporal quadrant 0 = absent; 1 = present; .a = missing; .b = not applicable; .c = can't grade	Dilated fundus examination using indirect ophthalmoscopy and standard grading form	See appendix for grading form

Category	Variable	Abbreviation	Description	Measurement	Comments
Fluorescein angiogram	Macular capillary non-perfusion	mac_cnp_re mac_cnp_le mac_cnp_w	Severity of macular capillary non-perfusion 0 = none; 1 = grade 1; 2 = grade 2; 3 = grade 3; 4 = grade 4; .a = missing; .b = not applicable; .c = can't grade	Dilated fundus photography 30 seconds to approximately 10 minutes after venous injection of sodium fluorescein	See appendix for grading form
	Peripheral capillary non-perfusion	per_cnp_re per_cnp_le per_cnp_w	Severity of peripheral capillary non-perfusion 0 = none; 1 = grade 1; 2 = grade 2; 3 = grade 3; 4 = grade 4; .a = missing; .b = not applicable; .c = can't grade	Dilated fundus photography 30 seconds to approximately 10 minutes after venous injection of sodium fluorescein	See appendix for grading form
	Furthest extent of retina seen	rag_per_cnp_le	Furthest extent of retina seen in images 0 = nothing beyond macula 1 = zone 1 in at least one quadrant 2 = zone 2 in at least one quadrant 3 = zone 3 in at least one quadrant .a = missing		Generated from variables describing each quadrant. See Faout_anal5.do Used for data from the left eye
	Disc leak	dl_re dl_le dl_w	Presence or absence of disc leak 0 = absent; 1 = present; .a = missing; .b = not applicable; .c = can't grade	Dilated fundus photography 30 seconds to approximately 10 minutes after venous injection of sodium fluorescein	See appendix for grading form

Category	Variable	Abbreviation	Description	Measurement	Comments
	Large focal leak	lfl_re lfl_le lfl_w	Number of sites of large focal leak Count of sites; .a = missing; .b = not applicable; .c = can't grade	Dilated fundus photography 30 seconds to approximately 10 minutes after venous injection of sodium fluorescein	See appendix for grading form
	Punctate focal leak	pfl_re pfl_le pfl_w	Number of sites of punctate focal leak 0 = none; 1 = 1-5; 2 = 6-20; 3 = 21-50; 4 = >50; .a = missing; .b = not applicable; .c = can't grade	Dilated fundus photography 30 seconds to approximately 10 minutes after venous injection of sodium fluorescein	See appendix for grading form
	Post-capillary venule leak	pcvl_re pcvl_le pcvl_w	Severity of post-capillary venule leak 0 = none; 1 = 1-5; 2 = 6-20; 3 = 21-50; 4 = >50; .a = missing; .b = not applicable; .c = can't grade	Dilated fundus photography 30 seconds to approximately 10 minutes after venous injection of sodium fluorescein	See appendix for grading form
	Large/small venule leak	lvl_re lvl_le lvl_w	Severity of leak from larger venules 0 = none; <1/3 of all segments; 1/3-2/3 of all segments; >2/3 of all segments; .a = missing; .b = not applicable; .c = can't grade	Dilated fundus photography 30 seconds to approximately 10 minutes after venous injection of sodium fluorescein	See appendix for grading form
	Intravascular filling defects (large arterioles)	Ivfd_la_re ivfd_la_le ivfd_la_w	Presence or absence of intravascular filling defects in large arterioles 0 = none; <1/3 of all segments; 1/3-2/3 of all segments; >2/3 of all segments; .a = missing; .b = not applicable; .c = can't grade	Dilated fundus photography 30 seconds to approximately 10 minutes after venous injection of sodium fluorescein	See appendix for grading form

Category	Variable	Abbreviation	Description	Measurement	Comments
	Intravascular filling defects (small arterioles)	Ivfd_sa_re ivfd_sa_le ivfd_sa_w	Presence or absence of intravascular filling defects in small arterioles 0 = none; <1/3 of all segments; 1/3-2/3 of all segments; >2/3 of all segments; .a = missing; .b = not applicable; .c = can't grade	Dilated fundus photography 30 seconds to approximately 10 minutes after venous injection of sodium fluorescein	See appendix for grading form
	Intravascular filling defects (pre-capillary arterioles)	Ivfd_pca_re ivfd_pca_le ivfd_pca_w	Presence or absence of intravascular filling defects in pre-capillary arterioles 0 = none; <1/3 of all segments; 1/3-2/3 of all segments; >2/3 of all segments; .a = missing; .b = not applicable; .c = can't grade	Dilated fundus photography 30 seconds to approximately 10 minutes after venous injection of sodium fluorescein	See appendix for grading form
	Intravascular filling defects (capillaries)	Ivfd_cap_re ivfd_cap_le ivfd_cap_w	Presence or absence of intravascular filling defects in capillaries 0 = none; <1/3 of all segments; 1/3-2/3 of all segments; >2/3 of all segments; .a = missing; .b = not applicable; .c = can't grade	Dilated fundus photography 30 seconds to approximately 10 minutes after venous injection of sodium fluorescein	See appendix for grading form
	Intravascular filling defects (post-capillary venules)	Ivfd_pcv_re ivfd_pcv_le ivfd_pcv_w	Presence or absence of intravascular filling defects in post-capillary venules 0 = none; <1/3 of all segments; 1/3-2/3 of all segments; >2/3 of all segments; .a = missing; .b = not applicable; .c = can't grade	Dilated fundus photography 30 seconds to approximately 10 minutes after venous injection of sodium fluorescein	See appendix for grading form

Category	Variable	Abbreviation	Description	Measurement	Comments
	Intravascular filling defects (small venules)	Ivfd_sv_re ivfd_sv_le ivfd_sv_w	Presence or absence of intravascular filling defects in small venules 0 = none; <1/3 of all segments; 1/3-2/3 of all segments; >2/3 of all segments; .a = missing; .b = not applicable; .c = can't grade	Dilated fundus photography 30 seconds to approximately 10 minutes after venous injection of sodium fluorescein	See appendix for grading form
	Intravascular filling defects (large venules)	Ivfd_lv_re ivfd_lv_le ivfd_lv_w	Presence or absence of intravascular filling defects in large venules 0 = none; <1/3 of all segments; 1/3-2/3 of all segments; >2/3 of all segments; .a = missing; .b = not applicable; .c = can't grade	Dilated fundus photography 30 seconds to approximately 10 minutes after venous injection of sodium fluorescein	See appendix for grading form
MRI brain variables	Pre-pontine csf space	csf2c	Distance between the clivus and the anterior wall of the pos, in mm, on a line drawn from the tip of the nose to the apex of the fourth ventricle, on a midline sagittal image Continuous variable; .a = missing	All scans were obtained on a 0.35T Signa Ovation Excite MRI scanner (GE Healthcare, Milwaukee, Wisconsin) (Potchen, 2012)	See (Seydel *et al.*, 2015)

Chapter 5 – Grading fluorescein angiograms in malarial retinopathy

5.1 Aim of chapter

Describe the type and severity of characteristic angiographic features of malarial retinopathy, and a reproducible method for systematically grading these features

5.2 Summary of chapter

5.2.1 What is known already

Malarial retinopathy is an important finding in *P. falciparum* cerebral malaria, since it strengthens diagnostic accuracy, predicts clinical outcome and appears to parallel cerebral disease processes. Several angiographic features of malarial retinopathy have been described, but observations in different populations can only be reliably compared if consistent methodology is used to capture and grade retinal images. Currently no grading scheme exists for fluorescein angiographic features of malarial retinopathy.

5.2.2 What this chapter involved

I devised a grading scheme for fluorescein angiographic images based on extensive personal review of archive images. I organised several consensus meetings of clinicians and researchers experienced in malarial retinopathy in children and adults to discuss angiographic features. These meetings led to agreed definitions for features and levels of severity. I supervised the implementation of this grading scheme in a professional retinal image reading centre, which performed dual grading with adjudication of admission fluorescein images from a large cohort of children with cerebral malaria. I then estimated inter-grader agreement for each angiographic feature.

5.2.3 What this adds to current knowledge

I provide a grading scheme with standard images to facilitate future studies of retinal angiography in severe malaria. Inter-grader agreement was >70% for most

variables. Intravascular filling defects are difficult to grade and tended to have lower inter-grader agreement (>57%) compared to other features. This grading scheme provides a consistent way to describe retinal vascular damage in paediatric cerebral malaria, and can facilitate comparisons of angiographic features of malarial retinopathy between different patient groups, and analysis against clinical outcomes. Inter-grader agreement is reasonable for a majority of angiographic signs. Dual grading with expert adjudication should be used to maximise accuracy. There is a lack of commonly agreed methods for validating the performance of ophthalmic reading centres.

5.3 Introduction

The clinical syndrome of cerebral malaria (CM) is a major cause of death and disability, yet the pathogenesis remains unclear (World Health Organization, 2014b). Improvements in diagnosis, treatment, and prognosis are likely to be possible only through an improved understanding of the disease process. The neurovasculature of the retina has attracted interest as a potential model of unseen cerebrovascular damage, both in CM (MacCormick *et al.*, 2014) and other neurological conditions, including stroke (Doubal *et al.*, 2009), cerebral small vessel disease (Wardlaw, 2010), and others (London *et al.*, 2013; MacGillivray *et al.*, 2014).

A system to classify and grade malarial retinopathy from ophthalmoscopy (Harding *et al.*, 2006; Lewallen *et al.*, 1999) and colour photographs has been widely used, in both children (Beare et al., 2002; Beare et al., 2004) and adults (Abu Sayeed *et al.*, 2011; Maude *et al.*, 2009). This has led to an awareness that malarial retinopathy in paediatric CM is a sensitive and specific indicator of cerebral sequestration (Taylor *et al.*, 2004), and that the severity of retinopathy correlates with the severity of retinal and cerebral sequestration (Barrera *et al.*, 2015), the intensity of cerebral haemorrhages (White *et al.*, 2001), and the likelihood of a fatal outcome (Beare et al., 2004). Retinopathy in adults with CM appears to involve fewer features than paediatric cases, but is also associated with death and other clinical markers of disease severity (Abu Sayeed *et al.*, 2011; Maude *et al.*, 2009).

Fundus fluorescein angiograms (FA) have been performed on children (Beare *et al.*, 2009; Hero *et al.*, 1997) and adults with CM (Davis *et al.*, 1992). This procedure involves injection of a fluorescent solution (fluorescein sodium) into a peripheral vein, and then taking photographs as it moves through the retinal circulation. When excited by short wavelength (blue) light fluorescein emits light of a longer wavelength (green). The light stimulus and corresponding signal are differentiated by a combination of filters, and the result is a map of retinal vessel structure and function. Structure because vessels, including capillaries, are highlighted by the dye, and function because any obstruction in or leakage from vessels is clearly seen (Dithmar and Holz, 2008; Maude *et al.*, 2011). FA in paediatric and adult CM shows several distinctive features in addition to those previously recognised from ophthalmoscopic examination or colour images of the retina (Beare *et al.*, 2009). Angiographic features may have important associations with cerebral pathology and clinical outcome. If such associations exist, they can only be quantified, replicated and compared between studies if observers of different populations use a consistent grading scheme. To the best of my knowledge a scheme for grading FA signs in severe malaria has not yet been described.

5.4 Methods

I reviewed angiographic features of CM in Malawian children and then presented representative images to an expert group with knowledge of severe malaria and malarial retinopathy, with the aim of developing terminology, definitions and selecting standard images. The grading scheme was developed from, and tested on, admission images from children admitted to the Paediatric Research Ward in Blantyre, Malawi, between 2006 and 2014, who were recruited to an on-going study of severe malaria (Taylor, 2009). The great majority of subjects had retinopathy-positive CM; a few had retinopathy-negative CM, or other malarial or non-malarial diagnoses. The majority of images were taken on the day or day after admission. Three cases were imaged at 48 or 96 hours from admission. Images were taken by an ophthalmologist using a Topcon 50-EX optical unit (Topcon, Japan) matched to a Nikon D1-H digital camera and desktop PC running

Imagenet2000 (Topcon, Japan). FA images were taken after injection of 1 to 5ml of sodium fluorescein 10-20% into a peripheral vein as described previously (Beare *et al.*, 2009). Images were generally low compression JPEG, or TIFF files with a 50º field of view. Some 20º images were also reviewed. A minority of JPEG files were of lower resolution.

A grading scheme was devised (Appendix 2) and used in dual grading with independent adjudication. Grading was performed by two professional graders in the Liverpool Ophthalmic Reading Centre, St Paul's Eye Unit, Liverpool, UK with 9.5 and 1.5 years experience in grading FA images for other retinal diseases, such as age-related macular degeneration. Images were viewed using Microsoft Office 2010 Picture Manager, on Dell P2412H screens with 1920×1020 resolution, and enhanced with standard tools as necessary (e.g. brightness, contrast). Montages were created using Imagenet IBase (Topcon, Japan), and a grid indicating retinal zones and quadrants was overlaid to facilitate grading and calibration (Figure 22 and 23) (In house software, Matlab, Mathworks). Graders reviewed montages and original FA images, and could check corresponding colour images.

Disagreement between graders was defined as ≥ two-level discrepancy for ordinal variables (i.e. variables with 3 or more levels), and any discrepancy in binary variables. Disagreement was adjudicated by one of two ophthalmologists with several years experience of FA in paediatric CM (IJCM, SPH). All observers were masked to subject identity and clinical characteristics, including outcome.

Grading data were imported to Stata 13 (StataCorp, Texas), and observed agreement was calculated for comparisons between grader 1 and grader 2. Large focal leak was compared after converting it from a count variable to an ordinal variable (no leak, 1 site of leak, >1 site of leak). Only data from the left eye were used.

Kappa statistics were weighted according to the number of levels in a variable, using a standard option in Stata[9]. Kappa values >0.75 was considered to indicate excellent agreement, 0.35-0.75 good agreement, and <0.35 poor agreement. Grader-1 was compared with grader-2 for all variables.

Admission examination was performed as described previously (Taylor, 2009). Respiratory distress was defined as any one of alar flare, chest recession, accessory muscle use, or deep breathing (Marsh *et al.*, 1995). Malarial retinopathy was diagnosed by an ophthalmologist on the basis of bilateral dilated indirect ophthalmoscopy and defined as any one of retinal haemorrhage, retinal whitening, or orange or white retinal vessels. Isolated papilloedema did not indicate malarial retinopathy (Taylor *et al.*, 2004). Admission investigations were performed: peripheral parasitaemia (microscopy of a finger prick blood sample); full blood count (Coulter Counter, Becton-Dickinson, Franklin Lakes, New Jersey); haematocrit (finger prick sample and centrifuged microhaematocrit tube); venous lactate (Lactate Pro point of care detector (Arkray Inc)), plasma HRP2 (Celabs ELISA); HIV status (Uni-Gold – Trinity Biotech, Carlsbad, CA; and Determine – Inverness Medical, Orlando, Florida).

This research was performed in accordance with the Declaration of Helsinki and was approved by the research ethics committees at Michigan State University, the University of Liverpool, and the University of Malawi College of Medicine. Informed consent to participate in the study was obtained from the parents or guardians of all participants.

9 The command wgt(w) specifies weights (1-(i-j)/(k-1), where i and j index the rows and columns of the ratings by the two raters and k is the maximum number of possible ratings.

Figure 22: FA montage and grading overlay.

A) A montage composed of several FA images from similar time points can provide a useful summary of FA features. B) Addition of a grading overlay assists identification of retinal areas. Detail of retinal areas are in Table 10 and Figure 23.

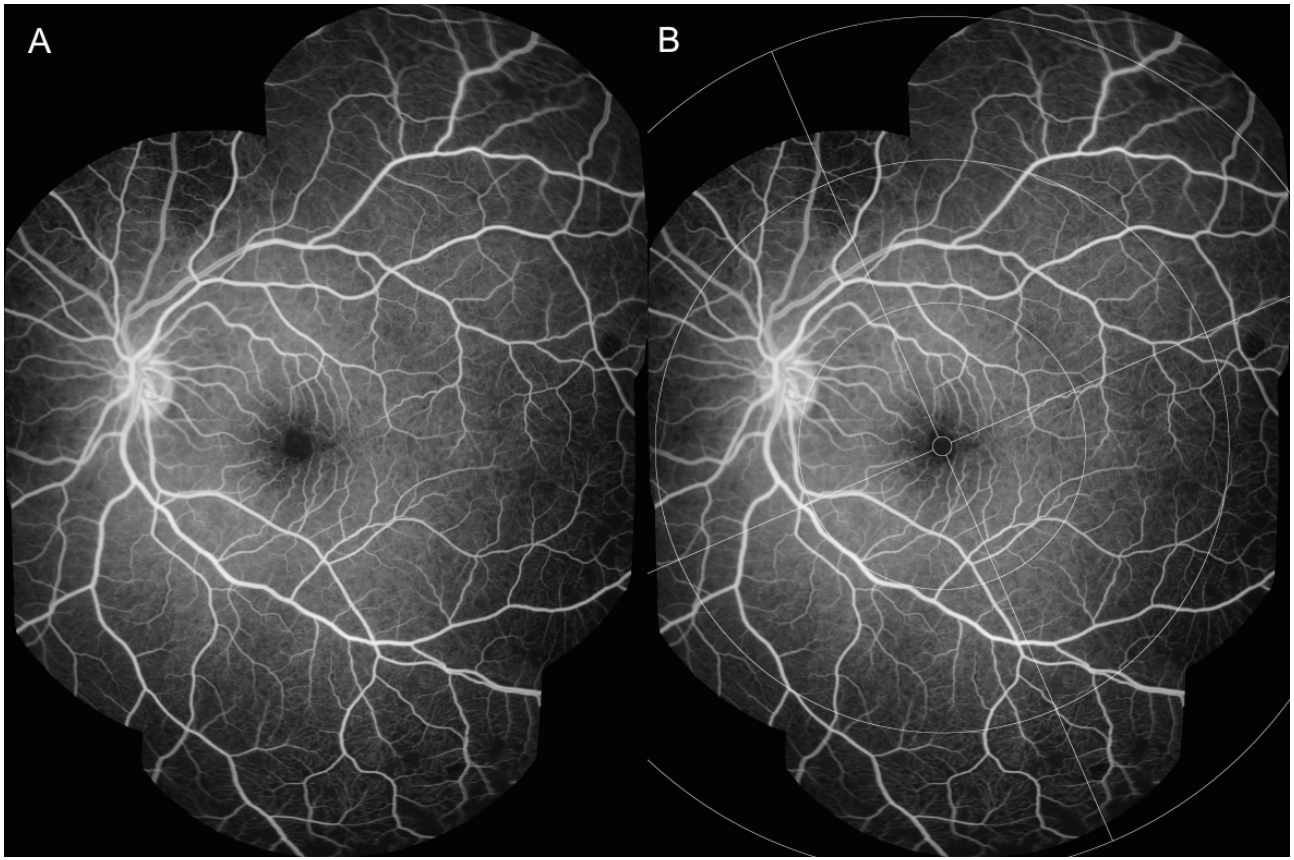

Figure 23: Definitions of retinal areas.

Schematic retina from (Harding *et al.*, 2006) adapted to show three different zones of peripheral retina for the right eye (Table 10). The disc and vessels are shown for reference. Note that the disc is always on the *nasal* edge of the macula. The distance from the outer edge of the disc to the centre of the fovea is referred to as one disc-fovea distance, and is equivalent to ~2.5 ETDRS disc diameters. Working from the centre of the image outwards, the fovea and macula are shown as circles (broken lines). The red circle indicates the limit of zone 1, which extends one disc-fovea distance beyond the macula. The blue circle indicates the limit of zone 2, which extends a further disc-fovea distance from zone 1. Zone 3 includes all retina out with the blue circle. The outer black circle nominally represents the ora serrata, but note the actual distance between the zone 2/3 boundary and the ora is much greater than suggested by this diagram. Superior, temporal, inferior, and nasal quadrants are shown by broken lines extending from the edge of the macula.

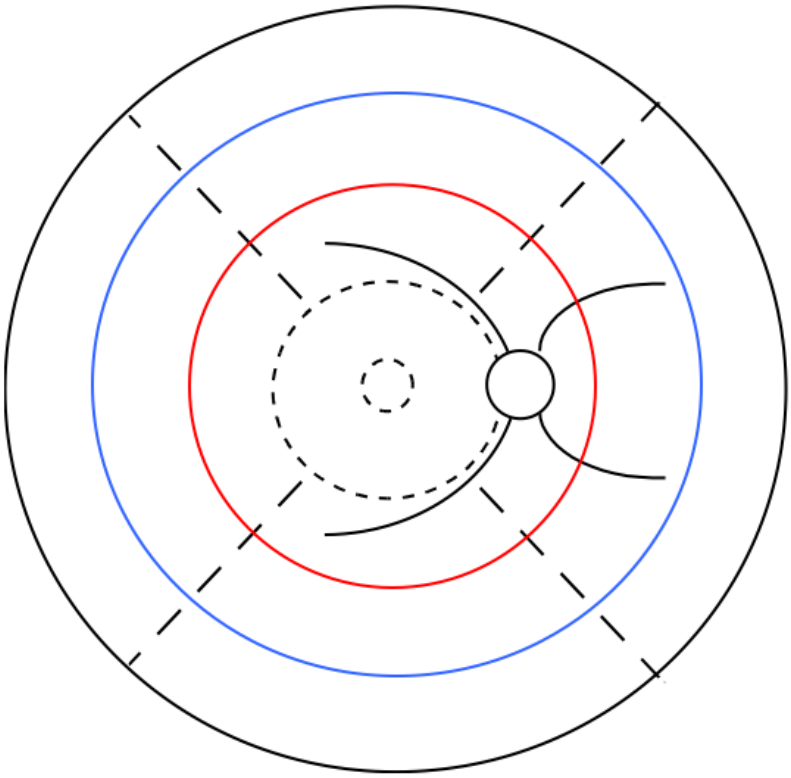

5.5 Results

My results are divided into three sections: principles of grading FA images, a description of specific FA features, and performance of the grading scheme in terms of inter-grader agreement. The grading form is provided in Appendix 2.

5.5.1 Principles of grading fluorescein angiogram images

In addition to recognising specific retinal features, consistent grading requires attention to several concepts relating to image acquisition, processing, viewing, and interpretation.

5.5.1.1 Image acquisition

My grading scheme is based on observations constrained by the limits of a 50º field of view and the limits of digital resolution for TIFF or high quality JPEG files. Suboptimal image resolution interferes with grading. I recommend that researchers acquire wide field images in a lossless format.

5.5.1.2 Image processing – Montages and grading overlay

Combining individual images into a montage allows a grader to view a large area of retina in one image (Figure 22). A montage can give a helpful overview of the retina before the full image set is examined, and can be used to prevent double counting of some retinal features from individual images.

However, inevitably FA montages are made up of images that are taken at slightly different times during the fluorescein run, and the process of selecting and then combining images risks loss of information. Ideally a montage should be made up of images from similar time points, and graders should use their judgement to make a grading based on both montages and individual images.

A grading overlay is applied to montages to help determine retinal areas (Figure 22B). A time stamp should be added to each FA image to show the time from fluorescein injection.

5.5.1.3 Viewing images

Images should be viewed in a darkened room on a large, high-resolution monitor (e.g. 1920×1200 pixel resolution). When available, information from colour images and montages of FA images should be used to help determine a grading. A good image-viewing software package with the ability to enhance the images should be used. In a formal reference grading centre a calibration is performed to correct for variable image size. Standard scale bars and discs are used as guides. Adjustments to brightness and contrast should be small in order not to lose the detailed features of lesions that were present in the original images.

5.5.1.4 Image interpretation

5.5.1.4.1 Retinal areas and minimum area visible

The retina is divided into several areas. The macula lies within a circle centred on the foveal centre and extending to the temporal border of the optic disc. I used the Early Treatment Diabetic Retinopathy Study (ETDRS) standard distance from the foveal centre to the temporal border of the disc (2.5 disc diameters, equivalent to 3.8mm) to define the radius of the macula, and as a standard measure: the "disc-fovea distance" (Early Treatment Diabetic Retinopathy Study research group, 1985). All retina beyond the macula is defined as peripheral retina. The periphery is divided into four quadrants. Each quadrant is divided into three zones, which cover areas of peripheral retina at increasing distances from the macula (Table 10, Figure 22 and 23).

Each retinal area is deemed visible for the purposes of grading if ≥75% of the area is captured in the image sequence. The exception is zone 3 which is deemed visible for a given quadrant if any retina is visible beyond the limit of zone 2. The amount of retina visible for grading is recorded on the grading form (Appendix 2).

Table 10: Definition of retinal areas.

Retinal areas are defined in terms of quadrants centred on the fovea, and concentric rings at increasing distance from the fovea. Distances are given in terms of retinal landmarks, such as proportions of optic disc diameter, and the distance from the disc to the fovea.

Retinal area	Definition
Macula	A circle centred on the centre of the fovea with a radius of 2.5 ETDRS disc diameters, or 3.8mm (Early Treatment Diabetic Retinopathy Study research group, 1985). The nasal edge is approximately in contact with the temporal border of the optic disc
Fovea	A circle centred on the centre of the fovea with a diameter of 1/3 disc diameter, or approximately 0.5mm
Zone 1 (Inner periphery)	The area between the macula and a circle extending 1 disc-fovea distance from the edge of the macula (Figure 23, red-circle)
Zone 2 (Mid periphery)	The area between the circle defining the extent of the inner periphery and a circle extending 2 disc-fovea distances from the edge of the macula (Figure 2, blue circle)
Zone 3 (Far periphery)	All retina beyond the extent of the mid periphery (Figure 23, beyond the blue circle)

5.5.1.4.2 Types of vessel segment

Some FA features in CM are localised to particular segments of vessels, and particularly venules. The simplest method to classify microvessels is to divide vessels into idealised groups. Other approaches include Horton-Strahler ordering and generation numbering (Pries and Secomb, 2008). Large retinal vessels often have multiple small 90º branches in between dichotomous branches. It is difficult for a human grader to describe this arrangement according to generation number or Horton-Strahler order. I therefore group vessels according to several types (Table 11).

Table 11: Definition of vessel types

Vessel type	Description
Capillary	Smallest vessel visible on a well focussed angiogram image
Post-capillary venule	Formed by the confluence of two or more capillaries, and extends up to the point where it is joined by a second post-capillary venule or other larger venular segment
Pre-capillary arteriole	Extends upstream from the divergence of two or more capillaries to the point where it branches from another pre-capillary arteriole or other larger arteriolar segment
Post-capillary venule complex	Extends approximately 1/3 of a disc diameter (~500μm) downstream from the capillaries along venular segments
Pre-capillary arteriole complex	Extends approximately 1/3 of a disc diameter (~500μm) upstream from the capillaries along arteriolar segments
Small venule	Extends from the edge of the post-capillary venule complex downstream to the point of confluence with another venule of similar or larger caliber
Small arteriole	Extends from the edge of the pre-capillary arteriole complex upstream to the point of branching with another arteriole of similar or larger caliber
Large venule	Extends downstream from the point of confluence that defines the upper caliber boundary of small vessel segments to the edge of the optic disc
Large arteriole	Extends upstream from the branching point that defines the upper caliber boundary of small arteriolar segments to the edge of the optic disc

5.5.1.4.3 Capillaries and the post-capillary venule complex

Capillaries are the smallest vessels visible on a well-focussed angiogram. A post-capillary venule is formed by the confluence of two or more capillaries, and extends up to the point where it is joined by a second post-capillary venule or other larger venular segment.

It is more practical to identify a larger group of vessels (the post-capillary venule complex) which extends approximately 1/3 of a disc diameter (~500μm) downstream from capillaries (Figure 24). An analogous selection of pre-capillary arterioles can also be considered (the pre-capillary arteriole complex), which

includes arteriolar segments 1/3 of a disc diameter upstream from the capillary bed.

5.5.1.4.4 Small and large venules

Small venules are defined as any section of vein between the edge of the post-capillary venule complex up to the point of confluence with another vessel of similar or larger calibre. Large venules extend from the point where two small venules converge to the edge of the optic disc (Figure 24). Separate sections of large vessels can be counted, since they begin and end at junctions between one large vessel and another large vessel of similar or larger calibre (Figure 25).

Analogous definitions exist for retinal arteriole segments (Table 11). Arterioles fill early in the angiogram are generally narrower than venules, which fill later.

Figure 24: The post-capillary venule complex, small venules, large venules. Left eye. Point A represents the beginning of a 'small venule' segment, which ends at point B when two small venules converge. Point B is also the beginning of a large venule, which ends at the optic disc. The scale bar shows 1/3 disc diameter (~500μm) from the convergence of capillaries on to the post-capillary venule, and approximates the length of the post-capillary venule complex. The post-capillary venule complex begins at the junction of two capillaries and extends a distance of 1/3 disc diameter downstream towards the small venules. Other visible features in this figure include disc leak, and intravascular filling defects (e.g. small venule at point A)

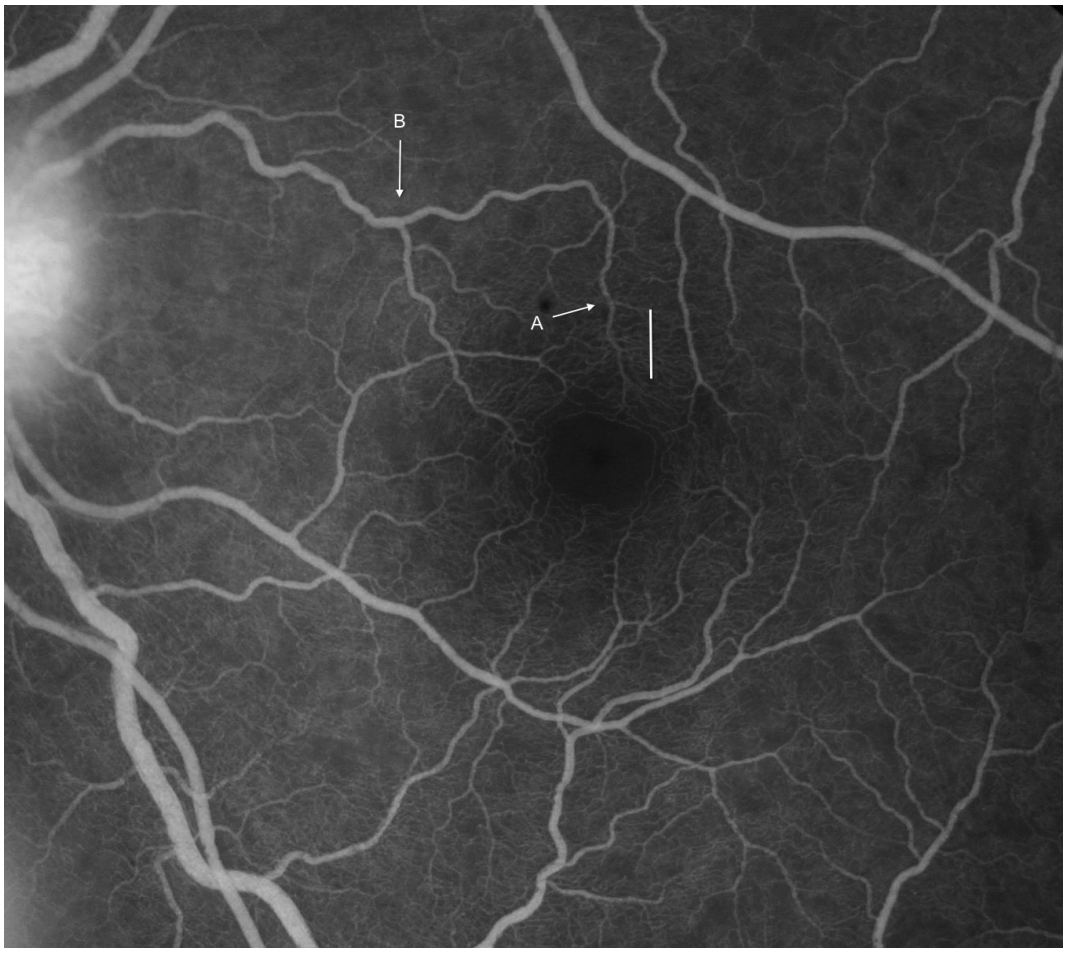

Figure 25: Segments of the venous network (small and large venules).
Montage of FA images, left eye. Large vessel segments are marked in red, and small vessel segments in yellow. A break in a line indicates the junction between two vessel segments. New vessel segments begin where a vessel meets another vessel of similar or larger calibre. Small vessels extend from the downstream limit of the post-capillary venule complex (~500μm from capillary bed) to the point where the small vessel joins another vessel of similar or larger calibre. Large vessels extend from this point to the disc. Sections of large vessels begin and end at junctions between one large vessel and another large vessel of similar or greater calibre. Other visible features in this figure include disc leak, and one site of large focal leak (inferior to the disc)

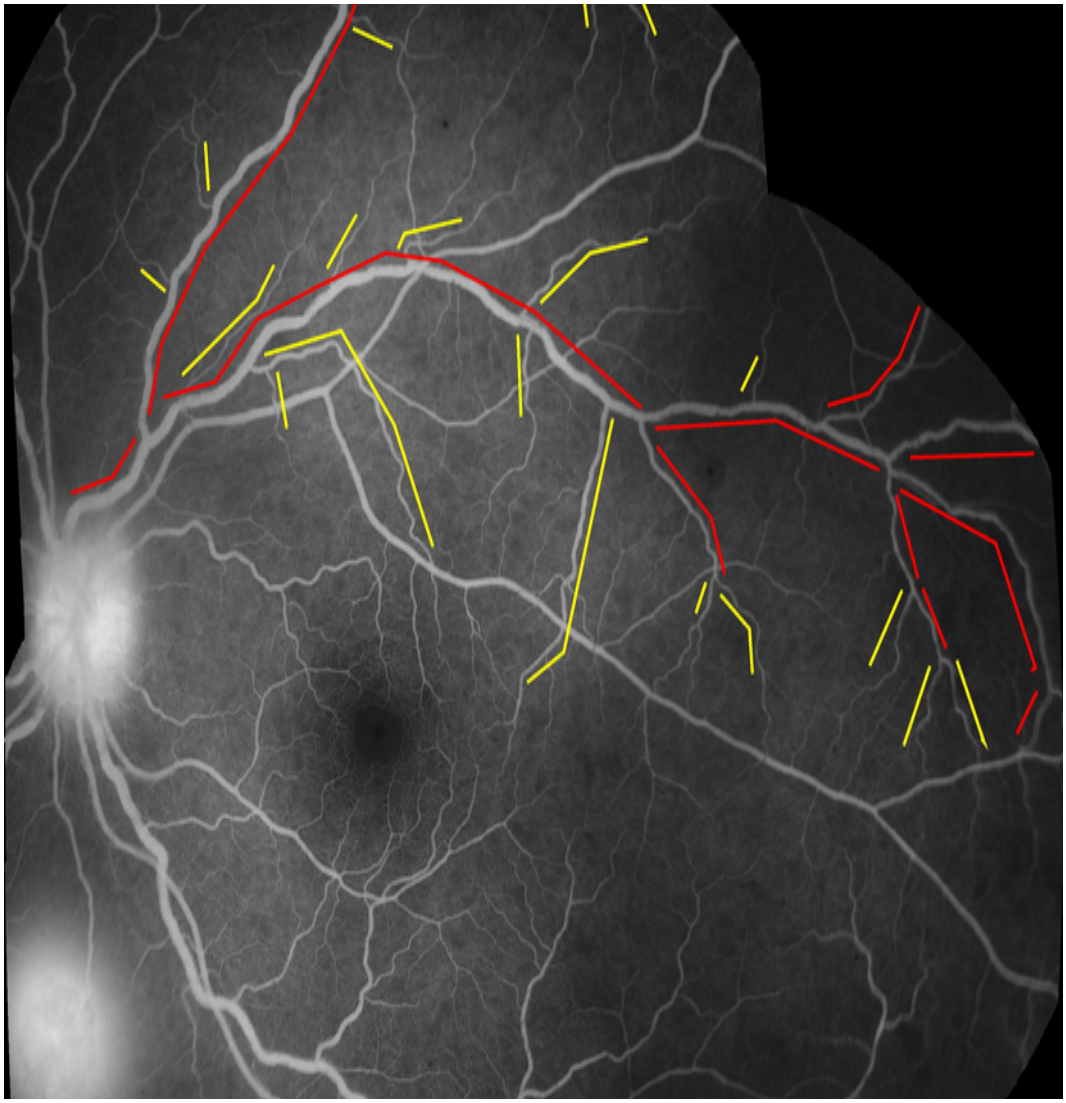

5.5.1.4.5 Grading image quality

Patients with CM are acutely unwell. They may be restless, and may have tonic or roving eye movements, nystagmus, or reduced corneal transparency secondary to incomplete lid closure. Grading of one or more features may be impossible if images are blurred, features are obscured by haemorrhages or leaking fluorescein, or if the area of retina to be graded has not been captured at an appropriate time point. Blurred images are a particular problem for grading vessel leak and intravascular filling defects (IVFD) (see sections on specific lesions).

Overall image quality is graded by evaluating the sharpness of FA images (Table 12). A score for image quality is assigned to the whole run for FA images for a given eye (Appendix 2).

Table 12: Definition of overall image quality

Image quality	Definition
Good	Focus is crisp, at least in the macular grid Focus and clarity are sufficient for grading of all features to be completed Retinal details (small capillaries) are sharply defined and have crisp boundaries. It should be possible to see the ends of the larger vessels approaching the foveal avascular zone (FAZ), if they are not obscured by pathology
Fair	The image is less well focused (than good), with it becoming more difficult to determine the ends of the larger vessels approaching the FAZ Retinal details are slightly fuzzy but subtle lesions, such as small retinal haemorrhages, can still be seen and graded
Poor gradeable	The image is less well focused (than fair), but it is possible to glean some information for grading Clarity is decreased so that subtle lesions might be missed, but is sufficient for assessment of large retinal haemorrhages and large retinal vessels
Poor ungradeable	This should be selected if the grader is unable to evaluate or distinguish (with more than 50% confidence) the absence or presence of any feature in all of the available images

Grades for individual retinal features should only be assigned when the grader is ≥50% certain that a feature is present, absent, or present at a given level of severity. A grade of ‘cannot grade’ (CG) is given if the grader is unable to tell if a feature is absent, present, or how severe it is on an ordinal scale. CG is not the same as ‘absent’. 'Absent' means the grader is ≥50% certain the feature is *not* present. The purpose of the CG category is to prevent an accumulation of false negative data by ensuring that subjects are not graded as having a lack of retinal signs when in fact they just have poor quality images.

5.6 Specific angiographic features in malarial retinopathy

5.6.1 Macular capillary non-perfusion (CNP)

CNP is an area of the capillary network that fails to fill with fluorescein by the late arteriovenous phase, with minimum linear dimension (MLD) ≥63µm. 63µm is approximately ½ the width of a retinal venule at the disc margin and is a conventional size circle used in the grading of drusen for age-related macular degeneration.

Macular CNP is graded on an ordinal scale (Table 13; Figures 26 27 28 29 30 31 32 33). Graders should use standard ETDRS circles to help mentally combine all CNP into the given circle (Early Treatment Diabetic Retinopathy Study research group, 1985), and should use images taken at or after the late arteriovenous phase to allow capillaries to fill completely. Grading should not include an area that notionally represents the normal foveal avascular zone (FAZ). Grade 1 macular CNP is very mild, and may capture subtle abnormalities that are not visible on indirect examination.

Table 13: Grades of macular capillary non-perfusion (CNP)

Lesion	Grading	Definition	Figures
Macular CNP	Cannot grade	No gradeable images of the macula exist	None
	Absent	One or more gradeable images of the macula exist, and no CNP is seen at the macula on any of these images	None
	Grade 1	A few, small areas of CNP (≥63µm MLD) are seen, often around the foveal avascular zone	26, 27
	Grade 2	Combined area of CNP is up to approximately 1/3 of a disc area	28, 29
	Grade 3	Combined area of CNP is approximately 1/3-1 disc area	30, 31
	Grade 4	Combined area of CNP at the macula exceeds 1 disc area. This can be due to a few large areas or many smaller areas of CNP	32. 33

Figure 26: Grade 1 macular capillary non-perfusion (CNP).

Right eye. A few small areas of CNP are seen at the macula (arrow), which is outlined by a white circle.

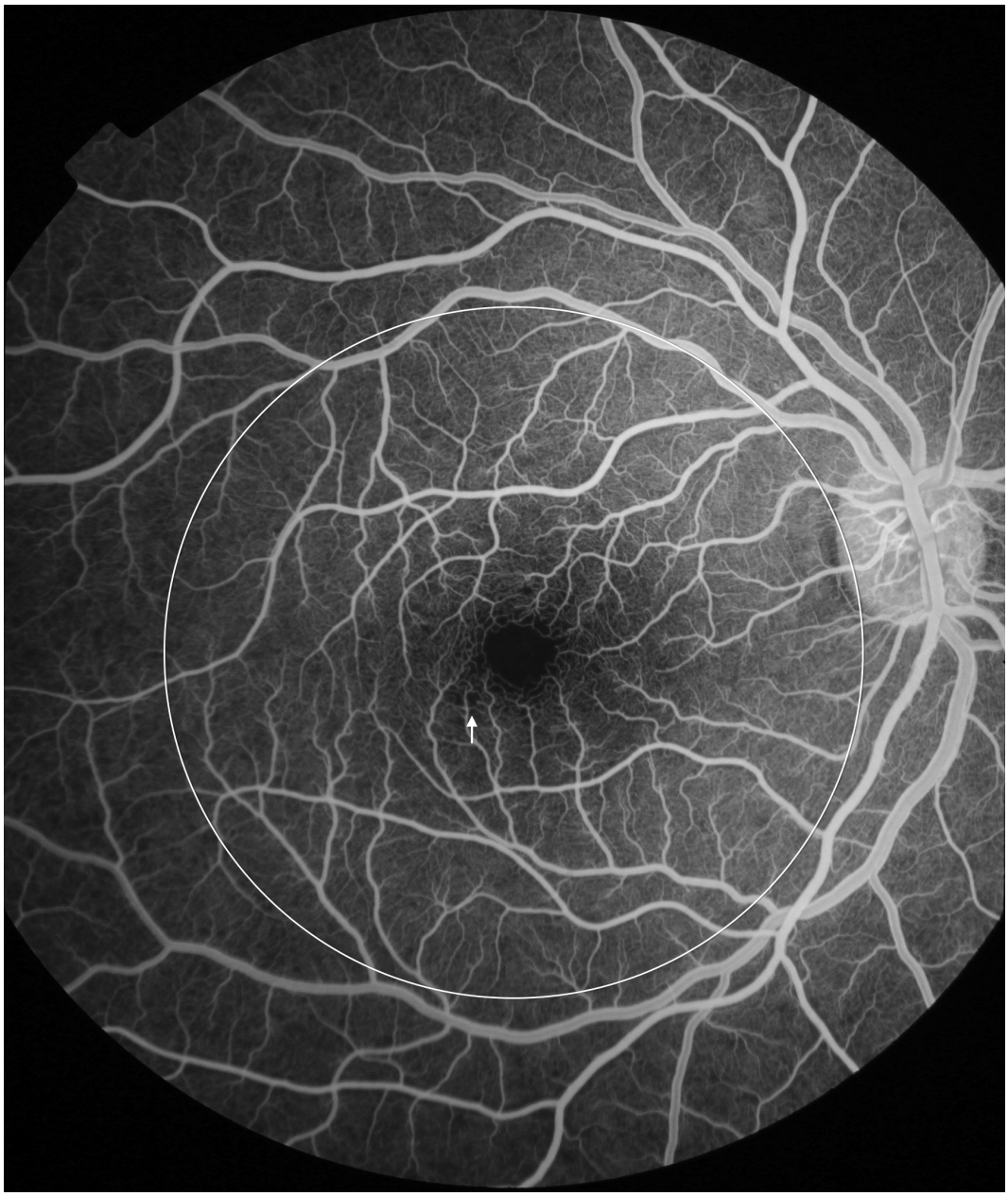

Figure 27: Grade 1 macular capillary non-perfusion (CNP).

Right eye. A few small areas of CNP are seen at the macula (arrow), which is outlined by a white circle

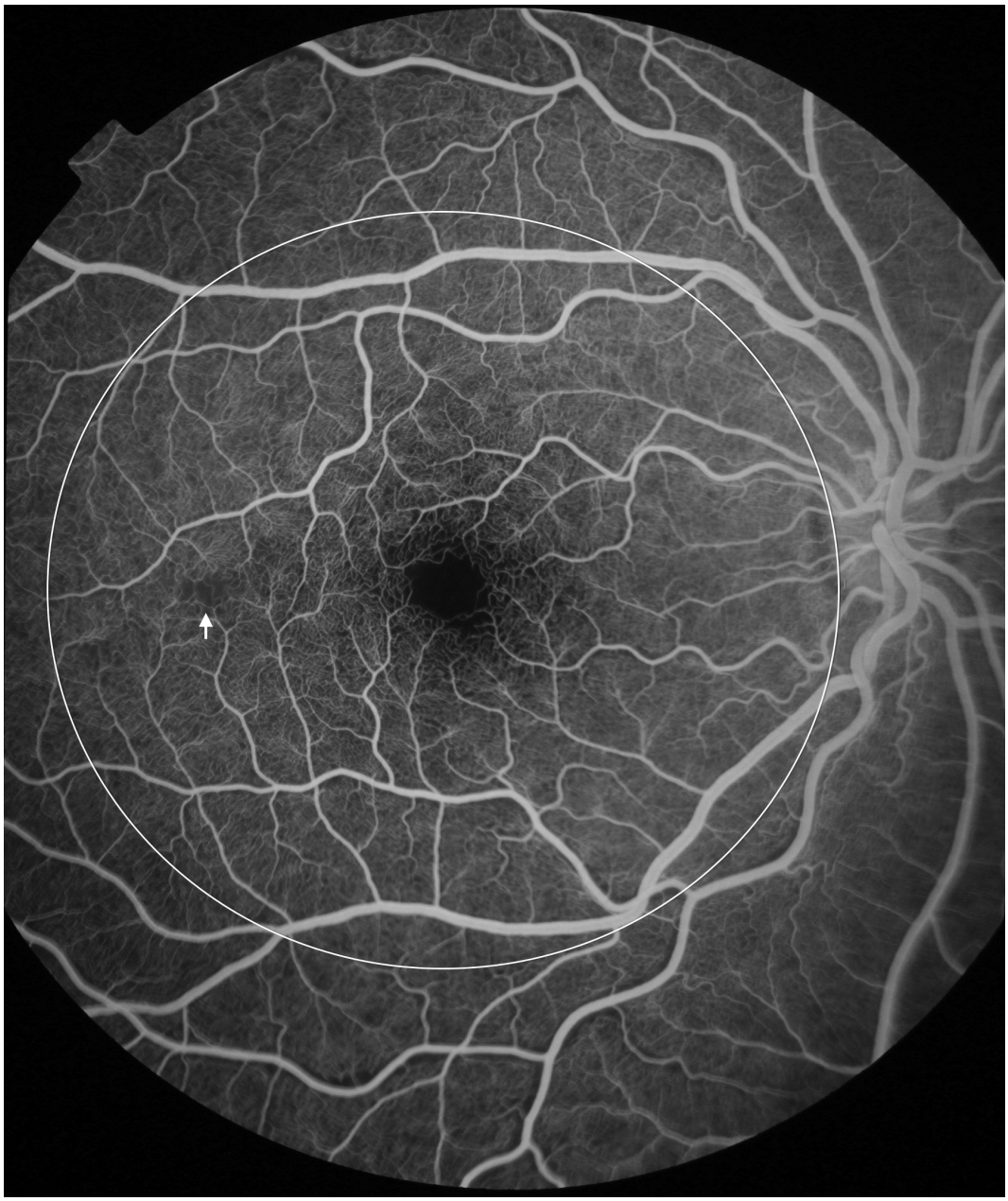

Figure 28: Grade 2 macular capillary non-perfusion (CNP).

Right eye. The upper limit of grade 2 macular CNP. Combined area of macular CNP is less than 1/3 disc area, after mentally subtracting a notional area for the normal foveal avascular zone. Macula, disc, and 1/3 disc area are shown as white circles. A single site of punctate focal leak is also visible in the macula (arrow)

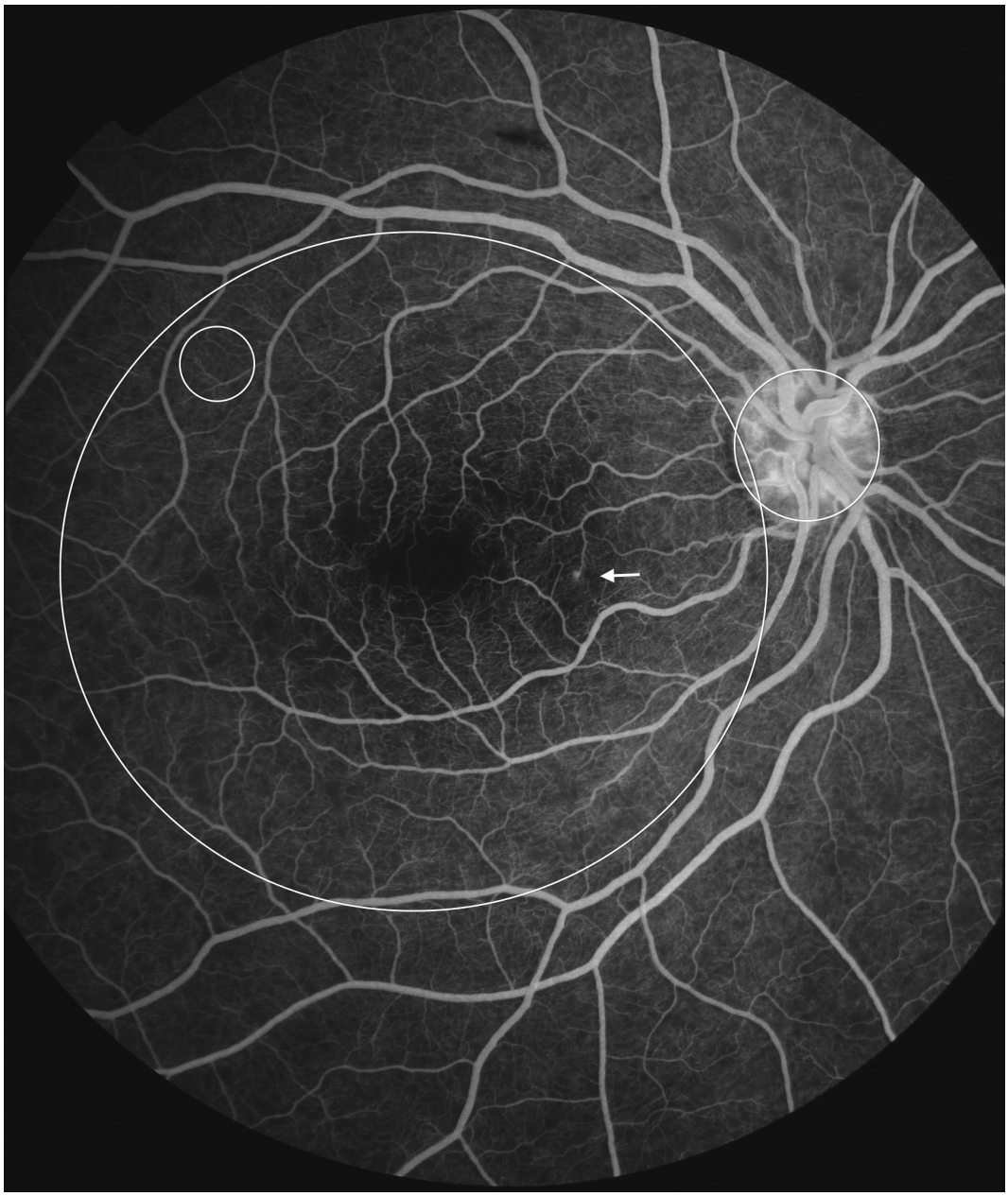

Figure 29: Grade 2 macular capillary non-perfusion (CNP).
Right eye. The upper limit of grade 2 macular CNP. Combined area of macular CNP is less than 1/3 disc area. CNP is clearly seen around the foveal avascular zone, and less obviously in the temporal macula (arrow). Macula and 1/3 disc area are shown as white circles. Masking of fluorescein from haemorrhage is also visible (double arrow). CNP has geographic boundaries (e.g. the abnormally irregular edge of the foveal avascular zone in this image), while haemorrhages tend to have rounded edges

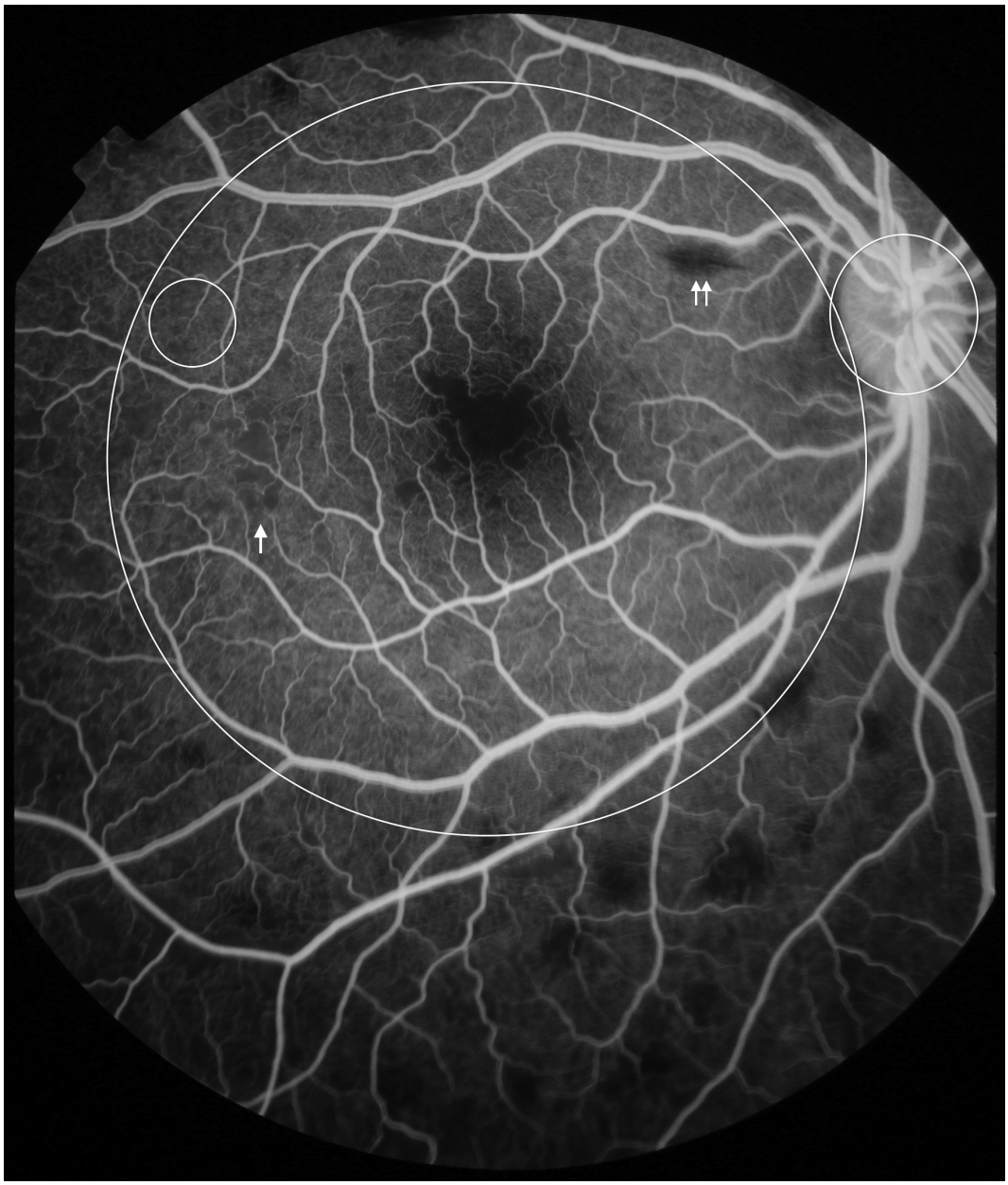

Figure 30: Grade 3 macular capillary non-perfusion (CNP).

Right eye. The upper limit of grade 3 macular CNP. Combined area of macular CNP is 1/3 to 1 disc area. Macula and 1 disc area are shown as white circles.

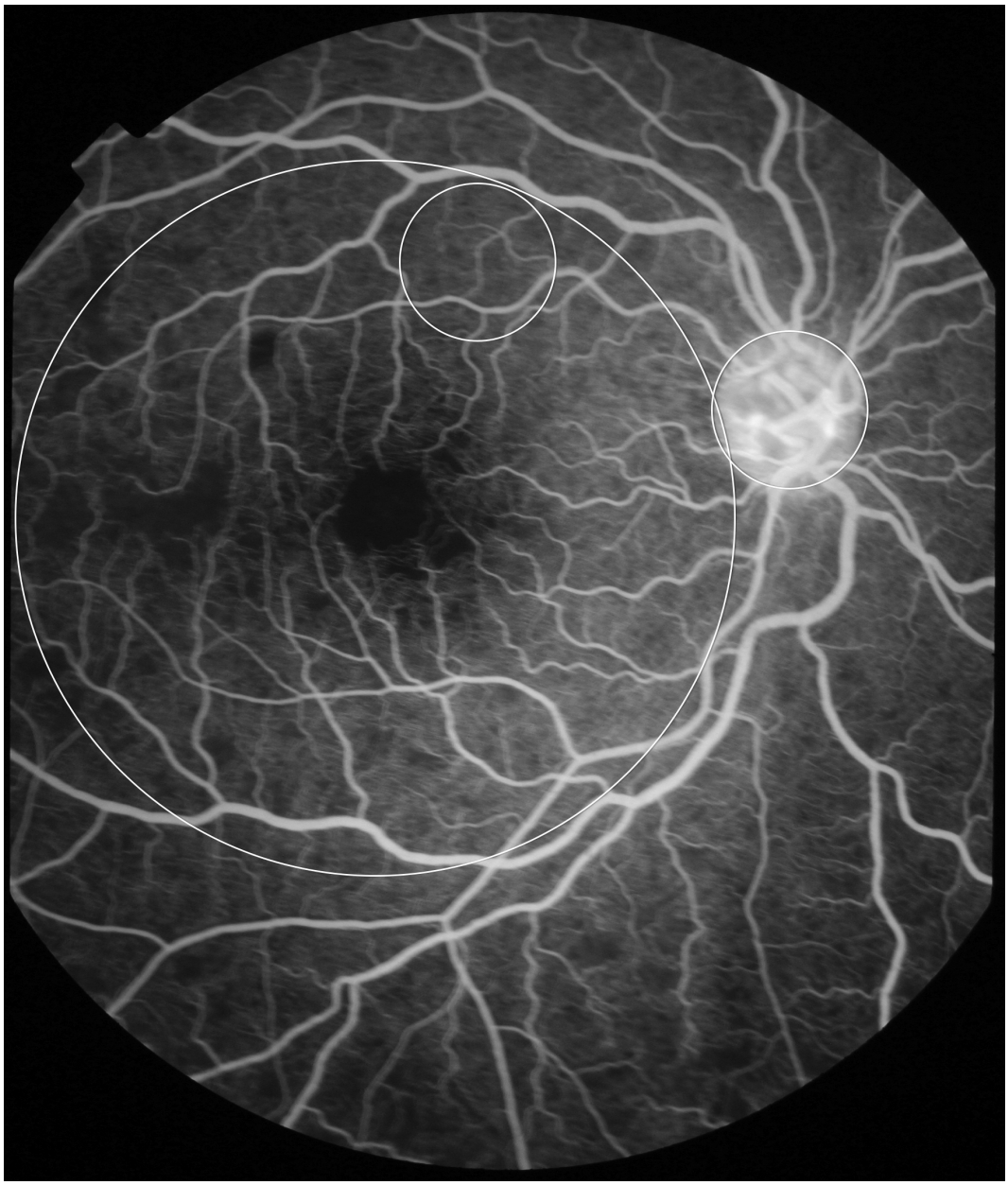

Figure 31: Grade 3 macular capillary non-perfusion (CNP).

Right eye. The upper limit of grade 3 macular CNP. Combined area of macular CNP is 1/3 to 1 disc area. Macula and 1 disc area are shown as white circles

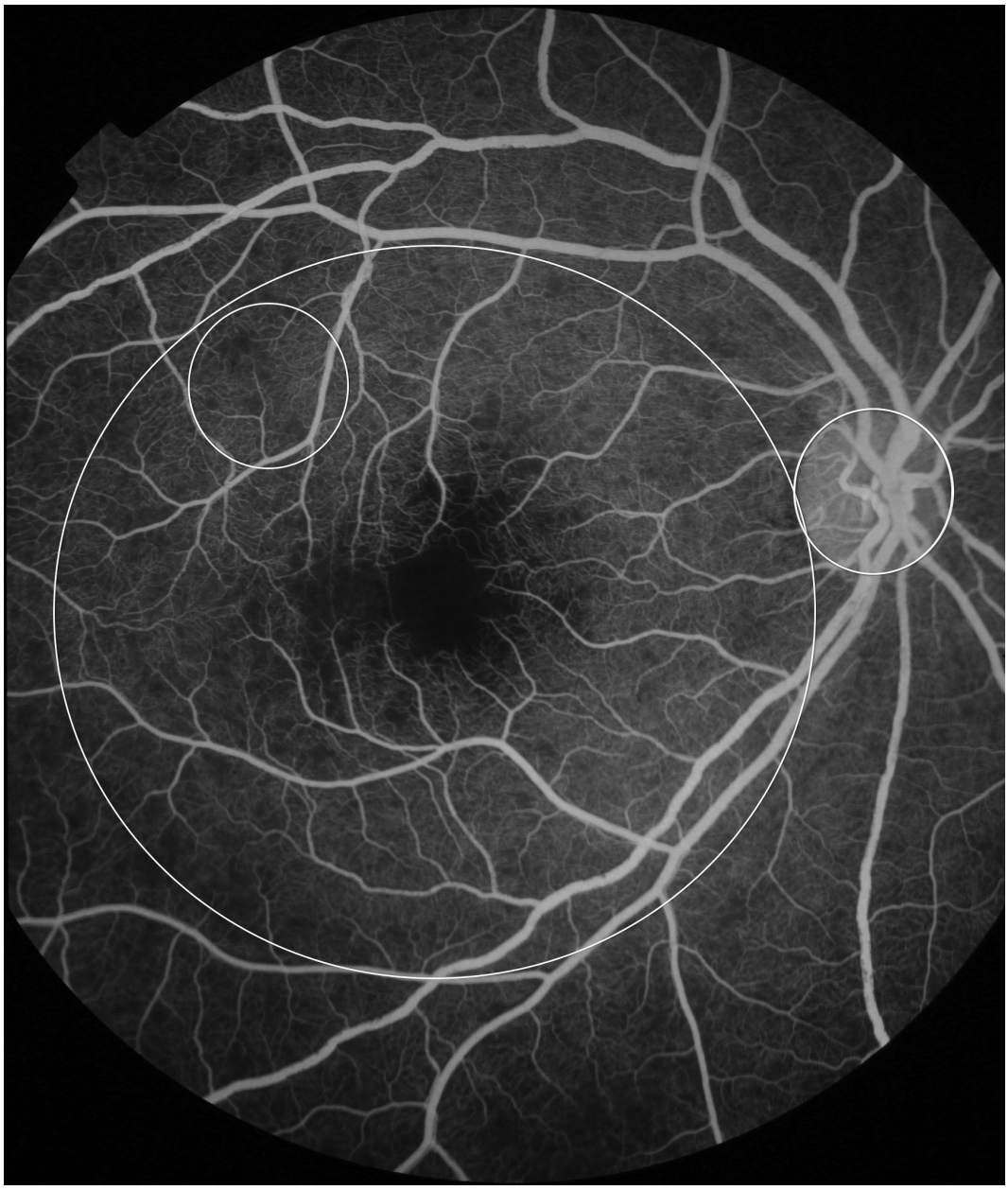

Figure 32: Grade 4 macular capillary non-perfusion (CNP).
Left eye. Combined areas of macular CNP are greater than 1 disc area. Macula and disc area are shown as white circles. Disc leak and punctate focal leak are also visible

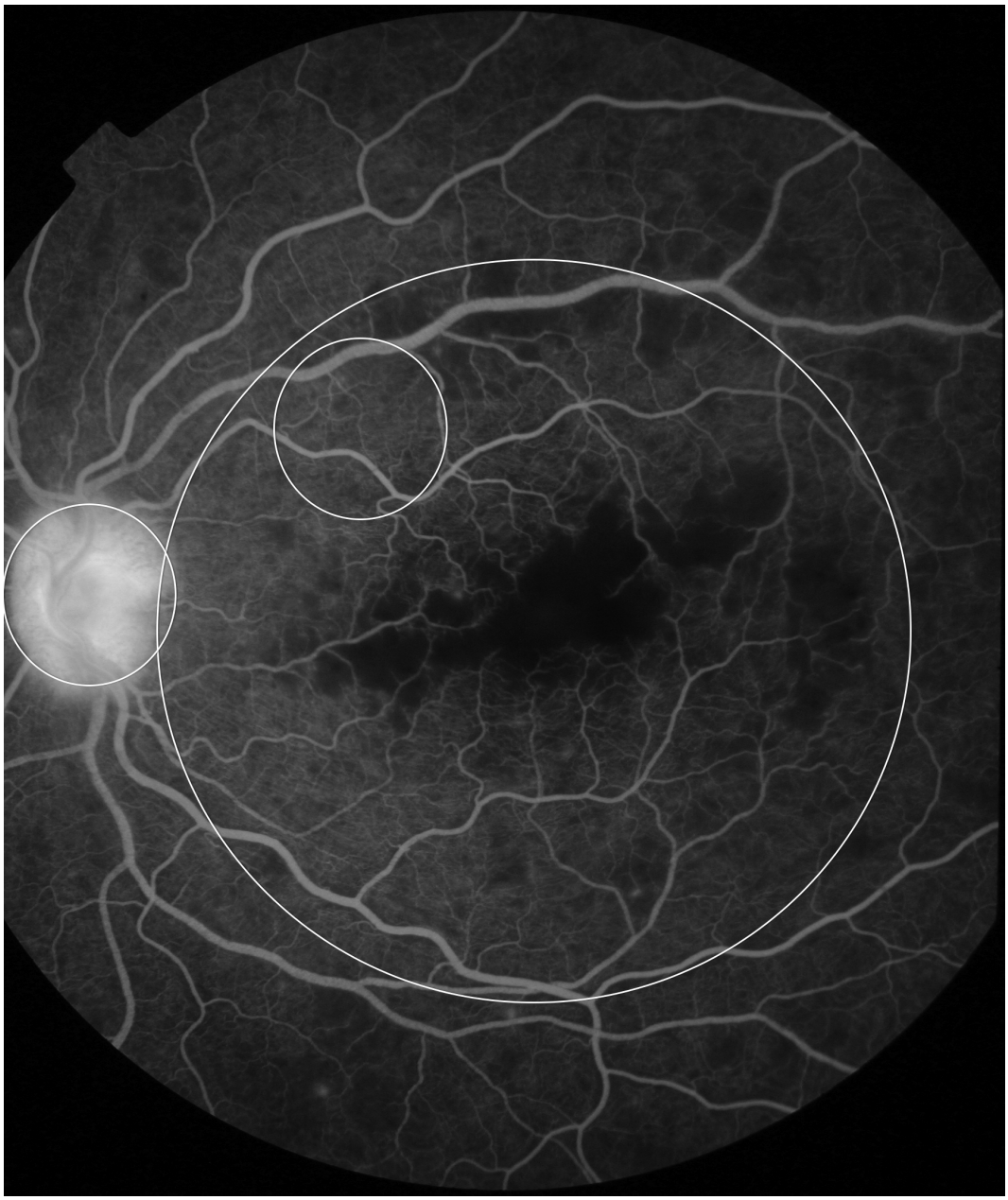

Figure 33: Grade 4 macular capillary non-perfusion (CNP).
Right eye. Combined areas of macular CNP are greater than 1 disc area. Macula and disc area are shown as white circles. Intravascular filling defects are visible in small and large venules

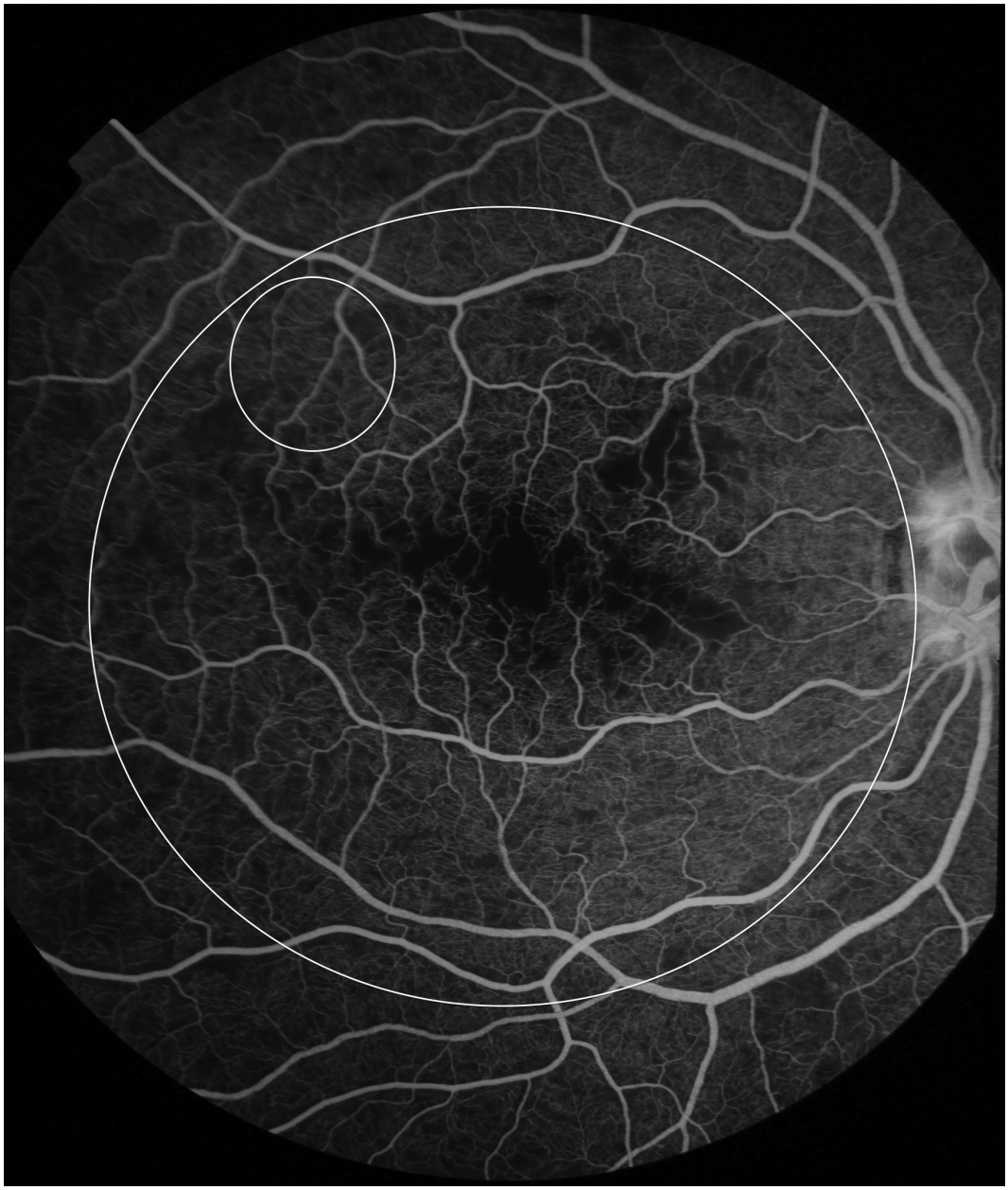

5.6.2 Peripheral capillary non-perfusion (CNP)

The definition for presence of any CNP in the periphery is the same as for CNP at the macula. For peripheral CNP to be gradeable there must be at least one well-focussed image of at least one minimum area of a particular quadrant of the periphery (i.e. ≥75% of zone 1, 2, or 3 in any quadrant). As for macular CNP, the image must be taken at or after the late arteriovenous phase. Images of the far retinal periphery may be magnified more than images of the posterior pole, owing to the optical characteristics of retinal photography done at an oblique angle through the cornea. This could potentially exaggerate the extent of CNP.

Peripheral CNP is graded on an ordinal scale (Table 14; Figures 34 35 36 37 38 39). Unlike macular CNP, peripheral CNP is graded according to the size of the largest single area of CNP, rather than the combination of all areas of CNP.

Table 14: Grades of peripheral capillary non-perfusion (CNP)

Lesion	Grading	Definition	Figures
Peripheral CNP	Cannot grade	No gradeable images of any retinal quadrant exist	None
	Absent	One or more gradeable images of one or more peripheral quadrants exist, and no CNP is seen on any of these images	None
	Mild Grade 1	Ranges from any CNP in the periphery to multiple areas of CNP that are *individually* not larger than 1/3 disc area	34. 35
	Grade 2	Multiple areas of CNP that are, *individually*, between 1/3 – 1 disc area	36. 37
	Grade 3	Includes features of previous grades, plus one or more large bays of peripheral CNP, each greater than 1 disc area	38
	Grade 4	One or more bays of CNP invade the superior, inferior, or temporal borders of zone 1, or zone 2 of the nasal retina.	39

Figure 34: Grade 1 peripheral capillary non-perfusion (CNP).
Superior retina, right eye. Individual areas of CNP are less than 1/3 disc area. 1/3 disc area is shown as a white circle. Note that the dark lesion (arrow) is a haemorrhage, and not CNP. Haemorrhage masks background fluorescence and has rounded edges, while CNP has a geographic boundary. Punctate focal leak is visible at the macula

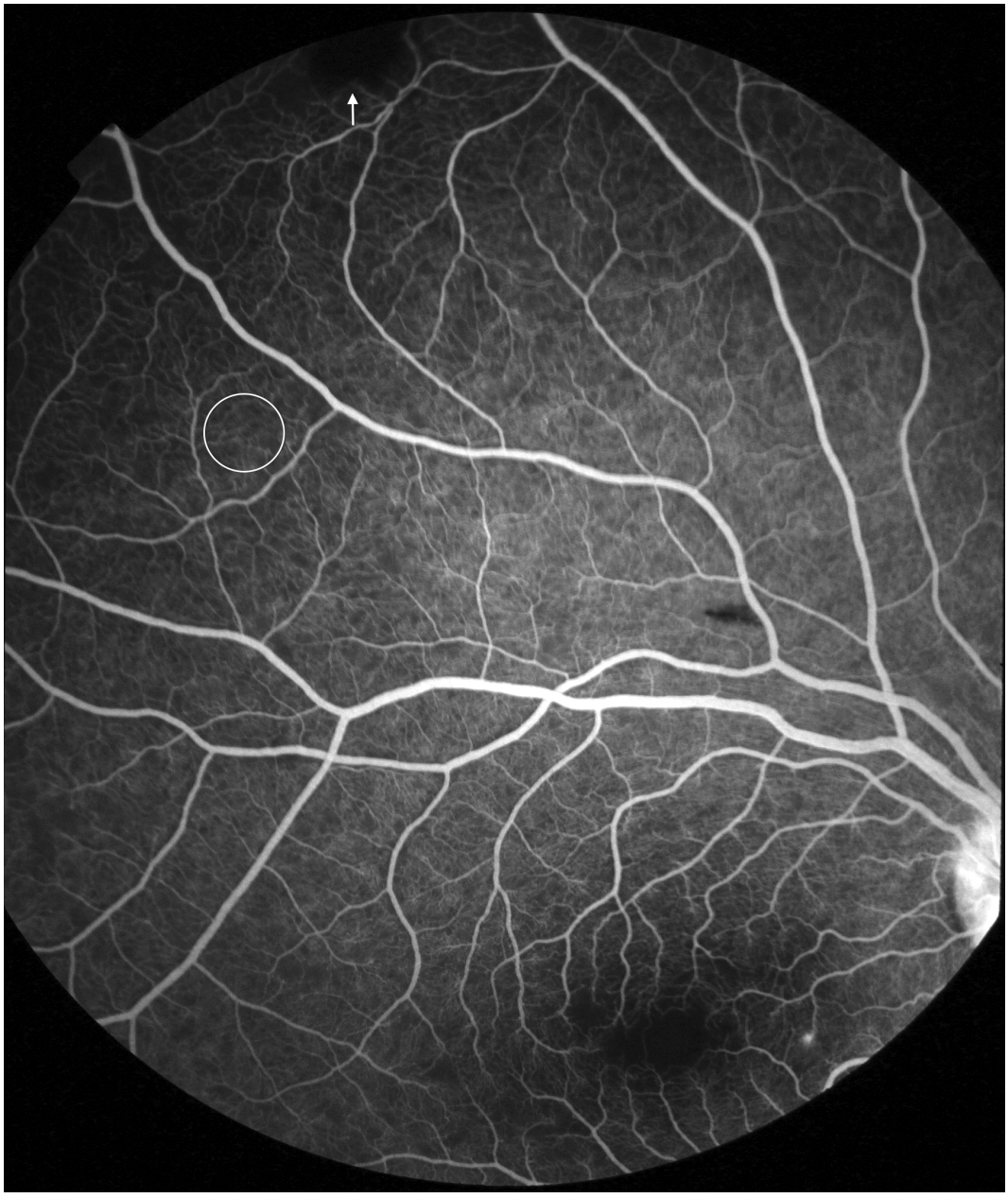

Figure 35: Grade 1 peripheral capillary non-perfusion (CNP).
Inferior retina, right eye. Individual areas of CNP are less than 1/3 disc area, which is shown by a white circle. Intravascular filling defects are visible in small venules (arrow), and adjacent large venules

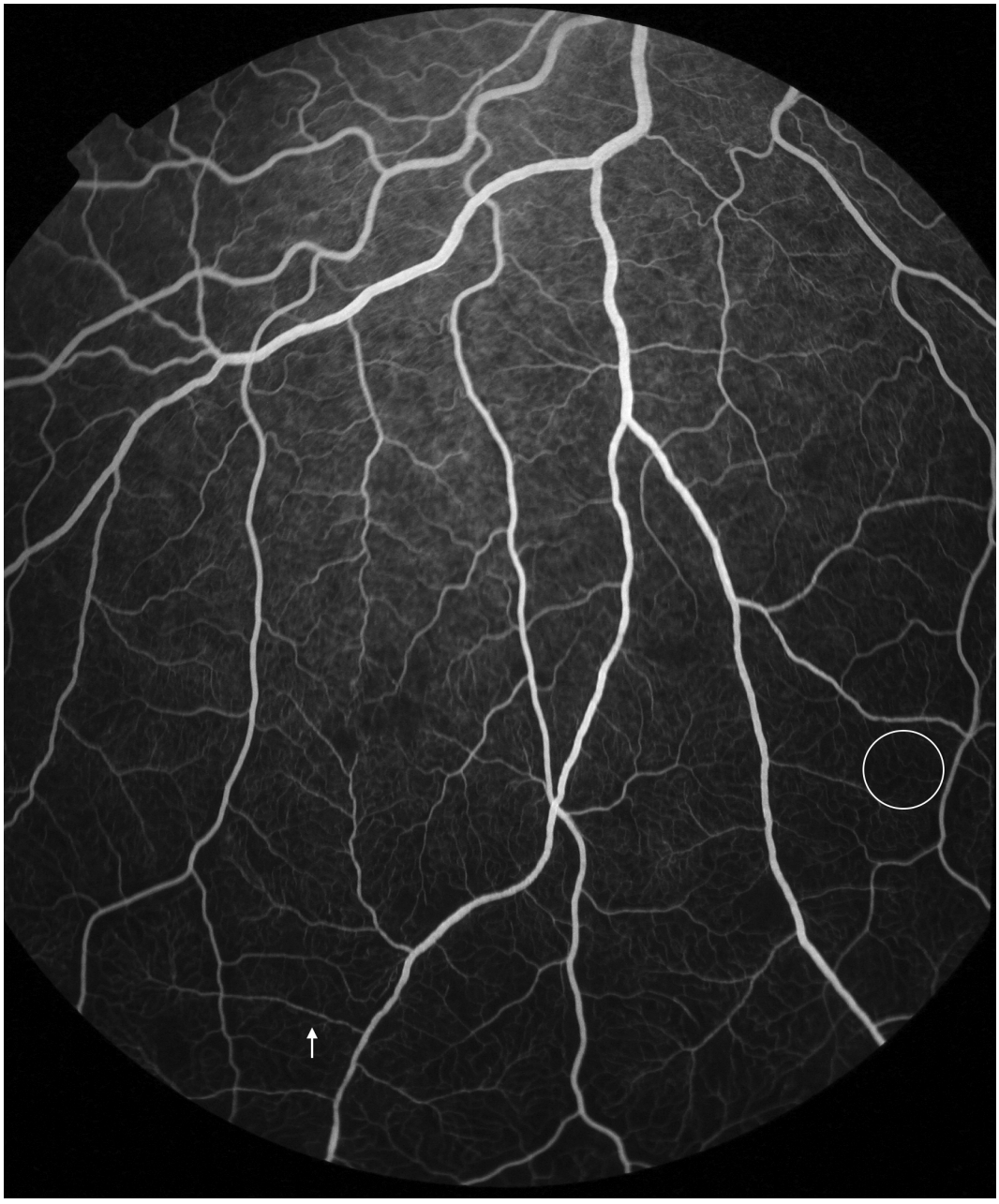

Figure 36: Grade 2 peripheral capillary non-perfusion (CNP).
Inferior retina, right eye. Individual areas of CNP are between 1/3 and 1 disc area. 1 disc area is shown as a white circle at the bottom of the image. An enlarged foveal avascular zone is seen at the top of the image

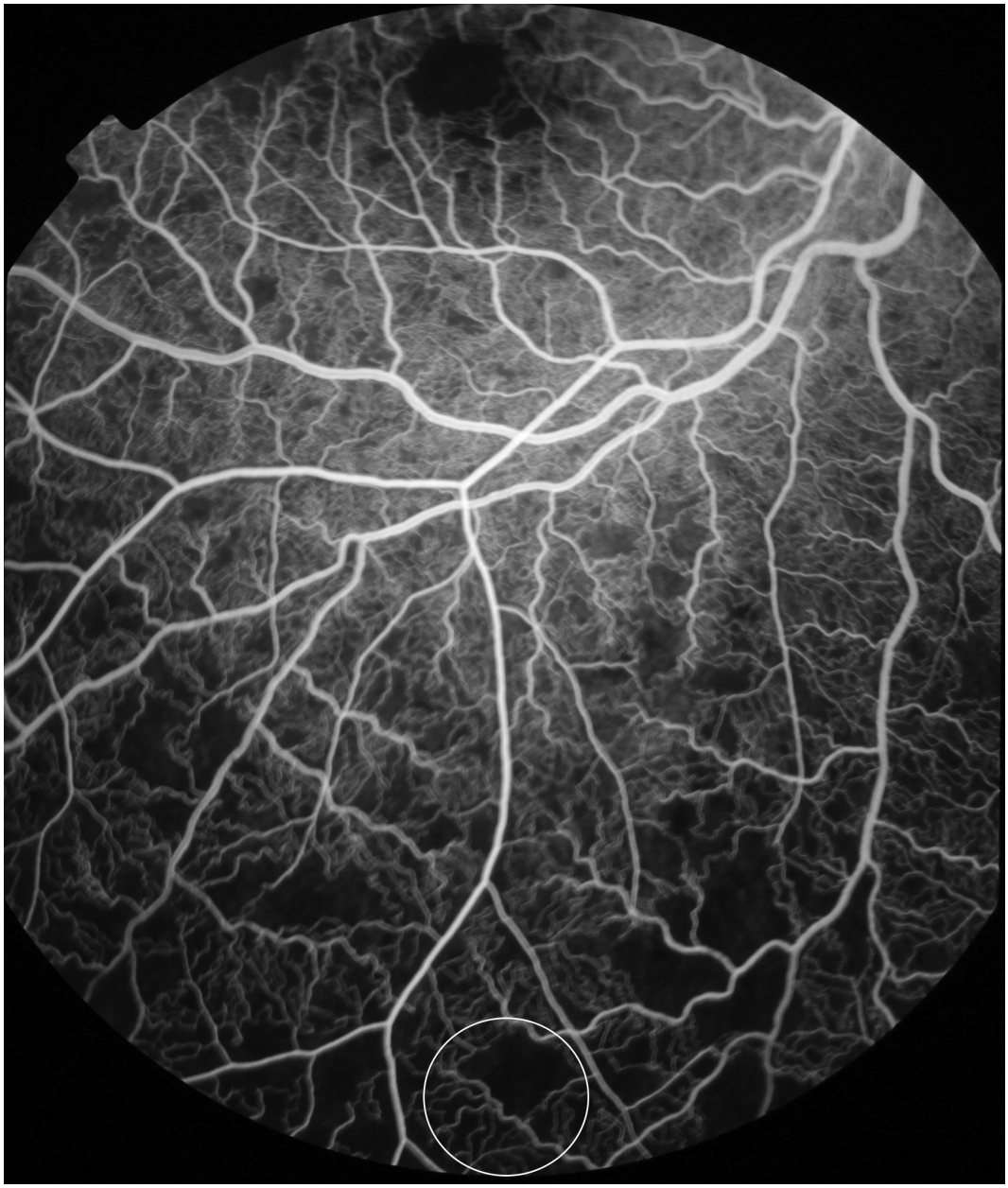

Figure 37: Grade 2 peripheral capillary non-perfusion (CNP).
Infero-nasal retina, right eye. Individual areas of CNP are between 1/3 and 1 disc area. Other visible features include disc leak, punctate focal leak, and intravascular filling defects in small and large venules (white arrows)

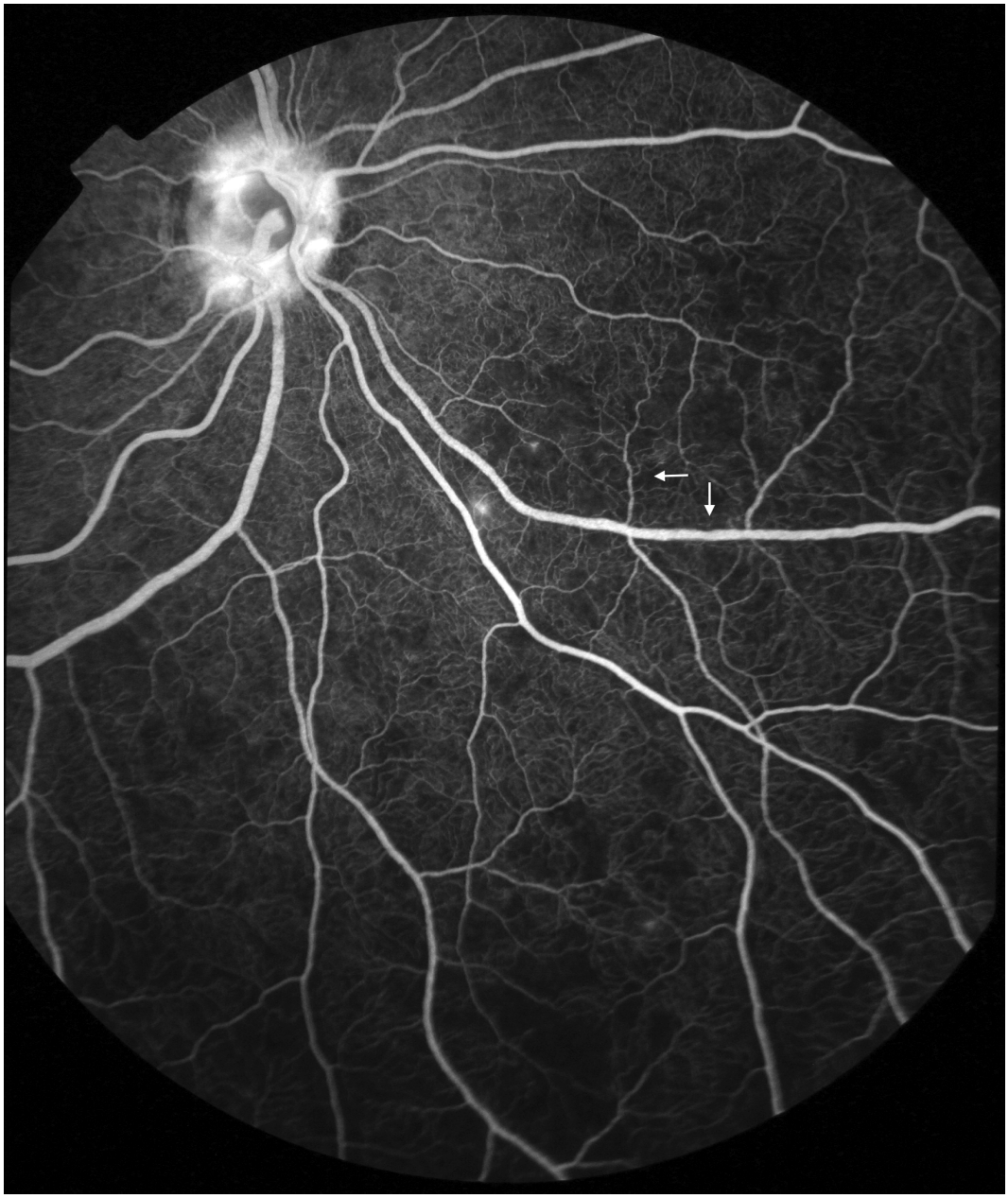

Figure 38: Grade 3 peripheral capillary non-perfusion (CNP).
Montage of FA images, left eye. Individual areas of CNP are greater than 1 disc area (superior and temporal quadrants), but do not extend into zone 2 nasally or zone 1 in other quadrants. Bays of CNP cut across large vessels and ghost vessels may be visible (e.g. temporal quadrant)

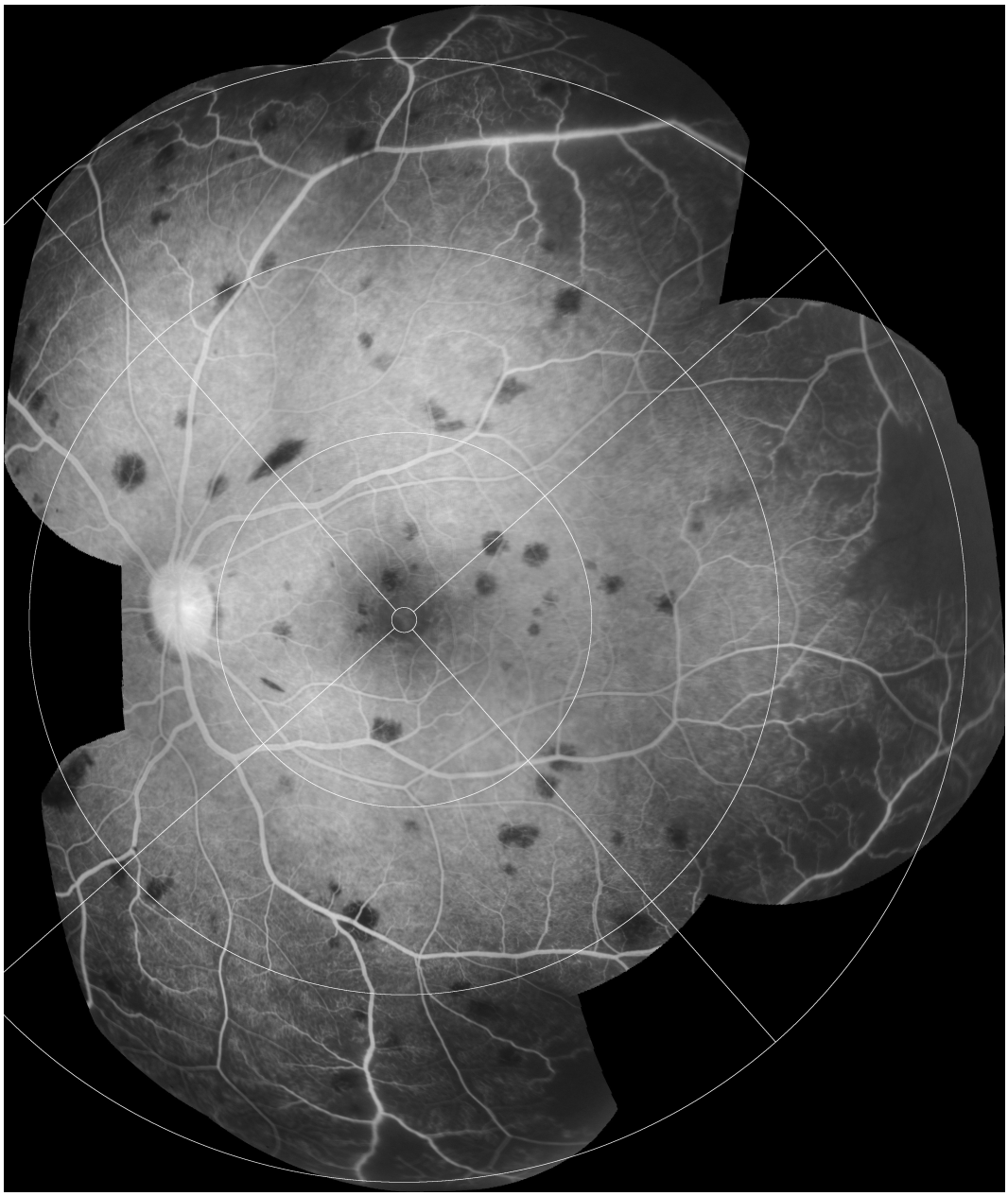

Figure 39: Grade 4 peripheral capillary non-perfusion (CNP).
Montage of FA images, right eye. One or more large bays of CNP encroach on zone 1 (inferior quadrant). Bays of CNP cut across large venules and arterioles, which may appear as ghost vessels in the affected area

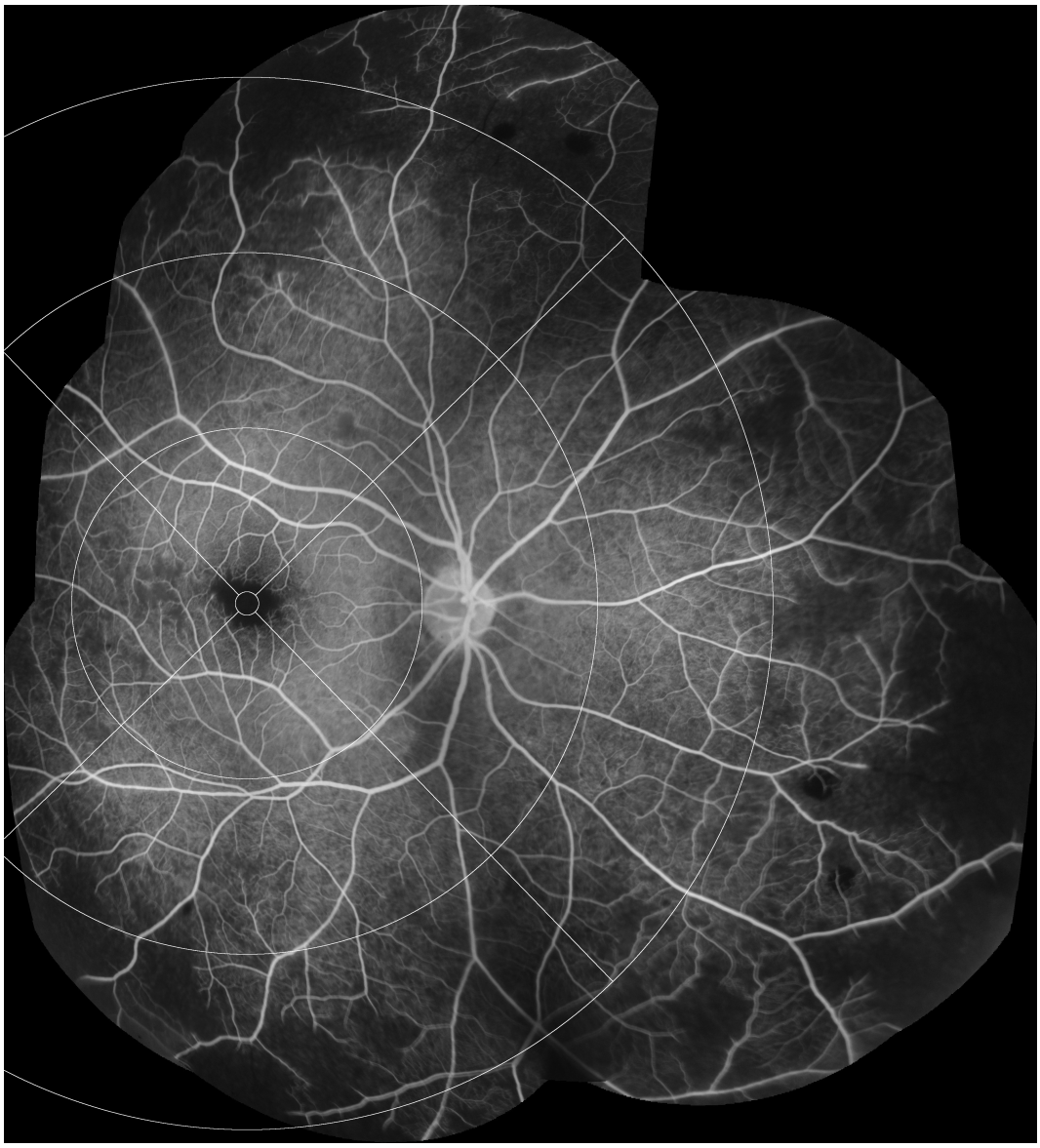

5.6.3 Large focal leak

Large focal leak involves one or more large (>125μm in greatest linear diameter), usually circular, areas of leak. 125μm is approximately the width of a major venule at the optic disc. Images are rarely ungradeable for large focal leak because it is very bright. However it is probably not appropriate to grade a subject as having 'absent' focal leak if they do not have at least one valid image of the macula and one valid peripheral image (≥75% of each area). Large focal leak is graded by counting each site of leak (Table 15; Figures 40 41).

Table 15: Grading large focal leak

Lesion	Grading	Definition	Figures
Large focal leak	Cannot grade	No gradeable images exist	None
	Absent	No large focal leak is seen on any gradeable image	None
	Count	A count of the number of leakage sites on a montage of fluorescein angiogram images that have been combined to illustrate the whole extent of retina captured during the fluorescein run.	40, 41

Figure 40: Large focal leak.

Right eye. One site of large focal leak is visible in the temporal macula (white arrow). Large focal leak appears to represent the evolution of retinal haemorrhage

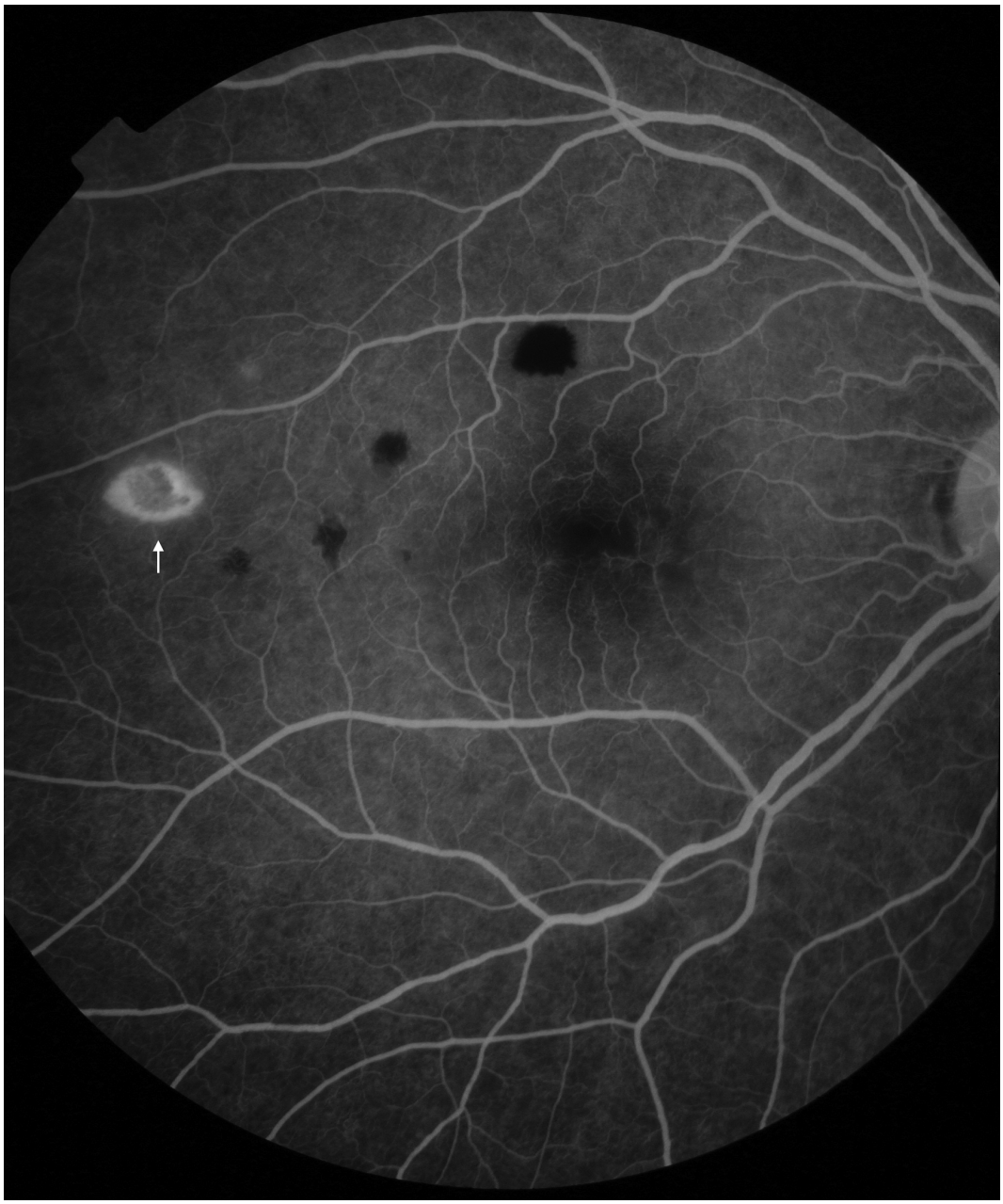

Figure 41: Large focal leak.

Montage of FA images, left eye. Many sites of large focal leak are visible in the context of severe retinal haemorrhage, which causes masking of background fluorescein and the appearance of multiple dark blots that obscure the vasculature. Disc leak is also visible. Distinguishing sites of large focal leak can be difficult in severe cases

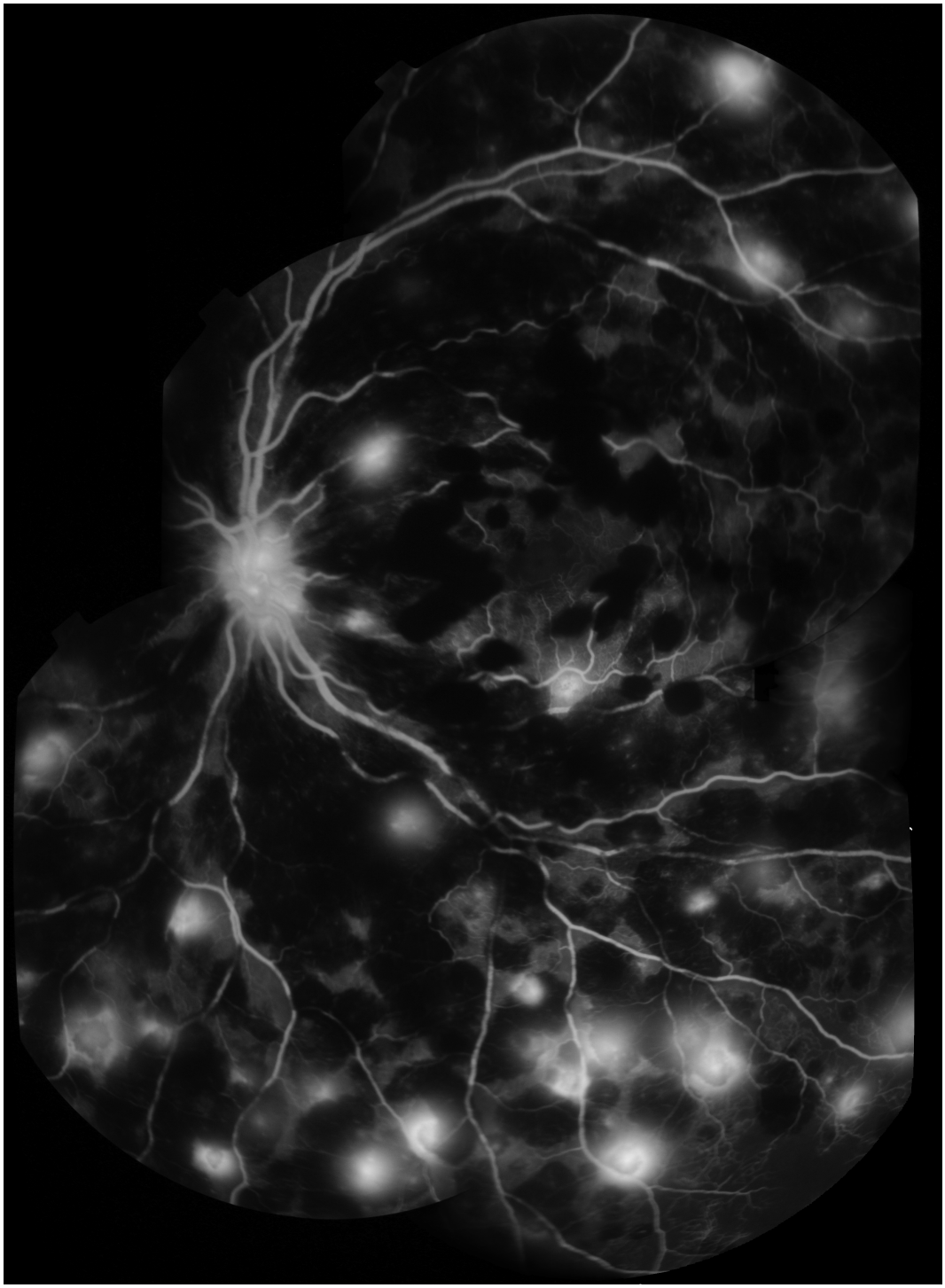

5.6.4 Punctate focal leak

This involves small (≤125μm) sites of leak. 125μm is approximately the width of a major venule at the optic disc. Ideally this type of leak should be graded from a montage of images, to avoid double-counting lesions. In some cases, the very early appearance of large focal leak can look punctate, before enlarging. To avoid confusion the size of leakage foci should be checked at different times during the angiogram. Punctate focal leak is graded on an ordinal scale (Table 16; Figure 42).

Table 16: Grading punctate focal leak

Lesion	Grading	Definition	Figures
Punctate focal leak	Cannot grade	No gradeable images exist	None
	Absent	No punctate focal leak is seen on any gradeable image	None
	Grade 1	1-5 sites are seen in the whole retina	34, 37
	Grade 2	6-20 sites are seen in the whole retina	None
	Grade 3	21-50 sites are seen in the whole retina	None
	Grade 4	>50 sites are seen in the whole retina	42

Figure 42: Punctate focal leak.

Left eye. Multiple sites of punctate focal leak are visible

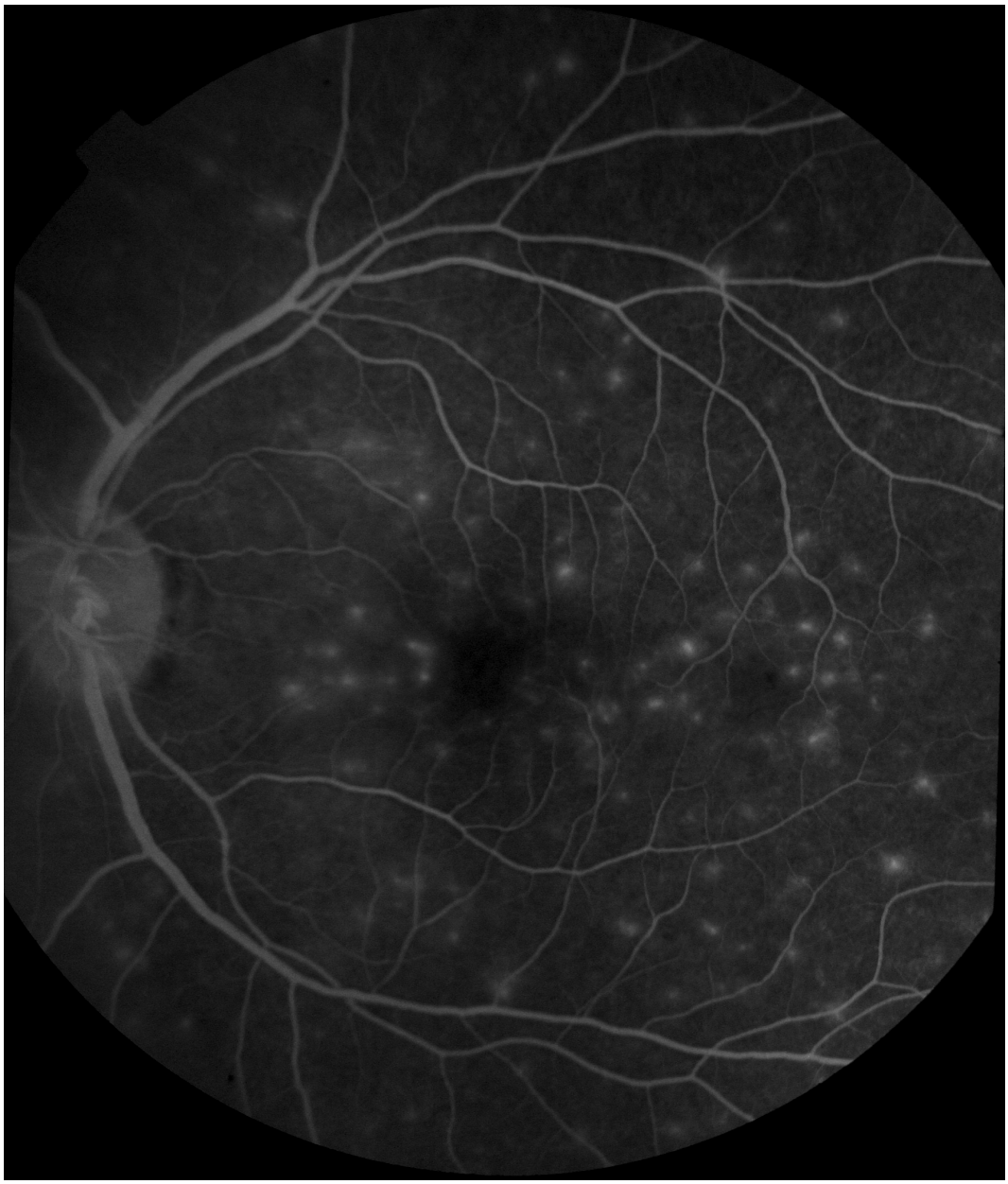

5.6.5 Post-capillary venule leak

This describes blurring of post-capillary venules within a distance 1/3 disc diameter (500μm) from the capillary bed (i.e. the post-capillary venule complex). When present, one or more post-capillary venules show blurring and/or increased brightness over time, compared to adjacent arterioles. Vessel segments cannot be graded for vessel leakage if adjacent vessels are not sharp enough to compare vessel margin blurring. If possible, leak should be confirmed by comparing the same vessel segments at different times during the fluorescein run. Post-capillary venule leak is graded on an ordinal scale (Table 17; Figures 43 44).

Table 17: Grading post-capillary venule leak

Lesion	Grading	Definition	Figures
Post-capillary venule leak	Cannot grade	No gradeable images exist	None
	Absent	No post-capillary venule leak is seen on any gradeable image	None
	Grade 1	1-5 post-capillary venules have leak	None
	Grade 2	6-20 post-capillary venules have leak	43, 44
	Grade 3	21-50 post-capillary venules have leak	None
	Grade 4	>50 post-capillary venules have leak	47

Figure 43: Post-capillary venule leak.

Left eye. Post-capillary venule leak affecting many vessel segments. Subtle leak from venules can be detected by comparing venules (e.g. double arrow) with corresponding arterioles (single arrow). The alternating pattern of arterioles and venules makes this sign particularly clear in well focussed images of the fovea (centre of image). Disc leak is also visible.

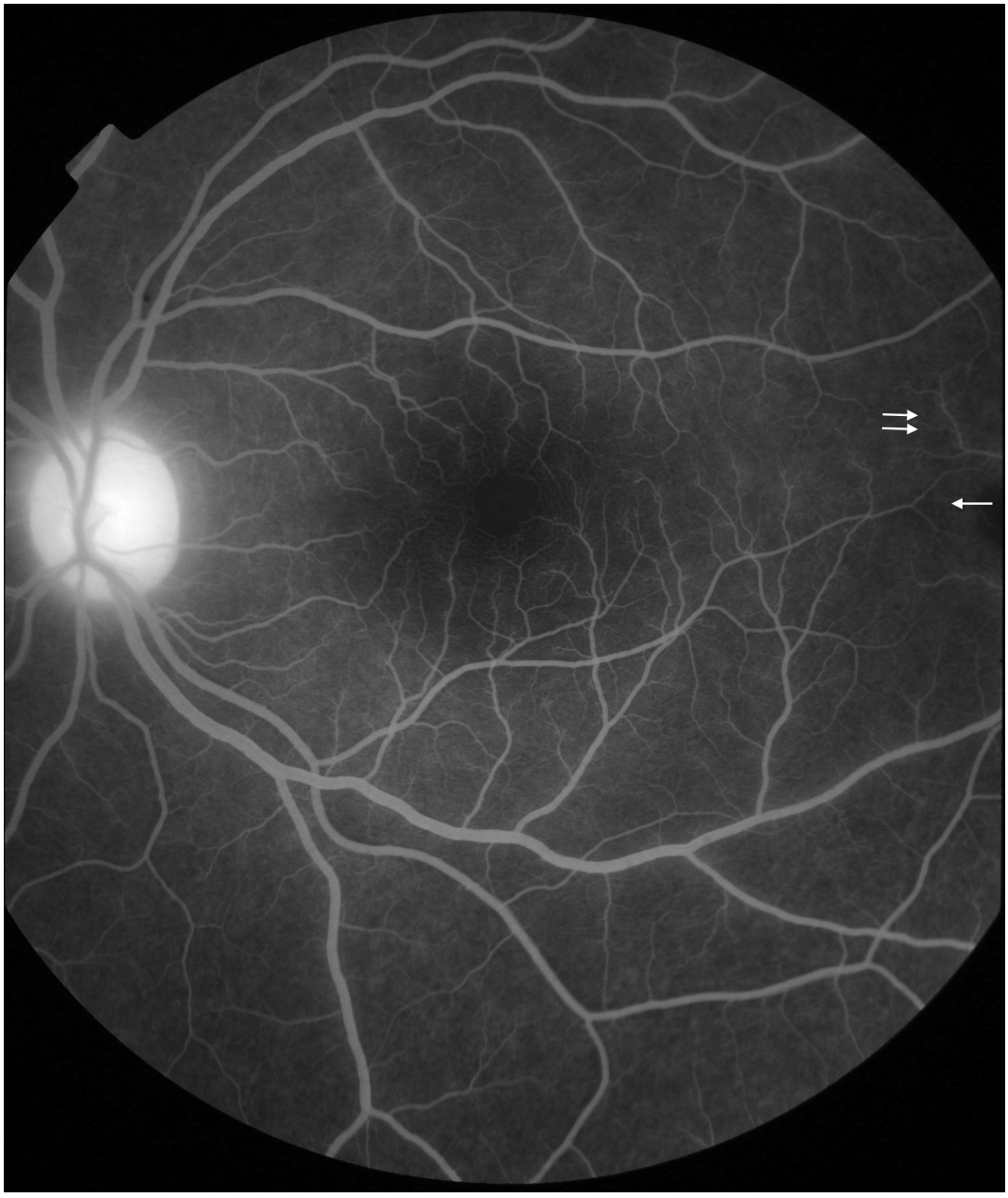

Figure 44: Post-capillary venule leak.

Left eye. Post-capillary venule leak around the fovea. Disc leak and large/small venule leak are also visible.

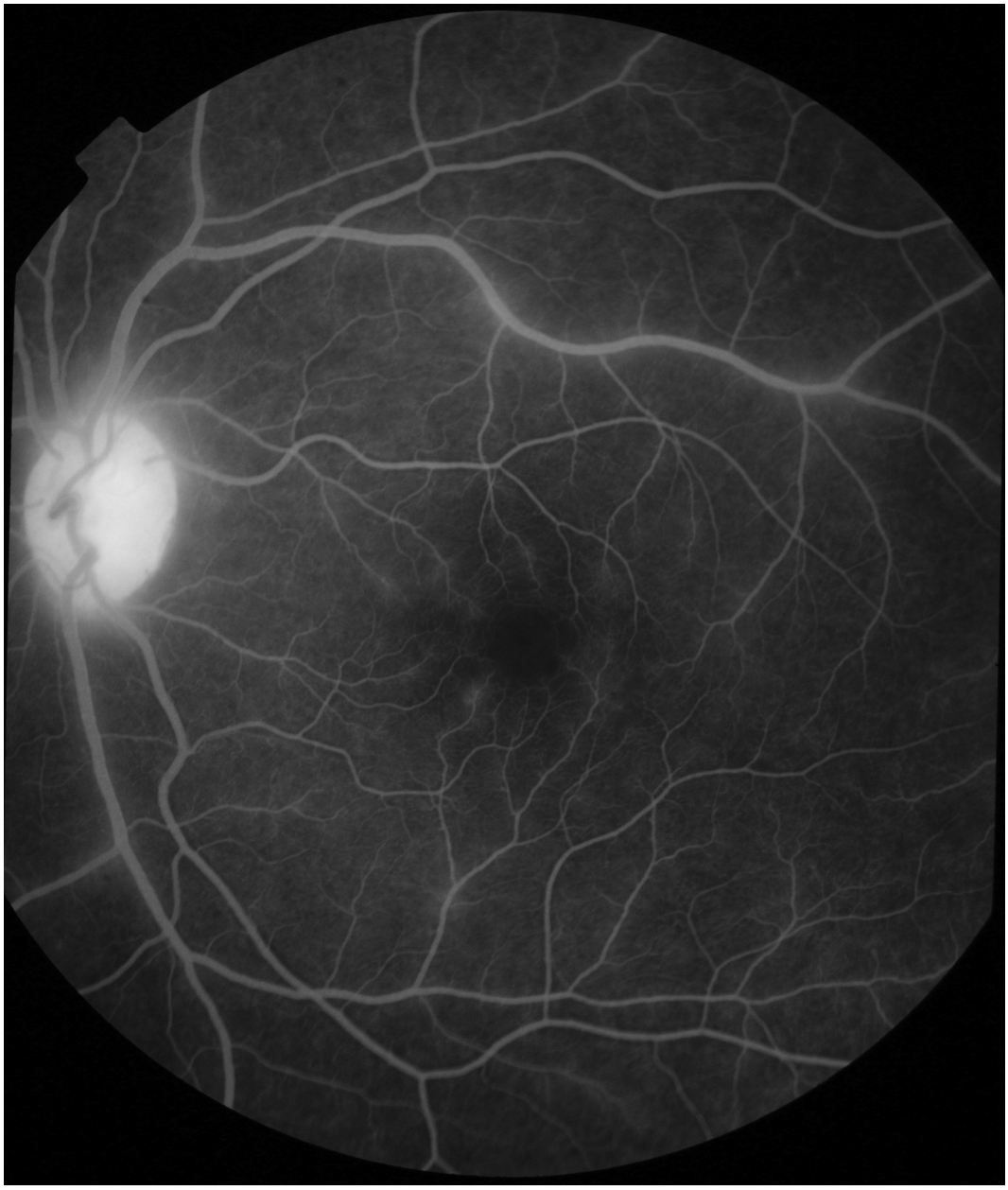

5.6.6 Large/small venule leak

Leakage can be inferred when the margins of venules downstream of the post-capillary venule complex are blurred, compared to adjacent arterioles. Venules may also have increased brightness over time. Ideally venule leak should be graded from a montage of images to prevent double counting of vessels. Images must be sharp enough to allow comparison of vessel margin blur between adjacent vessel segments. Large/small venule leak is graded on an ordinal scale (Table 18; Figures 45 46 47).

Table 18: Grading large/small venule Leak

Lesion	Grading	Definition	Figures
Large/small venule leak	Cannot grade	No gradeable images exist	None
	Absent	No large/small venule leak is seen on any gradeable image	None
	Grade 1	Less than 1/3 of all small and large venule segments are blurred and/or show increased brightness over time, compared to adjacent vessel segments, for the whole retina	45
	Grade 2	1/3-2/3 of all small and large venule segments are blurred and/or show increased brightness over time, compared to adjacent vessel segments, for the whole retina	46
	Grade 3	>2/3 of all small and large venule segments are blurred and/or show increased brightness over time, compared to adjacent vessel segments, for the whole retina	47

Figure 45: Grade 1 large/small venule leak.

Left eye. Less than 1/3 of all large/small venule segments are leaking (superior quadrant). Disc leak is visible.

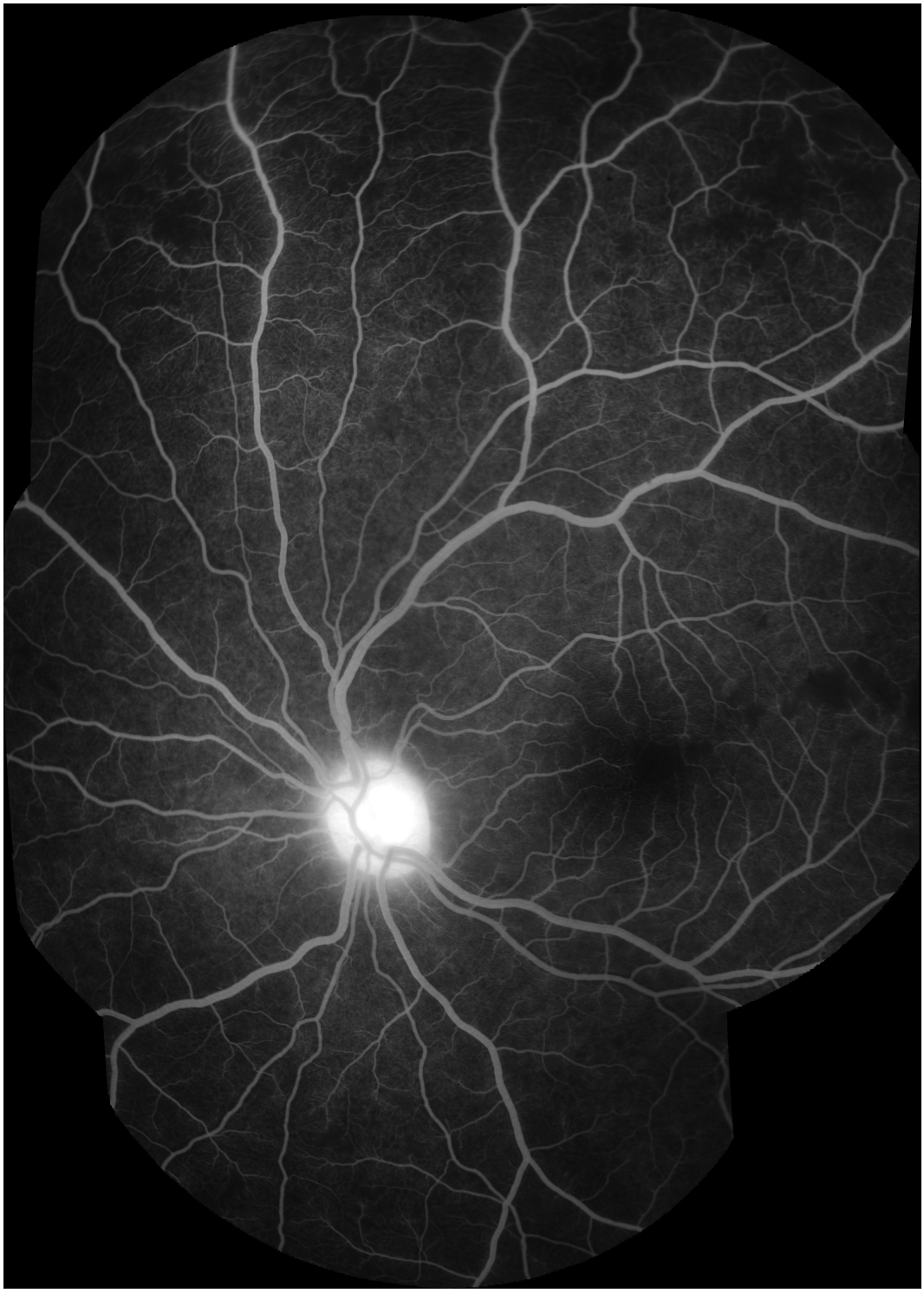

Figure 46: Grade 2 large/small venule leak.

Montage of FA images, left eye. Between 1/3 and 2/3 of all large/small venule segments are leaking. Very severe macular and peripheral CNP are also visible, with ghost vessels in areas of CNP in the temporal quadrant.

Figure 47: Grade 3 large/small venule leak.

Montage of FA images, right eye. Greater than 2/3 of all large/small venule segments are leaking. Image quality is affected by extensive leakage of fluorescein. Other visible features include very severe peripheral CNP (large bays enter zone 1 in temporal and inferior quadrants. Note ghost vessel in temporal quadrant – white arrow), grade 4 post-capillary venule leak, and disc leak.

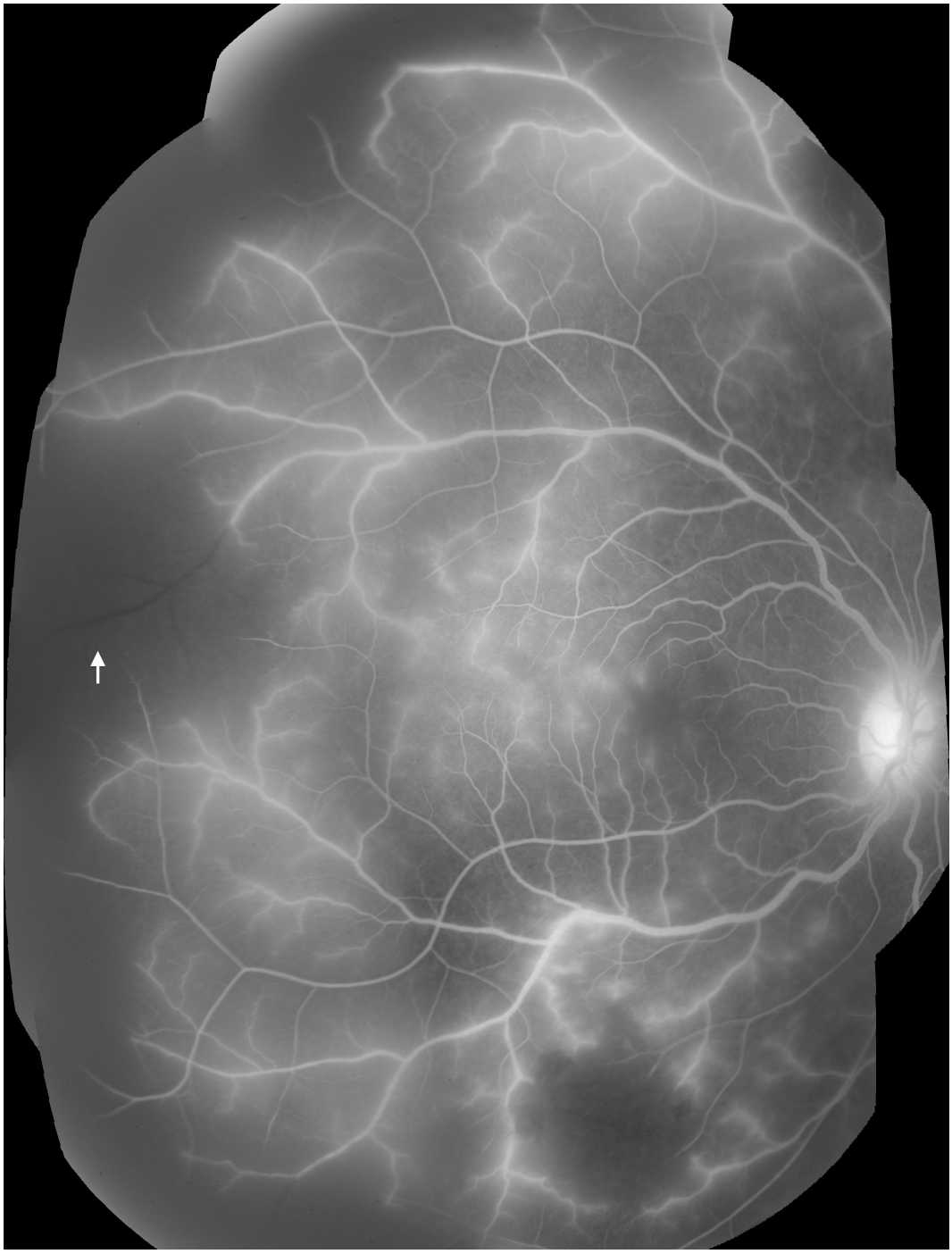

5.6.7 Disc leak

Disc leak is defined as an increase in brightness with blurring of the disc margin, over time during the fluorescein run. It can only be graded 'absent' by examination of images taken during mid to late phases of the fluorescein run. If no mid or late images exist, or if the disc is obscured, it should be graded 'CG' (Table 19; Figure 48).

Table 19: Grading disc leak

Lesion	Grading	Definition	Figures
Disc leak	Cannot grade	No gradeable images exist	None
	Absent	No disc leak is seen on any gradeable image	37, 45, 48
	Present	Disc leak is present on one or more gradeable images	37, 45, 48

Figure 48: Disc leak.

A – Normal disc with no leak (6min after injection of fluorescein). B – disc leak is visible as increasing brightness over time and blurring of the disc margin (in this case 2min after injection). Peri-disc haemorrhages are seen as black flame-shaped lesions, due to masking of background fluorescence

5.6.8 Intravascular filling defects (IVFD)

Intravascular filling defects are abnormalities of the blood column. They can occur in large and small retinal vessels of all types but appear to be most frequent and dense in post-capillary venules (Beare *et al.*, 2009). In larger vessels the appearance can range from slight irregularity to the impression that small 'bites' have been taken from the vessel. Small vessels can appear mottled. The observation of IVFD depends on being able to discern abnormal texture in vessels. This is not possible in images that are blurred, or where vessels are obscured by haemorrhage or leak. It may be possible to see severe IVFD in slightly blurred images, but confidently ruling out the presence of any defects requires images sharp enough to identify individual capillaries next to the vessels being graded. If image quality is poorer than this, filling defects cannot be ruled out, and the images should be graded 'CG' (Table 20; Figures 49 50).

Table 20: Grading intravascular filling defects (IVFD)

Lesion	Grading	Definition		Figures
Intravascular filling defects (IVFD)	Cannot grade	No gradeable images exist (adjacent capillaries are not clear). CG can be assigned to one or more vessel types		None
	Capillaries	Absent	IVFD are not seen in any capillaries	None
		Present	IVFD are seen in capillaries	None
	Post-capillary venule complex	Absent	IVFD are not seen in any post-capillary venules	None
		Present	IVFD are seen in post-capillary venules	None
	Pre-capillary arteriole complex	Absent	IVFD are not seen in any pre-capillary arterioles	None
		Present	IVFD are seen in pre-capillary arterioles	None
	Small venules	Absent	IVFD are not seen in any small venules	None
		Present	IVFD are seen in small venules	35,49, 50
	Small arterioles	Absent	IVFD are not seen in any small arterioles	None
		Present	IVFD are seen in small arterioles	49, 50
	Large venules	Absent	IVFD are not seen in any large venules	
		Present	IVFD are seen in large venules	37, 49, 50
	Large arterioles	Absent	IVFD are not seen in any large arterioles	None
		Present	IVFD are seen in large arterioles	49, 50

Figure 49: Intravascular filling defects (IVFD).

20º image, right eye. In this image IVFD are prominent in vessels at the disc (white arrow). The venules appear to be affected much more severely than corresponding arterioles.

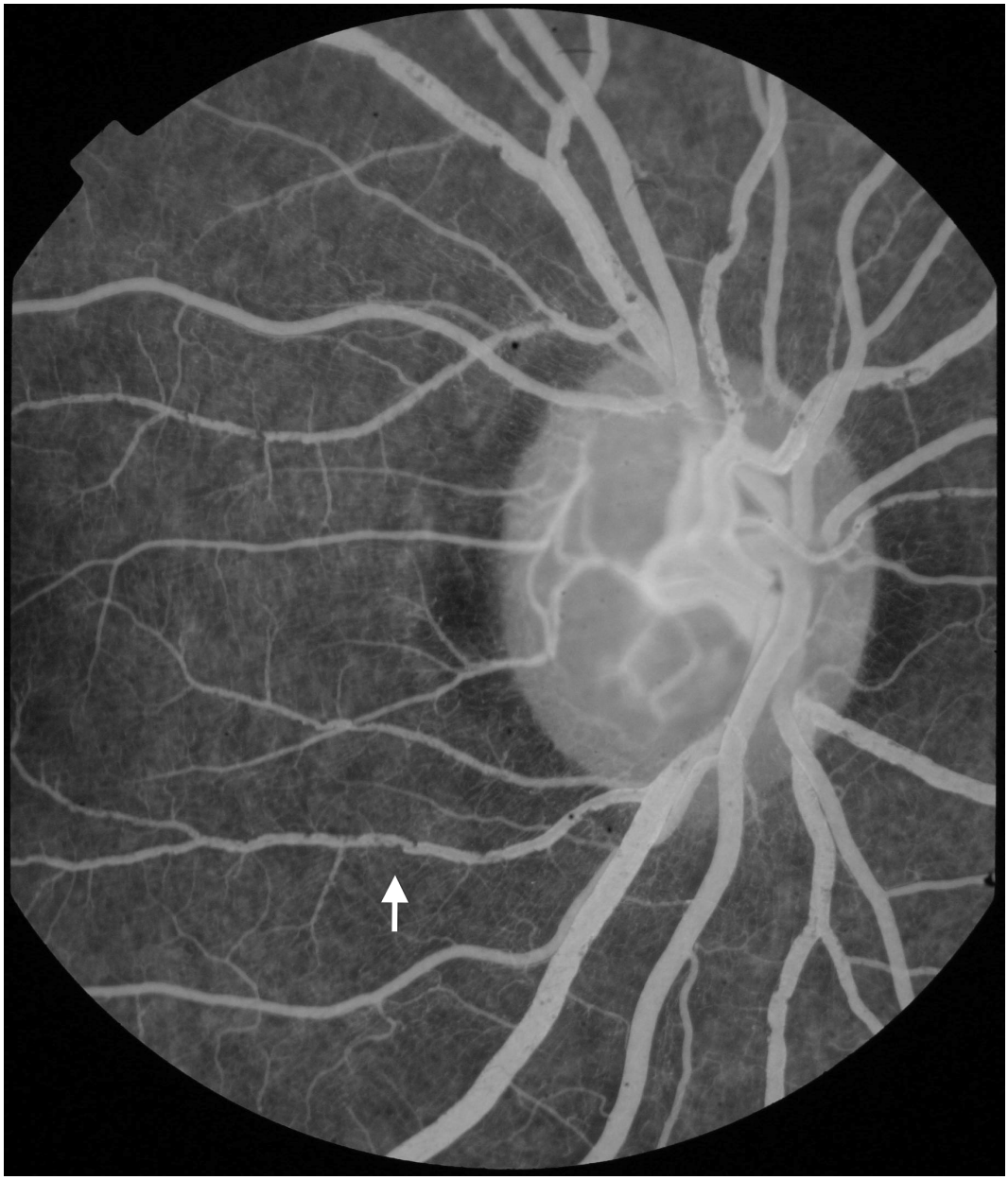

Figure 50: Intravascular filling defects (IVFD).

A – Left eye, 50º image of the macula and temporal periphery. IVFD are prominent in venules and arterioles. B – Full size image of the vessel junction marked in (A) (white arrow), illustrates mottling of the blood column.

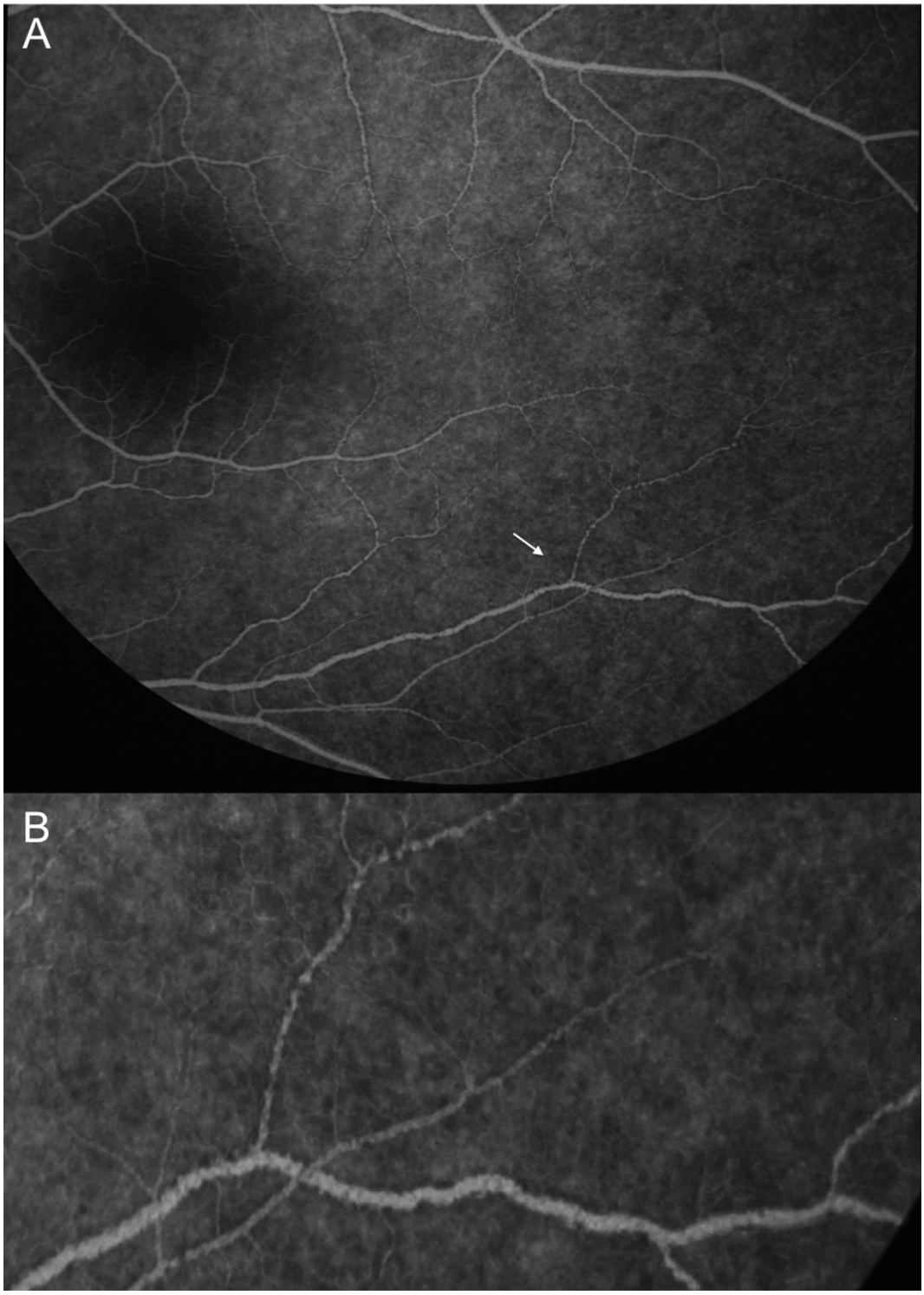

5.6.9 Other features

Other features besides those described above may be seen on FA in severe malaria. These include cystoid macular oedema and leakage from arterioles. If signs that are not part of the standardised grading scheme are observed this should be indicated on the grading form, with a description of the lesion.

5.7 Performance of the grading scheme

Between 2006 and 2014, 285 children had FA imaging of the left eye on admission to the Research Ward. The clinical characteristics of this group are listed in Table 21.

Grading scores were compared between grader 1 and grader 2 for all left eye images. Agreement was >80% for six features, 70-80% for three features, 60-69% for two features, and 50-59% for three features. The lowest levels of agreement were found for IVFD in capillaries, small arterioles, and large arterioles (Table 22). The weighted Kappa statistic was >0.35 ('good') for all variables except large/small venule leak, post-capillary venule leak, all IVFD variables, and macular CNP. In some cases low Kappa statistics were found for features that were also highly prevalent, and had high expected agreement (e.g. macular CNP, IVFD in small venules).

Dual grading with adjudication was performed on 285 left eye image sets from these subjects. The great majority of FA images in my sample were from children with CM with or without severe malarial anaemia (276/285, 96.84%). Similarly, the majority had malarial retinopathy visible on ophthalmoscopic exam (264/285, 92.63%). A minority (5/285) had other severe malarial syndromes, or non-malarial illness (4/285). The distribution of FA features for these groups is shown in Table 23. The data in this table are taken from the adjudicated grading for the left eye.

The most common FA feature in retinopathy-positive CM was CNP. Some level of macular CNP was seen in all cases, and peripheral CNP was seen in ~95%. Grade 1 macular CNP is extremely mild, and may well be present even when

macular whitening is not visible with indirect ophthalmoscopy. However ~80% of retinopathy-positive CM cases had grade 2 CNP or above. Of the leakage types, disc leak was seen in ~80% of retinopathy-positive CM cases, post-capillary venule leak in ~50%, Large venule leak in ~60%, punctate focal leak in ~30%, and large focal leak in ~12%. Venular IVFD were seen in 60-90%; arteriolar IVFD were seen in 8-40% (Table 23).

Table 21: Clinical characteristics of 285 subjects with admission FA

		Median	25th centile	75th centile	Number	Percent
Total		n/a	n/a	n/a	285	100.00
History						
Age		39.00	28.00	58.50	285	100.00
Gender	Male				137	48.07
	Female				148	51.93
Diagnosis	CM				124	43.51
	SMA				1	0.35
	CM+SMA				152	53.33
	Other malarial diagnosis				4	1.40
	Non-malarial illness				4	1.40
Examination						
Weight (kg)		12.00	10.00	15.00	285	100.00
Height (cm)		93.00	84.00	104.00	281	98.60
Mid-upper arm circumference (cm)		15.00	14.50	16.00	282	98.95
Temperature (rectal, C)		38.80	38.10	39.50	285	100.00
Heart rate (beat/sec)		150.00	133.50	169.00	285	100.00
Systolic blood pressure (mmHg)		97.00	90.00	106.00	268	94.04
Respiratory rate (breaths/sec)		44.00	36.00	52.00	285	100.00
Respiratory distress	Absent				195	68.42
	Present				90	31.58
Blantyre Coma Score	0				20	7.02
	1				130	45.61
	2				135	47.37
Retinopathy* (worst eye)	Absent				21	7.37
	Present				264	92.63
Investigations						
Peripheral parasitaemia (parasites/µl)		45,000.0	2,535.50	184,000.00	277	97.19
White cell count (cells)		10,050.0	7,200.00	14,500.00	270	94.74
Platelets (platelets)		62,500.0	33,000.00	105,000.00	268	94.04

		Median	25th centile	75th centile	Number	Percent
Haematocrit (%)		20.00	16.00	24.85	282	98.95
Venous lactate (mmol/L)		4.80	2.90	9.00	281	98.60
Plasma HRP2 (ng/ml)		7,405.00	3,117.00	10,452.00	263	92.28
HIV status	Negative				224	78.60
	Positive				39	13.68
Outcome						
Outcome	Full recovery				213	74.74
	Sequelae				36	12.63
	Death				36	12.63
* Retinopathy assessed by dilated bilateral indirect ophthalmoscopy						

Table 22: Inter-grader agreement (Left eye)

Variable	Number with data for comparison	Frequency of feature (grader 1)	Observed agreement between graders (%)	Weighted Kappa (95%CI)
Macular CNP	248	266/268 (99%)	74.9	0.17 (0.1-0.25)
Peripheral CNP	264	263/278 (95%)	80.40	0.38 (0.31-0.46)
Punctate focal leak	273	77/281 (27%)	89.10	0.38 (0.28-0.48)
Disc leak	278	237/283 (84%)	82.73	0.44 (0.31-0.58)
Post capillary venule leak	273	115/275 (42%)	84.25	0.39 (0.31-0.48)
Large venule leak	279	88/280 (31%)	71.92	0.18 (0.12-0.24)
Large focal leak*	285	34/285 (12%)	95.95	0.19 (0.07-0.31)
Capillary IVFD	212	62/220 (28%)	59.91	0.11 (-0.02-0.25)
Post-capillary venule unit IVFD	231	212/237 (89%)	75.32	0.21 (0.09-0.34)
Pre-capillary arteriole unit IVFD	235	52/243 (21%)	67.23	0.12 (-0.04-0.28)
Small venule IVFD	265	240/267 (90%)	84.91	0.17 (0.07-0.26)
Small arteriole IVFD	263	55/267 (21%)	57.79	0.26 (0.15-0.38)
Large venule IVFD	265	167/268 (62%)	69.43	0.13 (0.05-0.2)
Large arteriole IVFD	264	32/268 (12%)	59.47	0.17 (0.1-0.25)
CNP = Capillary non-perfusion IVFD = Intravascular filling defects *Large focal leak is a count variable with skewed distribution. Agreement estimated for categories “absent”, “1 site of leak”, “>1 site of leak”				

Table 23: Fluorescein angiogram features in 285 subjects with admission angiogram of the left eye, reported by clinical diagnosis.

*Only one subject with severe malarial anaemia, and one subject with a non-malarial diagnosis, had large focal leak. These numbers are absolute counts, not ranges. CNP = Capillary non-perfusion; IVFD = Intravascular filling defects; N/A = Not applicable

	Retinopathy negative				Retinopathy positive				
Diagnosis	Cerebral malaria	Cerebral malaria and severe malarial anaemia	Other malaria diagnosis	Non-malarial diagnosis	Cerebral malaria	Severe malarial anaemia	Cerebral malaria and severe malarial anaemia	Other malaria diagnosis	Non-malarial diagnosis
	Grade: Number (%)								
Macular CNP									
Absent	0 (0)	1 (50.00)	0 (0)	0 (0)	0 (0)	0 (0)	0 (0)	0 (0)	0 (0)
Grade 1	7 (46.67)	0 (0)	0 (0)	2 (66.67)	15 (13.76)	0 (0)	25 (16.67)	0 (0)	0 (0)
Grade 2	7 (46.67)	1 (50.00)	1 (100)	1 (33.33)	57 (52.29)	0 (0)	67 (44.67)	2 (66.67)	1 (100)
Grade 3	0 (0)	0 (0)	0 (0)	0 (0)	21 (19.27)	0 (0)	34 (22.67)	0 (0)	0 (0)
Grade 4	0 (0)	0 (0)	0 (0)	0 (0)	9 (8.26)	0 (0)	17 (11.33)	0 (0)	0 (0)
Cannot grade	1 (6.67)	0 (0)	0 (0)	0 (0)	7 (6.42)	1 (100)	7 (4.67)	1 (33.33)	0 (0)
Peripheral CNP									
Absent	0 (0)	0 (0)	0 (0)	1 (33.33)	5 (4.59)	0 (0)	0 (0)	0 (0)	0 (0)
Grade 1	14 (93.33)	2 (100)	1 (100)	2 (66.67)	63 (57.8)	0 (0)	71 (47.33)	1 (33.33)	0 (0)
Grade 2	0 (0)	0 (0)	0 (0)	0 (0)	15 (13.76)	1 (100)	36 (24)	1 (33.33)	1 (100)
Grade 3	1 (6.67)	0 (0)	0 (0)	0 (0)	12 (11.01)	0 (0)	23 (15.33)	0 (0)	0 (0)
Grade 4	0 (0)	0 (0)	0 (0)	0 (0)	12 (11.01)	0 (0)	15 (10.00)	0 (0)	0 (0)

	Retinopathy negative				Retinopathy positive				
Diagnosis	Cerebral malaria	Cerebral malaria and severe malarial anaemia	Other malaria diagnosis	Non-malarial diagnosis	Cerebral malaria	Severe malarial anaemia	Cerebral malaria and severe malarial anaemia	Other malaria diagnosis	Non-malarial diagnosis
	Grade: Number (%)								
Cannot grade	0 (0)	0 (0)	0 (0)	0 (0)	2 (1.8)	0 (0)	5 (3.3)	1 (3.3)	0 (0)
Punctate focal leak									
Absent	14 (93.3)	1 (50.0)	1 (100)	2 (66.6)	78 (71.5)	0 (0)	109 (72.6)	2 (66.6)	1 (100)
Grade 1	1 (6.6)	1 (50.0)	0 (0)	1 (33.3)	23 (21.1)	1 (100)	32 (21.3)	0 (0)	0 (0)
Grade 2	0 (0)	0 (0)	0 (0)	0 (0)	4 (3.6)	0 (0)	5 (3.3)	0 (0)	0 (0)
Grade 3	0 (0)	0 (0)	0 (0)	0 (0)	3 (2.7)	0 (0)	1 (0.6)	0 (0)	0 (0)
Grade 4	0 (0)	0 (0)	0 (0)	0 (0)	0 (0)	0 (0)	1 (0.6)	0 (0)	0 (0)
Cannot grade	0 (0)	0 (0)	0 (0)	0 (0)	1 (0.9)	0 (0)	2 (1.3)	1 (3.3)	0 (0)
Disc leak									
Absent	11 (73.3)	1 (50.0)	0 (0)	3 (100)	24 (22.0)	0 (0)	18 (12.0)	0 (0)	1 (100)
Present	4 (26.6)	1 (50.0)	1 (100)	0 (0)	84 (77.0)	1 (100)	131 (87.3)	2 (66.6)	0 (0)
Disc not seen	0 (0)	0 (0)	0 (0)	0 (0)	1 (0.9)	0 (0)	1 (0.6)	1 (33.3)	0 (0)
Post-capillary venule leak									
Absent	14 (93.3)	0 (0)	1 (100)	3 (100)	62 (56.8)	0 (0)	66 (44.0)	0 (0)	1 (100)
Grade 1	1 (6.6)	1 (50.0)	0 (0)	0 (0)	28 (25.6)	0 (0)	40 (26.6)	1 (33.3)	0 (0)
Grade 2	0 (0)	1 (50.0)	0 (0)	0 (0)	12 (11.0)	0 (0)	24 (16.0)	0 (0)	0 (0)
Grade 3	0 (0)	0 (0)	0 (0)	0 (0)	4 (3.6)	1 (100)	13 (8.6)	1 (33.3)	0 (0)
Grade 4	0 (0)	0 (0)	0 (0)	0 (0)	1 (0.9)	0 (0)	3 (2.0)	0 (0)	0 (0)
Cannot grade	0 (0)	0 (0)	0 (0)	0 (0)	2 (1.8)	0 (0)	4 (2.6)	1 (33.3)	0 (0)
Large venule leak									

	Retinopathy negative				Retinopathy positive				
Diagnosis	Cerebral malaria	Cerebral malaria and severe malarial anaemia	Other malaria diagnosis	Non-malarial diagnosis	Cerebral malaria	Severe malarial anaemia	Cerebral malaria and severe malarial anaemia	Other malaria diagnosis	Non-malarial diagnosis
	Grade: Number (%)								
Absent	12 (80.0)	1 (50.0)	1 (100)	3 (100)	79 (72.4)	0 (0)	80 (53.3)	1 (33.3)	1 (100)
Grade 1	3 (20.0)	1 (50.0)	0 (0)	0 (0)	22 (20.1)	0 (0)	50 (33.3)	0 (0)	0 (0)
Grade 2	0 (0)	0 (0)	0 (0)	0 (0)	5 (4.5)	1 (100)	12 (8.0)	1 (33.3)	0 (0)
Grade 3	0 (0)	0 (0)	0 (0)	0 (0)	1 (0.9)	0 (0)	6 (4.0)	0 (0)	0 (0)
Cannot grade	0 (0)	0 (0)	0 (0)	0 (0)	2 (1.8)	0 (0)	2 (1.3)	1 (33.3)	0 (0)
IVFD, capillaries									
Absent	7 (46.6)	0 (0)	0 (0)	2 (66.6)	31 (28.4)	0 (0)	30 (20.0)	1 (33.3)	0 (0)
Present	0 (0)	1 (50.0)	0 (0)	0 (0)	18 (16.5)	0 (0)	20 (13.3)	0 (0)	0 (0)
Cannot grade	8 (53.3)	1 (50.0)	1 (100)	1 (33.3)	60 (55.0)	1 (100)	100 (66.6)	2 (66.6)	1 (100)
IVFD, post-capillary venules									
Absent	1 (6.6)	1 (50.0)	0 (0)	1 (33.3)	3 (2.7)	0 (0)	4 (2.6)	0 (0)	0 (0)
Present	11 (73.3)	1 (50.0)	1 (100)	2 (66.6)	88 (80.7)	0 (0)	110 (73.3)	2 (66.6)	1 (100)
Cannot grade	3 (20.0)	0 (0)	0 (0)	0 (0)	18 (16.5)	1 (100)	36 (24.0)	1 (33.3)	0 (0)
IVFD, pre-capillary arterioles									
Absent	8 (53.3)	2 (100)	0 (0)	2 (66.6)	43 (39.4)	0 (0)	56 (37.3)	2 (66.6)	0 (0)
Present	4 (26.6)	0 (0)	1 (100)	1 (33.3)	47 (43.1)	0 (0)	48 (32.0)	0 (0)	0 (0)
Cannot grade	3 (20.0)	0 (0)	0 (0)	0 (0)	19 (17.4)	1 (100)	46 (30.6)	1 (33.3)	1 (100)
IVFD, small venules									
Absent	5 (33.3)	1 (50.0)	0 (0)	0 (0)	4 (3.6)	1 (100)	13 (8.6)	0 (0)	0 (0)
Present	9 (60.0)	1 (50.0)	1 (100)	3 (100)	98 (89.9)	0 (0)	126 (84.0)	2 (66.6)	1 (100)

	Retinopathy negative				Retinopathy positive				
Diagnosis	Cerebral malaria	Cerebral malaria and severe malarial anaemia	Other malaria diagnosis	Non-malarial diagnosis	Cerebral malaria	Severe malarial anaemia	Cerebral malaria and severe malarial anaemia	Other malaria diagnosis	Non-malarial diagnosis
	Grade: Number (%)								
Cannot grade	1 (6.6)	0 (0)	0 (0)	0 (0)	7 (6.4)	0 (0)	11 (7.3)	1 (33.3)	0 (0)
IVFD, small arterioles									
Absent	14 (93.3)	2 (100)	0 (0)	1 (33.3)	70 (64.2)	1 (100)	91 (60.6)	2 (66.6)	0 (0)
Present	0 (0)	0 (0)	1 (100)	2 (66.6)	31 (28.4)	0 (0)	46 (30.6)	0 (0)	1 (100)
Cannot grade	1 (6.6)	0 (0)	0 (0)	0 (0)	8 (7.3)	0 (0)	13 (8.6)	1 (33.3)	0 (0)
IVFD, large venules									
Absent	12 (80.0)	1 (50.0)	0 (0)	3 (100)	23 (21.1)	1 (100)	46 (30.6)	1 (33.3)	0 (0)
Present	3 (20.0)	1 (50.0)	1 (100)	0 (0)	79 (72.4)	0 (0)	94 (62.6)	1 (33.3)	1 (100)
Cannot grade	0 (0)	0 (0)	0 (0)	0 (0)	7 (6.4)	0 (0)	10 (6.6)	1 (33.3)	0 (0)
IVFD, large arterioles									
Absent	15 (100)	1 (50.0)	1 (100)	3 (100)	88 (80.7)	1 (100)	129 (86.0)	2 (66.6)	1 (100)
Present	0 (0)	1 (50.0)	0 (0)	0 (0)	15 (13.7)	0 (0)	12 (8.0)	0 (0)	0 (0)
Cannot grade	0 (0)	0 (0)	0 (0)	0 (0)	6 (5.5)	0 (0)	9 (6.0)	1 (33.3)	0 (0)
Large focal leak									
Absent	15 (100)	2 (100)	1 (100)	3 (100)	99 (91.6)	0 (0)	127 (84.6)	3 (100)	0 (0)
Present	0 (0)	0 (0)	0 (0)	0 (0)	9 (8.3)	1 (100)	23 (15.3)	0 (0)	1 (100)
Range	N/A	N/A	N/A	N/A	0-30	12*	0-32	N/A	7*
Cannot grade	0 (0)	0 (0)	0 (0)	0 (0)	0 (0)	0 (0)	0 (0)	0 (0)	0 (0)

5.8 Discussion

I have developed and tested a scheme for grading FA images of malarial retinopathy, along with example images to aid future interpretation of FA in this disease. This scheme can reliably classify dysfunction in the retinal vasculature seen in paediatric CM, in spite of challenges around image acquisition and quality that do not apply to most other retinal conditions. Unlike patients with diabetic retinopathy or age-related macular degeneration, patients with severe malaria are acutely unwell and capturing high quality images is difficult. Although I tested this scheme on images from children with CM, I believe that it will be applicable to future studies of severe malaria in general since malarial retinopathy is seen in some severe malarial syndromes other than CM, and in adults as well as children.

5.8.1 Angiographic features in paediatric severe malaria

FA features were commonly seen in children with retinopathy-positive CM, and could range from mild to severe. The same features were sometimes observed in children with other diagnoses (Table 23). This is consistent with previous observations of malarial retinopathy in severe non-cerebral, moderate, and uncomplicated paediatric malaria (Lewallen *et al.*, 1999). Cases without obvious retinopathy on ophthalmoscopic exam, or with diagnoses other than malaria, were included for completeness and to ensure the maximum number of cases for assessment of the grading scheme – which was the primary reason for this analysis. The number of subjects with non-CM diagnoses is not large enough to draw conclusions about the frequency of FA signs in these groups in the population in general, but my results indicate that retinal abnormalities do exist in patients without other signs of malarial retinopathy, and also in patients with diagnoses other than malaria. Increasingly sensitive retinal imaging modalities may potentially reveal previously unnoticed retinal dysfunction, both in CM and other neurological infections.

5.8.2 Inter-grader agreement

I found good levels of agreement between graders for the majority of features (Table 22), including CNP (75-80%) and four of the five types of leakage (>83%). Grading of large venule leak had an agreement of 72%, and may have been

affected by variable focus, brightness, and clarity during the FA run. Graders should review the full run of images to aid in this interpretation. Grading IVFD was more problematic, especially for the capillary network. Although they can be seen clearly on some exceptionally sharp images, experience suggests that capillary IVFD are probably beyond the resolution of standard FA, and that this feature should be treated with caution. Other existing or emerging imaging modalities may be more suitable for studying retinal capillaries in CM. Agreement for IVFD was consistently lower on the arteriolar compared to the venular side (57-67% vs 69-85% respectively). This may be a result of bleaching secondary to a greater concentration of fluorescein in arterioles compared to venules. Nevertheless, I found that expert adjudication of inter-grader discrepancies for arteriolar IVFD was much more feasible than for capillary IVFD and should provide reasonable quality data.

I found good (weighted kappa 0.35 to 0.7) inter-grader agreement for the majority of features in my grading scheme. This gives me reasonable confidence that my scheme can reliably measure most FA features of malarial retinopathy. Poor inter-grader agreement can occur for several reasons. Some features are difficult to grade and disagreements between graders are inevitable. I found that capillary IVFD was especially hard to record, and was heavily dependent on image quality. This is true for most, if not all, medical imaging quantified by human graders (E.g. reading chest x-ray films (Albaum *et al.*, 1996)).

However, low kappa values can also arise from the mathematical characteristics of this statistic. Kappa depends not only on measured and expected agreements, but also on the marginal distribution of disagreements, the prevalence of the feature in question, and the number of ordinal categories used (Marasini *et al.*, 2014). This suggests that low values for weighted kappa should not necessarily lead one to dismiss data for a particular feature as unreliable, but should prompt an examination of the two-way table comparing results from graders. For example, macular CNP is the most common FA feature in our group, with a frequency of 266/285 (93.3%). We found a measured agreement between graders of 74.9%, but a weighted kappa of 0.17 ('poor agreement'). Automated grading techniques

based on computerised image analysis may provide more reliable quantification than manual grading, but suitable statistics are also needed.

Disagreements between graders are inevitable and occur in most, if not all, medical imaging quantified by human observers. Adjudication of dual grading is an accepted approach to improving validity of grading systems and is widely used in research settings. Careful attention to training and quality control, and inclusion of adjudication gives me good confidence that my scheme can reliably be used to assess the FA features of malarial retinopathy. Automated grading techniques based on computerised image analysis may provide more reliable quantification than manual grading in the future (Zheng *et al.*, 2014).

5.8.3 Using this grading scheme in future studies of malarial retinopathy

In order to maximise the quality of grading data, studies of malarial retinopathy should ensure that images are taken by experienced retinal photographers and graded by observers who are familiar with grading retinal images. Ideally multiple graders should develop a mutual consensus on feature recognition by training on a set of malarial retinopathy test images before starting formal grading. I recommend that future studies of retinal imaging in malaria also perform dual grading with independent adjudication. Studies on malarial retinopathy should describe photographer and grader experience. Data on the overall quality of images and amount of retinal periphery captured give useful indications about the robustness of grading data in a study, and I suggest that these should be reported along with the frequency of specific FA features. These recommendations are not specific to FA images, but are applicable to collection and grading colour images and other retinal imaging modalities that may yet be applied to severe malaria.

5.9 Conclusions

This FA grading scheme offers a practical and consistent method to investigate malarial retinopathy in different populations and allow comparison between studies. I believe that my formal grading scheme will enhance understanding of severe malaria by allowing direct comparison of angiographic findings in malarial

retinopathy between children and adults, and between patients in different geographical areas. The reliability of grading is feature specific, and is also likely to depend on overall image quality and grader experience. Good levels of agreement can be achieved with experienced graders. Independent adjudication should be used to maximise grading accuracy.

Chapter 6 – Associations between ophthalmoscopic features and clinical outcomes

6.1 Aim of chapter

To describe associations between admission funduscopic exam and clinical outcomes in retinopathy positive paediatric cerebral malaria

6.2 Summary of chapter

6.2.1 What is known already

Many investigators have reported associations with malarial retinopathy in paediatric severe malaria. In general these results are based either on a comparison of children with and those without malarial retinopathy, or on samples of children with mixed retinopathy status. In paediatric cerebral malaria, malarial retinopathy has close associations with cerebral histopathology which suggest that the presence of retinopathy differentiates histopathologically defined cerebral malaria from coma of other cause with incidental parasitaemia. If this is the case, then analyses of associations within a sample of retinopathy positive cases may provide new and important information, different from previously reported findings from studies that compare retinopathy positive cases with retinopathy negative controls.

6.2.2 What this chapter involved

Structured funduscopic examinations have been recorded on children admitted to the paediatric research ward since 1999. I added to this dataset by examining patients from 2012 to 2014, designing a database, and entering and processing data from the entire cohort. I then estimated associations between features of malarial retinopathy visible with ophthalmoscopy and two clinical outcomes: death, and time to regain consciousness – defined as a Blantyre Coma Score of ≥3/5.

6.2.3 What this chapter adds to current knowledge

Previous reports describe associations between death and papilloedema, severity of retinal haemorrhages, and peripheral whitening. However these results are from datasets including retinopathy negative cases, which are likely to have histopathological diagnoses other than cerebral malaria, and as such are heterogeneous datasets. The analysis I report in this chapter found that, within retinopathy positive cases, >50 retinal haemorrhages and the presence of orange vessels are independently associated with death, and that >50 haemorrhages, severe foveal whitening, orange vessels, white vessels, and papilloedema are independently associated with longer time to recover from coma. Differences from previous reports may be explained by different selection criteria, greater sample size, and different statistical techniques. These results are arguably more relevant to disease mechanisms related to cerebral malaria pathology than studies on children with classically defined cerebral malaria.

6.3 Introduction

Cerebral malaria (CM) is a severe manifestation of infection with *P. falciparum*, which occurs predominantly in children in sub-Saharan Africa, where transmission is endemic, and adults in regions with lower transmission (World Health Organization, 2014b). Various associations have been reported between features of malarial retinopathy in paediatric CM, and clinical characteristics or outcomes. Such studies have usually been based on samples that include children meeting the standard case definition and thus include patients with, and also without, malarial retinopathy (Beare et al., 2004; Beare et al., 2004; Lewallen, 1998; Lewallen et al., 1993; Lochhead et al., 2010; Postels, Birbeck, et al., 2012; Seydel et al., 2012). These studies analyse retinopathy positive and negative subjects as one group. Other studies have taken a slightly different approach, and explicitly *compared* groups of children with and without malarial retinopathy (Conroy *et al.*, 2010, 2012; Lewallen *et al.*, 2008; Milner *et al.*, 2012; Phiri *et al.*, 2011; Postels *et al.*, 2014; Postels, Taylor, *et al.*, 2012; Potchen *et al.*, 2012).

These approaches have provided useful information about paediatric CM. In particular it appears that, in children, the presence of malarial retinopathy can

accurately differentiate between cases of histopathologically confirmed CM and cases of parasitaemic coma that appear to have CM according to standard clinical criteria, but in fact have alternative causes of death at autopsy (Taylor *et al.*, 2004). This is supported by similar results showing that the severity of malarial retinopathy is correlated with the severity of sequestration in both retina and brain (Barrera *et al.*, 2015).

Current clinical diagnostic criteria are broad, requiring the presence of coma, *P. falciparum* parasitaemia, and the absence of any other obvious cause of coma – such as hypoglycaemia, meningitis, or post-ictal state (World Health Organization, 2014b). In sub-Saharan Africa it is not usually possible to rule out aetiologies beyond this short list, and since parasitaemia is commonplace CM is likely to be over diagnosed. The results of Taylor et al., (2004) suggest this may occur in approximately 25% of cases. This finding is highly important, and particularly so for studies of CM pathogenesis, since it suggests that studies using the traditional definition of paediatric CM probably include a significant number of patients who only appear to have CM, but in fact are unlikely to have cerebral sequestration. Such sample heterogeneity may lead to errors in effect size estimates, and generally raises difficulties with interpreting results in terms of the specific pathogenesis of coma and death associated with cerebral sequestration.

Previously published reports of associations between features of malarial retinopathy and death in paediatric CM suggest that papilloedema is independently associated with death (Beare et al., 2004; Lewallen et al., 1993). This is consistent with the recent report of a strong link between death and severe brain swelling on admission MRI brain (Seydel *et al.*, 2015), and between death and clinical signs of brain herniation (Newton et al., 1991). Retinal haemorrhage (Beare et al., 2004) and whitening of the retinal periphery (Lewallen *et al.*, 1993) have also been associated with death, but only in one study each, both of which included subjects on the basis of the WHO clinical criteria for CM regardless of retinopathy status. It is therefore unclear if these associations also apply specifically to retinopathy-positive paediatric CM, a diagnosis which implies that coma and death are related to sequestration in the brain rather than other non-malarial causes of death (Taylor *et al.*, 2004).

In this chapter I present an analysis of ophthalmoscopic features observed on admission in children with retinopathy-positive CM. Malarial retinopathy is defined as at least one of the following signs: retinal haemorrhage (often white centred); retinal whitening of the fovea, macula, or periphery; and orange or white vessel discolouration. Isolated papilloedema, without any of these other findings, does not on its own identify a patient as having malarial retinopathy (Harding *et al.*, 2006).

The objective is to describe associations between these retinal features and two clinical outcomes: death, and time to regain consciousness – defined as Blantyre Coma Score of ≥3/5. Since the retina and brain share many features in common (MacCormick *et al.*, 2014), these associations may cast light on the pathogenesis of paediatric CM.

6.4 Methods

6.4.1 Study design

Prospective cohort study

6.4.2 Setting

This research took place within an ongoing study of severe malaria (Taylor, 2009) in the Paediatric Research Ward (PRW) of Queen Elizabeth Central Hospital (QECH), Blantyre, Malawi. Informed consent was given by the parents or guardians of all patients. This research adhered to the tenets of the Declaration of Helsinki, and was approved by the ethics committees of relevant academic institutions.

Patients were recruited to the study during malaria seasons (January to June) from 1999 to 2014. I personally recruited subjects in 2012, 2013 and 2014. Ophthalmoscopic examination was performed on admission and patients were followed during their hospital stay. Recovery from coma, or death, usually occur within a few days of admission.

6.4.3 Participants

Paediatric CM was defined according to World Health Organization (WHO) clinical criteria: peripheral *P. falciparum* parasitaemia, Blantyre Coma Score (BCS) <3, and no other evident explanation for coma. Hypoglycaemia, post-ictal state, and meningitis were explicitly ruled out as causes of coma in all cases (World Health Organization, 2014b). Patients could also have additional severe malarial syndromes, such as severe malarial anaemia. In addition, the presence of malarial retinopathy is interpreted as a diagnostic test to distinguish between coma associated with cerebral sequestration and coma with parasitaemia (Taylor et al., 2004; World Health Organization, 2014b). This was used to further classify patients into retinopathy-positive or retinopathy-negative groups. The former is a more stringent case definition of paediatric CM than described by the WHO criteria, and is likely to produce a more homogeneous sample which is of greater relevance to a study of disease mechanisms. Malarial retinopathy is defined as retinal haemorrhage (often white-centred), and/or retinal whitening, and/or orange or white vessel discolouration (Harding *et al.*, 2006; Lewallen *et al.*, 1999). Papilloedema in isolation does not indicate malarial retinopathy, but is associated with increased risk of death (Beare et al., 2004). I also considered that isolated peri-papillary haemorrhages in the context of papilloedema were not diagnostic of malarial retinopathy (Lewallen et al., 1999).

Patients were included in this analysis if they were admitted to the PRW with a diagnosis of WHO defined CM, and had one or more signs of malarial retinopathy based on ophthalmoscopic examination performed within 48 hours of admission. Patients were excluded if consent was withdrawn, if outcome data were missing, or if the initial coma score was greater than 2/5. This final exclusion refers to a very small minority of cases who had admission coma score >2 but then developed more profound coma just after admission.

6.4.4 Variables

6.4.4.1 Outcomes

Variable	Variable code	Description/comment	Measurement
Death	death	Binary variable describing which subjects lived or died	Clinical observation recorded in notes
Time to regain consciousness	timetocs3	Count variable describing the number of hours between admission and BCS≥3/5 Highly skewed with over-dispersion. Truncated as no subjects woke within 1 hour of admission	Clinical observation recorded in notes

6.4.4.2 Exposures

Variable	Variable code	Description	Measurement
Ophthalmoscopic features on funduscopic examination (within 48 hours of admission)			
Retinal haemorrhage	ahaem_w	Ordinal variable describing the number of haemorrhages in the worst affected eye, (none, 1-5, 6-20, 21-50, >50)	Dilated bilateral indirect ophthalmoscopy, done by ophthalmologist and recoded on standard form
Foveal whitening	acfa_w	Ordinal variable describing the severity of foveal whitening in the worst affected eye, (none, <1/3 foveal area involved, 1/3-2/3 involved. >2/3 involved)	
Macular whitening	awhitcmac_w	Ordinal variable describing severity of macular whitening in the worst affected eye, (none, <1/3 disc area, 1/3-1 disc area, >1 disc area)	
Orange vessels	orvess_temp_w	Binary variable, presence or absence of orange vessels in the temporal quadrant of the worst affected eye	
White vessels	wvess_temp_w	Binary variable, presence or absence of white vessels in the temporal quadrant of the worst affected eye	
White capillaries	wcap_temp_w	Binary variable, presence or absence of white capillaries in the temporal quadrant of the worst affected eye	
Disc hyperaemia	adiskhyp_w	Binary variable, presence of disc hyperaemia in the worst affected eye	

Papilloedema	apap_w	Binary variable, presence of papilloedema in the worst affected eye	
Clinical history			
Age	age	Continuous, age at admission in months	
Gender	sex	Binary, male or female	
Duration of coma	comadur	Count variable, number of hours between onset of coma and admission. Highly skewed	
Duration of fever	feverdur	Count variable, number of hours between onset of fever and admission. Highly skewed	
Clinical examination			
Pulse	pulse	Continuous, pulse rate per minute	
Coma score	comasc	Ordinal variable, depth of coma according to scale from 0 to 5	
Respiratory distress	respdis	Binary, describing the presence of any one of: nasal flare, chest indrawing, retraction, or deep breathing.	
Witnessed convulsions at admission	fitsonadm	Binary, positive if a convulsion of any duration was witnessed by nursing or clinical staff while the patient was in the admission bay	
Witnessed convulsions after admission	wardfits	Binary, positive if a convulsion of any duration was witnessed by nursing or clinical staff while the patient was in the main ward	
Investigations			
Blood pressure	bp	Continuous, systolic blood pressure in mmHg	
Temperature	temp	Continuous, rectal temperature in degrees centigrade	
Haematocrit	ahct	Continuous, fraction (%) of packed red cells from a finger prick sample	Finger prick sample
White cell count	abldwbc	Continuous, number of cells from full blood count	Coulter Counter, Beckman Coulter
Platelet count	platelet	Continuous, number of platelets from full blood count	(Coulter Counter, Beckman Coulter)
Lactate	admlact	Continuous, finger prick sample (mmol/L)	Lactate Pro point of care detector (Arkray Inc)
Parasitaemia	abldpta	Continuous, number of parasitised cells in finger prick sample	Microscopy
HRP2	hrp2	Continuous, stored frozen plasma	Celabs ELISA

		(ng/ml)	
Hypoglycaemia after admission	wardhypogl	Binary	
HIV	hivresults	Binary, two separate tests with confirmation by repeating one test if discrepant results	Uni-Gold Recombigen HIV-1/2, Trinity Biotech; and Determine HIV-1/2, Inverness Medical

6.4.5 Sources of data

Data collection took place during the Malawian malaria seasons (January to June) of 1999 to 2014 inclusive. All patients were initiated or continued on anti-malarial and supportive treatments. After clinical stabilisation an ophthalmologist performed dilated indirect ophthalmoscopy. Malarial retinopathy was graded using a standard form (Harding *et al.*, 2006).

Clinical data from the history, examination, and standard investigations were collected routinely at admission. These included rectal temperature, full blood count (Coulter Counter, Beckman Coulter), and HIV status using two separate tests (Uni-Gold Recombigen HIV-1/2, Trinity Biotech; and Determine HIV-1/2, Inverness Medical). One of the tests was repeated to decide rare discrepant cases. Finger prick blood samples were analysed to determine parasite species and density, packed-cell volume, blood glucose and blood lactate (Lactate Pro point of care detector (Arkay Inc)). Histidine rich protein 2 (HRP2) was measured retrospectively in stored plasma (Celabs ELISA). While peripheral parasitaemia reflects the number of circulating parasites, HRP2 is a parasite specific protein that may reflect the total mass of parasites in the host – whether circulating or sequestered (Dondorp *et al.*, 2005; Lucchi *et al.*, 2011). The eventual outcome of disease was recorded, including obvious neurological sequelae in survivors. Death or recovery typically occurs within 48 hours of admission.

6.4.6 Data handling

Data from the ophthalmoscopic examinations were written on to a standard paper form. I designed a custom database using REDCap (Harris *et al.*, 2009), and entered all ophthalmoscopic data. Audit of a random 10% sample found the

frequency of data entry errors to be approximately 0.5%. Data from the clinical history, exam, and investigations were written in the notes for each patient and subsequently double entered into a separate REDCap database (Harris *et al.*, 2009). I then merged, cleaned, and analysed datasets using Stata (StataCorp, Texas, version 13).

6.4.7 Bias

Potential selection bias was assessed by comparing subjects who did, and did not have admission retinal examination in terms of several variables related to severity of disease.

6.4.8 Study size

Starting with the sample of all patients with CM recruited between 1999 to 2014, subjects were progressively excluded for these reasons: consent withdrawn (1), outcome data missing (3), coma score >2 (5), no admission retinal exam (515), retinopathy negative (343).

6.4.9 Quantitative variables

Quantitative variables were not altered or transformed.

6.4.10 Statistical methods

Analysis was planned during and after data were collected.

6.4.10.1 Assessment of selection bias

Potential selection bias was assessed by comparing subjects who did, and did not have admission retinal examination in terms of several variables related to severity of disease. Logistic regression was used to generate unadjusted odds ratios, except in the case of the variable describing time between admission and death, which was analysed using the Kruskal-Wallis test as regression analysis seemed insensitive to differences in median time.

6.4.10.2 Evaluation of associations with death, or coma recovery time

The aim of the primary analysis was to describe associations between features of the funduscopic examination and two clinical outcomes – death, and time to recover consciousness. Unadjusted and adjusted associations between these outcomes and retinal variables were estimated using logistic regression (in the case of death) and truncated negative binomial regression (in the case of coma recovery time). Truncated negative binomial regression was chosen because the variable describing coma recovery time had a highly skewed distribution with over-dispersion. The data were truncated since no subjects awoke in less than 1 hour after admission.

A range of other variables from the history, examination, and admission investigations were also analysed for unadjusted associations with these outcomes using the same methods. These variables were chosen because associations with death had been reported in previous studies, and also on the basis of expert advice and review of the literature.

Variables were selected for multivariate models according to the following rules: the variable should have a statistically significant ($p<0.01$) unadjusted association with the outcome; and this association should be large enough to be clinically relevant; and the variable should be a plausible cause of the outcome, rather than an effect of the outcome. Plausible relationships were determined on the basis of expert advice.

A recent study from found that death in retinopathy-positive paediatric CM was closely related to severe brain swelling (Seydel *et al.*, 2015). Because of this, I selected variables for the multivariate model of death on the basis of presence or absent of plausible causal links to brain swelling. For example, depth of coma and papilloedema are traditionally included in models of death in CM, but both are likely to be effects of brain swelling rather than causes. Although these variables do undoubtably contain information that is useful for *predicting* death, their inclusion as independent 'exposures' in a model aimed at illuminating disease mechanisms (rather than simply predicting the outcome) could complicate later

biological interpretation, as well as potentially affecting the coefficients of more plausible causes of death (Beyea and Greenland, 1999; Greenland *et al.*, 1999). They were therefore excluded.

The same rules were applied to select variables for the model of time to coma resolution (BCS≥3). In this case depth of coma on admission is likely to directly affect the time taken to wake from coma, since one would expect that patients who are deeply comatose (BCS=0) might therefore take longer to wake than patients who are less so (BCS=2). Similar logic applies to papilloedema, since admission intracranial pressure could well have a direct effect on the time taken to wake.

Variables were also excluded if they were likely to represent the same process as another variable in the model. For example, macular whitening and foveal whitening are closely related and only one was included.

All regression models excluded subjects with missing data for any of the included variables. This is standard for regression analysis that does not involve multiple imputation.

6.5 Results

6.5.1 Participants

Between 1999 and 2014 1684 subjects with CM were recruited within the PRW. Nine were excluded because consent was withdrawn, or because of missing outcome data, or because admission coma score was >2. Of the remaining 1675, 515 did not have an admission retinal exam. Of 1160 who had indirect ophthalmoscopy within 48 hours of admission, 343 were retinopathy negative. This left 817 subjects for the analysis against clinical outcomes (Figure 51).

Figure 51: Derivation of the sample used to analyse associations between retinal features and clinical outcomes.

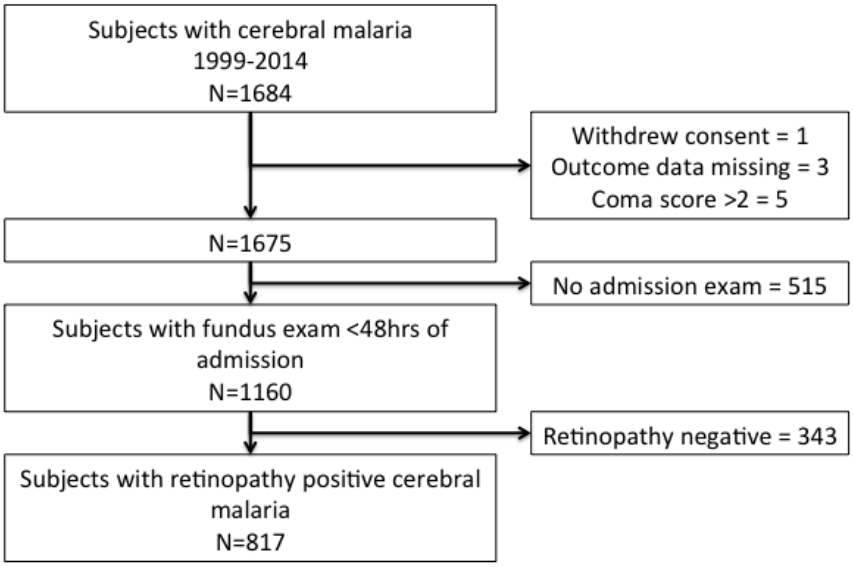

6.5.2 Descriptive data

The groups of subjects who did (n=1160) and did not (n=515) have an admission retinal exam were compared to assess possible selection bias (Table 24). It appears that subjects who did have admission retinal exam were generally less severely unwell than subjects who did not have admission retinal exam. Subjects with admission exam, which includes some retinopathy negative patients, tended to have lower blood lactate, longer time between admission and death, and less frequent death (all $p<0.01$). There was a trend towards lighter coma in the group with admission exam ($p=0.017$). Subjects who had admission retinal exam were also older than those without admission retinal exam (median (IQR): 39 (25-60) vs 34 (22-55) months, $p<0.001$).

Of the 817 subjects included in the analyses of clinical outcomes there were low numbers with missing data for most variables. The following exceptions were missing in more than approximately 10% of subjects: blood lactate, duration of coma pre-admission (both missing in approximately 20%), HIV status (15%), and

disc hyperaemia (12%) (Table 25). Blood lactate was missing more often in subjects with fatal outcomes (present in 67.2% vs 76.3%, p=0.02; two-sided test of z-ratio of two independent proportions).

6.5.3 Outcome data

Within the group of 817 subjects with retinopathy positive CM, who had admission retinal examination, there were 137 deaths (16.8%) (Table 25). 663 subjects had data on time to recover consciousness, and of these 200 (30.2%) reached BCS ≥3/5 within 12 hours, 214 (32.3%) did so between 12 and 24 hours, and 249 (37.6%) took over 24 hours (Table 26).

Table 24: Subjects with and without admission ophthalmoscopy.

Comparison of subjects who did (n=1160), and did not (n=515), have an admission retinal examination. Each of these groups contains a mixture of retinopathy positive and retinopathy negative cases. P-values ≤0.01 are bold. Some variables appear to have statistically significant associations with ophthalmoscopic exam that are unlikely to be clinically significant, e.g. a median difference of 0.2kg in weight. Subjects with a short time between admission and death were less likely to have a retinal examination (p=0.001). *This p-value was generated by Kruskal-Wallis test instead of logistic regression.

		Children without admission eye exam				Children with admission eye exam						
Variable	Detail	Median	IQR	Percent	Number	Median	IQR	Percent	Number	OR	95%CI	p
Total					515				1160			
Demographics												
Age	months	34	22-55		514	39	25-60		1158	1.01	1.00-1.01	**<0.001**
Weight	kg	11.8	9.4-14.2		515	12	10-15		1160	1.03	1.01-1.06	**0.005**
Height	cm	89	78-100		503	91	81-103		1141	1.01	1.00-1.02	**0.001**
Sex	boy			49.71	256			48.66	563			
	girl			50.29	259			51.34	594	1.04	0.85-1.28	0.69
Clinical												
Coma score	0			16.12	83			12.76	148			
	1			42.91	221			39.74	461	1.17	0.86-1.6	0.326
	2			40.97	211			47.5	551	1.46	1.07-2.00	0.017
Respiratory distress	absent			58.51	299			61.6	714			
	present			41.49	212			38.4	445	0.88	0.71-1.09	0.233
History of convulsions	absent			22.79	116			21.6	248			

		Children without admission eye exam				Children with admission eye exam						
Variable	Detail	Median	IQR	Percent	Number	Median	IQR	Percent	Number	OR	95%CI	p
	present			77.21	393			78.4	900	1.07	0.83-1.37	0.59
Convulsions at admission	absent			83.46	429			82.88	954			
	present			16.54	85			17.12	197	1.04	0.79-1.38	0.78
Laboratory												
Parasitaemia	#cells	78395.5	15330-227000		500	68012	11250-278000		1108	1	0.99-1.00	0.095
White cell count	#cells	9800	6800-15025		470	9700	6800-14300		1058	0.99	0.99-1.00	0.685
Haematocrit	%	22	16-28		511	22	17-28		1150	1	0.99-1.02	0.499
Lactate	mmol/L	7	3.4-12.1		321	5.6	3.2-9.4		821	0.95	0.92-0.98	**<0.001**
HRP2	ng/ml	6915	3312.25-12102.5		152	5855.5	2360.5-10434		774	0.99	0.99-1.00	0.06
HIV	negative			84.31	360			84.49	850			
	positive			15.69	67			15.51	156	0.99	0.72-1.35	0.93
Outcomes												
Recovery status	full recovery			68.54	353			75.69	878			
	sequelae			10.68	55			8.53	99	0.72	0.51-1.03	0.07
	died			20.78	107			15.78	183	0.69	0.53-0.90	**0.006**
Time to consciousness	hours	16	8-40		396	16	8-36		952	0.99	0.99-1.00	0.75
Time to death	hours	8	3-24		107	17	6-31		183			**0.001***

Table 25: Unadjusted associations with death in subjects who had admission ophthalmoscopy.

Estimates of association are from logistic regression. p-values <0.01 are bold.

Variable	Description	Subjects who died				Subjects who lived				Association with death		
		Median	25th centile	75th centile	n	Median	25th centile	75th centile	n	OR	95%CI	p
Number					137				680			
Age	months	35	23	59	136	39	27	58.75	680	0.99	0.00-1.00	0.432
Parasitaemia	#cells parasitised	79052	16695	357000	134	68076	11700	298000	649	1	0.99-1.00	0.271
White cell count	#cells	11300	6925	18225	120	9200	6600	13725	630	1	1.00-1.00	**0.004**
Haematocrit	%	19.5	15	24.75	136	20	15.8	25	673	0.99	0.97-1.02	0.689
Lactate	mmol/L	8.75	5.375	12.775	92	5.3	3.2	9.9	519	1.11	1.06-1.16	**<0.001**
HRP2	ng/ml	8838.5	4435.5	15102.25	120	5765	2471.5	10031	609	1	1.00-1.00	**0.004**
Temperature	Degrees C	38.7	37.8	39.5	137	38.9	38	39.7	680	0.89	0.77-1.03	0.121
Systolic blood pressure	mmHg	100	90	110	127	100	90	110	652	0.99	0.99-1.01	0.633
Pulse	Beats/min	156	136.5	170.5	137	152	136.75	169	678	1	0.99-1.01	0.983
Duration of coma	hours	7	4	18	110	7	4	17	558	0.99	0.98-1.01	0.291
Duration of fever	hours	48	33.25	72	130	60	43.25	72	652	0.99	0.99-1.00	0.087
Platelet	#platelets	52000	30250	82750	112	58000	34000	94500	609	1	0.99-1.00	0.844
CSF opening pressure	mmCSF	160	119.3	207.5	64	160	110	220	380	0.99	0.99-1.00	0.67
			number	percent	total		number	percent	total			
Sex	boy		66	48.89	135		342	50.29	680	1.06	0.73-1.53	0.766
	girl		69	51.11			338	49.71				
Coma score	0		32	23.36	137		67	9.85	680	Reference		
	1		57	41.61			256	37.65		0.47	0.28-0.78	**0.003**
	2		48	35.04			357	52.5		0.28	0.17-0.47	**<0.001**
Respiratory distress	absent		70	51.09	137		415	61.03	680			
	present		67	48.91			265	38.97		1.5	1.04-2.17	0.031
Witnessed convulsions at admission	absent		120	87.59	137		574	85.42	672			
	present		17	12.41			98	14.58		0.83	0.45-1.44	0.51

Variable	Description	Subjects who died				Subjects who lived				Association with death		
Witnessed convulsions after admission	absent		82	60.29	136		435	63.97	680			
	present		54	39.71			245	36.03		1.17	0.80-1.71	0.42
HIV	negative		100	77.52	129		503	85.11	591			
	positive		29	22.48			88	14.89		1.66	1.03-2.66	0.036
Hypoglycaemia on ward	absent		117	85.4	137		626	92.19	679			
	present		20	14.6			53	7.81		2.02	1.16-3.5	0.012
Retinal haemorrhage (worst eye)	None		37	27.01	137		183	26.95	679	Reference		
	1 to 5		45	32.85			291	42.86		0.76	0.48-1.23	0.266
	6 to 20		18	13.14			129	19		0.69	0.38-1.27	0.231
	21 to 50		15	10.95			44	6.48		1.69	0.85-3.34	0.135
	>50		22	16.06			32	4.71		3.4	1.78-6.5	**<0.001**
Macular whitening (worst eye)	None		14	10.45	134		101	14.92	677	Reference		
	<1/3		50	37.31			306	45.2		1.18	0.63-2.22	0.611
	1/3 to 1		38	28.36			170	25.11		1.61	0.83-3.12	0.156
	>1		32	23.88			100	14.77		2.31	1.16-4.59	0.017
Foveal whitening (worst eye)	None		21	15.79	133		179	26.48	676	Reference		
	<1/3 foveal area		57	42.86			316	46.75		1.54	0.90-2.62	0.114
	1/3 to 2/3 foveal area		24	18.05			103	15.24		1.99	1.05-3.74	**0.034**
	>2/3 foveal area		31	23.31			78	11.54		3.39	1.83-6.26	**<0.001**
Temporal whitening (worst eye)	None		31	23.85	130		172	25.56	673	Reference		
	1		54	41.54			290	43.09		1.03	0.64-1.67	0.894
	2		32	24.62			124	18.42		1.43	0.83-2.47	0.197
	3		13	10			87	12.93		0.83	0.41-1.66	0.598
Orange vessels, temporal quadrant (worst eye)	absent		72	55.38	130		523	78.29	668			
	present		58	44.62			145	21.71		2.9	1.96-4.3	**<0.001**
White vessels, temporal	absent		97	74.62	130		506	75.75	668			

Variable	Description	Subjects who died				Subjects who lived				Association with death		
quadrant (worst eye)	present		33	25.38			162	24.25		1.06	0.69-1.64	0.783
White capillaries (worst eye)	absent		95	73.08	130		447	66.92	668			
	present		35	26.92			221	33.08		0.75	0.49-1.13	0.17
Papilloedema (worst eye)	absent		83	61.03	136		530	78.17	678			
	present		53	38.97			148	21.83		2.29	1.55-3.38	**<0.001**
Disc hyperaemia	absent		57	51.35	111		388	64.67	600			
	present		54	48.65			212	35.33		1.73	1.15-2.61	**0.008**

Table 26: Unadjusted associations with time to reach Blantyre Coma Score ≥3/5.

Association with coma resolution time tested using truncated negative binomial regression. p-values <0.01 are bold

Variable	Description	Recovery to BCS=3 in <12hrs				Recovery to BCS=3 in 12 to 24hrs				Recovery to BCS=3 in >24hrs				Unadjusted association with coma resolution time			
		Median	25th centile	75th centile	n	Median	25th centile	75th centile	n	Median	25th centile	75th centile	n	Coefficient	p	95% CI low	95% CI high
Number					200				214				249				
Age	months	35	22	53.75	200	40.5	26	61.25	214	40	29	60.5	249	0.002	0.073	0.000	0.005
Parasitaemia	#cells parasitised	192000	39841	463000	191	57583	4136	269000	205	40200	4594	195000	239	0.000	**<0.001**	0.000	0.000
White cell count	#cells	8894	6600	14025	188	9200	6600	13400	203	9650	6525	13975	224	0.000	0.592	0.000	0.000
Haematocrit	%	18.85	15	25	198	20.4	17	25	211	20	16	25	247	0.008	0.182	-0.004	0.019
Lactate	mmol/L	6.2	3.3	11.5	129	4.6	2.9	8.7	177	5.8	3.3	10.2	199	0.014	0.153	-0.005	0.032
HRP2	ng/ml	4762	1869	9525	175	5296	2328	9975	191	7150	3158.75	11074	230	0.000	0.166	0.000	0.000
Temperature	Degrees C	38.9	38.2	39.7	200	38.9	38	39.6	214	38.8	37.8	39.6	249	-0.045	0.154	-0.107	0.017
Systolic blood pressure	mmHg	100	90	110	192	99	90	106	204	100	90	110	240	0.001	0.776	-0.004	0.006
Pulse	Beats/min	157	140	172	199	149.5	134.75	168	214	150	132	168	248	-0.003	0.016	-0.006	-0.001
Duration of coma	hours	4	3	8	162	8	4	18.25	170	8	5	23	210	0.006	0.037	0.000	0.012
Duration of fever	hours	48	36	72	192	72	48	72	206	72	48	72	239	0.002	0.07	0.000	0.003
Platelet	#platelets	56000	37000	88000	179	59000	32000	99000	199	56500	33000	94000	214	0.000	0.416	0.000	0.000
			Number	Percent	Total		Number	Percent	Total		Number	Percent	Total				
Sex	boy		100	50	200		117	54.67	214		111	44.58	249				
	girl		100	50			97	45.33			138	55.42		0.094	0.214	-0.054	0.242

Variable	Description	Recovery to BCS=3 in <12hrs			Recovery to BCS=3 in 12 to 24hrs			Recovery to BCS=3 in >24hrs			Unadjusted association with coma resolution time			
Coma score	0	16	8	200	19	8.88	214	31	12.45	249				
	1	54	27		80	37.38		113	45.38		-0.043	0.746	-0.302	0.216
	2	130	65		115	53.74		105	42.17		-0.380	**0.003**	-0.631	-0.128
Respiratory distress	absent	114	57	200	141	65.89	214	150	60.24	249				
	present	86	43		73	34.11		99	39.76		-0.029	0.705	-0.182	0.123
History of convulsions	absent	53	26.9	197	47	22.38	210	57	23.17	246				
	present	144	73.1		163	77.62		189	76.83		0.070	0.431	-0.105	0.246
Witnessed convulsions at admission	absent	169	84.5	200	179	85.65	209	212	86.18	246				
	present	31	15.5		30	14.35		34	13.82		0.024	0.821	-0.185	0.234
Witnessed convulsions after admission	absent	163	81.5	200	142	66.36	214	119	47.79	249				
	present	37	18.5		72	33.64		130	52.21		0.596	**<0.001**	0.449	0.742
HIV	negative	161	89.94	179	148	82.68	179	185	84.09	220				
	positive	18	10.06		31	17.32		35	15.91		0.105	0.361	-0.121	0.331
Hypoglycaemia on ward	absent	183	91.5	200	198	92.52	214	230	92.74	248				
	present	17	8.5		16	7.48		18	7.26		0.173	0.223	-0.105	0.450
Retinal haemorrhage (worst eye)	None	56	28	200	60	28.04	214	62	25	248				
	1 to 5	104	52		87	40.65		96	38.71		0.137	0.138	-0.044	0.318
	6 to 20	28	14		43	20.09		54	21.77		0.088	0.436	-0.134	0.310
	21 to 50	8	4		16	7.48		17	6.85		0.125	0.457	-0.204	0.454
	>50	4	2		8	3.74		19	7.66		0.518	**0.006**	0.151	0.886
Macular whitening (worst eye)	None	40	20.1	199	33	15.57	212	22	8.87	248				
	<1/3 disc area	103	51.76		98	46.23		101	40.73		0.270	0.015	0.053	0.486
	1/3 to 1 disc area	45	22.61		57	26.89		66	26.61		0.385	**0.001**	0.150	0.621
	>1 disc area	11	5.53		24	11.32		59	23.79		0.864	**<0.001**	0.598	1.130
Foveal whitening	None	73	36.87	198	54	25.35	213	44	17.81	247				
	<1/3 fovea	96	48.48		104	48.83		115	46.56		0.344	**<0.001**	0.170	0.519

Variable	Description	Recovery to BCS=3 in <12hrs			Recovery to BCS=3 in 12 to 24hrs				Recovery to BCS=3 in >24hrs				Unadjusted association with coma resolution time			
(worst eye)	1/3 to 2/3 fovea	24	12.12			38	17.84			38	15.38		0.405	**0.001**	0.175	0.635
	>2/3 fovea	5	2.53			17	7.98			50	20.24		0.876	<**0.001**	0.621	1.131
Temporal whitening (worst eye)	None	68	34.17	199		56	26.67	210		42	17	247				
	1	87	43.72			88	41.9			109	44.13		0.326	<**0.001**	0.144	0.508
	2	34	17.09			41	19.52			48	19.43		0.283	0.012	0.061	0.504
	3	10	5.03			25	11.9			48	19.43		0.642	<**0.001**	0.392	0.891
Orange vessels, temporal quadrant (worst eye)	absent	182	92.39	197		172	82.3	209		157	64.08	245				
	present	15	7.61			37	17.7			88	35.92		0.608	<**0.001**	0.435	0.780
White vessels, temporal quadrant (worst eye)	absent	157	79.7	197		164	78.47	209		176	71.84	245				
	present	40	20.3			45	21.53			69	28.16		0.222	0.012	0.048	0.396
White capillaries (worst eye)	absent	131	66.5	197		142	67.94	209		165	67.35	245				
	present	66	33.5			67	32.06			80	32.65		0.138	0.088	-0.020	0.296
Papilloedema (worst eye)	absent	172	86.43	199		175	82.16	213		169	67.87	249				
	present	27	13.57			38	17.84			80	32.13		0.512	<**0.001**	0.338	0.685
Disc hyperaemia (worst eye)	absent	106	67.09	158		146	73.74	198		127	55.46	229				
	present	52	32.91			52	26.26			102	44.54		0.353	<**0.001**	0.196	0.509

6.6 Main results

Several unadjusted estimates of association with death were found, including (OR, 95%CI): higher blood lactate (1.11, 1.06-1.16), more profound coma, the presence of >50 retinal haemorrhages (3.4, 1.78-6.5), severe foveal whitening (>2/3 foveal area 3.4, 1.8-6.3), presence of orange vessels (2.9, 1.9-4.3), presence of papilloedema (2.3, 1.6-3.4) and presence of disc hyperaemia (1.7, 1.2-2.6) (all $p<0.01$) (Table 25).

Respiratory distress, positive HIV status, hypoglycaemia on the ward (after admission), and severe macular whitening were associated with death at $p<0.05$, and generally had smaller OR than the variables listed above.

White cell count and HRP2 had statistically significant associations with death, but with very small effect sizes (OR not distinguishable from 1). These associations are unlikely to be clinically significant.

Retinal variables were included with blood lactate and HIV status in a multiple logistic regression with death as the outcome variable. Papilloedema was excluded as an uninformative confounder of brain swelling closely associated with death.

In this model, blood lactate (1.2, 1.1-1.2), >50 retinal haemorrhages (4.2, 1.6-10.7), and orange vessels (2.9, 1.6-5.1) were associated with death at $p<0.01$. This model included 512 of 817 subjects, largely because of subjects missing data for blood lactate (Table 27).

The model was repeated, but with respiratory distress substituted for lactate (Table 28). The presence of respiratory distress is thought to indicate metabolic acidosis (Marsh *et al.*, 1995), so may contain information about similar processes as blood lactate. In this model, >50 retinal haemorrhages (3.2, 1.4-7.3) and the presence of orange vessels (2.1, 1.3-3.4) were still significantly associated with death ($p<0.01$). Respiratory distress was not associated with death ($p=0.1$), and borderline associations were seen between death and severe foveal whitening

(p=0.06) and disc hyperaemia (p=0.03). This model used data from 606 of 817 subjects. The Akaike information criterion (AIC) for this second model is poorer than the model in Table 27, consistent with the lack of information in a binary variable (respiratory distress) compared to a continuous variable (blood lactate).

Table 27: Model of ophthalmoscopic variables against death.
Variables with negligible unadjusted associations with death were excluded from this model (HRP2, white cell count). Admission variables associated with death are: blood lactate, >50 retinal haemorrhages, and orange vessels (all p<0.01, in bold).

Logistic regression				Number of obs		512
				LR chi2(11)		57.85
				Prob > chi2		0
Log likelihood = -189.57298				Pseudo R2		0.1324
Death	Odds Ratio	Std. Err.	z	P>z	95% CI low	95% CI high
Lactate	1.14	0.03	4.64	**<0.001**	1.08	1.21
HIV	1.23	0.43	0.6	0.55	0.62	2.43
Retinal haemorrhage						
1 to 5	0.92	0.30	-0.26	0.796	0.48	1.75
6 to 20	0.50	0.23	-1.53	0.126	0.21	1.22
21 to 50	1.08	0.54	0.14	0.885	0.40	2.88
Over 50	4.16	2.01	2.95	0.003	1.62	10.73
Foveal whitening						
<1/3 foveal area	1.65	0.71	1.17	0.243	0.71	3.83
1/3 to 2/3 foveal area	1.28	0.66	0.48	0.632	0.47	3.52
>2/3 foveal area	1.91	0.96	1.3	0.194	0.72	5.09
Orange vessels, temporal quadrant	2.88	0.83	3.68	**<0.001**	1.64	5.05
Disc hyperaemia	1.15	0.33	0.48	0.629	0.66	2.01
Constant	0.03	0.01	-6.96	**<0.001**	0.01	0.07
Model fit	Obs	ll(null)	ll(model)	df	AIC	BIC
.	512	-218.5	-189.6	12	403.0	454.0

Table 28: Second model of ophthalmoscopic variables against death.
Blood lactate was missing in a substantial number of cases, and appeared to be missing significantly more often in subjects who died. The model in Table 27, was re-run but including respiratory distress instead of blood lactate. Respiratory distress is a binary variable summarising the presence of any one of several examination features, and is thought to broadly reflect metabolic acidosis. P-values <0.01 are in bold.

Logistic regression				Number of obs		606
				LR chi2(11)		42.68
				Prob > chi2		0
Log likelihood = -250.08371				Pseudo R2		0.0786
Death	Odds Ratio	Std. Err.	z	P>z	95%CI low	95%CI high
Respiratory distress	1.47	0.34	1.63	0.103	0.93	2.32
HIV	1.22	0.35	0.68	0.497	0.69	2.15
Retinal haemorrhage						
1 to 5	0.86	0.24	-0.54	0.593	0.49	1.50
6 to 20	0.59	0.23	-1.37	0.172	0.27	1.26
21 to 50	1.47	0.62	0.93	0.354	0.65	3.35
Over 50	3.23	1.35	2.81	**0.005**	1.42	7.31
Foveal whitening						
<1/3 foveal area	1.58	0.55	1.31	0.189	0.80	3.11
1/3 to 2/3 foveal area	1.66	0.68	1.23	0.218	0.74	3.69
>2/3 foveal area	2.18	0.89	1.92	0.055	0.98	4.84
Orange vessels, temporal quadrant	2.12	0.52	3.04	**0.002**	1.31	3.44
Disc hyperaemia	1.70	0.41	2.22	0.027	1.06	2.71
Constant	0.07	0.03	-6.92	**<0.001**	0.03	0.14
Model fit	Obs	ll(null)	ll(model)	df	AIC	BIC
.	606	-271.4	-250.1	12	524.2	577.05

Unadjusted associations with time to recover consciousness included (coefficient, 95%CI): depth of coma (BCS=2, -0.4, -0.6 to -0.1), witnessed convulsions after admission (0.6, 0.4 to 0.7), >50 haemorrhages (0.5, 0.2 to 0.9), moderate or severe macular whitening (>1 disc area, 0.9, 0.6 to 1.1), any grade of foveal whitening (>2/3 foveal area, 0.9, 0.6 to 1.1), peripheral whitening (severe, 0.6, 0.4 to 0.9), orange vessels (0.6, 0.4 to 0.8), papilloedema (0.5, 0.3 to 0.7) and disc hyperaemia (0.4, 0.2 to 0.5) (Table 26).

Peripheral parasitaemia had a statistical association with coma recovery time but with very small coefficient indistinguishable from 0.

Pulse, duration of coma pre-admission, mild macular whitening, grade 2 peripheral whitening, and white retinal vessels were directly associated with longer time to recovery of coma at $0.01<p<0.05$, and generally had smaller effect sizes that the variables listed above.

Retinal variables with significant ($p<0.05$) unadjusted associations with coma resolution time were included in a multivariate model along with admission coma score, and witnessed convulsions on the ward. This model used data from 569 of 663 subjects. The following variables had significant independent associations with coma resolution time (coefficient, 95%CI): admission coma score (BCS 2, -0.5, -0.7 to -0.2), witnessed convulsions (0.5, 0.4 to 0.7), >50 haemorrhages (0.4, 0.1 to 0.8), severe foveal whitening (0.5, 0.3 to 0.8), orange vessels (0.5, 0.3 to 0.7). All associations were $p<0.01$ (Table 29).

The presence of white vessels and papilloedema were associated less strongly with coma resolution time, with coefficients of approximately 0.2, significant at $p<0.05$.

Table 29: Ophthalmoscopic and clinical variables against coma resolution time. Truncated negative binomial regression model, with time to reach Blantyre Coma Score ≥3/5 as the dependent variable. P-values <0.01 are in bold.

Truncated negative binomial regression				Number of obs		569
Truncation point: 0				LR chi2(14)		191.49
Dispersion = mean				Prob > chi2		0
Log likelihood = -2430.7911				Pseudo R2		0.0379
Time to reach coma score ≥3/5	Coefficient	Std. Err.	z	P>z	95%CI low	95%CI high
Admission coma score						
1	-0.077	0.120	-0.64	0.522	-0.313	0.158
2	-0.475	0.116	-4.1	**<0.001**	-0.703	-0.248
Witnessed convulsions after admission	0.543	0.071	7.57	**<0.001**	0.403	0.684
Retinal haemorrhage						
1 to 5	0.075	0.084	0.9	0.369	-0.089	0.240
6 to 20	0.049	0.102	0.48	0.633	-0.152	0.250
21 to 50	-0.143	0.149	-0.96	0.336	-0.437	0.149
>50	0.434	0.164	2.63	0.008	0.110	0.757
Foveal whitening						
<1/3 fovea	0.187	0.086	2.15	0.031	0.016	0.357
1/3 to 2/3 fovea	0.179	0.111	1.61	0.107	-0.039	0.397
>2/3 fovea	0.512	0.122	4.17	**<0.001**	0.271	0.752
Orange vessels	0.507	0.083	6.1	**<0.001**	0.344	0.671
White vessels	0.197	0.080	2.44	0.015	0.038	0.355
Papilloedema	0.220	0.087	2.53	0.012	0.049	0.391
Disc hyperaemia	0.135	0.077	1.75	0.08	-0.016	0.287
Constant	2.911	0.137	21.2	**<0.001**	2.642	3.180
/lnalpha	-0.536	0.065			-0.664	-0.408
Alpha	0.584	0.038			0.514	0.664
Likelihood-ratio test of alpha=0: chibar2(01) = 8958.17 Prob>=chibar2 = 0.000						

6.7 Discussion

6.7.1 Key results

To the best of my knowledge this is the largest study of clinical outcomes and malarial retinopathy to date. Severe retinal haemorrhages, and orange vessels, are associated with death from paediatric CM after controlling for blood lactate and other retinal variables. This is in contrast to previous reports, which did not find any relationship with orange vessels (Beare et al., 2004; Lewallen et al., 1993), or reported an association with retinal whitening (Lewallen *et al.*, 1993).

Similar retinal features appear to be relevant, not just to fatal disease, but also to prolongation of coma, since severe haemorrhage, severe foveal whitening, and orange vessels are associated with longer time to recover consciousness. These associations are independent of depth of coma on admission, and consistent with the concept that coma and death result from similar neurovascular processes that vary by degree, duration, speed of onset, or some other qualifier, rather than from distinct mechanisms. The significant relationship with witnessed convulsions on the ward suggests that cerebral pathology underpinning coma can be perpetuated by seizures.

6.7.2 Limitations

This analysis does have several limitations. The reasons why certain subjects did not have a retinal exam were not recorded, but it appears that subjects with milder disease were more likely to have an admission retinal exam than subjects with severe disease (Table 24). This means that my sample may not fairly represent the more severe end of the disease severity spectrum, and that my estimates of effect size may be inaccurate. I think it is likely that my results are an underestimate, since failure to include severe cases is likely to dilute effect size.

Blood lactate was available less often for fatal cases, and this could potentially bias the multivariate model by excluding subjects with more severe disease. However associations between retinal haemorrhage, orange vessels, and death were stable when lactate was replaced with respiratory distress.

6.7.3 Interpretation

Various severe signs of malarial retinopathy are associated with death, and also with duration of coma in patients who recover consciousness. Since retinal manifestations of CM appear to reflect cerebral pathology (Barrera *et al.*, 2015; MacCormick *et al.*, 2014), this suggests that a combination of neurovascular pathologies may contribute to processes leading to fatal and non-fatal cerebral dysfunction.

Severe retinal haemorrhage suggests large scale disruption of the blood-brain barrier, since the number of haemorrhages in retina and brain are correlated in fatal cases (White *et al.*, 2001). This could produce severe brain swelling through large scale extravasion of intravascular fluid (including erythrocytes), which could be considered a form of vasogenic oedema. Haemorrhage is not significantly related to death or duration of coma unless it is very severe. This may reflect the importance of on-going haemorrhage over haemorrhage which has occurred but stopped. Personal experience suggests that cases with >50 haemorrhages often have haemorrhages that look 'fresh', while in other cases blood may even appear to be in the process of being reabsorbed. This would be consistent with associations between large focal leak, which is an evolving haemorrhage, and death.

Orange vessels suggest accumulation of parasite related material within the neurovasculature. The orange colour could result from partial digestion of haemoglobin by sequestered parasites (Lewallen *et al.*, 2000), or possibly the accumulation of haemozoin. Orange vessels may therefore point to the severity of neurovascular sequestration as an important disease mechanism. Whether damage from sequestration is mediated via degrees of local obstruction or congestion (White *et al.*, 2013), or dysfunctional interactions with receptors crucial for regulation of inflammation and coagulation (Moxon *et al.*, 2013; Turner *et al.*, 2013), or both, is less clear. Retinal imaging may help to investigate this question further. For example, orange vessels may have intravascular filling defects but are not typically blocked completely on FA, in contrast to white vessels overlying large areas of retinal whitening, which are typically blocked completely. Patterns of retinal leakage associated with orange vessels might suggest that disruption of

the blood-brain barrier can occur in the absence of profound obstruction (see Chapter 5), though a degree of local hypoxia is likely to play at least some role in any vasogenic oedema (Klatzo, 1987).

The association between retinal whitening and longer coma recovery time suggests that ischaemia and cytotoxic oedema are also important, independent of severe haemorrhage or orange vessels. The lack of association between retinal whitening and death may have to do with controlling for blood lactate, which is likely to reflect total body hypoxia as well as the severity of disease. It may be useful to repeat these analyses without lactate. Retinal whitening is often present in combination with retinal haemorrhages and orange vessels, and it may be that associated cytotoxic oedema does not contribute as much to fatal outcome as does the pathology related to haemorrhage or orange vessels.

These retinal features are not biologically independent, but statistically independent associations suggest that they may each have distinctly different roles, or that each can lead to the same final common pathway through different mechanisms. Neither haemorrhage nor orange vessels appear to be necessary for death – only contributory. It seems likely that fatal CM involves a multiplicity of mechanisms that interact in different ways to produce outcomes.

This analysis produced results that are different from previous reports. The reasons for this may include the larger sample size of the current study, with the explicit selection of only retinopathy-positive cases, and also perhaps with the way retinal features were analysed. For example, Beare et al., (2004) analysed orange and white vessels together as a single factor, and retinal haemorrhage as if it were a continuous variable. They found an independent association between haemorrhage (on a scale from 0 to 4) and death. While the presence of any retinal haemorrhage is important for diagnosing malarial retinopathy in paediatric cerebral malaria, my analysis in this chapter suggests that only very severe retinal haemorrhage is relevant to the overall association between haemorrhage and death.

6.7.4 Generalisability

It seems likely that disease processes related to orange discolouration of the neurovasculature, and severe haemorrhage, are important for progression to death or prolonged coma. The estimates in this study may not take account of patients at the severe end of the disease spectrum, since patients with rapidly fatal disease were less likely to have ophthalmoscopic examination than those with milder disease. However, while this analysis may have missed some features associated with the most severe cases, it seems reasonable to conclude that orange vessel discolouration should receive more attention as a clue to the pathogenesis of paediatric CM. Previously retinal haemorrhage and papilloedema appeared to have the strongest associations with death (Beare et al., 2004). It now appears as if papilloedema is probably an imperfect marker of severe brain swelling (Seydel *et al.*, 2015), and that haemorrhage is only relevant if it is very severe. To the best of my knowledge, orange vessels have not been reported in cases of severe malaria in adults (Abu Sayeed *et al.*, 2011; Maude *et al.*, 2009). The associations in children between orange retinal vessels, death, and coma recovery time, appear to be another example of how differently *P. falciparum* can manifest in these two age groups (World Health Organization, 2014b).

Chapter 7 – Associations between admission fluorescein angiography and clinical outcomes

7.1 Aim of chapter

Investigate associations between angiographic features of malarial retinopathy and clinical outcomes in retinopathy positive paediatric cerebral malaria

7.2 Summary

7.2.1 What is known already

Malarial retinopathy involves occlusion of and leakage from blood vessels. These features, and other angiographic features not previously described were quantified in Chapter 5. Associations between clinical outcomes and angiographic features have not yet been estimated. In this chapter I report an analysis of these associations, which is relevant to the pathogenesis of paediatric cerebral malaria, since fatal disease is thought to result from severe brain swelling. Such swelling could be caused by blockage of or leakage from the cerebral neurovasculature (cytotoxic and vasogenic oedema, respectively). Since the retinal and cerebral vasculatures have much in common, retinal angiography may shed light on mechanisms leading to death in paediatric cerebral malaria.

7.2.2 What this chapter involved

I took fluorescein angiogram images in children with retinopathy positive cerebral malaria on admission from 2012 to 2014. I added these images to a pre-existing dataset (started in 2006), and then analysed data from retinal angiograms taken within 48 hours of admission against two clinical outcomes – death, and time to reach coma score ≥3/5. Selection bias was assessed by comparing groups of eligible subjects who did, or did not, have admission retinal angiography. Unadjusted associations were estimated, and then associations were further evaluated in multivariate models.

7.2.3 What this chapter adds to current knowledge

The main angiographic features related to outcome are specific types of leakage. Although leakage is commonly seen in retinopathy positive paediatric cerebral malaria, it seems that only specific types of leak are associated with poor outcome. Other angiographic features with significant unadjusted (but not adjusted) associations may contribute to leak. These observations are consistent with animal models of cerebral oedema, where initial leakage can be followed by secondary angiogenesis and further blood-brain barrier breakdown; and in which cytotoxic and vasogenic types of oedema typically co-exist. Specific types of blood-brain barrier breakdown may play a key role in brain swelling in paediatric cerebral malaria.

7.3 Introduction

Cerebral malaria (CM) is a severe complication of infection with the parasite *P. falciparum*. Malaria caused an estimated 584,000 deaths in 2014. These were largely among children in sub-Saharan Africa, and most of these deaths resulted from severe malarial syndromes such as CM (WHO, 2014). Children who survive CM are at increased risk of neuropsychiatric disabilities. Sequestration of parasitised erythrocytes in the neurovasculature of the brain is the histopathological hallmark of CM, and sequestration is thought to be the initiating event in the pathological process leading to death (World Health Organization, 2014b), which is almost always associated with increased brain volume (Seydel *et al.*, 2015). However the mechanisms by which the *P. falciparum* parasite causes fatal damage to the central nervous system remain unclear (World Health Organization, 2014b).

Children with CM have retinal signs (Lewallen *et al.*, 1999) that appear to mirror the neuropathology of the brain. The severity of paediatric malarial retinopathy is directly proportional to the intensity of sequestration in both retina and brain (Barrera *et al.*, 2015), and the retina shares many histopathological features with the brain in fatal CM (MacCormick *et al.*, 2014). Such associations are biologically plausible since the retina and brain have similar embryology, anatomy, and physiology – including similar blood-tissue barriers (MacCormick

et al., 2014; Patton *et al.*, 2005). Indeed the retina is a specialised part of the central nervous system; but, in contrast to the brain itself, the retina can be observed directly and non-invasively during life.

Retinal angiographic features have been described previously in paediatric (Beare *et al.*, 2009) and adult (Davis *et al.*, 1992; Maude *et al.*, 2011) CM. I aimed to quantify fluorescein abnormalities and discover whether blockage of, or leakage from, the retinal neurovasculature is associated with death or time to recover consciousness in children with CM. Because the inner retinal circulation has much in common with the cerebral circulation, such associations would suggest that blood-brain barrier breakdown is an important contributor to clinical outcomes. Since few studies of FA have been performed in patients with severe malaria, I also sought to characterise angiographic features in terms of other relevant clinical variables. This may suggest hypotheses for further research. Possible mechanisms for fatal brain swelling include cytotoxic oedema, vasogenic oedema, and vascular congestion. None is mutually exclusive, and particular features of malarial retinopathy could suggest each mechanism. For example, capillary non-perfusion and retinal whitening probably represent local ischaemia and loss of retinal transparency secondary to cell membrane pump failure (*cf.* cytotoxic oedema) (Beare *et al.*, 2009). Leakage of fluorescein results from breakdown of the blood-retinal barrier (*cf.* Vasogenic oedema), and the severity of intravascular filling defects (IVFD) could represent degrees of vascular congestion. Independent associations between one or more retinal features and death could suggest which mechanism is most important.

7.4 Methods

7.4.1 Study design

Prospective cohort study

7.4.2 Setting

This research took place within an ongoing study of severe malaria (Taylor, 2009) in the Paediatric Research Ward (PRW) of Queen Elizabeth Central Hospital (QECH), Blantyre, Malawi. Informed consent was given by the parents

or guardians of all patients. This research adhered to the tenets of the Declaration of Helsinki, and was approved by the ethics committees of relevant academic institutions.

Paediatric CM was defined according to World Health Organization (WHO) clinical criteria: peripheral *P. falciparum* parasitaemia, Blantyre Coma Score (BCS) <3, and no other evident explanation for coma. Hypoglycaemia, post-ictal state, and meningitis were explicitly ruled out as causes of coma in all cases (World Health Organization, 2014). Patients could also have additional severe malarial syndromes, such as severe malarial anaemia. In addition, the presence of malarial retinopathy is interpreted as a diagnostic test to distinguish between coma associated with cerebral sequestration and coma with incidental parasitaemia (Taylor et al., 2004; World Health Organization, 2014). This is used to further classify patients into retinopathy-positive or retinopathy-negative groups. The former is a stricter case definition of paediatric CM than described by the WHO criteria, and is likely to produce a more homogeneous sample which is of greater relevance to a study of disease mechanisms. In children, retinopathy-negative status in the context of apparent CM implies a greater likelihood that coma and death are the result of other, non-malarial causes (World Health Organization, 2014b). It is not clear whether this association also applies to CM in adults, which is different from paediatric disease in several important respects (World Health Organization, 2014).

Malarial retinopathy is defined as retinal haemorrhage (often white-centred), and/or retinal whitening, and/or orange or white vessel discolouration (Harding *et al.*, 2006; Lewallen *et al.*, 1999). Papilloedema in isolation does not indicate malarial retinopathy, but is associated with increased risk of death (Beare et al., 2004).

7.4.3 Participants

Subjects were included in the analysis if they had a diagnosis of retinopathy-positive CM, and had a fundus fluorescein angiogram (FA) on the day or day after admission. Subjects were excluded if their guardians withdrew consent, if they did not have ophthalmoscopic assessment of malarial retinopathy, or if they did

not have FA in the specified time frame (<48hours from admission). Angiography was not performed on patients whose clinical condition was deteriorating, or on those rapidly regaining consciousness, or if the ophthalmologist was not available.

7.4.4 Variables

7.4.4.1 Predictor variables

Macular CNP (categorical, 0-2)

Peripheral CNP (categorical, 0-2)

Disc leak (binary)

Punctate focal leak (categorical, 0-2)

Large focal leak (categorical, 0-2)

Vessel segment leak (categorical, 0-2)

Post-capillary venule leak (categorical, 0-2)

IVFD in large, small, and peri-capillary vessels on either the arterial or venous circulation (six binary variables)

Blood lactate (continuous, bimodal)

7.4.4.2 Outcome variables

7.4.4.2.1 Primary outcomes

Death (binary)

Time between admission and recovery of Blantyre Coma Score 3 (truncated count variable)

7.4.4.2.2 Secondary outcomes

Haematocrit (continuous)

Blood lactate (continuous, bimodal)

HRP2 (continuous)

Blood white cell count (continuous)

Duration of coma pre-admission (count, skewed)

Fluorescein variables were originally described in terms of more categories (see grading form, appendix 2), but were collapsed to 3 levels before analysis to ensure adequate numbers of subjects in each strata. All fluorescein variables were from

the worst affected eye, except for peripheral CNP, which was taken from the left eye and controlled for the extent of peripheral retina seen in that eye.

7.4.5 Data sources

Data collection took place during the Malawian malaria seasons (January to June) of 2006 to 2014 inclusive, excluding 2011—a year in which FA were not done for operational reasons. Descriptions of angiograms from 2006 have been published, but these were not formally graded or tested for associations with death (Beare et al., 2009).

All patients were initiated or continued on anti-malarial and supportive treatments. After clinical stabilisation an ophthalmologist performed dilated indirect ophthalmoscopy. Malarial retinopathy was graded using a standard form (Harding et al., 2006).

The ophthalmologist then took 50 degree colour and FA retinal images using a table mounted camera (Nikon D1-H; Topcon TRC-50EX, Topcon, Japan; Imagenet 2000, Topcon, Japan), if this was deemed clinically appropriate by the supervising physicians. A nurse gave an intravenous injection of 1-5ml (depending on patient weight) 10-20% sodium fluorescein and also monitored the condition of the patient during the angiogram. Images of both eyes were taken for 10 to 15 minutes after injection, and as much of the retina was captured as possible. Although comatose, patients with CM often have tonic, nystagmoid, or roving eye movements. Corneal transparency may be reduced by incomplete lid closure. As a result the extent and quality of retinal images varied between patients. Angiographic images were then graded (dual grading with adjudication) in a professional reading centre according to a standard protocol (see Chapter 5).

Clinical data from the history, examination, and standard investigations were collected routinely at admission. These included rectal temperature, full blood count (Coulter Counter, Beckman Coulter), and HIV status using two separate tests (Uni-Gold Recombigen HIV-1/2, Trinity Biotech; and Determine HIV-1/2, Inverness Medical). Finger prick blood samples were analysed to determine parasite species and density, packed-cell volume, blood glucose and blood lactate

(Lactate Pro point of care detector (Arkay Inc)). Histidine rich protein 2 (HRP2) was measured retrospectively in stored plasma (Celabs ELISA). While peripheral parasitaemia reflects the number of circulating parasites, HRP2 is a parasite specific protein that may reflect the total mass of parasites in the host – whether circulating or sequestered (Dondorp *et al.*, 2005; Lucchi *et al.*, 2011). The eventual outcome of disease was recorded, including obvious neurological sequelae in survivors. Death or recovery typically occurs within 48 hours of admission.

7.5 Statistical methods

Analysis was planned during and after data acquisition

7.5.1 Assessment of selection bias

Potential selection bias was assessed by comparing eligible patients who had admission FA with eligible patients who did not by generating unadjusted odds ratios with logistic regression.

7.5.2 Evaluation of associations with death, or coma recovery time

My primary analysis involved evaluation of angiographic features with multivariate models, with the aim of gaining information about possible disease mechanisms. This is different from developing models with the aim of predict outcomes in individual patients, and this distinction informed my rules for variable selection (Altman and Royston, 2000; Hemingway et al., 2013). I assessed angiographic features against two co-primary outcomes: death, and time to coma resolution. The latter describes the time between admission and recovery of consciousness (defined as BCS=≥3/5). It is highly skewed with over-dispersion, and is truncated at zero since no patients regained consciousness in less than 1 hour from admission.

I assessed several risk factors for death, based on published results from other studies of severe malaria. These included: age, peripheral parasitaemia, white cell

count, jaundice, venous lactate, respiratory distress, depth of coma, witnessed convulsions at admission, papilloedema, and retinal haemorrhages (Beare et al., 2004; Jallow et al., 2012; Marsh et al., 1995; Molyneux et al., 1989; von Seidlein et al., 2012; World Health Organization, 2014b). I tested a broad range of variables against time to regain BCS=3 since associations with prolonged coma recovery time are less clear than associations with death in severe paediatric malaria. I generated odds ratios or coefficients for unadjusted associations with each outcome, using logistic regression and truncated negative binomial regression for binary and continuous outcomes, respectively.

I selected variables for separate multivariate models of each clinical outcome on the basis of two criteria.

Firstly, I sought to include variables with significant pairwise associations to the outcome of interest ($p<0.1$). Secondly, I attempted to select variables describing possible biological causes, rather than effects, of the given outcome. This is because I am interested in potential mechanistic relationships between angiogram features and outcomes, rather than in predicting outcome. So for example, papilloedema is more likely to describe an effect of severe brain swelling (and rapid death) than a cause, and so was excluded from the multivariate model of death. The same is true for depth of coma at admission. However papilloedema at admission (as a marker of brain swelling) may represent a plausible cause of prolonged coma in patients who survived, and so was included in the model of coma recovery time. In cases where two or more variables were judged to represent very similar disease processes I selected only one variable for inclusion in a multivariate model to avoid problems with collinearity. For example, my images strongly suggest that large focal leak represents the evolution of retinal haemorrhage, and so retinal haemorrhage was excluded from models with large focal leak. Similarly, other ophthalmoscopic features of malarial retinopathy are co-localised to angiographic variables (Beare *et al.*, 2009) and are likely to represent very similar processes.

I tested multivariate associations using logistic regression and truncated negative binomial regression for binary and continuous outcomes, respectively. In the case

of time to regain BCS≥3, assessment of over-dispersion indicated that the model was appropriate for pairwise and multivariate tests. Pairwise associations were done to inform variable selection rather than for hypothesis testing, and were not adjusted for multiple comparisons. Within the multivariate models, associations at $p<0.025$ were regarded as statistically significant. This value was chosen by dividing the conventional $p=0.05$ level by two, since I have two models.

In a secondary descriptive analysis, univariate associations between fluorescein features and six continuous clinical variables of interest in severe malaria were tested (age, haematocrit, lactate, HRP2, white cell count, and duration of coma pre-admission). No correction for multiple tests was made. For these tests I report odds ratios and 95% confidence intervals rather than p-values in order to emphasise effect size rather than an arbitrary threshold for significance, which in some cases may have been reached purely by chance. Univariate associations between angiographic features and continuous clinical variables of interest were graphed using box plots and tested using ordered logistic or logistic regression depending on the nature of the fluorescein variable.

7.6 Results

7.6.1 Participants

Between 2006 and 2014 813 patients admitted to the PRW had a diagnosis of CM or CM with severe malarial anaemia. Three patients were excluded because guardians withdrew consent (n=1) or the patient had an admission coma score >2 which dropped after admission (n=2). 80 patients were recruited in 2011, when no angiograms were performed. Of 730 patients, 549 had one or more signs of malarial retinopathy, 164 were retinopathy negative, and 17 did not have an eye exam. Of 549 patients with retinopathy-positive CM, 260 had a FA within 24 hours of admission, and 289 did not. Of 164 patients without retinopathy, 18 had an angiogram within 48 hours of admission (Figure 52). There were no adverse reactions to fluorescein.

Figure 52: Derivation of sample used to estimate associations between angiographic features and clinical outcomes.

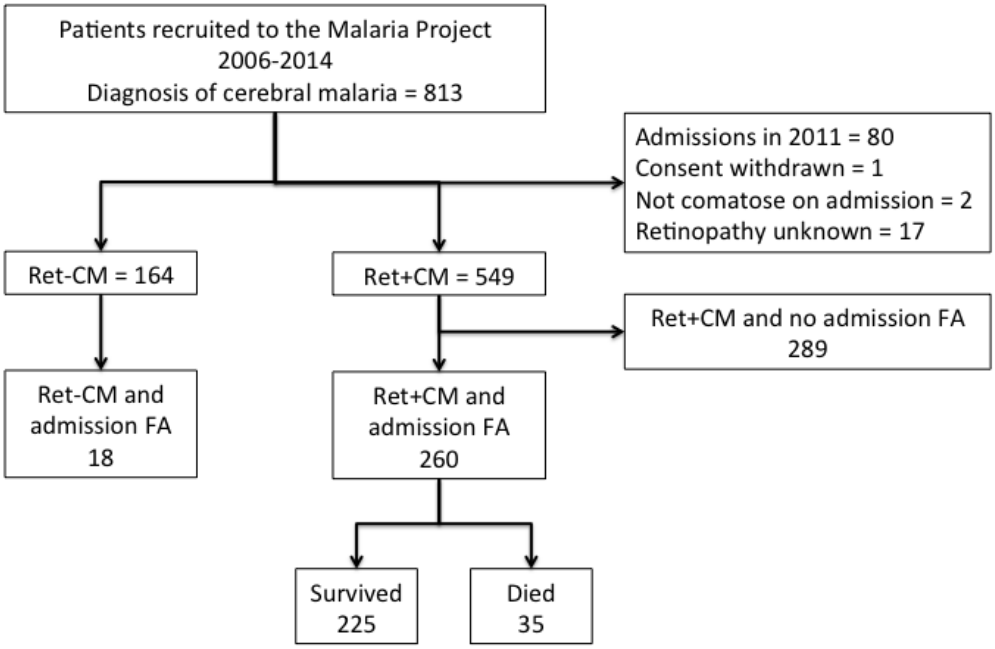

7.6.2 Descriptive and outcome data

7.6.2.1 Characteristics of subjects who had an admission angiogram, compared to subjects who did not

Patients who had FA had more severe retinopathy, different coma recovery times (fewer children who had angiography woke within 12hrs, and more recovered in >24hrs), a higher chance of convulsions during the hospital stay, and a greater chance of developing neurological sequelae evident on discharge than patients who did not have an angiogram. Patients who had FA also had statistically significant ($p<0.05$) but clinically trivial differences in maximum duration of convulsion pre-admission, pulse rate, respiratory rate, CSF opening pressure, and venous lactate (Table 30).

Table 30: Subjects who did or did not have admission angiography.

Comparison of patients with retinopathy positive cerebral malaria who did or did not have a fluorescein angiogram within 48 hours of admission. Retinal data are from the worst affected eye unless otherwise specified. Retinal features are all reported from the eye with most severe signs in each case. Groups were compared using logistic regression with group as the dependent variable and clinical feature as the sole independent variable. P values in bold indicate p<0.01

	Retinopathy positive cerebral malaria No admission FA				Retinopathy positive cerebral malaria Admission FA				Association		
	Median	25th centile	75th centile	number	Median	25th centile	75th centile	number	OR	95%CI	p
Number	n/a	n/a	n/a	289	n/a	n/a	n/a	260			
Age	39	27	57.5	289	38.5	28	56	260	1	0.99-1.01	0.68
Duration of fever pre-admission (hours)	60	43.5	72	284	60	48	72	247	1	0.99-1.01	0.26
Duration of coma pre-admission (hours)	7	4	12	227	9	5	22.75	200	1.01	0.99-1.02	0.12
Duration of convulsions pre admission (hours)	7	3	12	223	8	4	20	189	1.02	1.00-1.03	**0.007**
Weight (kg)	12.2	10.1	14.95	289	12	10	15	260	0.99	0.96-1.03	0.73
Height (cm)	92	84	103	283	92.5	84	104	256	0.99	0.99-1.01	0.87
Mid upper arm circumference (cm)	15	14	16	281	15	14.1	16	257	1.03	0.93-1.13	0.59
Rectal temperature (ºC)	39	38.05	39.6	289	38.8	38.1	39.575	260	0.97	0.85-1.12	0.7
Pulse (beat/sec)	160	140	176	289	151	134	171	260	0.99	0.98-0.99	**0.009**
Systolic blood pressure (mmHg)	95	87.5	104	277	97	89.25	105.75	244	1.01	0.99-1.02	0.077
Respiratory rate (breath/sec)	48	40	56	287	42.5	36	52	260	0.98	0.97-0.99	**0.008**
CSF opening pressure (mmCSF)	150	110	190	148	170	116.25	220	134	1	1.00-1.01	0.046
Peripheral parasitaemia (cells)	72807.5	15792	301000	280	47720	3295.5	210000	252	0.99	0.99-1.00	0.19
White cell count (cells)	9950	6800	15100	274	10000	7200	14400	247	1	0.99-1.00	0.84

		Retinopathy positive cerebral malaria No admission FA				Retinopathy positive cerebral malaria Admission FA				Association		
Platelet count		54000	31000	84000	275	59000	31000	103000	245	1	0.99-1.00	0.14
Haematocrit (%)		19.9	15.5	24.05	285	19.3	15.3	24.1	257	1.01	0.98-1.03	0.66
Lactate (mmol/L)		6.9	3.8	11.6	287	4.85	2.9	9.175	256	0.94	0.90-0.97	**0.001**
HRP2 (ng/ml)		6765.5	2827	12203	280	7641	3275	10471	259	1	0.99-1.00	0.73
			number	%	total		number	%	total	OR	95%CI	p
Jaundice	negative		228	92.31	247		218	92.37	236	0.99	0.51-1.94	0.98
	positive		19	7.63			18	7.63				
Respiratory distress	negative		178	61.59	289		175	67.31	260	0.78	0.55-1.11	0.16
	positive		111	38.41			85	32.69				
Hypoglycaemia on the ward	negative		255	88.24	289		234	90	260	0.83	0.49-1.43	0.51
	positive		34	11.76			26	10				
Transfusion on the ward	negative		147	50.87	289		123	47.31	260	1.15	0.82-1.61	0.41
	positive		142	49.13			137	52.69				
Blood culture positive	negative		270	94.41	286		226	93.78	241	1.12	0.54-2.31	0.76
	positive		16	5.59			15	6.22				
Diagnosis	CM		133	46.02	289		110	42.31	260	1.08	0.91-1.28	0.38
	CM+SMA		156	53.98			150	57.69				
Sex	male		146	50.52	289		126	48.46	260	1.09	0.78-1.52	0.63
	female		143	49.48			134	51.54				
Coma score	0		29	10.03	289		18	6.92	260			
	1		122	42.21			120	46.15		1.58	0.84-3.00	0.158
	2		138	47.75			122	46.92		1.42	0.75-2.69	0.276
Hours to reach coma score	< 12hrs		82	34.45	238		27	12.39	218			

		Retinopathy positive cerebral malaria No admission FA				Retinopathy positive cerebral malaria Admission FA				Association		
3	12 to 24 hrs		82	34.45			82	37.61		3.04	1.78-5.17	**<0.001**
	> 24 hrs		74	31.09			109	50		4.47	2.64-7.57	**<0.001**
Clinical outcome	full recovery		225	77.85	289		194	74.62	260			
	sequelae		13	4.5			31	11.92		2.77	1.41-5.43	**0.003**
	death		51	17.65			35	13.46		0.8	0.5-1.27	0.342
History of convulsions pre-admission	negative		64	22.3	287		47	18.29	257	1.28	0.84-1.95	0.25
	positive		223	77.7			210	81.71				
Witnessed convulsions on admission	negative		251	87.46	287		222	86.38	257	1.1	0.67-1.81	0.71
	positive		36	12.54			35	13.62				
Witnessed convulsions after admission	negative		192	66.44	289		143	55	260	1.62	1.15-2.29	**0.006**
	positive		97	33.56			117	45				
HIV status	negative		223	86.1	259		203	84.94	239	1.1	0.67-1.81	0.71
	positive		36	13.9			36	15.06				
Retinal haemorrhages	none		76	28.46	267		60	23.17	259			
	1 to 5		104	38.95			92	35.52		1.12	0.72-1.74	0.612
	6 to 20		53	19.85			52	20.08		1.24	0.75-2.07	0.404
	21 to 50		19	7.12			23	8.88		1.53	0.76-3.07	0.228
	>50		15	5.62			32	12.36		2.7	1.34-5.44	**0.005**
Papilloedema	negative		204	76.4	267		175	67.57	259	1.55	1.06-2.28	0.024
	positive		63	23.6			84	32.42				
Disc hyperaemia	negative		183	69.58	263		177	69.96	253	0.98	0.67-1.43	0.925
	positive		80	30.42			76	30.04				
Macular whitening	none		29	11.07	262		21	8.14	258			
	<1/3DA		159	60.69			97	37.6		0.84	0.46-1.56	0.585

		Retinopathy positive cerebral malaria No admission FA				Retinopathy positive cerebral malaria Admission FA				Association		
	1/3-1DA		49	18.7			78	30.23		2.2	1.13-4.28	0.02
	>1DA		25	9.54			62	24.03		3.42	1.65-7.1	**0.001**
	none		58	22.22	261		35	13.62	257			
	<1/3 fovea		150	57.47			111	43.19		1.23	0.75-2.0	0.411
	1/3-2/3 fovea		30	11.49			52	20.23		2.87	1.55-5.31	**0.001**
Foveal whitening	>2/3 fovea		23	8.81			59	22.96		4.25	2.24-8.05	**<0.001**
	none		73	28.19	259		35	13.78	254			
	grade 1		140	54.05			101	39.76		1.5	0.93-2.43	0.09
	grade 2		28	10.81			53	20.87		3.95	2.15-7.27	**<0.001**
Temporal whitening	grade 3		18	6.95			65	25.59		7.53	3.89-14.56	**<0.001**
Orange vessels, temporal periphery	absent		196	77.78	252		122	62.89	194	2.07	1.36-3.13	**0.001**
	present		56	22.22			72	37.11				
White vessels, temporal periphery	absent		179	71.03	252		148	76.29	194	0.76	0.5-1.17	0.214
	present		73	28.97			46	23.71				
White capillaries, temporal periphery	absent		154	61.11	252		143	73.71	194	0.56	0.37-0.84	**0.005**
	present		98	38.89			51	26.29				

7.6.3 Associations between FA features and death

The FA features observed in paediatric CM have been described in detail in Chapter 5 and (Beare *et al.*, 2009). Briefly, these include: capillary non-perfusion (CNP) at the macula or periphery, punctate focal leak, large focal leak, post-capillary venule leak, large venule leak, and intravascular filling defects (IVFD) in vessels of different types and sizes (Figures 32, 39, 41, 42, 44, 47, 50 in Chapter 5).

In the 260 patients with retinopathy-positive CM who had an admission FA, the following FA features were positively associated with death on pairwise analysis (unadjusted OR, 95%CI, all $p<0.1$): severe macular CNP (7.3, 0.9-56.8), punctate focal leak (1 to 5 sites: 4.4, 2.0-10.0; >5 sites: 10.3, 3.1-34.4), >1 site of large focal leak (13.9, 5.6-34.6), and IVFD in pre-capillary (2.5, 0.9-6.5) and large arterioles (2.8, 1.2-6.7). Grade 2 post-capillary venule leak was associated with recovery (0.2, 0.05-1.0) (Table 31).

In terms of clinical features, admission venous lactate, depth of coma, papilloedema, and severity of retinal haemorrhages were also associated with death ($p<0.1$, Table 31). Of these, lactate was selected for inclusion in a multivariate model of FA features against death.

When FA features were analysed together with admission lactate, the presence of >5 sites of punctate focal leak (OR 6.9, 95%CI 1.5-31.3) remained significantly and independently associated with death ($p<0.02$). The odds ratio relating venous lactate to death was also significant at $p<0.02$ (OR 1.1, 95%CI 1.0-1.3). The association between death and large focal leak was not significant at $p<0.02$ (OR 3.6, 95%CI 1.1-12.1, $p=0.04$) (Table 32).

Table 31: Unadjusted associations with death in subjects with retinopathy positive cerebral malaria and admission fluorescein angiogram. Unadjusted pairwise associations with death tested in 260 children with retinopathy positive cerebral malaria who also had a fluorescein angiogram within 48hrs of admission. Since the grade of peripheral capillary non-perfusion is likely to depend on the extent of peripheral retina captured in the fluorescein image series, this feature was tested according to measurements from the worst affected eye, the left eye only, and finally the left eye controlling for the furthest extent of retina visible in the left eye. Retinal findings are reported for the worst eye affected in all cases except when stated otherwise. CNP = capillary non-perfusion; IVFD = intravascular filling defects; Respiratory distress is defined as any one of: deep breathing, nasal flare, tracheal tug, or intercostal in-drawing. Differences between groups of patients who lived or died were tested with logistic regression, with death as the dependent variable against a sole independent variable. P-values in bold indicate <0.1. *No subjects had grade 0 (absent) macular CNP. **6 subjects who lived had peripheral retinal imaged, but these images were ungradeable. One Subject who died had peripheral retinal images, but these images were ungradeable.

		Subjects who lived				Subjects who died				Association with death		
Variable	Detail	Median	IQR	Percent	Number	Median	IQR	Percent	Number	OR	95%CI	p
Number					225				35			
Demographics												
Age	months	38	28.5-55		225	41	23-69		35	1	0.99-1.02	0.65
Body mass index		14.22	13.22-15.42		222	14.23	13.18-15.84		34	1.04	0.85-1.28	0.68
Mid-upper arm circumference	cm	15.5	14.5-16		223	15	14-15.5		34	0.86	0.68-1.08	0.2
Clinical												
Blantyre coma score	0			6.22	14			4	11.43			

		Subjects who lived				Subjects who died				Association with death		
Variable	Detail	Median	IQR	Percent	Number	Median	IQR	Percent	Number	OR	95%CI	p
	1			44	99			21	60	0.74	0.22-2.48	0.63
	2			49.78	112			10	28.57	0.31	0.09-1.13	**0.076**
Witnessed convulsions on admission	no			85.59	190			32	91.43			
	yes			14.41	32			3	8.57	0.56	0.16-1.93	0.355
Witnessed convulsions after admission	no			54.67	123			21	60			
	yes			45.33	102			14	40	0.8	0.34-1.66	0.56
Respiratory distress	no			68.89	155			20	57.14			
	yes			31.11	70			15	42.86	1.66	0.80-3.43	0.17
Jaundice	no			92.12	187			31	93.94			
	yes			7.88	16			2	6.06	0.75	0.17-3.44	0.72
Laboratory												
Venous lactate	mmol/L	4.6	2.8-8.9		222	8.1	3.65-13.35		34	1.14	1.05-1.23	**0.001**
Peripheral parasitaemia	calls	40140	2001-187000		217	78904	17707-471000		35	1	0.99-1.0	0.23
HRP2	ng/ml	7222	3135.5-10425.5		224	8358	5204-16772		35	1	0.99-1.00	0.21
White blood count	calls	9900	7250-14450		213	10750	6975-14200		34	0.99	0.99-1.00	0.89
CSF opening pressure	mmCSF	170	119-220		118	170	102.8-237.5		16	1	0.99-1.01	0.76

		Subjects who lived				Subjects who died				Association with death		
Variable	Detail	Median	IQR	Percent	Number	Median	IQR	Percent	Number	OR	95%CI	p
Hypoglycaemia on the ward	no			91.11	205			29	82.86			
	yes			8.89	20			6	17.14	2.12	0.79-5.72	0.14
HIV	negative			85.51	177			26	81.25			
	positive			14.49	30			6	18.75	1.36	0.52-3.59	0.532
Retinal												
Papilloedema	no			71.88	161			14	40			
	yes			28.12	63			21	60	3.83	1.84-8.00	**<0.001**
Retinal haemorrhage	none			23.66	53			7	20			
	1 to 5			36.61	82			10	28.57	0.92	0.33-2.58	0.88
	6 to 20			20.54	46			6	17.14	0.99	0.31-3.15	0.98
	21 to 50			8.93	20			3	8.57	1.14	0.27-4.83	0.86
	>50			10.27	23			9	25.71	2.96	0.98-8.92	**0.053**
Orange vessels, temporal quadrant	absent			65.09	110			12	48			
	present			34.91	59			13	52	2.02	0.87-4.71	0.103
Macular CNP	grade 1*			13.39	30			1	3.23			
	grade 2			48.21	108			9	29.03	2.5	0.30-20.52	0.39
	grade 3 or 4			38.39	86			21	67.74	7.33	0.94-56.83	**0.06**
Peripheral CNP, worst eye	None or grade 1			44	99			12	35.29			

		Subjects who lived				Subjects who died				Association with death		
Variable	Detail	Median	IQR	Percent	Number	Median	IQR	Percent	Number	OR	95%CI	p
	Grade 2			23.56	53			10	29.41	1.56	0.63-3.84	0.34
	Grade 3 or 4			32.44	73			12	35.29	1.36	0.58-3.19	0.49
Peripheral CNP, left eye	None or grade 1			54.63	118			18	54.55			
	Grade 2			21.3	46			5	15.15	0.71	0.25-2.03	0.53
	Grade 3 or 4			24.07	52			10	30.3	1.26	0.54-2.92	0.59
Furthest peripheral retina seen, left eye**	None			0.45	1			0	0			
	Zone 1			18.47	41			4	11.76	0.47	0.15-1.5	0.2
	Zone 2			48.65	108			15	44.12	0.67	0.31-1.45	0.31
	Zone 3			32.43	72			15	44.12	Omitted because of collinearity	Omitted because of collinearity	Omitted because of collinearity
Peripheral CNP, left eye, controlling for furthest extent of retina seen	None or grade 1			N/a	N/a			N/a	N/a			
	Grade 2			N/a	N/a			N/a		0.64	0.22-1.85	0.41

		Subjects who lived				Subjects who died				Association with death		
Variable	Detail	Median	IQR	Percent	Number	Median	IQR	Percent	Number	OR	95%CI	p
	Grade 3 or 4			N/a	N/a			N/a		1.16	0.49-2.72	0.74
Disc leak	absent			14.67	33			3	8.57			
	present			85.33	192			32	91.43	1.83	0.53-6.33	0.34
Punctate focal leak	None			72.89	164			12	34.29			
	1 to 5 sites			23.56	53			17	48.57	4.38	1.97-9.77	**<0.001**
	>5 sites			3.56	8			6	17.14	10.25	3.06-34.37	**<0.001**
Large focal leak	None			86.22	194			19	54.29			
	1 site			8.89	20			1	2.86	0.51	0.06-4.02	0.52
	>1 site			4.89	11			15	42.86	13.92	5.6-34.58	**<0.001**
Post capillary venule leak	None or grade 1			69.2	155			27	81.82			
	grade 2			21.88	49			2	6.06	0.23	0.054-1.02	**0.053**
	grade 3 or 4			8.93	20			4	12.12	1.15	0.36-3.62	0.81
Large venule leak	None			57.33	129			17	51.52			
	grade 1			28.44	64			10	30.3	1.19	0.51-2.74	0.69
	grade 2 or 3			14.22	32			6	18.18	1.42	0.52-3.9	0.49
Post capillary venule IVFD	absent			1.47	3			1	3.85			

		Subjects who lived				Subjects who died				Association with death		
Variable	Detail	Median	IQR	Percent	Number	Median	IQR	Percent	Number	OR	95%CI	p
	present			98.53	201			25	96.15	0.37	0.04-3.7	0.4
Pre capillary arteriole IVFD	absent			43.81	85			6	24			
	present			56.19	109			19	76	2.47	0.94-6.45	**0.065**
Small venule IVFD	absent			1.86	4			1	3.33			
	present			98.14	211			29	96.67	0.55	0.06-5.09	0.6
Small arteriole IVFD	absent			57.14	124			14	48.28			
	present			42.86	93			15	51.72	1.43	0.66-3.11	0.37
Large venule IVFD	absent			20.74	45			4	13.33			
	present			79.26	172			26	86.67	1.7	0.56-5.12	0.35
Large arteriole IVFD	absent			86.76	190			21	70			
	present			13.24	29			9	30	2.81	1.17-6.72	**0.02**

Table 32: Multivariate model of angiographic features against death.
Logistic regression model of fluorescein features and clinical variables, with death as the dependent variable, in 243 subjects with retinopathy positive cerebral malaria who had a fluorescein angiogram within 24 hours of admission. Variables were chosen on the basis of univariate significance with death, and also a priori biological rationale. Bold text indicates p<0.02. CNP = capillary non-perfusion; IVFD = intravascular filling defects; *No subjects had grade 0 (absent) macular CNP

		Odds Ratio	Std. Err.	z	P>z	95%CI low	95%CI high
Macular CNP	grade 1*						
	grade 2	2.08	2.31	0.66	0.50	0.23	18.35
	grade 3 or 4	3.20	3.54	1.05	0.29	0.36	28.05
Punctate focal leak	None						
	1 to 5 sites	2.36	1.23	1.65	0.1	0.84	6.60
	>5 sites	6.90	5.32	2.51	**0.012**	1.52	31.30
Large focal leak	None						
	1 site	0.26	0.29	-1.18	0.239	0.02	2.43
	>1 site	3.59	2.21	2.07	0.038	1.07	12.05
Post-capillary venule leak	None or grade 1						
	grade 2	0.14	0.15	-1.8	0.072	0.01	1.19
	grade 3 or 4	0.59	0.48	-0.64	0.524	0.11	2.96
Large arteriole IVFD		1.79	1.04	1.01	0.311	0.57	5.60
Lactate		1.13	0.06	2.36	**0.018**	1.02	1.26
Constant		0.01	0.01	-3.82	**<0.001**	0.001	0.12

7.6.4 Associations between FA features and time to regain consciousness (BCS=3)

I found positive unadjusted associations between the following angiographic variables and coma recovery time (unadjusted coefficient, 95%CI, all p<0.1): severe macular capillary non-perfusion (0.39, 0.07-0.71), 1 site of large focal leak (0.48, 0.12-0.84), punctate focal leak (1-5 sites: 0.42, 0.19-0.66; >5 sites: 0.77, 0.24-1.29), and intravascular filling defects in arterioles (pre-capillary: 0.32, 0.09-0.55; small: 0.30, 0.09-0.51; large: 0.38, 0.08-0.68) (Table 33).

Pairwise testing also suggested associations between clinical and ophthalmoscopic variables and time to recover consciousness (unadjusted coefficient, all at p<0.1): peripheral parasitaemia (<-0.001, <-0.001 to <-0.001), lactate (0.03, 0.002-0.05), witnessed convulsions at admission (0.26, -0.03-0.56), witnessed convulsions after admission (0.31, 0.10-0.51), severe macular whitening (0.45, 0.04-0.87), foveal whitening (moderate: 0.41, 0.07-0.75; severe: 0.51, 0.15-0.87), orange vessels (0.3, 0.05-0.55), papilloedema (0.47, 0.25-0.69), disc hyperaemia (0.23, 0.004-0.46) (Table 33).

When angiographic variables with significant associations to coma resolution time on pairwise testing were analysed in a multivariate model that included lactate, papilloedema, and witnessed convulsions after admission, significant independent associations were found between longer coma recovery time and the presence of the following variables (coefficient, 95%CI) (all p<0.02): punctate focal leak (>5 sites: 0.67, 0.17-1.17), 1 site of large focal leak (0.42, 0.09-0.75), papilloedema (0.31, 0.10-0.52), and convulsions after admission (0.32, 0.13-0.50) (Table 34).

Table 33: Unadjusted associations with coma resolution

Data for a range of clinical variables of interest and angiographic features listed for groups of patients who recovered consciousness (Blantyre coma score = 3) in <12 hours, 12-24 hours, or >24 hours after admission. Unadjusted associations from truncated negative binomial regression are shown. P-values <0.05 are in bold. Retinal variables are from the worst affected eye in each case unless specified. CNP = capillary non-perfusion; IVFD = intravascular filling defects; Macular whitening is measured in terms of disc areas; Foveal whitening is measured in terms of foveal area. *no subjects had grade 0 (absent) macular CNP.

Variable	Detail	Median	IQR	%	n	Median	IQR	%	n	Median	IQR	%	n	Coef.	p	95%CI
Number					27				82				109			
Demograpics																
Age	months	37	28-49		27	44	29-66		82	37	28.5-53.5		109	-0.002	0.384	-0.006 to 0.002
Sex	boy			48.15	13			52.44	43			44.95	49			
	girl			51.85	14			47.56	39			55.05	60	-0.053	0.614	-0.259 to 0.153
Clinical																
Temperature	C	39	38.4-39.8		27	38.8	37.675-39.3		82	38.8	38.05-39.7		109	-0.007	0.886	-0.098 to 0.085
Systolic blood pressure	mmHg	96	85-109.5		25	99	91-108		77	96	90-104		103	-0.003	0.523	-0.011 to 0.006

Variable	Detail	Median	IQR	%	n	Median	IQR	%	n	Median	IQR	%	n	Coef.	p	95%CI
Pulse	Beats/min	148	139-161		27	142	130-167.25		82	156	134-174.5		109	0.001	0.736	-0.003 to 0.004
Duration of coma pre-admission	hours	7	5.25-13.5		20	10	4.25-23.75		60	9	5-22.5		86	0.004	0.317	-0.004 to 0.011
Duration of fever pre-admission	hours	72	48-72		25	72	48-72		79	54	48-72		105	0.001	0.498	-0.001 to 0.002
Coma score	0			3.7	1			2.44	2			9.17	10			
	1			29.63	8			45.12	37			46.79	51	-0.031	0.891	-0.473 to 0.411
	2			66.67	18			52.44	43			44.04	48	-0.297	0.185	-0.736 to 0.142
Respiratory distress	absent			62.96	17			73.17	60			65.14	71			
	present			37.04	10			26.83	22			34.86	38	0.007	0.948	-0.213 to 0.228
History of convulsions	absent			22.22	6			12.66	10			17.43	19			
	present			77.78	21			87.34	69			82.57	90	0.016	0.906	-0.265 to 0.299
Laboratory																
Parasitaemia		156000	34000 - 463000		27	38010	763.5 - 232000		78	30480	1803.5-108000		106	-0.000	**0.009**	-0.000 to -0.000

Variable	Detail	Median	IQR	%	n	Median	IQR	%	n	Median	IQR	%	n	Coef.	p	95%CI
White cell count	cells	8600	6800-14525		26	10300	7350-13500		77	9800	7250-14725		104	0.000	0.194	-0.000 to 0.000
Haematocrit	%	18	15.4-23.2		27	21	17-25.75		80	19.1	14.925-24.625		108	0.005	0.516	-0.011 to 0.021
Lactate	mmol/L	4.8	2.4-9.8		27	3.85	2.45-7.1		80	5.1	3.025-9.1		108	0.027	**0.033**	0.002 to 0.051
HRP2	ng/ml	5462	3117-9660		27	7344.5	2942.5-10400		82	8025.5	3195-13898		108	0.000	0.504	-0.000 to 0.000
Platelet count	platelets	51000	30000-97000		27	64000	39000-111000		77	57500	30750-98500		102	-0.000	0.294	-0.000 to 0.000
HIV	negative			96	24			87.01	67			82.83	82			
	positive			4	1			12.99	10			17.17	17	0.002	0.986	-0.308 to 0.314
Hypoglycaemia on ward	absent			88.89	24			91.46	75			90.83	99			
	present			11.11	3			8.54	7			9.17	10	0.163	0.367	-0.192 to 0.519
Retinal																
Retinal haemorrhage	None			23.08	6			26.83	22			21.1	23			

Variable	Detail	Median	IQR	%	n	Median	IQR	%	n	Median	IQR	%	n	Coef.	p	95%CI
	1 to 5			42.31	11			37.8	31			34.86	38	0.176	0.201	-0.094 to 0.447
	6 to 20			15.38	4			17.07	14			24.77	27	0.000	0.997	-0.309 to 0.310
	21 to 50			7.69	2			10.98	9			6.42	7	0.130	0.536	-0.283 to 0.544
	>50			11.54	3			7.32	6			12.84	14	0.252	0.191	-0.125 to 0.631
Macular whitening	None			7.69	2			11.11	9			6.42	7			
	<1/3			53.85	14			45.68	37			32.11	35	-0.025	0.898	-0.410 to 0.359
	1/3 to 1			26.92	7			29.63	24			32.11	35	0.177	0.378	-0.217 to 0.572
	>1			11.54	3			13.58	11			29.36	32	0.454	**0.031**	0.042 to 0.865
Foveal whitening	None			11.54	3			20.73	17			11.11	12			
	<1/3			61.54	16			50	41			38.89	42	0.145	0.349	-0.158 to 0.449
	1/3 to 2/3			26.92	7			15.85	13			25.93	28	0.411	**0.018**	0.071 to 0.751
	>2/3			0	0			13.41	11			24.07	26	0.513	**0.005**	0.154 to 0.871
Temporal whitening	None			15.38	4			9.88	8			15.6	17			

Variable	Detail	Median	IQR	%	n	Median	IQR	%	n	Median	IQR	%	n	Coef.	p	95%CI
	1			26.92	7			46.91	38			37.6	41	-0.219	0.185	-0.542 to 0.104
	2			34.62	9			22.22	18			19.27	21	-0.186	0.302	-0.541 to 0.168
	3			23.08	6			20.99	17			27.52	30	-0.018	0.918	-0.365 to 0.329
Orange vessels, temporal quadrant	absent			83.33	15			71.43	50			56	42			
	present			16.67	3			28.57	20			44	33	0.296	**0.02**	0.046 to 0.545
White vessels, temporal quadrant	absent			72.22	13			80	56			76	57			
	present			27.78	5			20	14			24	18	-0.017	0.908	-0.305 to 0.271
White capillaries	absent			61.11	11			75.71	53			77.33	58			
	present			38.89	7			24.29	17			22.67	17	-0.065	0.643	-0.343 to 0.212
Papilloedema	absent			80.77	21			79.27	65			64.22	70			
	present			19.23	5			20.73	17			35.78	39	0.473	**0**	0.253 to 0.692
Disc hyperaemia	absent			84	21			74.39	61			66.04	70			
	present			16	4			25.61	21			33.96	36	0.230	**0.046**	0.004 to 0.457

Variable	Detail	Median	IQR	%	n	Median	IQR	%	n	Median	IQR	%	n	Coef.	p	95%CI
Convulsions at admission	absent			96.3	26			85	68			84.26	91			
	present			3.7	1			15	12			15.74	17	0.264	0.081	-0.032 to 0.561
Convulsions after admission	absent			70.37	19			62.2	51			45.87	50			
	present			29.63	8			37.8	31			54.13	59	0.307	**0.003**	0.104 to 0.511
Macular CNP	Grade 1*			14.81	4			19.75	16			9.17	10			
	Grade 2			51.85	14			49.38	40			45.87	50	0.182	0.252	-0.129 to 0.495
	Grade 3 or 4			33.33	9			30.86	25			44.95	49	0.390	**0.017**	0.069 to 0.711
Peripheral CNP	Grade 0 or 1			44.44	12			56.1	46			35.78	39			
	Grade 2			18.52	5			23.17	19			25.69	28	0.032	0.806	-0.226 to 0.291
	Grade 3 or 4			37.04	10			20.73	17			38.53	42	0.281	**0.02**	0.044 to 0.517
Peripheral CNP, left eye	Grade 0 or 1			55.56	15			65.38	51			48.57	51			
	Grade 2			22.22	6			19.23	15			22.86	24	0.055	0.68	-0.207 to 0.318
	Grade 3 or 4			22.22	6			15.38	12			28.57	30	0.336	**0.01**	0.080 to 0.592

Variable	Detail	Median	IQR	%	n	Median	IQR	%	n	Median	IQR	%	n	Coef.	p	95%CI
Amount of periphery seen, left eye	none			0	0			1.25	1			0	0			
	zone 1			14.81	4			12.5	10			25	27	0.575	0.464	-0.964 to 2.115
	zone 2			44.44	12			51.25	41			47.22	51	0.524	0.502	-1.005 to 2.053
	zone 3			40.74	11			35	28			27.78	30	0.251	0.748	-1.282 to 1.784
Large focal leak	None			92.59	25			93.9	77			77.98	85			
	1 site			7.41	2			1.22	1			14.68	16	0.477	**0.009**	0.120 to 0.835
	>1 site			0	0			4.88	4			7.34	8	0.235	0.298	-0.208 to 0.679
Punctate focal leak	None			92.59	25			80.49	66			60.55	66			
	1 to 5 sites			7.41	2			19.51	16			32.11	35	0.424	**0**	0.193 to 0.655
	>5 sites			0	0			0	0			7.34	8	0.765	**0.004**	0.243 to 1.287
Post-capillary venule leak	Grade 0 or 1			70.37	19			73.17	60			66.67	72			
	Grade 2			14.81	4			20.73	17			24.07	26	0.065	0.615	-0.189 to 0.319
	Grade 3 or 4			14.81	4			6.1	5			9.26	10	0.057	0.76	-0.312 to 0.428

Variable	Detail	Median	IQR	%	n	Median	IQR	%	n	Median	IQR	%	n	Coef.	p	95%CI
Large venule leak	None			55.56	15			65.85	54			52.29	57			
	Grade 1			29.63	8			24.39	20			29.36	32	0.198	0.101	-0.038 to 0.435
	Grade 2 or 3			14.81	4			9.76	8			18.35	20	0.216	0.156	-0.082 to 0.514
IVFD, large venules	Absent			18.52	5			28.75	23			16.35	17			
	Present			81.48	22			71.25	57			83.65	87	0.216	0.097	-0.039 to 0.472
IVFD, small venules	Absent			0	0			2.53	2			1.94	2			
	Present			100	27			97.47	77			98.06	101	0.191	0.628	-0.584 to 0.968
IVFD, post-capillary venules	Absent			0	0			2.67	2			1.04	1			
	Present			100	27			97.33	73			98.96	95	0.360	0.437	-0.548 to 1.269
IVFD, pre-capillary arterioles	Absent			55.56	15			51.39	37			34.83	31			
	Present			44.44	12			48.61	35			65.17	58	0.322	**0.005**	0.094 to 0.549
IVFD, small arterioles	Absent			66.67	18			63.75	51			49.04	51			
	Present			33.33	9			36.25	29			50.96	53	0.302	**0.004**	0.093 to 0.510

Variable	Detail	Median	IQR	%	n	Median	IQR	%	n	Median	IQR	%	n	Coef.	p	95%CI
IVFD, large arterioles	Absent			88.89	24			92.59	75			81.9	86			
	Present			11.11	3			7.41	6			18.1	19	0.378	**0.014**	0.076 to 0.681
Disc leak	Absent			29.63	8			14.63	12			11.93	13			
	Present			70.37	19			85.37	70			88.07	96	0.290	**0.047**	0.003 to 0.578

Table 34: Model of angiographic features against coma resolution.

Truncated negative binomial regression model of coma resolution time, including fluorescein angiogram features and also admission lactate, papilloedema, and the presence or absence of witnessed convulsions after admission (n=208). These additional variables were selected on the basis of significant pairwise associations with coma resolution time, and also because each had a plausible hypothetical causal relationship with prolonged coma (e.g. admission papilloedema was taken as a marker of increased intracranial pressure). Bold text indicates p<0.02. IVFD = intravascular filling defects; CNP = capillary non-perfusion

		coefficient	Std. Err.	z	p	95% CI low	95% CI high
Lactate		0.017	0.012	1.390	0.163	-0.007	0.040
Papilloedema		0.312	0.106	2.950	**0.003**	0.105	0.520
Witnessed convulsions after admission		0.317	0.095	3.32	**0.001**	0.129	0.504
Macular CNP	grade 1*						
	grade 2	0.219	0.146	1.49	0.135	-0.068	0.506
	grade 3 or 4	0.177	0.156	1.14	0.254	-0.128	0.483
Punctate focal leak	None						
	1 to 5 sites	0.171	0.120	1.42	0.154	-0.064	0.406
	>5 sites	0.670	0.254	2.64	**0.008**	0.172	1.167
Large focal leak	None						
	1 site	0.423	0.168	2.52	**0.012**	0.093	0.752
	>1 site	0.020	0.219	0.09	0.927	-0.410	0.449
Pre-capillary arteriolar IVFD		0.161	0.147	1.10	0.273	-0.127	0.448
Constant		2.913	0.158	18.42	**0.000**	2.603	3.222
/lnalpha	-0.858	0.104				-1.062	-0.655
alpha	0.424	0.044				0.346	0.520
Likelihood-ratio test of alpha=0: chibar2(01) = 2437.57 Prob>=chibar2 = 0.000							

7.6.5 Associations between fluorescein features and clinical variables

I visualised individual pairwise associations between fluorescein variables and age, venous lactate, haematocrit, HRP2, white cell count, and duration of coma pre-admission (Table 35). Effect sizes are small, but this series of analyses suggests several links. Age appears to be inversely related to peripheral CNP and leakage from venules of all sizes. Lactate was positively associated with the severity of macular CNP and the presence of intravascular filling defects in large arterioles. Haematocrit was negatively associated with disc leak, large focal leak, and leak from venules of all sizes. HRP2 and white cell count appeared to have trivial associations with leak from venules. Duration of coma pre-admission was not associated with any FA variables linked with death. The one association with intravascular filling defects in post-capillary venules involved a comparison between very imbalanced groups, since this FA sign was virtually ubiquitous.

Table 35: Unadjusted associations between selected fluorescein and clinical variables

All fluorescein variables measured from the worst affected eye, except where stated otherwise. CNP = capillary non perfusion; IVFD = intravascular filling defects. Logistic or ordinal regression used to test associations, depending on the nature of the fluorescein variable. Bold text indicates p<0.01. Peripheral CNP in the left eye was tested after controlling for the furthest extent of peripheral retina seen. Other tests include only one independent variable and use data from the worst affected eye. *no subjects had grade 0 (absent) macular CNP.

		Age			Lactate			Haematocrit			HRP2			White cell count			Time from coma onset to admission		
		n	OR	95%CI	n	OR	95%CI	n	OR	95%CI	n	OR	95%CI	n	OR	95%CI	n	OR	95%CI
Macular CNP	grade 1*	31	0.99	0.98-1.0	30	**1.07**	**1.02-1.14**	30	0.97	0.93-1.00	30	1	0.99-1.00	29	1	0.99-1.00	23	1	0.99-1.02
	grade 2	117			115			115			117			113			91		
	grade 3 or 4	107			106			107			107			100			82		
Peripheral CNP	None or grade 1	45	**0.98**	**0.97-0.99**	45	1.02	0.97-1.08	45	0.95	0.91-0.99	44	1	0.99-1.00	43	1	0.99-1.00	110	1.01	0.99-1.02
	Grade 2	121			118			118			121			112			37		
	Grade 3 or 4	83			82			83			83			81			44		
Disc leak	absent	36	0.99	0.98-1.00	36	1.04	0.95-1.13	36	**0.93**	**0.88-0.98**	36	0.99	0.99-1.00	36	1	0.99-1.00	28	1.06	1.01-1.12
	present	224			220			221			223			211			172		
Punctate focal leak	none	176	1	0.99-1.01	175	1.06	0.99-1.12	175	1.03	0.99-1.08	175	1	0.99-1.00	166	0.99	0.99-1.00	135	1.01	0.99-1.03
	1 to 5 sites	70			67			68			70			67			57		
	>5 sites	14			14			14			14			14			8		

		Age			Lactate			Haematocrit			HRP2			White cell count			Time from coma onset to admission		
		n	OR	95%CI	n	OR	95%CI	n	OR	95%CI	n	OR	95%CI	n	OR	95%CI	n	OR	95%CI
Large focal leak	none	213	0.99	0.98-1.00	210	1.06	0.99-1.14	211	**0.93**	**0.88-0.98**	213	1	0.99-1.00	201	1	0.99-1.00	159	0.99	0.98-1.02
	1 site	21			21			21			20			21			19		
	>1 sites	26			25			25			26			25			22		
Post-capillary leak	none or grade 1	182	**0.96**	**0.95-0.98**	179	1.04	0.98-1.11	179	**0.94**	**0.89-0.98**	181	**0.99**	**0.99-0.99**	173	**1**	**1.00-1.00**	143	1.01	0.99-1.03
	grade 2	51			51			51			51			48			37		
	grade 3 or 4	24			23			24			24			23			19		
Large venule leak	none	146	**0.97**	**0.95-0.98**	144	1.06	1.00-1.12	145	**0.93**	**0.89-0.97**	145	0.99	0.99-0.99	140	**1**	**1.00-1.00**	115	1	0.99-1.02
	grade 1	74			73			72			74			68			52		
	grade 2 or 3	38			37			38			38			37			32		
IVFD, large veins	absent	49	1	0.99-1.02	48	0.95	0.89-1.02	49	1.01	0.96-1.06	48	1	0.99-1.00	48	1	0.99-1.00	39	1.01	0.99-1.04
	present	198			195			195			198			186			151		
IVFD, Post-capillary venules	absent	2	1.02	0.97-1.07	3	1.25	0.8-1.97	4	1.01	0.86-1.18	4	1	0.99-1.00	4	0.99	0.99-1.00	4	**0.96**	**0.93-0.99**
	present	226			223			223			225			213			170		
IVFD, pre-capillary arterioles	absent	91	0.99	0.99-1.01	90	1	0.94-1.07	90	1.02	0.98-1.07	90	1	0.99-1.00	87	1	0.99-1.00	70	1.01	0.99-1.03
	present	128			125			126			128			121			93		

		Age			Lactate			Haematocrit			HRP2			White cell count			Time from coma onset to admission		
		n	OR	95%CI	n	OR	95%CI	n	OR	95%CI	n	OR	95%CI	n	OR	95%CI	n	OR	95%CI
IVFD, large arterioles	absent	211	0.99	0.98-1.01	207	**1.09**	**1.02-1.18**	208	0.98	0.92-1.03	210	1	0.99-1.00	199	0.99	0.99-1.00	163	0.97	0.93-1.01
	present	38			38			38			38			37			29		

7.6.6 Co-existence of punctate focal leak, large focal leak, and death

Punctate focal leak was independently associated with death. Large focal leak was associated with death on pairwise analysis, but this effect was reduced to a non-significant trend after controlling for punctate leak and other variables. Punctate and large focal leak types were found to coexist in 26 patients. This was out of 47 patients with large focal leak (55%), and 84 with punctate leak (31%). 7 of 35 patients who died (20%) had no evidence of either type of leak (Figure 53).

Of 84 survivors, 61 patients had some punctate leak (73%), but 53 of these 61 patients had 5 or less leak sites and 8/61 (13%) had greater than 5 sites of leak. This is in contrast to 6/23 (26%) fatal cases with >5 sites of leak (Fisher's exact, p=0.19). 31/84 survivors had large focal leak, but all of these patients had relatively few sites of leak (median 1, range 1-5), while in patients who died with large focal leak (n=16) the number of sites was greater (median 4, range 1-30) (Kruskal-Wallis test, $p<0.001$).

Figure 53: Venn diagram illustrating the co-existence of any large focal leak, any punctate focal leak, and death.
The circles are proportional to the patient numbers in each area, and the whole sample of 260 patients is illustrated by a proportionately scaled black outline.
LFL = large focal leak; PFL = punctate focal leak.

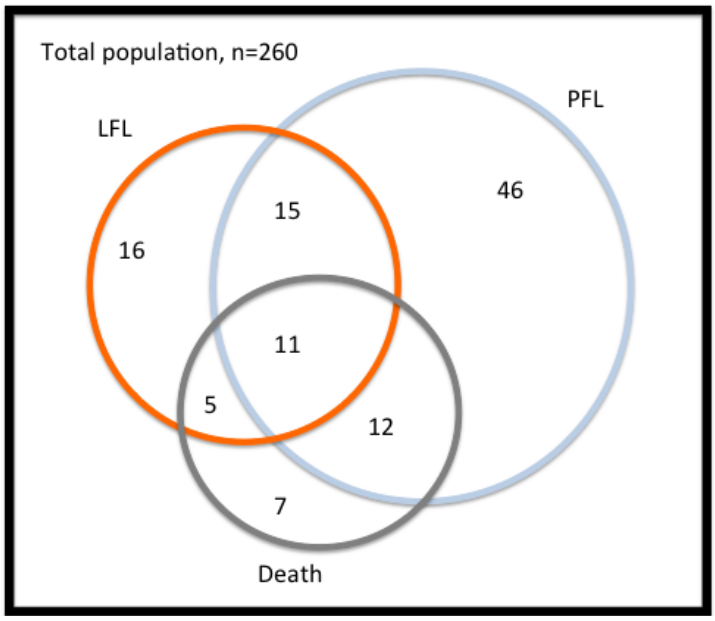

7.7 Discussion

Punctate leakage of fluorescein through defects in the inner blood-retinal barrier is independently associated with death in children with retinopathy-positive CM, after controlling for venous lactate and other angiographic features. A recent study found that increased brain volume was present in almost all fatal cases of paediatric CM (Seydel *et al.*, 2015). In view of the close similarity between blood-retinal and blood-brain barriers (Patton *et al.*, 2005), my results suggest that the cerebral vasculature may be sustaining damage similar to what I have observed in the retina, and that blood-*brain* barrier breakdown may be an important cause of increased brain volume in this disease.

The existence of several visually distinct types of retinal leak suggests that the specific type of leakage is more important, with respect to fatal outcome, than the presence or absence of blood-tissue-barrier breakdown in general.

Punctate and large focal leak were also independently associated with longer time to regain consciousness, after controlling for admission lactate, papilloedema, and witnessed convulsions after admission. This suggests that, as well as being related to disease mechanisms leading to death, these types of blood-tissue barrier damage may also contribute to clinically significant tissue dysfunction in non-fatal cases. The implication is that neurovascular endothelial leakage may have important roles in the pathogenesis or maintenance of coma, as well as progression to death. The independent association with papilloedema at admission is consistent with the observation that increased brain volume occurs in non-fatal as well as fatal cases, but that it resolves over time in children who recover from retinopathy-positive CM (Seydel *et al.*, 2015).

As in the brain, the inner blood-retina barrier involves junctions between endothelial cells that operate in concert with supportive cells such as pericytes, astrocytes and (in the retina) Müller cells. Several mechanisms are associated with leakage from retinal vessels in hypoxic conditions, including hyperviscosity, increased production of vascular endothelial growth factor (VEGF) and nitric oxide (NO), inflammatory mediators, and free radicals (Kaur et al., 2008). In addition to its role in haemostasis the protein C pathway is also involved in regulating barrier function (Bouwens *et al.*, 2013). For example, blockade of the endothelial protein-C receptor (EPCR) has been linked to increased blood-brain barrier permeability in a mouse model of cerebral venous sinus thrombosis (Nagai *et al.*, 2010). Moxon et al., recently found that sequestered parasitised erythrocytes are co-localised with focal loss of EPCR in the neurovasculature in fatal paediatric CM. This loss could result from receptor shedding into the cerebrospinal fluid (Moxon *et al.*, 2013) pathological binding of parasitised erythrocytes EPCR (Turner *et al.*, 2013), or both phenomena.

The morphological features of both punctate leak and large focal leak suggest that each results from processes that are highly localised to short microvascular segments. This is consistent with the possibility that focal endothelial barrier dysfunction, involving loss of EPCR and/or activation of protease activated receptor 1 (PAR1), results from the localised binding of parasitised erythrocytes (Moxon et al., 2014; Turner et al., 2013).

Punctate focal leak involves small (≤125μm linear diameter) sites of leak, and stereoscopic images from a few cases suggest that it arises from the deep capillary plexus within the outer retinal layers. Punctate leak was not associated with any of the clinical variables that I tested (Table 35). Although it can co-exist with large focal leak, it appears not to be simply a precursor of this other leakage type, either within a given angiogram series or on serial images from subsequent days after admission. A punctate leak does not develop into haemorrhage after the angiogram, or on subsequent days of the hospital admission (Figure 54). Venular leak may be a sign of recovery, a hypothesis which is consistent with trends between post-capillary venule leak and survival on pairwise and multivariate analysis (Table 31 and 32), as well as animal models of blood-brain barrier breakdown (Nag *et al.*, 2011).

Punctate leak also occurred in children who survived, and in children with any punctate leak the number of punctate leak sites was not significantly different between patients who lived or died. My analysis of angiogram features against time to recover from coma suggests that children with punctate leak who survive go on to spend a significantly longer time in coma than children without this type of leak. This is consistent with MRI assessment of brain swelling in retinopathy positive paediatric CM. Seydel et al. found severe brain swelling at admission in 39/143 (28%) of non-fatal cases, but in these cases brain volume decreased over subsequent days (Seydel *et al.*, 2015).

In the case of large focal leak, barrier loss is apparently severe enough to allow a large amount of fluorescein to move rapidly out from the vessel, and in addition the endothelial break is large enough to permit movement of erythrocytes and produce a haemorrhage. Each site of large focal leak involves a large (>125μm diameter) area, and in our series are consistently co-localised with retinal haemorrhage in subsequent images (Figure 55). Although the effect size is small, large focal leak appears to be related to low haematocrit (Table 35), consistent with reported associations between retinal haemorrhage and anaemia from non-malarial causes (Carraro *et al.*, 2001; Holt and Gordon-Smith, 1969).

Figure 54: Change in punctate leak over time.

The natural history of punctate focal leak does not appear to involve haemorrhages similar to those seen with large focal leak. In this case punctate focal leak on admission is seen in association with severe retinal whitening at the fovea (left two images). Repeat imaging the day after admission does not show haemorrhage (right two images), but post-capillary venule leak has developed.

Figure 55: Development of large focal leak.

The natural history of large focal leak appears to involve sudden onset of a rapid leak of fluorescein followed by blood. Colour photography of sites of large focal leak immediately after the angiogram consistently reveals retinal haemorrhage at the same location – often with a surrounding halo of fluorescein.

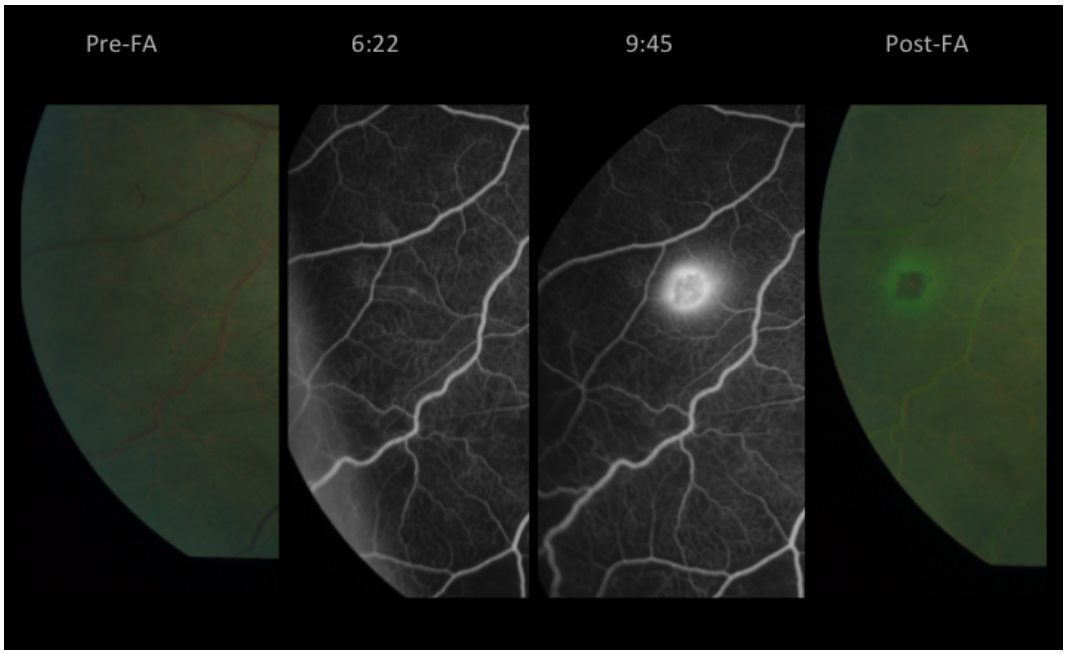

In children with large focal leak, the number of large focal leak sites was greater in fatal than in non-fatal cases. The positive association between the severity of large focal leak and death is consistent with results of our analysis of angiographic features against coma recovery time. The presence of a single site of large focal leak was associated with greater time to regain consciousness, whereas a greater number of sites was not – presumably because many of these children did not recover at all.

CNP at the macula was associated with death on pairwise testing (Table 31), but this was not significant after controlling for other variables linked to death on multivariate analysis (Table 32). The macular CNP in paediatric malarial retinopathy ranges from mild to severe, and is positively associated with lactate on pairwise testing (Table 35). Since lactate is a marker of systemic anaerobic metabolism, this association is consistent with local failure of perfusion in the retina, as well as an association between retinal whitening (which tends to be co-

localised to CNP) (Beare *et al.*, 2009) and lactate in adults with severe malaria (Maude et al., 2009). Hyperlactitaemia and macular CNP may both reflect underlying neurovascular ischaemia, which could cause cytotoxic oedema and increased brain volume.

IVFD in large arterioles were also associated with death on univariate, but not multivariate analysis (Table 31 and 32). These features may represent sequestration of parasitised erythrocytes within vessel segments (Beare *et al.*, 2009; Lewallen *et al.*, 2000). Histopathological studies of brain vessels in CM report that sequestration is most common and intense in capillaries and post-capillary venules, possibly related to favourable haemodynamic characteristics in these vessel segments, such as lower flow velocity compared to arterioles (MacCormick *et al.*, 2014). I found that IVFD were almost ubiquitous in retinal venules, and particularly post-capillary venules, but were less common in arterioles (see also Table 23 in Chapter 5). The presence of this feature in large arterioles may suggest a greater severity of sequestration within the neurovasculature, possibly as a result of reductions in arteriolar flow velocity secondary to severe venous sequestration and congestion. An association between IVFD in large arterioles and death would be consistent with this hypothesis.

Neither CNP at the macula, nor large arteriolar IVFD were independently associated with death after controlling for other risk factors. This could occur if CNP and filling defects contribute to the pathogenesis of these other features (such as punctate or large focal leak), or if non-perfusion and filling defects both represent different aspects of the same phenomenon: reduced perfusion of neuronal tissue secondary to sequestration. This process may be captured to some extent by measurements of systemic lactate. The failure of these features to reach significance in a multivariate model certainly does *not* prove that they are irrelevant to CM pathogenesis. Logistic regression involves the assumption that exposure variables are independent of each other. In reality it is likely that IVFD, CNP, and various types of leak are related in complex ways—for example, sequestration (perhaps represented by IVFD) may cause both CNP and leakage. Such hypotheses could be tested on observational data using structural equation modelling.

Strengths of this study include a strict case definition based on retinopathy positive CM, rather than the standard WHO clinical definition (World Health Organization, 2014b). Retinopathy positive cases are more likely to have cerebral sequestration than otherwise similar cases of paediatric CM without retinopathy (Barrera *et al.*, 2015; Taylor *et al.*, 2004), and so this case definition should deliver a sample that is more pathologically homogenous, and therefore more relevant to questions about disease mechanisms, than one based on the WHO case definition. Limitations include a relatively low inclusion rate (260/549, 47.4%), and a tendency to preferentially perform angiograms on patients with more severe malarial retinopathy (Table 30). This suggests that my results may be more relevant to moderate and severe retinopathy positive CM than to mild cases. My sample also had a higher prevalence of convulsions after admission, neurological sequelae on discharge, and longer time to reach consciousness (BCS=3) (Table 30). These characteristics may be a result of inadvertently selecting cases from the more severe end of the disease spectrum.

In conclusion, an independent association between death and punctate leakage suggests that a specific type of blood-brain barrier breakdown may be an important cause of fatal increases in brain volume in this paediatric CM. Similar independent associations exist between punctate and large focal leak, and duration of coma in children who survive CM. This suggests that neurovascular barrier leakage is important to the pathology of coma as well as death. I discuss possible disease mechanisms further in Chapter 9. The retina provides a useful means to study paediatric CM disease mechanisms, and the angiographic features we describe may be profitable targets for further research into the interaction of host and parasite factors, how these relate to clinical outcomes, and ultimately strategies to disrupt these processes with novel treatments.

Chapter 8 – Associations between retina and brain swelling

8.1 Aim of chapter

Investigate associations at admission between retinal variables and brain swelling in retinopathy positive paediatric cerebral malaria

8.2 Summary of chapter

8.2.1 What is known already

Certain features of malarial retinopathy, and also certain MRI brain characteristics, are known to be related to death from paediatric cerebral malaria. Since retinal and MRI brain images may provide complementary information about fatal disease processes, evaluating associations between them may provide clues about the causes of brain damage in this disease.

8.2.2 What this chapter involved

After collecting original retinal data in the form of ophthalmoscopic exams and fluorescein angiographic images from admission and adding these to an existing dataset, I tested associations between brain swelling (measured as pre-pontine CSF space) and blood-retinal barrier breakdown (measured on fluorescein angiography), with reference to the ultimate outcome of the disease process – death or recovery.

8.2.3 What this chapter adds to current knowledge

Associations between retina and brain are unclear, probably because of previously unrecognised selection bias. Further work on associations between the change in retinal and brain variables may be more profitable. Future studies of retinal and brain features in cerebral malaria should be careful to minimise selection bias.

8.3 Introduction

Significant associations between retina and brain in paediatric cerebral malaria (CM) are suggested by biological similarity between the two CNS regions, previously demonstrated associations between retina and brain (MacCormick *et*

al., 2014), and links between both retinal and brain features and death (Chapter 6 and 7).

Previous studies have reported associations between retinal features and cerebral histology (Barrera *et al.*, 2015; Taylor *et al.*, 2004; White *et al.*, 2001), and between retinal features at admission and follow up MRI brain (Kampondeni *et al.*, 2013). Associations between various retinal features and death have been reported in the literature (Beare et al., 2004; Lewallen et al., 1996), and also in earlier chapters of this thesis (Chapter 6 and 7). No analysis has yet been done on retinal and MRI brain features recorded at admission in children with CM.

Admission MRI brain suggests that most children who die from retinopathy positive CM have severely increased brain volume (Seydel *et al.*, 2015). This is consistent with clinical observations of pre-morbid children and previous research suggesting that respiratory arrest was accompanied by other signs of brain stem dysfunction (Newton et al., 1991; Newton et al., 1994, 1997).

The volume of the brain can increase for several reasons, and it is not yet clear which is responsible for the brain swelling seen in paediatric CM. Note that *cerebral oedema* is only one cause of *brain swelling*. Causes of brain swelling include:

- Vasogenic oedema. This involves leakage from blood vessels, and can occur because of blood-brain barrier breakdown or from increased hydrostatic pressure
- Cytotoxic oedema, which involves swelling of tissue as a result of cellular membrane pump failure, often in the context of ischaemia
- Osmotic oedema, from an imbalance in brain and plasma osmolality, as in diabetic hyperosmolar hyperglycaemia
- Interstitial oedema, from a breakdown of the blood-cerebrospinal fluid (CSF) barrier, usually associated with hydrocephalus

In addition to one or more types of cerebral oedema, brain volume can also increase because of enlargement in the volume of blood or CSF compartments,

and intracranial masses such as tumour or haemorrhage (Nag *et al.*, 2009; Yachnis, 2013).

The relationship between intracranial volume and pressure is non-linear, and depends on the elasticity of the craniospinal system (or its inverse, compliance). Consequently relatively small changes in volume (such as from obstructions to venous outflow) can potentially lead to large fluctuations in intracranial pressure in patients already suffering from compromised cerebrospinal elastance (Shapiro *et al.*, 1980; Timmons, 2013)).

Therefore sequestration could exert effects through obstruction and local ischaemia (cytotoxic oedema), damage to the blood-brain barrier (vasogenic oedema), and local reductions in venous outflow.

Vasogenic and cytotoxic mechanisms are likely to be the types of oedema most relevant to increases in brain volume in paediatric CM, since severe changes in blood osmolality and hydrocephalus are not seen in this disease. Processes similar to vasogenic and cytotoxic oedema appear to take place in the retina in children with malarial retinopathy (Beare *et al.*, 2009).

For example, several types of retinal leakage are seen (Chapter 5). These types of leak could occur for different reasons, including damage to the blood retina barrier secondary to sequestration, inflammation and local coagulopathy (Moxon *et al.*, 2013; Turner *et al.*, 2013), as well as increased hydrostatic pressure. Pressure within vessels will increase if there is an imbalance between inflow and outflow. Global cerebral blood flow is increased in response to seizure activity, and microvascular outflow is likely to decrease in relation to the density of venous sequestration, congestion (Barrera *et al.*, 2015; Ponsford *et al.*, 2012), and blood viscosity (Kee and Wood, 1984; Pries and Secomb, 2003; Suwanarusk *et al.*, 2004). Vessel rupture and retinal haemorrhage may be the consequence of increased venous pressure, as in other conditions with raised blood viscosity (Ring et al., 1976; Ling and James, 1998). In addition, the co-existence of retinal whitening in regions of capillary non-perfusion suggests that in these areas neural

tissue has become swollen and opaque as a result of local ischaemia (Beare *et al.*, 2009), i.e. cytotoxic oedema.

Retinal observations may therefore help to explain which mechanisms are responsible for increased brain volume in paediatric CM, and perhaps also other acute manifestations visible on MRI brain features, such as abnormalities of cerebral grey or white matter, or the basal ganglia (Potchen *et al.*, 2012). If strong associations exist between retinal and MRI brain it may even be possible to substitute retinal measurements for MRI in future studies of adjuvant treatments for CM (Chapter 2 and 3).

The aim of this chapter is to report associations between retinal features and MRI brain features measured at admission in children with retinopathy positive CM. The retinal features include components of the indirect ophthalmoscopic exam and fluorescein angiography (FA). The MRI brain feature of interest is brain swelling indicated by a measurement of pre-pontine CSF space. This measurement was chosen because it was independently associated with death in paediatric CM, and has the advantage of being continuous rather than binary or ordinal (Seydel *et al.*, 2015).

In the analyses I presented in previous chapters I found three retinal vascular features to be significantly associated with death: orange vessels, punctate focal leak, and large focal leak. The objective of this chapter is to test the hypothesis that one or more of these features are significantly associated with brain volume. If so I will go on to test whether we can consider any of these features as effectively equivalent to severely increased brain volume, with respect to the information they contain about risk of death. See Chapter 3 for conceptual background about evaluating a retinal feature for equivalence with an analogous brain feature.

This requires the application of a statistic – the proportion of information gain (PIG) – which was not originally designed for use on observational data. Because of this, I test this statistic using three control scenarios to determine whether it is able to function properly in this setting. The first is a “positive control” where

PIG ought to be very high, the second is a “negative control” where PIG ought to be low, and the third evaluates a traditional marker of brain swelling using this novel metric to give a sense of scale to further tests of malarial retinopathy features.

Following assessment of these control scenarios I will test two hypotheses: firstly, that punctate focal leak provides equivalent information to MRI brain swelling about death; and secondly, that large focal leak provides equivalent information to MRI brain swelling about death.

Statistical assessment of surrogacy sets a very high bar for my data. If the proportion of information gain does not produce useful information, I will test associations between brain swelling and a range of retinal features using linear regression.

8.4 Methods

8.4.1 Study design

Prospective longitudinal study

8.4.2 Setting

See Chapter 4 for details. Briefly, subjects were recruited from the Paediatric Research Ward in Queen Elizabeth Central Hospital, Blantyre. This ward receives children with severe malaria from other units within the hospital, which serves Blantyre and surrounding areas of Southern Malawi. Recruitment took place within a long running study of severe malaria (Taylor, 2009). The subjects who provided data for this particular analysis were admitted between 2009 (when an MRI scanner was installed at the hospital) and 2014. Investigations were performed within 48 hours of admission on children with retinopathy positive CM during each malaria season (January to June), with the exception of 2011 when FA was not done. In 2014 retinal exam was performed only on the left eye because of other studies being performed on the same subjects. Subjects received treatment for CM in accordance with national guidelines (intravenous quinine until 2013,

intravenous artesunate in 2014) and with adjunctive measures as needed (Taylor, 2009). Informed consent was given by the parents or guardians of all patients. This research adhered to the tenets of the Declaration of Helsinki, and was approved by the ethics committees of relevant academic institutions.

8.4.3 Participants

Patients were recruited consecutively from the Paediatric Research Ward, and were eligible for this study if

- They had CM according to the WHO criteria (Blantyre Coma Score <3, and peripheral *P. falciparum* parasitaemia, and no other identifiable cause of coma). Hypoglycaemia, meningitis, and post-ictal state were specifically ruled out as alternative causes of coma.
- They had one or more signs of malarial retinopathy. These are retinal whitening, retinal haemorrhage, and orange or white discolouration of retinal vessels. Papilloedema in isolation (which may include one or more peri-disc haemorrhages) was not sufficient to diagnose malarial retinopathy.
- Their guardian gave consent

Subjects were excluded from the analysis if

- They did not have MRI brain within 48 hours of admission (i.e. on the day, or day after admission)

Subjects who did not have a fluorescein angiogram (FA) within 48 hours of admission were excluded from the analysis of associations between angiographic features and MRI signs, but not from the analysis of retinal exam features and MRI signs. A similar rule applied to subjects who had admission angiogram but not admission retinal exam.

The reasons for not performing retinal or MRI brain were not recorded for each case, but in general subjects did not undergo retinal or MRI imaging if they were thought to be too unwell to be moved, or if their level of consciousness was increasing such that they were likely to be uncooperative. Other reasons for non-

investigation included absence of the ophthalmologist due to other clinical commitments, and servicing of the MRI scanner. Consequently the sample of subjects who did have complete admission investigations is likely to exclude cases from both ends of the spectrum of severity.

8.4.4 Variables

Predictor variables:

Test case one – Papilloedema in the left eye (binary)

Test case two – Retinal haemorrhage in the left eye (none, 1-5, 6-20, 21-50, >50)

Test case three – Papilloedema in the left eye (none, mild, moderate, severe)

Hypothesis one – Severity of punctate focal leak (none, 1 to 5 sites, >5 sites)

Hypothesis one – Severity of large focal leak (none, 1 site, >1 site)

Outcome variables:

Test case one – Papilloedema in the right eye (binary)

Test case two – Foveal whitening in the right eye (none, <1/3 foveal area, 1/3-2/3, >2/3 foveal area)

Test case thee, hypotheses 1 & 2 – Pre-pontine CSF space (continuous, normally distributed)

Reference variable:

All analyses – Death (binary)

Punctate leak was originally described in five levels (0-4), and large focal leak as a count variable. These were collapsed into three levels each, for consistency with previous chapters.

8.4.5 Data sources

Severe brain swelling was determined on the basis of MRI brain images taken on a 0.35T Signa Ovation Excite MRI scanner (General Electric). Two radiologists interpreted each MRI study. Interpretation included a measurement of brain swelling in terms of the CSF space around the brain stem, on a line drawn from the tip of the nose to the apex of the fourth ventricle on a midline sagittal T1

FLAIR image. The pre-pontine space is measured between the clivus and the anterior wall of the brainstem (Figure 56). Various other features were scored as present, absent, or on a range of severity. Each radiologist was masked to the grading of the other radiologist, and to clinical outcome and retinopathy status. Differences were resolved by consensus according to pre-specified criteria (Potchen *et al.*, 2013). The appearance of the cerebral hemispheres in terms of brain volume was scored from 1 to 8. Scores 7 and 8 indicate life threatening increases in brain volume (Seydel *et al.*, 2015). Scores based on the MRI scans were entered directly into a database (NeuroInterp, Michigan State University, USA).

Retinal leakage (punctate focal leak and large focal leak) was detected with FA using a table mounted camera (Nikon D1-H; Topcon TRC-50EX, Topcon, Japan; Imagenet 2000, Topcon, Japan). 1 to 5ml 10-20% sodium fluorescein was injected into a peripheral vein, after which an ophthalmologist took repeated 50 degree images of the macula and as much peripheral retina as possible until approximately 10 to 15 minutes post-injection. Although comatose, patients with CM often have tonic, nystagmoid, or roving eye movements. Corneal transparency was sometimes reduced by incomplete lid closure. As a result the extent and quality of retinal images varied between patients.

Angiographic images were dual graded according to a standard protocol, and disagreements were resolved by arbitration. See Chapter 5 for details of the grading scheme and implementation. Grading data from angiograms were entered directly to a database (Microsoft Access).

An ophthalmologist performed dilated indirect ophthalmoscopy to detect orange vessels (as well as other signs of malarial retinopathy, and the severity of papilloedema). They recorded their findings on a standard form (Appendix) (Harding *et al.*, 2006; Lewallen *et al.*, 1999). These forms were then entered to a database (single entry with audit of random 10% sample; Research Electronic Data Capture (Harris *et al.*, 2009)).

Clinical data from the history, examination, and standard investigations were collected routinely at admission. These included rectal temperature, full blood count (Coulter Counter, Beckman Coulter), and HIV status using two separate tests (Uni-Gold Recombigen HIV-1/2, Trinity Biotech; and Determine HIV-1/2, Inverness Medical). Finger prick blood samples were analysed to determine parasite species and density, packed-cell volume, blood glucose and blood lactate. Histidine rich protein 2 (HRP2) was measured retrospectively in stored plasma (ELISA). The eventual outcome of disease was recorded, including obvious neurological sequelae in survivors. Death or recovery typically occurs within 48 hours of admission. The ultimate outcome of each subject was entered, along with other clinical details, in the clinical notes and then into a database (Research Electronic Data Capture (Harris *et al.*, 2009)). Datasets were cleaned and merged using Stata (version 13, StataCorp, Texas).

Figure 56: Pre- and post-pontine CSF space.

The pre-pontine and post-pontine spaces are measured on a mid sagittal T1 image, on a line drawn from the tip of the nose to the apex of the 4th ventricle. The pre-pontine space is shown (arrow) between the clivus and the anterior wall of the pons.

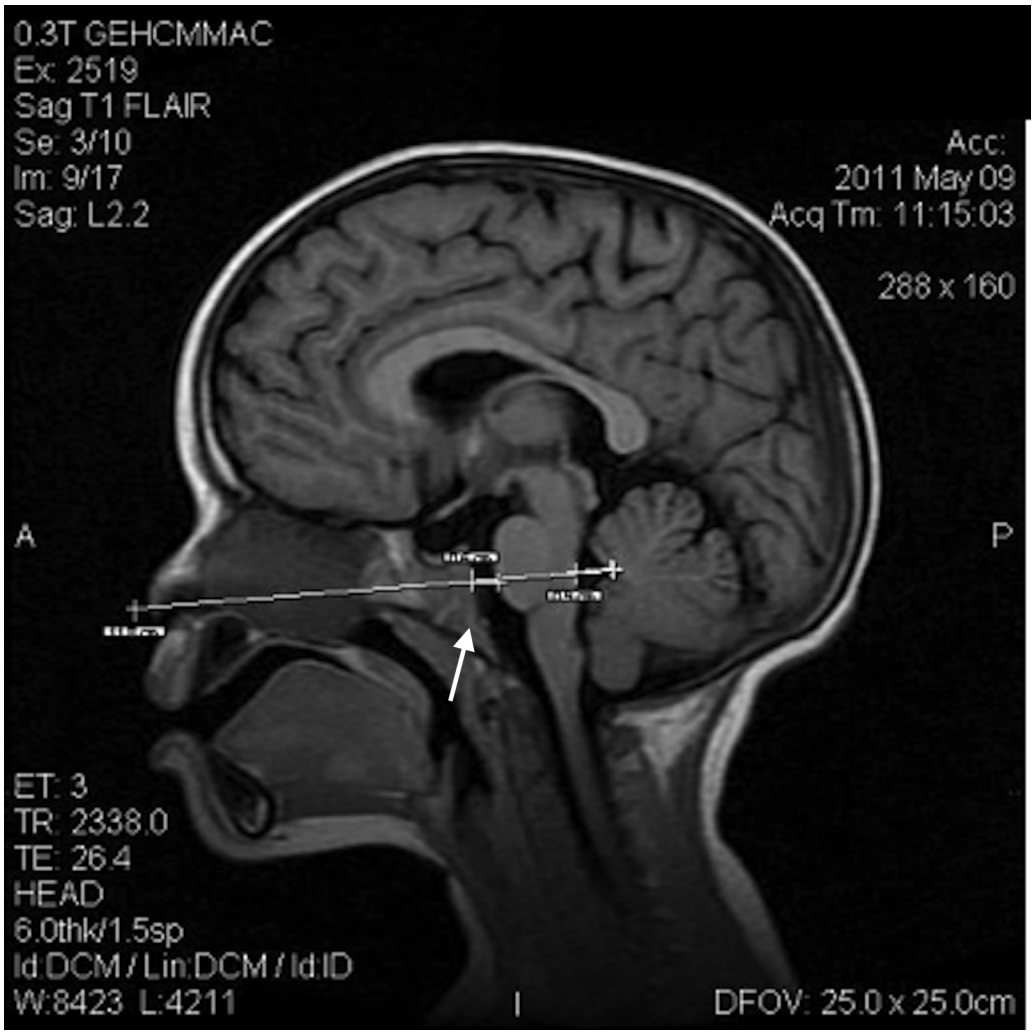

8.4.6 Bias

Potential selection bias was assessed by comparing groups of eligible subjects who did or did not have retinal and MRI imaging.

8.5 Statistical methods

Analysis was planned during and after data collection.

8.5.1 Assessment of selection bias

I compared the clinical characteristics of eligible subjects who were included or excluded using unadjusted odds ratios generated from logistic regression.

8.5.2 Evaluation of unadjusted associations between retinal variables and brain swelling

I used logistic, ordered logistic, and linear regression models to generate unadjusted odds ratios and test whether univariate associations exist between pre-pontine CSF space and retinal leak (punctate or large focal).

8.5.3 Evaluation of the proportion of information gain applied to observational data

The proportion of information gain (PIG) was originally developed to evaluate surrogate endpoints for randomised clinical trials (Qu and Case, 2007) (see chapter 3 for details). Briefly, it is a measure of the degree to which a variable S quantifies the effect of Z on T (Figure 57). This is done by comparing the amount of information in S about T with the amount of information in S and Z about T. Information is measured according to the Kullback-Leibler principle i.e. by comparing the likelihoods of T. If S and T are effectively interchangeable, then adding Z should make very little difference to the fit (as measured by the likelihood) of T by S thus leading to a PIG close to 1. In the context of a randomised clinical trial, this result would be consistent with S being a good surrogate for T. Alternatively if S and T share little information about Z, PIG is close to 0. PIG is a ratio and is bounded by 0 and 1. It is calculated by generating log likelihoods, or the residual sum of squares, for regression models with T alone (LL T), S and T (LL TS), and S, T and Z (LL TSZ). PIG = [(LL TS) – (LL T)] /

[(LL TSZ) / (LL T)]. Note that, because PIG is a ratio of model fit without and with the Z variable, it is probably not appropriate to use this statistic in situations where Z is not associated with S and T. Log likelihoods are only comparable if they are generated from the same type of model, and when evaluated on the same measures from the same patients.

Figure 57: The relationship between retina, brain, and ultimate outcome.
S = Retinal variable; T = MRI brain variable; Z = Ultimate outcome

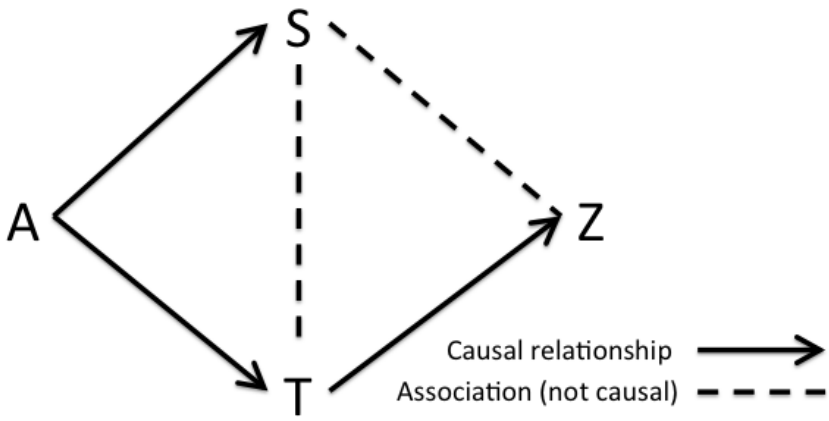

Because it has rarely been used on observational data, and never to evaluate a retinal biomarker of brain disease, I first estimated PIG for three test cases. Firstly, a positive control where the statistic should be close to maximal. In this case a retinal feature (papilloedema) from the left eye is evaluated as a proxy (S) for the same feature in the right eye (T), with reference to risk of death (Z). Papilloedema is known to be associated with death, and since the mechanisms that produce papilloedema tend to affect both eyes symmetrically the severity of papilloedema in the left eye is likely to contain almost identical information about death as the severity of papilloedema in the right eye.

Secondly, a negative control where the statistic should be lower. In this case I evaluated the severity of haemorrhage in the left eye (S) against a different feature in the right eye (T) (foveal whitening), with reference to death. These variables were selected because they are the same type (ordered categorical) and previous analyses suggested (Chapter 6) that both are associated with death. However

because they are different retinal features they are likely to share a smaller proportion of information about death than a comparison of identical features between eyes.

Thirdly, a control involving a traditional marker of brain swelling. This was tested to provide a comparison for evaluations of retinal features as markers of brain swelling. Traditionally, papilloedema is regarded as a specific (though insensitive) sign of raised intracranial pressure secondary to brain swelling, which commonly leads to death. How much information about death is shared by the retinal variable papilloedema, and an assessment of brain swelling based on MRI brain? In this case, severity of papilloedema in the left eye (S) was evaluated as a proxy for pre-pontine CSF space (T), with reference to death (Z).

Note that the structure of my analyses assumes that there are no confounders of associations between S, T, and Z (none of which are measured under conditions of experimental randomisation); and that Z adequately captures information relevant to both S and T.

8.5.4 Evaluating retinal vascular features as proxy markers of MRI brain swelling

I then applied the methods described in the previous paragraphs to evaluate punctate focal leak and large focal leak as markers of brain swelling, with reference to death. These angiographic features were chosen because they are significantly associated with death (Chapter 7), and if death is related to brain swelling (Seydel *et al.*, 2015) this may plausibly occur as a result of neurovascular leakage.

All statistical work was done using Stata 13 (StataCorp, Texas, USA). Regression models were run only on subjects with complete data. Bias corrected confidence intervals were estimated using bootstrap with 200 repetitions.

8.5.5 Secondary analysis – regression model of pre-pontine CSF space

Several retinal variables previously found to be associated with death were tested for univariate associations with pre-pontine CSF space. Associations found to be significant at $p<0.1$ were included in an ordinary least squares regression model.

8.6 Results

8.6.1 Participants with retinal exam and MRI on admission

Between 2009 and 2014, 524 children with CM were recruited to the parent study. Of these, 402/524 were retinopathy positive, 121/524 were retinopathy negative, and 1/524 did not have any retinal exam. Of the 402 subjects with retinopathy positive CM, 332 had a retinal exam within 48 hours of admission and 70 only had an exam after this point. Of the 332 retinopathy positive subjects with an admission retinal exam, 225 also had an MRI brain scan within 48 hours of admission, and 107 did not (Figure 58).

Participants with retinal angiogram and MRI on admission

Between 2009 and 2014 (but excluding 2011 when no angiograms were performed) 444 children with CM were recruited to the parent study. Of these, 338/444 were retinopathy positive, and 106/444 were retinopathy negative. All subjects had a retinal exam during their hospital stay. Of the 338 subjects with retinopathy positive CM, 161 had an FA within 48 hours of admission and 177 did not. Of the 161 retinopathy positive subjects who had an admission angiogram, 134 also had an MRI brain scan within 48 hours of admission, and 27 did not (Figure 59).

Specific reasons for failure to undergo investigations were not recorded, but in general subjects did not have retinal or brain imaging if they were either very unwell or if recovery was imminent, if imaging could not be done because staff had other clinical commitments, or if the equipment was being serviced.

Figure 58: Subjects with both admission ophthalmoscopy and MRI

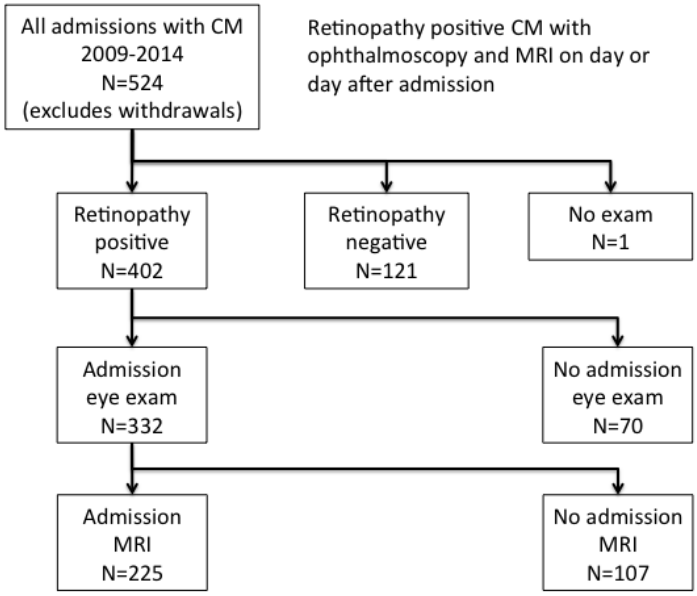

Figure 59: Subjects with with admission fluorescein angiogram and MRI

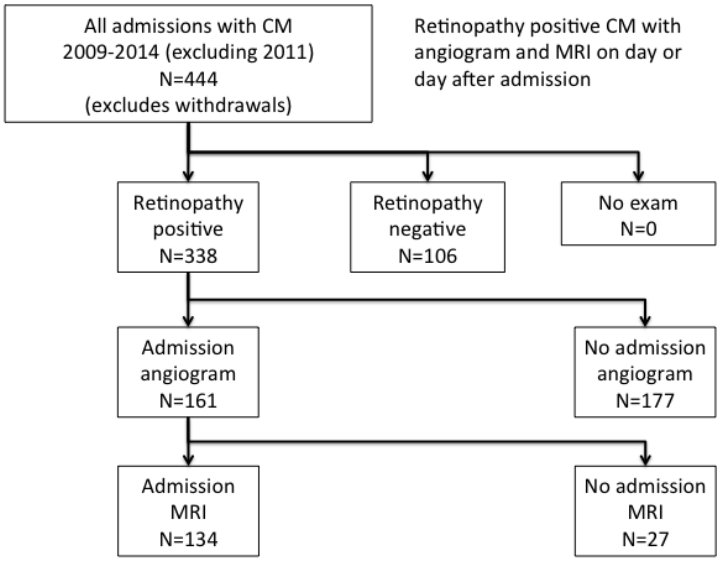

8.6.2 Descriptive and outcome data

8.6.2.1 Characteristics of subjects who had an admission MRI

The characteristics of study participants, along with comparisons to subjects who did not have MRI, are shown in Table 36 and Table 37.

29 of 225 subjects (12.9%) with admission retinal exam and MRI brain data died. 72 of 219 (32.9%) had orange vessels on admission, and 47/224 (21%) had severely increased brain volume. Median (IQR) pre-pontine cistern CSF space was 5.35 (4.5-6.5)mm.

19 of 134 subjects (14.2%) with admission FA and MRI brain data died. 40 of 108 with data had orange vessels (37.0%); 38/134 (28.4%) had 1-5 sites of punctate leak and 11/134 had >5 sites (8.2%). 9/134 had one site of large focal leak (6.7%), 13/134 (9.7%) had >1 site of large focal leak). 21/133 (16%) had severely increased brain volume. Median (IQR) pre-pontine CSF space was 5.5 (4.5-6.5)mm.

8.6.2.2 Differences between subjects who did and did not have an admission MRI

Subjects with admission retinal exam who also had an admission MRI were different from subjects who were eligible for the study but were excluded because they did not have an admission MRI (Table 36). In general subjects who had an MRI took longer to wake from coma (median 28hrs vs 12 hrs), longer to die (24hrs vs 7hrs), and had a higher incidence of neurological sequelae (OR, 95%CI: 3.8, 1.1-12.9) than subjects who did not have an MRI ($p<0.001$ for all). The former group also had a higher prevalence of HIV (3.2, 1.3-7.9), and more severe retinal whitening and orange vessel discolouration.

Similarly, subjects with admission retinal angiogram who also had an admission MRI were different from those who did not (Table 37). Subjects with admission MRI generally took longer to wake from coma (median 28hrs vs 16hrs, $p=0.006$) than subjects who did not have an MRI.

These results suggest that the sample of children who underwent MRI may not be representative of the general population of children with CM who are admitted to the paediatric research ward. This point is relevant to several of the main results since the exclusion of subjects from both the very severe and much less severe ends of the disease spectrum may have led to abnormally low variation in important factors.

Table 36: Subjects who had ophthalmoscopy – with and without admission MRI.

Characteristics of subjects with admission retinal exam and MRI, compared to subjects who were otherwise eligible but did not have an admission MRI. Differences that are likely to be clinically significant exist for the following variables: time to reach coma score 3; time between admission and death; witnessed convulsions on the ward; HIV results; foveal whitening; orange vessels (all p≤0.01). All variables are greater or more frequent in subjects who did have admission MRI. Bold p-values are ≤0.01; p-values with * indicate values from Kruskal-Wallis test. All other p-values are from logistic regression. n/a = not applicable

		Ret+CM subjects with eye exam and MRI <48hrs admission				Ret+CM subjects with admission eye exam but without MRI <48hrs admission				Associations			
Variable	Detail	Median	IQR	number	%	Median	IQR	number	%	OR	p	95% CI low	95% CI high
Demographics													
Age	months	46	31-69	225		42	27-57	107		1.01	**0.005**	1.00	1.02
Weight	Kg	13	10.95-16	225		12.8	10.2-15	107		1.05	0.084	0.99	1.10
Height	cm	95	86-109	223		95	82-104	103		1.02	0.036	1.00	1.03
Sex	boy			110	48.89			56	52.34				
	girl			115	51.11			51	47.66	1.15	0.557	0.72	1.82
Clinical													
Duration of fever pre-admission	hours	72	48-72	218		48	35-72	105		1.00	0.656	1.00	1.01
Duration of coma pre-admission	hours	10	5-24	186		7	4-12	94		1.02	**<0.001***	1.00	1.03
Temperature	C	39	38.1-	225		38.7	37.7-39.5	107		1.19	0.062	0.99	1.42

		Ret+CM subjects with eye exam and MRI <48hrs admission				Ret+CM subjects with admission eye exam but without MRI <48hrs admission				Associations			
Variable	Detail	Median	IQR	number	%	Median	IQR	number	%	OR	p	95% CI low	95% CI high
			39.75										
Pulse	Beat/min	149	132-167	225		150	136-168	107		1.00	0.589	0.99	1.01
Systolic pressure	mmHg	96	89-106.25	206		94.5	88.75-101.25	102		1.01	0.191	0.99	1.03
Respiratory rate	breath/min	42	36-52	225		44	38-54	107		0.99	0.267	0.97	1.01
CSF opening pressure	mmCSF	160	110-220	103		130	105-195	57		1.00	0.189	1.00	1.01
Jaundice	no			206	91.56			97	91.51				
	yes			19	8.44			9	8.49	0.99	0.989	0.43	2.28
Respiratory distress	no			165	73.33			71	66.36				
	yes			60	26.67			36	33.64	0.72	0.191	0.44	1.18
Diagnosis	CM			113	50.22			55	51.40				
	CM+SMA			112	49.78			52	48.60	1.02	0.841	0.81	1.29
Admission coma score	0			16	7.11			10	9.35				
	1			112	49.78			39	36.45	1.79	0.188	0.75	4.28
	2			97	43.11			58	54.21	1.05	0.919	0.44	2.46
Convulsions during admission	no			187	84.23			93	87.74				

		Ret+CM subjects with eye exam and MRI <48hrs admission				Ret+CM subjects with admission eye exam but without MRI <48hrs admission				Associations			
Variable	Detail	Median	IQR	number	%	Median	IQR	number	%	OR	p	95% CI low	95% CI high
	yes			35	15.77			13	12.26	1.34	0.403	0.68	2.65
Convulsions after admission	no			114	50.67			73	68.22				
	yes			111	49.33			34	31.78	2.09	**0.003**	1.29	3.39
Laboratory													
Parasitaemia	cells	48320	2008-250000	219		102000	27010-347000	104		1.00	0.109	1.00	1.00
White cell count	cells	9100	6600-13650	213		8600	6400-12400	103		1.00	0.865	1.00	1.00
Platelets	platelets	55500	30000-91250	212		49000	23000-83000	103		1.00	0.190	1.00	1.00
Haematocrit	%	20.9	17.7-25.225	222		21	16.325-25	104		1.02	0.275	0.98	1.06
Blood lactate	mmol/L	4.9	3-8.85	225		5.7	3.3-9.9	101		0.97	0.317	0.92	1.03
HRP2	ng/ml	8279	3604-13882.25	224		5886.5	1859.5-10707	106		1.00	0.109	1.00	1.00
Time from admission to reach coma score ≥3/5	hours	28	18-52	193		12	7.5-18	90		1.04	**<0.001**	1.02	1.06
Time from admission to death	hours	24	18.5-33.5	29		7	3-15	15		1.00	**<0.001***	0.99	1.02

		Ret+CM subjects with eye exam and MRI <48hrs admission				Ret+CM subjects with admission eye exam but without MRI <48hrs admission				Associations			
Variable	Detail	Median	IQR	number	%	Median	IQR	number	%	OR	p	95% CI low	95% CI high
Pre-pontine CSF space	mm	5.35	4.5-6.5	225		N/A	N/A	N/A		N/A			
Severe brain swelling on MRI	no			177	79.02			n/a	n/a				
	yes			47	20.98			n/a	n/a	N/A			
HIV	negative			175	82.94			94	94.00				
	positive			36	17.06			6	6.00	3.22	**0.011**	1.31	7.93
Retinal													
Retinal haemorrhages	None			65	28.89			30	28.04				
	1 to 5			86	38.22			45	42.06	0.88	0.662	0.50	1.55
	6 to 20			42	18.67			18	16.82	1.08	0.836	0.53	2.17
	21 to 50			18	8.00			8	7.48	1.04	0.937	0.41	2.65
	>50			14	6.22			6	5.61	1.08	0.89	0.38	3.08
Papilloedema	no			164	72.89			83	77.57				
	yes			61	27.11			24	22.43	1.29	0.362	0.75	2.21
Disc hyperaemia	no			147	66.52			80	76.19				
	yes			74	33.48			25	23.81	1.61	0.077	0.95	2.73
Macular whitening	None			21	9.42			17	16.19				
	<1/3 DA			104	46.64			58	55.24	1.45	0.307	0.71	2.97

		Ret+CM subjects with eye exam and MRI <48hrs admission				Ret+CM subjects with admission eye exam but without MRI <48hrs admission				Associations			
Variable	Detail	Median	IQR	number	%	Median	IQR	number	%	OR	p	95% CI low	95% CI high
	1/3 to 1 DA			57	25.56			18	17.14	2.56	0.026	1.12	5.88
	>1 DA			41	18.39			12	11.43	2.77	0.028	1.12	6.85
Foveal whitening	None			36	16.14			33	31.73				
	<1/3 fovea			111	49.78			46	44.23	2.21	**0.008**	1.23	3.97
	1/3 to 2/3 fovea			30	13.45			18	17.31	1.53	0.269	0.72	3.24
	>2/3 fovea			46	20.63			7	6.73	6.02	**<0.001**	2.39	15.19
Orange vessels, temporal quadrant	no			147	67.12			89	88.12				
	yes			72	32.88			12	11.88	3.63	**<0.001**	1.87	7.07
White vessels, temporal quadrant	no			178	81.28			73	72.28				
	yes			41	18.72			28	27.72	0.60	0.07	0.35	1.04
White capillaries, temporal quadrant	no			173	79.00			67	66.34				
	yes			46	21.00			34	33.66	0.52	0.016	0.31	0.89
Outcomes													
Clinical outcome	full			174	77.33			89	83.18				

		Ret+CM subjects with eye exam and MRI <48hrs admission				Ret+CM subjects with admission eye exam but without MRI <48hrs admission				Associations			
Variable	Detail	Median	IQR	number	%	Median	IQR	number	%	OR	p	95% CI low	95% CI high
	recovery												
	sequelae			22	9.78			3	2.80	3.75	0.036	1.09	12.87
	died			29	12.89			15	14.02	0.99	0.974	0.50	1.94

Table 37: Subjects who had fluorescein angiography – with and without admission MRI

Retinal variables (ophthalmoscopic and angiographic) are from the worst affected eye unless stated otherwise. p-values with an * were generated from Kruskal-Wallis test. All other p-values are from logistic regression. Highlighted p-values are P≤0.01

		Ret+CM subjects with eye exam and MRI <48hrs admission				Ret+CM subjects with admission eye exam but without MRI <48hrs admission				Associations			
Variable	Detail	Median	IQR	Number	%	Median	IQR	Number	%	OR	p	95%CI low	95%CI high
Demographics													
Age	months	43.00	27.00-66.25	134.00		33.00	23.00-54.00	27.00		1.01	0.217	0.99	1.03
Weight	kg	11.95	10.00-15.43	134.00		11.90	8.90-15.00	27.00		1.03	0.510	0.94	1.14
Height	cm	93.00	81.13-106.00	132.00		93.00	80.75-104.25	26.00		1.01	0.492	0.98	1.04
Sex	boy			69	51.49			12	44.44				
	girl			65	48.51			15	55.56	0.75	0.505	0.33	1.73
Clinical													
Duration of fever pre-admission	hours	64.00	48.00-72.00	128.00		48.00	42.00-72.00	26.00		1.00	0.524	0.99	1.02
Duration of coma pre-admission	hours	9.00	5.00-21.50	105.00		9.00	5.00-18.50	21.00		1.01	0.571	0.98	1.04
Temperature	degrees C	38.95	38.10-39.70	134.00		38.80	38.10-39.40	27.00		1.06	0.738	0.74	1.52
Pulse	beat/sec	149.00	132.75-169.00	134.00		152.00	130.00-171.00	27.00		1.00	0.972	0.98	1.02
Systolic pressure	mmHg	96.00	89.00-104.00	120.00		95.00	86.75-101.00	26.00		1.02	0.230	0.99	1.06

Respiratory rate	breath/min	41.00	36.00-52.00	134.00		48.00	38.00-56.00	27.00		0.99	0.444	0.95	1.02
CSF opening pressure	mmCSF	170.00	130.00-232.50	62.00		185.00	122.50-217.50	16.00		1.00	0.923	0.99	1.01
Jaundice	no			129	96.27			25	92.59				
	yes			5	3.73			2	7.41	0.48	0.402	0.09	2.64
Respiratory distress	no			97	72.39			18	66.67				
	yes			37	27.61			9	33.33	0.76	0.549	0.31	1.85
Diagnosis	CM			57	42.54			14	51.85				
	CM+SMA			77	57.46			13	48.15	1.21	0.375	0.80	1.83
Admission coma score	0			9	6.72			2	7.41				
	1			69	51.49			9	33.33	1.70	0.535	0.32	9.16
	2			56	41.79			16	59.26	0.78	0.762	0.15	3.97
Convulsions during admission	no			24	17.91			5	19.23				
	yes			110	82.09			21	80.77	1.09	0.873	0.37	3.18
Convulsions after admission	no			112	85.50			25	92.59				
	yes			19	14.50			2	7.41	2.12	0.332	0.46	9.70
Laboratory													
Parasitaemia	cells	39360.00	1270.50-176000.00	129.00		50550.00	19200.75-182000.00	26.00		1.00	0.436	1.00	1.00
White cell count	cells	10200.0	6500.00-	125.00		9500.00	7650.00-	26.00		1.00	0.635	1.00	1.00

		0	14850.00				12950.00						
Platelets	plaetlets	58000.00	30000.0-97000.00	123.00		47500.00	25750.00-86750.00	26.00		1.00	0.679	1.00	1.00
Haematocrit	%	20.00	17.00-25.10	131.00		18.70	15.60-23.20	27.00		1.05	0.179	0.98	1.12
Blood lactate	mmol/L	4.60	2.80-8.95	134.00		4.60	3.00-11.30	23.00		0.96	0.452	0.87	1.06
HRP2	ng/ml	8415.00	4133.00-13690.75	134.00		9470.00	2790.00-11070.00	27.00		1.00	0.919	1.00	1.00
HIV	negative			72	53.73			16	59.26				
	positive			62	46.27			11	40.74	1.25	0.599	0.54	2.90
Retinal													
Retinal haemorrhages	None			107	84.25			23	88.46				
	1 to 5			20	15.75			3	11.54	1.43	0.586	0.39	5.23
	6 to 20			36	27.07			8	29.63				
	21 to 50			49	36.84			8	29.63	1.36	0.572	0.47	3.97
	>50			24	18.05			5	18.52	1.07	0.918	0.31	3.65
Papilloedema	no			9	6.77			2	7.41	1.00	1.000	0.18	5.55
	yes			15	11.28			4	14.81	0.83	0.790	0.22	3.19
Disc hyperaemia	no			97	72.93			17	62.96				
	yes			36	27.07			10	37.04	0.63	0.299	0.26	1.51
Macular whitening	None			91	70.00			22	84.62				
	<1/3 DA			39	30.00			4	15.38	2.36	0.137	0.76	7.29

	1/3 to 1 DA			13	9.85			1	3.70				
	>1 DA			40	30.30			12	44.44	0.26	0.211	0.03	2.17
Foveal whitening	None			43	32.58			5	18.52	0.66	0.717	0.07	6.18
	<1/3 fovea			36	27.27			9	33.33	0.31	0.285	0.04	2.67
	1/3 to 2/3 fovea			21	15.91			4	15.38				
	>2/3 fovea			51	38.64			12	46.15	0.81	0.738	0.23	2.80
Orange vessels, temporal quadrant	no			22	16.67			5	19.23	0.84	0.811	0.20	3.55
	yes			38	28.79			5	19.23	1.45	0.609	0.35	5.98
White vessels, temporal quadrant	no			68	62.96			15	75.00				
	yes			40	37.04			5	25.00	1.76	0.305	0.60	5.22
White capillaries, temporal quadrant	no			93	86.11			15	75.00				
	yes			15	13.89			5	25.00	0.48	0.216	0.15	1.53
Macular CNP	Grade 1			9	6.87			3	11.54				
	Grade 2			62	47.33			13	50.00	1.59	0.527	0.38	6.69
	Grade 3			60	45.80			10	38.46	2.00	0.355	0.46	8.68
Peripheral CNP	Grade 0			53	39.85			7	25.93	0.62	0.413	0.20	1.94
	Grade 2			33	24.81			7	25.93	0.48	0.147	0.18	1.30
	Grade 3			47	35.34			13	48.15				

Punctate focal leak	None			85	63.43			18	66.67				
	Grade 1			38	28.36			9	33.33	0.89	0.805	0.37	2.17
	Grade 2			11	8.21			0	0.00	1.00	-	-	-
Large focal leak	None			112	83.58			21	77.78				
	Grade 1			9	6.72			0	0.00	1.00	-	-	-
	Grade 2			13	9.70			6	22.22	0.41	0.100	0.14	1.19
Large venule leak	None			75	56.39			12	46.15				
	Grade 1			43	32.33			7	26.92	0.98	0.973	0.36	2.68
	Grade 2			15	11.28			7	26.92	0.34	0.053	0.12	1.01
Post-capillary venule leak	None			100	75.19			14	53.85				
	Grade 2			23	17.29			7	26.92	0.46	0.133	0.17	1.27
	Grade 3			10	7.52			5	19.23	0.28	0.039	0.08	0.94
Disc leak	Absent			25	18.66			0	0.00				
	Present			109	81.34			27	100.00	0.00	-	-	-
IVFD, large arterioles	Absent			112	86.15			17	77.27				
	Present			18	13.85			5	22.73	0.55	0.288	0.18	1.67
Outcomes													
Clinical outcome	full recovery			99	73.88			21	77.78				
	sequelae			16	11.94			1	3.70	3.39	0.248	0.43	27.02

	died			19	14.18			5	18.52	0.81	0.699	0.27	2.40
Time to reach coma score ≥3/5	hours	28.00	18.00-52.00	109.00		16.00	10.00-28.00	23.00		1.01	**0.006 ***	0.99	1.02
Time from admission to death	hours	24.00	17.00-34.00	19.00		14.00	4.00-121.50	5.00		0.99	0.279	0.97	1.01

8.7 Main results

8.7.1 Evaluation of statistical approach

8.7.1.1 Test case one – Positive control

Papilloedema in the left eye was tested as a proxy (S) for papilloedema in the right eye (T), with reference to death (Z), using all subjects with admission retinal exam, regardless of whether or not they had and MRI (n=331 for left eye data, n=269 for right eye data). Significant univariate associations were present between all variables except between death and papilloedema in the left eye, which was borderline (p=0.09) (Table 38). The strength of association between death and papilloedema in either eye was lower than expected. However PIG was not significantly different from 1 with narrow confidence intervals (PIG, 95%CI) (1.00, 0.96-1.00).

Table 38: Test case one

Unadjusted associations and proportion of information gain (PIG) for test case one – a positive control where PIG should be close to 1. The presence or absence of papilloedema in the left eye is treated as a marker (S) of the same feature in the right eye (T), with reference to death (Z).

	Model	Relationship		OR	p	95% low	95% high	n
Unadjusted association	logit	ST		107.66	0.001	41.86	276.9	268
	logit	SZ		1.84	0.086	0.92	3.70	331
	logit	TZ		2.19	0.032	1.07	4.49	269
	Model	LL T	LL TS	LL TSZ	PIG	95% low	95% high	n
PIG	logit x3	-149.88	-69.52	-69.14	1.00	0.96	1.00	268

Bias corrected confidence intervals for PIG were estimated from 200 bootstrap samples
S = papilloedema LE (binary)
T = papilloedema RE (binary)
Z = death (binary)
logit = logistic regression
This is used to compare models in the calculation of the proportion of information gain

8.7.1.2 Test case two – Negative control

Retinal haemorrhage in the left eye was tested as a proxy (S) for foveal whitening in the right eye (T) with reference to death (Z), again in subjects with admission retinal exam regardless of MRI (n=331 for left eye, 265 for right eye). In this case significant univariate associations were found between each variable and every other variable, at one level of severity (Table 39). PIG was lower than for test case 1, with very wide confidence intervals (0.82, 0.41-0.99), suggesting that retinal haemorrhage and foveal whitening do share a proportion of information about death, but the precise extent may be less than 0.5.

8.7.1.3 Test case three – Conventional marker of brain swelling

The severity of papilloedema in the worst affected eye was tested as a proxy (S) for pre-pontine CSF space on admission MRI (T), with reference to death (Z). In this case the analysis was performed on a restricted group of subjects who had both admission retinal exam and MRI brain (n=225). As expected, significant univariate associations were found between papilloedema and brain swelling, and between brain swelling and death. However the association between papilloedema and death was only present for the most severe grade of papilloedema (OR, 95%CI; 4.6, 1.02-20.9), and this grade was seen in only 8/225 subjects (3.6%).

PIG was low with wide confidence intervals (0.5, 0.2-0.8) (Table 40). This is consistent with the low sensitivity for the presence of papilloedema to 'detect' a reference standard of severe brain swelling on MRI in the same group (statistic, 95%CI: sensitivity 0.33, 0.19-0.48; specificity 0.79, 0.73-0.85; n=223). However if my sample is missing a proportion of subjects with both severe papilloedema and brain swelling these results may underestimate the performance of papilloedema against CSF space.

Table 39: Test case two

Unadjusted associations and proportion of information gain (PIG) for test case two – a negative control where PIG should be low. the severity of retinal haemorrhage in the left eye (S) is treated as a marker of the severity of foveal whitening in the right eye (T), with reference to death (Z).

	Model	Relationship	Level	OR	p	95% low	95% high	number
Unadjusted association	ologit	ST	foveal area					263
			<1/3	1.65	0.057	0.99	2.75	
			1/3-2/3	1.58	0.250	0.72	3.44	
			>2/3	2.71	0.019	1.18	6.21	
	logit	SZ	haemorrhage number					330
			1 to 5	0.69	0.348	0.31	1.51	
			6 to 20	0.32	0.080	0.09	1.14	
			21 to 50	1.38	0.597	0.42	4.62	
			>50	4.28	0.006	1.50	12.17	
	logit	TZ	foveal area					265
			<1/3	1.55	0.329	0.64	3.72	
			1/3-2/3	0.73	0.702	0.15	3.67	
			>2/3	4.06	0.013	1.34	12.27	
	Models	LL T	LL TS	LL TSZ	PIG	95% low	95% high	number
Proportion of information gain	ologit x3	-310.33	-303.52	-302.01	0.82	0.41	0.99	263

Bias corrected confidence intervals for PIG were estimated from 200 bootstrap samples
S = severity of haemorrhage LE (0-4)
T = severity of foveal whitening RE (0-3)
Z = death (binary)
logit = logistic regression
ologit = ordered logistic regression
LL = log likelihood. This is used to compare models in the calculation of the proportion of information gain

Table 40: Test case three

Unadjusted associations and proportion of information gain (PIG) for test case three – a conventional marker of brain swelling. The severity of papilloedema in the worst affected eye (S) is treated as a marker of pre-pontine CSF space (T), with reference to death (Z).

	Model	Relationship	Level	coefficient	p	95% low	95% high	number
Unadjusted associations	regress	ST	papilloedema					225
			mild	-0.44	0.129	-1.00	0.13	
			moderate	-1.29	0.009	-2.25	-0.33	
			severe	-1.41	0.018	-2.57	-0.24	
	logit	SZ		OR				
			papilloedema					225
			mild	1.10	0.862	0.38	3.14	
			moderate	1.54	0.597	0.31	7.55	
			severe	4.61	0.047	1.02	20.85	
	logit	TZ		OR				
			death					
				0.59	<0.001	0.45	0.77	225
	Models	RSS T	RSS TS	RSS TSZ	PIG	95% low	95% high	number
Proportion of information gain	regress x3	620.69	585.97	548.74	0.48	0.20	0.85	225

Bias corrected confidence intervals for PIG were estimated from 200 bootstrap samples
S = severity of papilloedema (worst affected eye) (0-3)
T = pre-pontine CSF space in mm (continuous normal)
Z = death (binary)
logit = logistic regression
ologit = ordered logistic regression
regress = linear regression
RSS = residual sum of squares, and is used to compare models to estimate the proportion of information gain in the same way as log likelihood.

8.7.2 Primary hypotheses

8.7.2.1 Punctate focal leak as a proxy for reduced pre-pontine CSF space

Significant univariate associations were found between each variable and every other variable (Table 41 - see rows for tests of ST, TZ, and SZ), although associations with punctate leak (S) were only significant for >5 sites of leak – a small group of subjects (11/134. 8.2%). Consistent with this, confidence intervals for PIG were very wide (0.39, 0.02-0.86), making the statistic uninterpretable.

8.7.2.2 Large focal leak as a proxy for reduced pre-pontine CSF space

Similar results were found for large focal leak (Table 42). Significant associations with large focal leak existed only for subjects with >1 site of leak, which again is a small subgroup of the sample (13/134, 9.7%), and confidence intervals for PIG were also very wide (0.42, 0.07-0.91).

Orange vessels were not significantly associated with pre-pontine CSF space (OR 0.86, 0.7-1.0, p=0.08), and so further tests were not performed.

Table 41: Punctate leak as a marker for brain swelling (pre-pontine CSF space)

Unadjusted associations and proportion of information gain (PIG) for hypothesis one – punctate focal leak in the worst affected eye (S) is treated as a marker of pre-pontine CSF space (T), with reference to death.

Unadjusted associations	Model	Relationship	level	Coefficient	p	95% low	95% high	n
	regress	ST	punctate leak					134
			1 to 5 sites	-0.28	0.40	-0.93	0.38	
			>5 sites	-1.46	0.01	-2.53	-0.39	
	logit	SZ	punctate leak	OR				134
			1 to 5 sites	2.52	0.11	0.82	7.77	
			>5 sites	9.29	0.001	2.25	38.28	
	logit	TZ		OR				134
				0.54	0.001	0.39	0.75	
PIG	Models	RSS T	RSS ST	RSS STZ	PIG	95% low	95% high	n
	regress x3	394.80	373.66	338.97	0.38	0.02	0.86	134

Bias corrected confidence intervals for PIG were estimated from 200 bootstrap samples
S = punctate leak worst eye (0-2)
T = pre-pontine csf space (continuous normal)
Z = death (binary)
regress = linear regression
logit = logistic regression
RSS = residual sum of squares, and is used to compare models to estimate the proportion of information gain in the same way as log likelihood.

Table 42: Large focal leak as a marker for brain swelling
Unadjusted associations and proportion of information gain (PIG) for hypothesis one – large focal leak in the worst affected eye (S) is treated as a marker of pre-pontine CSF space (T), with reference to death.

Unadjusted associations	Model	Relationship	Level	Coefficient	p	95% low	95% high	n
	regress	ST	Large focal leak					134
			1 site	0.73	0.21	-0.42	1.88	
			>1 site	-1.24	0.01	-2.22	-0.27	
	logit	SZ	Large focal leak	OR				125
			1 site	1				
			>1 site	6.53	0.001	1.90	22.43	
	logit	TZ		OR				134
				0.54	0.001	0.39	0.75	
PIG	Models	RSS T	RSS ST	RSS STZ	PIG	95% low	95% high	n
	regress x3	394.80	370.72	337.55	0.42	0.07	0.91	134

Bias corrected confidence intervals for PIG were estimated from 200 bootstrap samples
S = large focal leak worst eye (0-2)
T = pre-pontine csf space (continuous normal)
Z = death (binary)
regress = linear regression
logit = logistic regression
RSS = residual sum of squares, and is used to compare models to estimate the proportion of information gain in the same way as log likelihood.

8.7.3 Secondary analysis

8.7.3.1 Regression model of pre-pontine CSF space

Several features of the retinal angiogram (Chapter 7) and ophthalmoscopic exam (Chapter 6) are significantly associated with death. Several retinal features have univariate associations with pre-pontine CSF space (Table 43) - including temporal whitening, punctate and large focal leak, and large arteriolar IVFD (all $p \leq 0.01$). These were included in a multiple linear regression model. Other retinal variables related to CSF space ($p=0.01$-0.05) were orange vessels and white capillaries.

The multiple linear regression model showed a significant inverse association with large arteriolar IVFD (coefficient, 95%CI: -1.10, -1.92 to -0.27) (Table 44), and a *direct* association between temporal whitening and CSF space (coefficient, 95%CI; grade 2: 1.7, 0.6-2.7; grade 3: 1.3, 0.3-2.3). In other words, retinal arteriolar IVFD was associated with brain swelling, while peripheral whitening was associated with the *absence* of swelling. Other associations were not significant at $p<0.05$, but there was a trend towards a direct association between punctate focal leak (>5 sites) and reduced pre-pontine CSF space.

Table 43: Unadjusted associations – pre-pontine CSF space and retinal variables.

Retinal variable	Level	coefficient	p	95% low	95% high	n
Haemorrhage						
	1 to 5	0.09	0.741	-0.45	0.63	225
	6 to 20	0.16	0.635	-0.49	0.81	
	21 to 50	0.23	0.607	-0.65	1.11	
	>50	-0.52	0.296	-1.49	0.46	
Macular whitening						
	<1/3 DA	0.12	0.755	-0.66	0.91	223
	1/3 to 1	0.63	0.140	-0.21	1.47	
	>1 DA	0.14	0.758	-0.74	1.02	
Foveal whitening						
	<1/3 fovea	0.15	0.645	-0.48	0.78	223
	1/3 to 2/3	0.60	0.151	-0.22	1.41	
	>2/3 fovea	0.33	0.372	-0.40	1.07	
Temporal whitening						
	1	0.28	0.346	-0.31	0.88	221
	2	0.89	**0.015**	0.18	1.60	
	3	0.82	**0.019**	0.14	1.50	
Orange vessels		-0.42	0.081	-0.89	0.05	219
White vessels		-0.15	0.610	-0.72	0.42	219
white capillaries		0.54	0.053	-0.01	1.08	219
Macular CNP						
	Grade 2	0.53	0.374	-0.65	1.71	131
	Grade 3 or 4	0.00	0.997	-1.18	1.18	
Disc leak		-0.13	0.727	-0.89	0.62	134
Punctate leak						
	1 to 5 sites	-0.28	0.403	-0.93	0.38	134
	>5 sites	-1.46	**0.008**	-2.53	-0.39	
Large focal leak						
	1 site	0.73	0.214	-0.42	1.88	134
	>1 site	-1.24	**0.013**	-2.22	-0.27	
large venule leak						
	Grade 1	0.11	0.733	-0.54	0.76	133
	Grade 2 or 3	-0.27	0.575	-1.24	0.69	
Post-capillary venule leak						
	Grade 2	0.42	0.287	-0.36	1.21	133
	Grade 3 or 4	-0.38	0.507	-1.50	0.75	
Large arteriole IVFD		-1.44	**0.001**	-2.25	-0.63	130
All associations were tested using linear regression p<0.05 in bold						

Table 44: Multivariate linear regression against pre-pontine CSF space

Linear regression model of pre-pontine CSF space as the dependent variable, and retinal features as independent variables. Retinal features were included if they were found to have significant unadjusted associations with CSF space (at p<0.01, see Table 43). All measurements are from the worst affected eye.

Independent variable name	Level	Coef.	Std. Err.	t	P>t	95%CI low	95%CI high
Temporal whitening							
	Grade 1	0.90	0.51	1.79	0.077	-0.10	1.91
	Grade 2	1.65	0.54	3.06	**0.003**	0.58	2.71
	Grade 3	1.27	0.51	2.50	0.014	0.26	2.27
Large arteriole IVFD		-1.10	0.42	-2.62	**0.01**	-1.92	-0.27
Punctate focal leak							
	1-5 sites	-0.16	0.32	-0.49	0.625	-0.80	0.48
	>5 sites	-1.19	0.58	-2.03	0.044	-2.35	-0.03
Large focal leak							
	1 site	0.75	0.54	1.39	0.169	-0.32	1.82
	>1 site	-0.69	0.53	-1.30	0.195	-1.73	0.36
Constant		4.71	0.48	9.78	**0.001**	3.75	5.66

p-values ≤0.01 highlighted
IVFD = Intravascular filling defects
Coef. = Coefficient
Std. Err. = Standard error
P>t = p-value
95%CI low and 95%CI high are lower and upper bounds of 95% confidence intervals, respectively

8.8 Discussion

8.8.1 Key results

Punctate focal leak and large focal leak both have significant unadjusted associations with low pre-pontine CSF space. However these associations only exist for particular grades of each leak type: >5 sites of punctate leak, and >1 site of large focal leak; and these grades were seen in relatively few subjects who had admission MRI. A small number of subjects with relevant data is consistent with wide confidence intervals for estimates of PIG. However, severe brain swelling was present in approximately twice as many subjects as had relevant grades of punctate or large focal leak, suggesting that blood-retina barrier breakdown (and by implication, blood-brain barrier breakdown) is not a necessary feature of severe brain swelling. Based on these results retinal leakage seems unlikely to be a good biomarker of brain swelling, or provide much help in explaining the mechanisms behind brain swelling in CM.

This result is puzzling given that punctate leak is associated with death (Chapter 7), and that severe brain swelling appears to be the likely cause of death in most cases (Seydel *et al.*, 2015). Is it possible that punctate and large focal leak point to some mechanism for death that is measured poorly by MRI? For example, vasogenic oedema, manifestations of which are captured by retinal angiography soon after admission, could potentially cause death before MRI scanning is possible. It is also possible, though unlikely, that retinal leakage is pointing to fatal disease mechanisms that are independent of severe brain swelling.

The inconsistency is probably related to the composition of the group of subjects who had both admission angiogram and admission MRI. In subjects with retinopathy positive CM who had an angiogram within 48 hours of admission (n=260), there are significant unadjusted associations between death and all grades of punctate leak (1-5 sites OR, 95%CI: 4.4, 2.0-10.0; >5 sites: 10.3, 3.1-34.4). In contrast, only the top grade of punctate leak is associated with death in subjects who had both admission MRI and angiogram (n=134). A similar pattern is present for associations between papilloedema and death. In subjects with admission angiogram (2006-2014, n=260), the presence of papilloedema (worst

eye) is significantly associated with death (OR, 95%CI: 3.8, 1.8-8.0) (see Chapter 6), whereas this association does not exist in the group who had both admission MRI and retinal exam (1.5, 0.7-3.4, p=0.34, n=225) or the group who had both admission MRI and retinal angiogram (2.2, 0.8-6.1, p=0.12, n=133). The practical constraints on performing MRI on children with CM appear to have led to an inadvertent selection of subjects who are not representative of children with retinopathy positive CM in general, and this could explain weaker than expected associations with retinal features in this sample.

The secondary analysis of retinal features against pre-pontine CSF space suggests that IVFD in large arterioles are significantly associated with brain swelling, and that this relationship is independent of other features (such as punctate leak) which were previously found to have much larger associations with death in Chapter 7. Since IVFD are frequently visible in venules, but less commonly seen in arterioles (Chapter 5), it is possible that arteriolar IVFD represent severe neurovascular sequestration and congestion. Sequestration could produce brain swelling through several related mechanisms, including direct interference with endothelial barrier function (vasogenic oedema), in combination with impaired perfusion and tissue hypoxia (cytotoxic oedema) (Klatzo, 1987). In addition intracranial congestion can cause brain swelling purely through an increase in the size of the vascular compartment. Consequently there are several plausible explanations for an association between arteriolar IVFD and reduced pre-pontine CSF space. However, it is difficult to interpret this result in the light of Chapter 7, which showed that arteriolar IVFD was not associated with death after controlling for other retinal features, such as punctate leak. Again, part of the explanation may lie with the different composition of groups who had admission angiogram (2006-2014), and who had admission angiogram and MRI (2009-2014).

Peripheral retinal whitening was associated with greater pre-pontine CSF space, implying lesser rather than greater brain volume. Retinal whitening in the periphery has been associated with T2 signal in the periventricular white matter, on follow up MRI scans in survivors after discharge (Kampondeni *et al.*, 2013). Other associations with MRI brain features remain to be explored. It may be the case that retinal whitening remains, or even becomes more dense, in spite of

improvement in underlying CNP (personal observation) (Figure 6 in Chapter 1). Paradoxically, 'severe' peripheral whitening could potentially be a sign of recovery – at least in the subgroup of patients who manage to survive the initial stages of illness.

8.9 Limitations

As discussed above, this analysis is likely to be limited by selection bias. Unintentional exclusion of subjects at both the severe and mild ends of the disease spectrum may have produced a sample in which associations with death and brain swelling are smaller than expected, or absent, without producing a significant difference in overall mortality rate.

The utility of PIG depends on the choice of a variable for Z, which forms the reference point for associations between S and T. In a randomised clinical trial, Z would be the treatment variable, and Z-S and Z-T associations would be estimated under conditions of experimental randomisation. Experimental randomisation does not apply to observational studies of disease mechanisms, but nonetheless Z ought to capture as much information as possible about either a disease exposure or disease outcome that is relevant to both S and T. Such variables are difficult to come by. Mortality is completely captured by a variable describing which subjects live or die, and is clinically meaningful. However a binary variable cannot contain as much information as a continuous variable. Other possibilities for Z include HRP2, which may approximate total body parasite body mass (Dondorp *et al.*, 2005), and blood lactate. These are continuous variables. However HRP2 appears to have only weak associations with retinal angiogram variables (see Chapter 7), and lactate is likely to only describe one facet of the CM disease process. The analyses with PIG described above could be repeated using other Z variables, and this may produce different results.

8.10 Conclusion

Several retinal angiographic features are associated with reduced pre-pontine CSF space, including punctate and large focal leak, and IVFD in the large arterioles. These three features were also found to have significant unadjusted – in the case of arteriolar IVFD – or adjusted associations with death in a different (overlapping) sample (Chapter 7). Neither punctate nor large focal leak can be said to be statistically equivalent to reduced CSF space on the basis of the PIG ratio, and these results do not prove that brain swelling in paediatric CM is largely the result of vasogenic oedema. It is important to note that this result does not rule out such a mechanism, particularly since the confidence intervals around PIG are so wide. The results of the multivariate linear regression suggest that vascular sequestration and congestion, represented by IVFD, may have an important role in brain swelling that is independent of vascular leakage. However it is difficult to reconcile this with associations between angiographic features and death found in Chapter 7, and this inconsistency could also be a result of insufficient spread of the MRI (pre-pontine CSF space) and FA (leakage) data secondary to lower sampling rates of subjects at the mild and severe ends of the disease spectrum. These results should be replicated in further studies before being accepted as generally true for retinopathy-positive paediatric CM. Future work on associations between retina and MRI brain markers of disease should aim to include a higher proportion of eligible subjects, and aim for a significantly larger sample.

Chapter 9 – Discussion

9.1 Aim of chapter

Discuss the results from each chapter in the context of the thesis aim and objectives, and existing literature

9.2 Introduction

The aim of this thesis was to develop retinal features as markers of brain damage in paediatric cerebral malaria (CM). The chapter begins with a brief summary of concepts from the literature on malarial retinopathy that influenced the thesis. The thesis objectives are summarised and the chapter concludes with a summary addressing the extent to which the objectives were achieved. I discuss the results from previous chapters in an attempt to place them within the broader context of current medical literature, and suggest areas for further work.

9.3 Background to the thesis objectives

Extensive research had been carried out on paediatric malarial retinopathy prior to 2012—particularly in Malawi. Key findings included associations between features of malarial retinopathy and death (Beare et al., 2004), frequency of retinal and cerebral haemorrhage (White *et al.*, 2001), and perhaps most importantly the ability of ophthalmoscopy to differentiate between autopsy cases with histopathologically confirmed CM and autopsy cases with peripheral parasitaemia but no neurovascular sequestration (Taylor *et al.*, 2004). These findings and others in the same vein (discussed in Chapter 2 and (Birbeck, Beare, *et al.*, 2010; Lewallen *et al.*, 1999; MacCormick *et al.*, 2014)) led to the concept that, in paediatric CM, the retina could be considered a "window to the brain". This was articulated most explicitly in an MD thesis by Beare (Beare, 2005), and two major lines of thinking have gone on to shape the direction of work since then.

The first idea was that, at least in paediatric CM, retinal features tend to mirror corresponding brain features. This influenced the interpretation of results from retinal research (e.g. (Beare et al., 2009; Beare et al., 2004)), and provided the motivation for further investigations into associations between retinal and MRI brain features. The retinal "window" was demonstrated to have important potential as a diagnostic tool (Taylor *et al.*, 2004), and in general appeared able to provide information about neurovascular processes that would otherwise remain hidden. For example, evidence of blood-retina barrier dysfunction and deficits in neurovascular perfusion (Beare *et al.*, 2009), and results suggesting that retinal vessel discolouration resulted from neurovascular sequestration (Lewallen *et al.*, 2000).

The second idea was simply that not all children who appear to have CM actually have sequestration in the brain. Patients with cerebral sequestration could be distinguished from those who did not using ophthalmoscopy (Beare *et al.*, 2006, 2011; Taylor *et al.*, 2004). In a sense this is only one example of how the retina appears to function as a window into the rest of the central nervous system (CNS). However, as well as being consistent with the concept that the retina mirrors the brain, this particular conclusion also led to the concept of "retinopathy positive" and "retinopathy negative" cases of paediatric CM, and to the use of retinopathy negative patients as control subjects in a range of published reports (Conroy et al., 2010, 2012; Lewallen et al., 2008; Milner et al., 2012; Phiri et al., 2011; Postels et al., 2014; Postels, Taylor, et al., 2012; Potchen et al., 2012). In effect, paediatric CM now had a new definition (Beare *et al.*, 2011).

These ideas inevitably shaped the questions being addressed in this current thesis, and also the approach I used to answer them.

I was struck by the terminology used to justify inferences about the brain from the retina in paediatric CM. It often included references to embryological origins (Beare *et al.*, 2009; White *et al.*, 2001), and suggested that an *analogy* could be drawn between the retina and brain on the basis of these similarities (e.g. (Beare, 2005; Beare *et al.*, 2009)), but did not go into detail. Similar terminology is present in literature about other diseases (London *et al.*, 2013), apparently

indicating a fairly widespread notion that the retina might somehow provide a model, or surrogate for the brain, or even that the retina should be considered a visible extension of the brain (Dowling, 2012).

However, I was aware that an argument from analogy is only valid insofar as subject and object are similar in relevant ways[10]. Failure to appreciate the epistemology of analogy could lead to serious misinterpretation, and the controversy that had just then erupted over the utility of animal models in malaria research seemed to illustrate the sort of issues that could eventually arise from this fundamental point (Craig *et al.*, 2012). This prompted me to try thinking about associations between retina and brain in terms of warranted analogy, and what evidence would be needed to justify an appeal to an analogy between retina and brain as a way of allowing inferences to be drawn. It seemed to me that an attempt to develop the concept of retina-brain analogy would be potentially useful either, at best, for allowing greater insights into the brain from the retina, or at least for limiting illegitimate conclusions. Furthermore this approach ought to be relevant to a range of neurological diseases in addition to paediatric CM.

Helpful insights to this question were provided at various points by guidelines for clinical trials (International Conference on Harmonisation, 1998), extensive literature on surrogate end points (which assume an analogy between true and surrogate end points) (Lassere, 2007; Weir and Walley, 2006), and The Stanford Encyclopedia of Philosophy (Bartha, 2013).

The thesis objectives developed from these thoughts. It became clear that biologically plausible relationships between (and within) subject and object were of primary importance. It also seemed that traditional statistical methodology would not be able to exploit information about the structure of biological relationships central to a valid analogy. In addition I faced practical issues about how to quantify the information within retinal images so that they could be analysed. Therefore the aim and objectives of the thesis were:

10 I am grateful to Dr James Anderson for pointing this out so clearly while he was at New College, University of Edinburgh. Incidentally his blog is titled “Analogical thoughts” (Anderson, 2015)

Aim: Develop retinal features as markers of brain disease in paediatric cerebral malaria

O1: Review the biological plausibility of associations between retina and brain
O2: Review methods for evaluating surrogate-like relationships between retina and brain
O3: Design a grading system for fluorescein angiography
O4: Estimate associations between admission retinal features and death
O5: Estimate associations between admission retinal features and MRI features

This aim and objectives were achieved in large part through collecting new retinal data during the malaria seasons from 2012 to 2014 and by designing a robust data collection and analysis plan.

Regarding objective one, it seemed that there probably was reasonable evidence that the retina sustained similar damage to the brain in paediatric CM, particularly from the extensive histopathological work done in Blantyre. However I thought that this evidence had not yet been collected and examined in the systematic way necessary to address questions about whether or not associations between retina and brain were biologically plausible, and if so, what common mechanisms could be invoked to explain these associations. The review in Chapter 2 was my attempt to achieve this objective.

Regarding objective two, the literature describing statistical methodology for evaluating surrogate end points in randomised clinical trials is extensive, but there was little written about how these approaches might be applied to observational studies (Walker *et al.*, 2013). Therefore I attempted to do this in Chapter 3.

Objective three was necessary because up to this point there was no standardised way to grade angiographic features of malarial retinopathy. Without this I could not achieve objectives 4 and 5. My method for grading retinal angiograms is dealt with in Chapter 5.

A valid analogy ought to have relevant associations within domains as well as between them. In the case of an analogy between retina and brain in paediatric CM, intra-domain relationships exist between a given retinal (or brain) feature, and particular causes or effects of that feature. I illustrate this concept with an example taken from Bartha (2013), of an analogy between the Earth and Mars. This analogy will better support the claim that Mars supports life if the cited similarities between the two planets are related to this particular outcome (Bartha, 2013) (Table 45). The most obvious outcome of interest in CM is whether or not a patient dies. Retinal and brain features are primarily of interest because they, and the associations between them, might help explain this event.

Table 45: Vertical and horizontal relationships in analogical reasoning.
An analogy between a source (S) and a target (T) can be described in terms of horizontal and vertical relationships. Horizontal relationships indicate similarities (or dissimilarities) between domains, and vertical relationships describe the relevance of listed features to the outcome relevant to the inferred similarity. These relationships may, or may not, provide warrant for belief in the further inferred similarity. Important questions include whether the first four features of the analogy in S are relevant to the further feature (supports life), and whether these vertical relationships also apply in the target domain. Adapted from (Bartha, 2013).

↑ Vertical relationships ↓	Earth Source domain (S)		Mars Target domain (T)
		Known similarities	
	Orbits the Sun Has a moon Revolves on axis Subject to gravity	← Horizontal relationships →	Orbits the Sun Has moons Revolves on axis Subject to gravity
		Inferred similarity	
	Supports life	→ Therefore →	*May* support life

It was becoming apparent that severe brain swelling was very closely related to death in paediatric CM (Seydel *et al.*, 2015). Certain retinal features had previously been associated with death (Beare et al., 2004), however this analysis had been performed before the diagnostic importance of retinopathy was known,

on a mixed sample of retinopathy positive and negative children. It was possible that estimates of associations between death and ophthalmoscopic features were not accurate, and no attempt had yet been made to estimate associations between angiographic features and mortality. This led to objective four, which is addressed in Chapters 6 and 7. Several associations were found between retinal features and death.

Retinal features were associated with death (Chapter 6 and 7), as was brain swelling on MRI (Seydel *et al.*, 2015). Might one or more retinal features effectively account for this brain swelling in children with carefully defined retinopathy-positive CM? This was the question motivating objective five, and indeed each objective leading up to it. This was dealt with in Chapter 8.

In summary, the thesis aim and each objective fit within the context of major themes arising from previous work on malarial retinopathy in African children – the idea that the retina reflects the brain, and the idea that retinopathy positive status identifies a more homogenous sample that is more suitable for research into disease mechanisms than the traditional WHO definition. The objectives developed from an awareness of the temptation to make analogical inferences without rigorous justification for them, and the expectation that an attempt to provide this justification would be relevant to neurological disease generally as well as CM in particular. The objectives were set out to specifically address the often assumed analogy between retina and brain, by examining the strength and biological plausibility of associations between retina and brain features, and between retinal features and death, and interpreting these within a unified framework.

9.4 Discussion of specific objectives and results

9.4.1 Biological plausibility of associations between retina and brain in paediatric cerebral malaria

Considering the number of reports referring to the retina as a source of biomarkers of brain dysfunction (several are reviewed in London et al., (2013)), detailed comparisons of the anatomy and physiology of retina and brain appear to be

uncommon, and particularly so for reviews aiming to illuminate a specific neurological condition. An example is the review by Patton et al., (2005), which compares retina and brain as the context for a discussion of retinal imaging techniques relevant to cerebrovascular disease. Other comparisons exist, but tend to describe characteristics in general rather than those likely to be important for particular disease manifestations (Cogan and Kuwabara, 1984; Klaassen *et al.*, 2013; Schlosshauer and Steuer, 2002; Steuer *et al.*, 2005). Green et al., (2010) and Archibald et al., (2009) give detailed descriptions of retinal pathology in multiple sclerosis and Parkinson's disease, respectively, but there is little emphasis on explicitly comparing these descriptions with the corresponding situation in the brain.

The biological plausibility of associations between biomarkers and outcomes has been discussed as a (rather weak) auxiliary to statistical evaluation based on randomised controlled trials (Buyse *et al.*, 2010). However biological context is also intimately bound up in the discovery and selection of particular candidate markers. A lack of reviews attempting to systematically compare the source and target domains relevant to biomarkers could help to explain the general lack of success in validating candidates (Buyse *et al.*, 2010). Surveys of retina and brain disease features in multiple sclerosis, Alzheimer's and Parkinson's disease may lead to a stronger biological rationale for certain candidate markers, and in so doing help direct time and money to the most effective empirical studies.

There are practical limitations to this approach. It is time consuming. Its starting point – the choice of which specific features to give most attention – is dictated by the prevailing theoretical model, which will not be entirely correct, and may even be almost entirely wrong (Kuhn, 1984). Published data about the most relevant retina and brain characteristics may be incomplete, only exist for certain groups of people, or for animal models. Even so reviews ought to at least highlight areas of the field that need further work. Ideally the process should be iterative and incorporate major new findings as they are made.

In the case of paediatric CM histopathological data were reasonably abundant, allowing the conclusion that retina and brain share many disease features. The

distribution of features with microvascular network architecture, and the known effects of *P. falciparum* on the erythrocyte, suggested that the combination of haemorheological changes with the basic energy demands of neuronal tissue might help to explain some of these similarities (Chapter 2) (MacCormick *et al.*, 2014).

How might this comparative review be improved in the light of results from this thesis? Chapters 6 and 7 revealed several new associations between retinal features and clinical outcomes. These features can broadly be considered as types of endothelial pathology and types of leakage. Regarding endothelial pathology, orange vessel discolouration is independently associated with death in retinopathy positive cases, and appears to co-localise with IVFD but not total vascular occlusion (Figures 60 and 61). There is limited information about what produces the orange colour (Lewallen *et al.*, 2000), but it seems likely that these lesions could lead to parenchymal damage through congestion and pathological interactions with the endothelium related to inflammation and coagulation (Moxon *et al.*, 2013; Turner *et al.*, 2013). The potential impact of congestion within particular vascular beds is discussed in Chapter 2, but I do not compare the retinal and cerebral vascular endothelium.

This is also likely to be relevant to associations between death and retinal leakage. The strongest association is with punctate focal leak. Large focal leak appears to be less important after controlling for other retinal signs. Both indicate focal breakdown of the blood-retinal barrier. However these specific leakage types are distinct from other types of retinal leakage that are either not associated with death or tend towards an association with recovery. These results point to comparison of the blood-retina and brain barriers as an area worthy of further research.

Figure 60: Co-localisation of orange material and intravascular defects. Fluorescein angiogram and colour image of the same venule segment, showing a close spatial relationships between intravascular filling defects and orange discolouration (arrows). Images are from MP3212

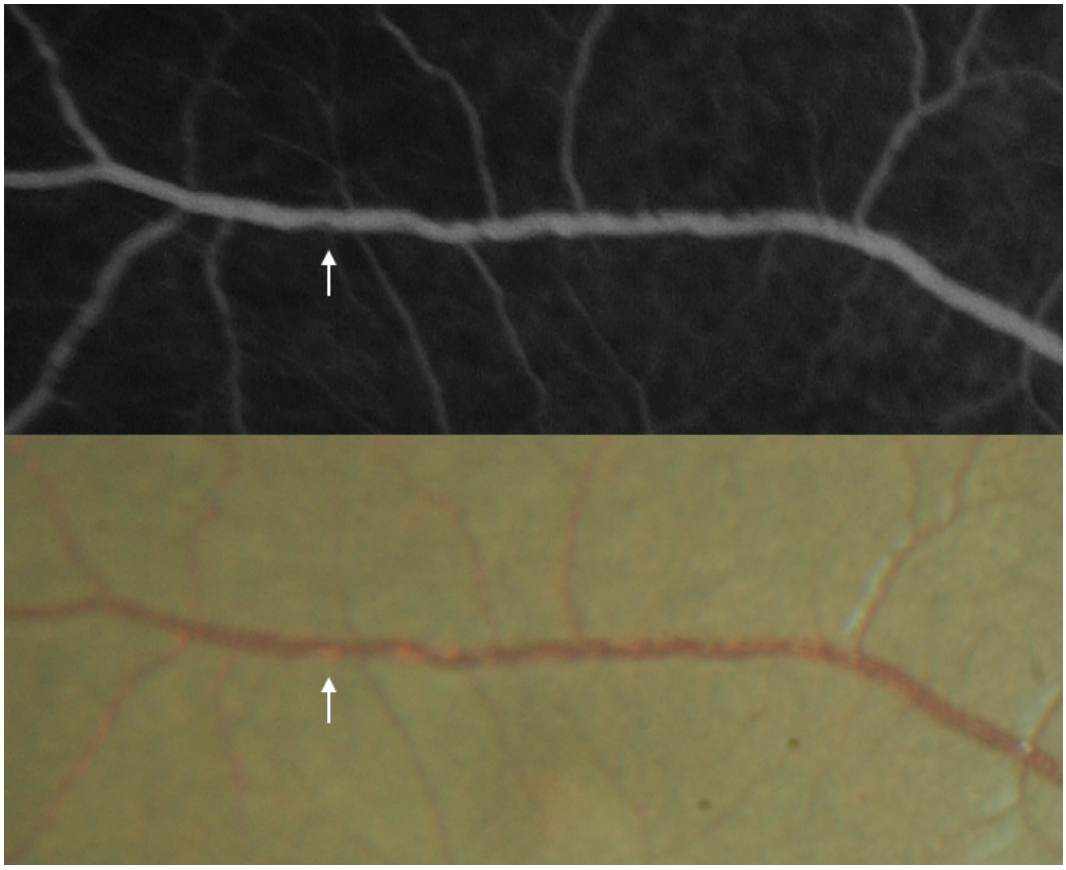

Figure 61: Change in vessel features over time

Matching colour and fluorescein images of the same vessel segment over subsequent days from admission. Images are from MP3189. Column A shows the admission images (02/03/13). A venule with marked orange discolouration and intravascular filling defects is shown (arrows, upper and lower panels respectively). Column B and C show corresponding images from 03/03/13 and 04/03/13. Note that the orange material is not clearly visible in colour images two days after admission. Similarly, intravascular filling defects become much less clear after the first image, although vessel segment leak has developed and this may obscure the view. The vessel appears to widen with time, and the area of capillary non-perfusion drained by the venule initially becomes more extensive before starting to reperfuse with post-capillary venule leak.

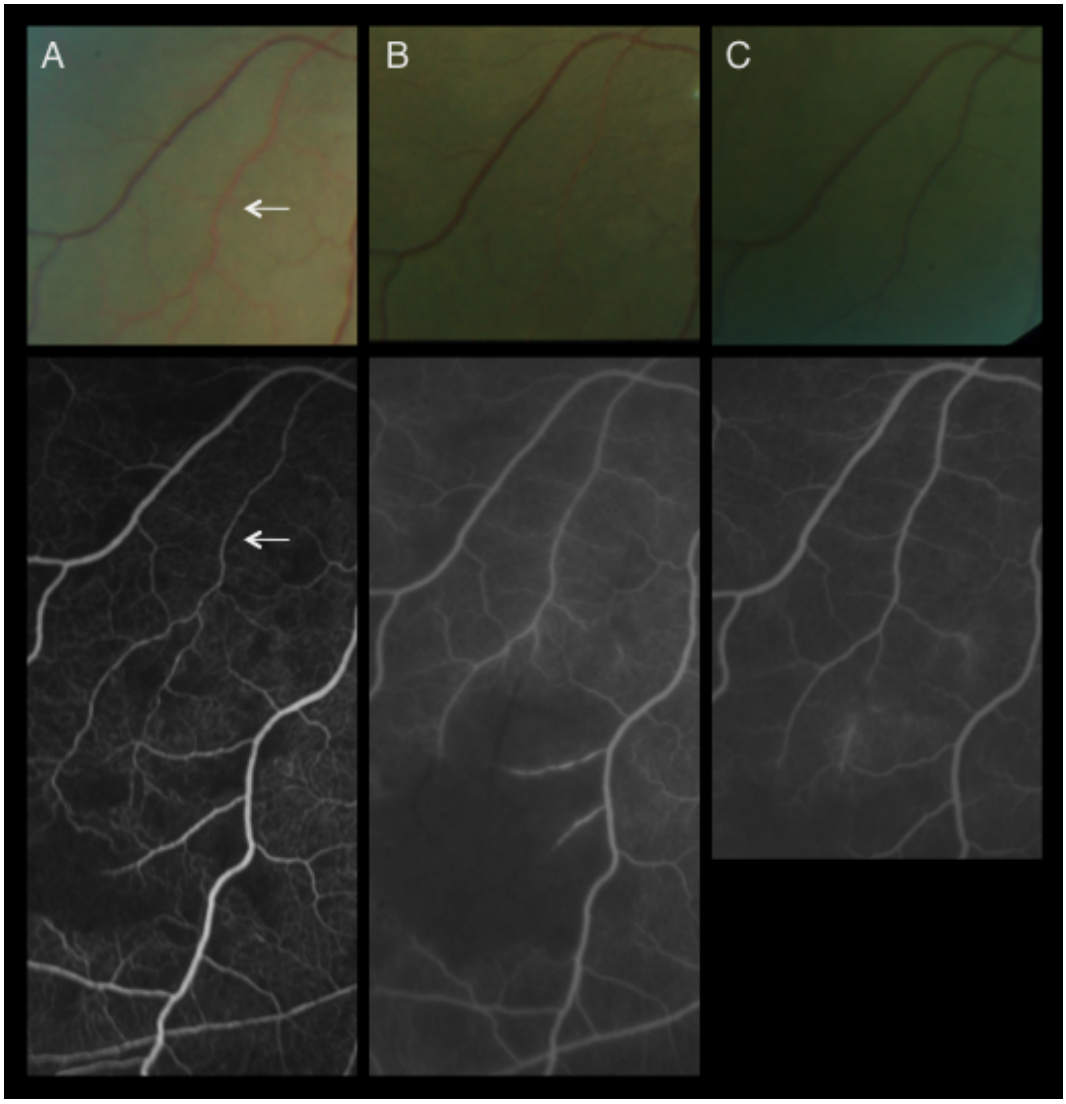

9.4.1.1 Comparison of retinal and brain barrier systems

Unlike the brain, the retina has inner (visible) and outer (choroidal) circulations, each of which have distinct barrier systems. I will focus on the inner retinal circulation, since this is affected by sequestration much more severely than the choriocapillaris (Barrera *et al.*, 2015). Recently a new perivascular pathway has been described which may be relevant to removal of waste products from the brain interstitium into the cervical nodes (the glymphatic system) (Iliff et al., 2012; reviewed by Jessen et al., 2015). It is not yet clear whether there is a similar system in the inner retina, where interstitial fluid is removed across the retinal pigment epithelium and into the choroidal circulation (Kaur *et al.*, 2008).

A short summary of recent reviews summarising the blood brain and blood retina barriers (Kaur *et al.*, 2008; Nag, 2011; Nag *et al.*, 2011) suggests that the two systems are similar in many respects.

In both sites the purpose of the barrier system is to control the exchange of fluid, metabolites and waste products between blood and neural tissues. This is achieved by interactions between several cell types. These include endothelial cells, pericytes, and astrocytes. A notable difference is that Müller cells are involved in retinal barrier function but are not present in the brain. These are involved in the homeostasis of retinal interstitial fluid. They also secrete factors that influence barrier integrity (e.g. pigment epithelium derived growth factor, PEDF), and breakdown (vascular endothelial growth factor (VEGF), and matrix metalloproteases (MMP)) (Kaur *et al.*, 2008).

Retinal and cerebral endothelial cells have scanty caveolae compared to vascular endothelium outside the central nervous system, and are linked by tight junctions and adherens junction complexes. Tight junctions are composed of transmembrane proteins (occludin, claudins, junction adhesion molecules (JAM)), linked to scaffolding proteins (zonula occludens (ZO)), which in turn are connected to the actin cytoskeleton. Adherens junction complexes are composed of vascular endothelial (VE) cadheren linked to catenins and ultimately to the

cytoskeleton. In the brain their function is thought to include selective modulation of permeability (Kaur *et al.*, 2008; Nag, 2011).

In the brain organisation of tight junctions varies with vessel type and calibre. Some venules have discontinuous tight junctions, which provide a possible route for migrating leukocytes (Nag *et al.*, 2011). I am not aware of variation in tight junctions between retinal vessels. It is possible that, in different regions of the CNS, the composition of tight junctions and adherens junction complexes may involve slightly different members of the protein families listed above (reviewed in (Nag, 2011)).

Pericytes are more frequent in the neurovasculature than outside the central nervous system, with ratios to endothelial cells of 1:1 in the retina and approximately 1:3 in the brain. They induce barrier function, and modulate blood flow (Hall *et al.*, 2014). In the brain they also appear to function as a multi-potent stem cell. Astrocytes also induce and maintain barrier function, *via* angiopoietin 1 (Ang-1), amongst other factors. In the brain they are implicated in control of highly local changes in blood flow in concert with neuronal activity (Nag, 2011), and Ang-1 is low in patients with malarial retinopathy (Conroy *et al.*, 2010, 2012).

Differences in the number and type of support cell (pericytes, Müller cells) could conceivably lead to different responses to sequestration in retinal and cerebral circulations, as could the specific composition of tight junctions. Interactions between parasitised erythrocytes and specific tight junction components may give insights into the causes of barrier breakdown. However a much more detailed review is required to fully assess similarities and differences between retinal and brain barriers, relevant to paediatric CM.

9.4.2 An analytical approach to evaluate analogical inferences in observational research

Inferences about the brain from retinal data, and about true outcomes from surrogate end points, are examples of analogical reasoning. Consistent with this, some statistical approaches to evaluating surrogate end points appear to have a

structure that is particularly similar to that of analogy. For example, the relative effect (RE) can be thought of as expressing a concept similar to nomic isomorphism, where the behaviour of two different physical entities can be described by the same equations (e.g. volumetric flow of a liquid and electrical current) (Bartha, 2013; Buyse and Molenberghs, 1998).

However, to the best of my knowledge no-one has yet attempted to evaluate retinal markers of brain disease using approaches derived from the surrogate endpoint literature.

In Chapter 3 I outlined the potential, and also some possible pitfalls, of this approach. The results of Chapter 8 further suggest that a statistic such as the proportion of information gain functions best with high-quality data. By this I mean data from a large sample, with a reasonable amount of variation (Alonso *et al.*, 2004). In addition continuous normal data is more versatile than binary variables, and also allows more scope for running structural equation models (Kline, 2011). The designation of the "reference" variable (A or Z in Figure 16 in Chapter 3) can have a large impact on associations between S and T, and so should be chosen carefully. These points should be taken into consideration when designing future studies.

Further work on biomarker evaluation may provide more tools to investigate associations between the retina and brain. For example, current statistics operate by describing the amount of information (or signal) shared by the biomarker and the true endpoint. These might be improved by also considering the amount of noise common to both factors (Czanner, MacCormick, Faragher, unpublished work).

Overall, Chapter 3 provides a novel link between scientific inference based on the epistemology of analogical reasoning, and existing statistical techniques. This suggests broader applications for these methods beyond their originally intended field of randomised controlled trials. This approach can potentially give useful information about associations between retina and brain, and the interactions of

each with measurements of disease exposure and outcomes, that go beyond existing results from individual multivariate models.

9.4.3 Fluorescein angiographic grading scheme

Fluorescein angiograms (FA) had been taken in Malawian children with CM since 2006, and the qualitative description of images made it clear that a broad range of microvascular problems occurred in this disease – including unusual IVFD (Beare *et al.*, 2009).

However associations between these features and clinical outcomes could not be estimated because there was no formal method for quantitively grading the images. Development of this grading scheme required several steps. I began by reviewing existing fluorescein images and listing the types of abnormalities. This revealed a new type of leak (punctate focal leak) that had not been described by Beare et al., (2009). I convened a panel of experts on malarial retinopathy to discuss these features and decide on grades and terminology, as well as a way of accounting for the inevitable variation in the amount of retina captured on images between patients. Image montages were very important for measuring this feature. Finally, the grading scheme was implemented. We used dual grading with adjudication to give results with maximum reliability.

This process led to the grading scheme that was essential for the analyses in Chapter 7 and 8. Dual manual grading according to a standard system has the advantage of describing a range of severity for specific retinal features, and should give more consistent results than grading by a single observer. Future studies using this scheme will be able to compare their results with the data in this thesis. On the other hand, manual grading is time consuming, and inter-observer agreement depends on the feature in question. Inter-grader agreement was acceptable for the majority of features. Some variation in agreement is understandable given the large diversity in retinal features graded in the scheme – ranging from large areas of focal leak to microscopic abnormalities of the vessel wall.

Developing the grading scheme also assisted the development of automated grading techniques by focusing attention on questions about the nature of each vascular feature, what ought to be measured in each case, identifying a new feature and sub-classifying existing ones. These automated techniques are described (Zhao, MacCormick, Parry, Beare, *et al.*, 2015; Zhao, MacCormick, Parry, Leach, *et al.*, 2015; Zheng *et al.*, 2014). Automated techniques may provide greater accuracy than human graders, and also analyse images much more quickly.

9.4.4 Associations between ophthalmoscopy and clinical outcomes

Prior to this thesis associations between death and ophthalmoscopic features of malarial retinopathy had been described by several authors (Beare et al., 2004; Lewallen et al., 1993, 1996, 2008). What is the benefit of returning again to this same question?

One result of studies on CM over the past several decades is that concepts about the disease have changed. As discussed above, a major example of these changes was the finding that only a proportion of children who appeared to have CM actually had sequestration in cerebral vessels (Taylor *et al.*, 2004), and that the presence of neurovascular sequestration and retinopathy were closely associated. Previous analyses of ophthalmoscopic features of malarial retinopathy have not looked at associations within a sample of children with retinopathy positive CM. This is necessary to investigate retinal features as markers of disease processes specific to neurovascular sequestration, as opposed to disease processes common to comatose children with what may only be incidental parasitaemia. Including children without any retinopathy in the sample risks obscuring true associations with cerebral sequestration.

Although the distinction implied by malarial retinopathy came to be widely acknowledged (World Health Organization, 2014b) the use of ophthalmoscopy to ensure a more homogenous study population was by and large limited to research in Malawi, with studies in other locations continuing to report results from

patients meeting the much broader traditional definition provided by the WHO. The WHO case definition raises problems with interpreting results since associations are estimated in a heterogeneous sample, and therefore will not reflect disease processes specific to cerebral sequestration as clearly as they might if they were estimated in a sample defined by malarial retinopathy.

This criticism applies to studies on malarial retinopathy before its diagnostic significance was realised (Taylor *et al.*, 2004), but is also sadly relevant to much research since then. For example, two recent proteomic studies did not include retinopathy in their case definition of paediatric CM (Bachmann *et al.*, 2014; Gitau *et al.*, 2013) - and this is a type of research where conclusions may be especially vulnerable to extraneous noise from a heterogeneous sample.

There are signs that plasma HRP2 might provide a more user-friendly diagnostic test for retinopathy positive paediatric CM than ophthalmoscopy (Kariuki *et al.*, 2014; Seydel *et al.*, 2012), and this may lead to greater consistency in research methodology and paediatric CM case definition.

The results of my analysis of ophthalmoscopic features are different from previous studies (Beare et al., 2004), and point to orange vessels as an important feature for further research. Orange discolouration appears to represent, at least in some cases, the same process as IVFD (Figure 60), and is likely to have something to do with neurovascular sequestration, whether this is via consumption of haemoglobin (Lewallen *et al.*, 2000) or production of haemozoin, or another process. This retinal feature suggests that obstruction of vessels (not complete occlusion) may be important. Sequestration may also produce adverse effects on the local endothelium and blood-retinal barrier, as suggested by associations between angiographic leak and death independent of IVFD (Chapter 7).

Retinal haemorrhages seem to have an important link with fatal outcome, but only when very severe. It may be that the association between >50 haemorrhages and death reflects a process of ongoing, or uncontrolled haemorrhage, in contrast to haemorrhage that occurred at some point before admission but has since stopped.

This would be consistent with the link between large focal leak and death (Chapter 7), and appears to occur in only a minority of patients.

Although orange vessels and retinal haemorrhages can co-exist, independent associations with death suggest that the neurovascular processes involved are complex and multifactorial. No single retinal feature (or even the combination of features) fully explains clinical outcomes. Unfortunately orange vessels are one of the most difficult retinal features to see on ophthalmoscopy, and further progress may be made by applying more advanced imaging that allows precise measurements within vessels of different types or sizes, and track changes over time from admission. Ultra high resolution optical coherence tomography is just becoming commercially available, and provides detailed images of the peri-foveal capillaries. Further histopathological work to elucidate the nature of the orange material will also help to explain the cause of death in this disease.

It is important to remember that children with CM may also have other infections, and in particular they may be HIV positive. Microvascular retinopathy is common in adults with AIDS, and includes signs similar to those seen in malarial retinopathy and diabetic retinopathy (e.g. cotton wool spots, blot haemorrhages) (reviewed by (Vrabec, 2004). Notably, these signs appear to be much less common in children with vertically acquired HIV (Ikoona *et al.*, 2003; Kestelyn *et al.*, 2000). However even if HIV microvasculopathy is unlikely to be the sole cause of retinal signs in paediatric cerebral malaria, it certainly seems plausible that HIV co-infection could exacerbate malarial neurovascular injury, and future analyses of retinal signs in terms of HIV status deserve attention.

9.4.5 Associations between fluorescein angiography and clinical outcomes

Previous literature on retinal angiographic features of malaria had largely reported the presence or absence of abnormalities. Early case reports (Jean *et al.*, 1987; Yospaiboon *et al.*, 1984) were followed by studies in Thai adults (Davis *et al.*, 1992) and African children (Beare *et al.*, 2009; Hero *et al.*, 1997). Hero et al., (1997) observed mild capillary non-perfusion, vessel leakage, and disc leakage.

They did not see an association between retinal whitening and capillary non-perfusion, in contrast to (Beare *et al.*, 2009), who found whitening and capillary non-perfusion involved almost exactly the same areas. Beare *et al.*, (2009) also reported a broader range of abnormalities than previously published, and described the distribution of features in different vessel types and sizes. These abnormalities included intravascular filling defects, occlusion of large vessels (at sites of widespread capillary non perfusion) and leakage from small and large venules. The contrast in results with Hero et al., (1997) may be explained by the larger sample size and better camera used by Beare et al., (2009). In addition, (Hero *et al.*, 1997) did not describe when images were taken after admission, and some signs may have resolved before photography.

Informal review of fluorescein images from Malawi suggested that several features existed in addition to those previously described in Beare et al., (2009), namely large focal leak and punctate focal leak. These other features were quantified using dual grading with adjudication according to a standard grading scheme (Chapter 5).

The results of my analysis of admission fluorescein features against clinical outcomes (Chapter 7) suggest that retinal leak is a major risk factor for death and prolonged coma. The types of leak related to clinical outcomes (punctate leak, large focal leak) had not been described in previous literature, whereas vessel segment leak and post-capillary venule leak had (Beare *et al.*, 2009).

Each type of leak has a strikingly unique appearance, suggesting not only that blood-retina barrier breakdown is an important pathological process in malarial retinopathy, but also that the specific type of breakdown is clinically significant. This is in keeping with the general pattern of blood-brain barrier breakdown in cold injury models, where initial leakage from the acute injury is followed by inflammation, and then a period of repair and angiogenesis in which further leakage occurs (Nag *et al.*, 2011). Post-capillary venule leak, in particular, appears to develop around the margins of CNP, and it seems plausible that this specific type of leak represents recovery rather than an acute insult (Figure 61).

This is consistent with the trend between post-capillary venule leak and recovery (Chapter 7) (grade 2, unadjusted OR, 95%CI: 0.23, 0.05-1.02, p=0.053).

On the other hand, large focal leak, with its close spatio-temporal relationship to retinal haemorrhage (Figure 62) implies sudden rupture of a microvessel, creating a hole large enough to permit rapid flow of a relatively large volume of fluorescein and erythrocytes. Bleeding seems to be consistent with a local coagulopathy produced by loss of normal endothelial protein-c receptor (EPCR) (Moxon *et al.*, 2013). The observation of >1 site of large focal leak is associated with death (at p=0.04). Taken together with the previous finding that retinal haemorrhages are only associated with death when 50 or more are seen, this suggests that the important pathological characteristic may be uncontrolled, or on-going neurovascular haemorrhage, rather than haemorrhage *per se*. It seems that patients who have developed multiple retinal haemorrhages pre-admission, but in whom this bleeding has stopped, have less risk of death than those who have active bleeding at the time of angiography. Absence of pericytes is linked to cerebral haemorrhage in animal models (Nag, 2011 p137). It may be that intense local sequestration could cause reductions of platelet derived growth factor beta (PDGF-β) from endothelial cells severe enough to produce secondary loss of pericytes, and subsequent haemorrhage.

Figure 62: Large focal leak and haemorrhage

Matching colour and fluorescein images taken before, during, and immediately after the angiogram. A) Colour image before the angiogram, B) fluorescein angiogram image taken 6 minutes after injection; C) Fluorescein image taken 10 minutes after injection. Large focal leak is clearly visible; D) Colour image taken immediately after the angiogram, showing a haemorrhage at the site of large focal leak, with a halo of fluorescein. Images are from MP3280.

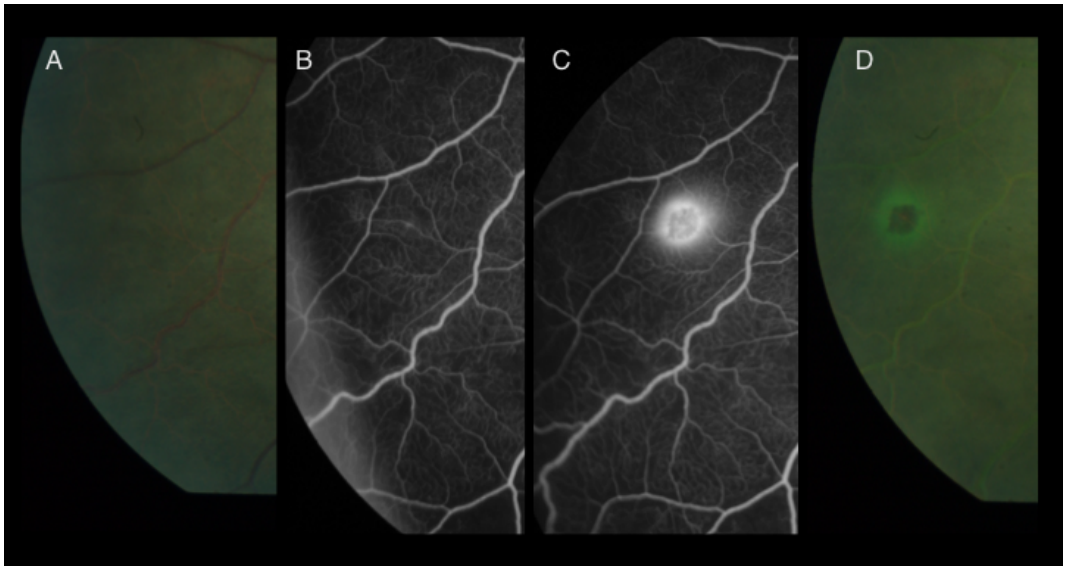

Punctate focal leak involves very small sites of leak which look like pinpricks on light in a dark sky (Figure 63). While it is easy to imagine that extensive large focal leak might cause death if it occurred in the brain, the association between punctate leak and death is less intuitive. How can such small breaks in the neurovasculature lead to fatal brain swelling?

Figure 63: Punctate focal leak.

Fluorescein angiogram image showing severe punctate focal leak. Multiple small sites of leak appear to arise from the capillary plexus of the inner retina.

The process represented by punctate leak is not entirely clear, but seems to involve rapid leakage through small breaks in the endothelium – smaller than the width of an erythrocyte. Stereoscopic images suggest these breaks occur in the inner retinal circulation, rather than in the retinal pigment epithelium (RPE). Damage to the RPE also seems less likely, given that the density of sequestration

in choriocapillaris is low compared to the inner retina (Barrera *et al.*, 2015). Interestingly, the RPE and choriocapillaris appear to have several features in common with the choroid plexus in the brain (Nag, 2011), and so evidence of damage to these retinal structures might point to blood-CSF barrier breakdown.

My impression is that severe punctate focal leak is often seen in cases with severe orange vessels, and it may be that this leakage represents part of a process involving severe sequestration, inflammation and focal endothelial damage, and blood-retinal barrier breakdown. One possibility is that punctate leak occurs when a weakened endothelium is exposed to additional vascular stress – such as a combination of increased arterial inflow acting against high venous resistance secondary to congestion. This might force fluorescein (free or bound to albumin) through tiny gaps in the blood-retina barrier. In this case the leak itself would be just one effect of increased neurovascular blood volume amd transmural pressure. This root cause could lead to brain swelling, most likely with at least some associated vasogenic and cytotoxic oedema. This would be consistent with unadjusted associations between death, IVFD and CNP, since these features would represent processes that contributed to the combination of endothelial instability and vascular congestion. Several components of the blood-retinal and blood-brain barriers (e.g. occludin, JAM-A) respond to haemodynamic forces, and these could plausibly link pathological changes in sheer stress and transmural pressure to focal loss of barrier function (Schmitt *et al.*, 2014). Angiopoietin 2 (Ang-2) is related to blood-brain barrier breakdown, and has been associated both with features of malarial retinopathy (such as number of haemorrhages) and death in children with CM (Conroy *et al.*, 2012).

Ideally these results should be replicated in an independent sample. The sample in this thesis includes subjects with worse than average malarial retinopathy, and the frequency of angiographic signs may be overestimated for the general population. Useful future work could investigate different populations, such as adults, or children in a different region of Africa; and use computerised methods alongside manual grading (e.g. Zheng et al., (2014)). Before this, the next step should be to analyse serial angiograms from Malawi. This may suggest patterns of change associated with deterioration or recovery. In addition, leakage

phenotypes could be evaluated against plasma markers of blood-brain barrier breakdown, such as Ang-1 and Ang-2 (Conroy *et al.*, 2012), and histopathological specimens could be analysed for specific barrier proteins.

9.5.6 Associations between retinal features, brain swelling, and death

Prior to this thesis, MRI brain features of paediatric CM had been analysed by comparing children with and without retinopathy (Postels *et al.*, 2014; Potchen *et al.*, 2012), and also in terms of associations with death in retinopathy positive cases (Seydel *et al.*, 2015). One study from Malawi reported associations between features of malarial retinopathy on admission and follow up MRI scans performed after discharge in survivors (Kampondeni *et al.*, 2013).

These studies pointed to several MRI features that were more common in retinopathy positive CM, compared to retinopathy negative cases, including abnormal signal in the basal ganglia, cortical T2 abnormalities, and cerebral white matter T2 abnormalities (Potchen *et al.*, 2012), amongst others. However the main features associated with death in retinopathy positive disease were brain swelling (measured in three different ways), DWI signal in the cortical grey matter, predominantly posterior (i.e. occipital) involvement, and patchy cortical T2 abnormalities which may represent local cerebritis in the context of diffuse venous congestion (Seydel *et al.*, 2015).

However, it is still unclear exactly which mechanisms cause brain swelling in paediatric CM. Brain volume depends on the volume of tissue, which is increased in cerebral oedema of various types. It also depends on cerebral blood volume, which can be raised if there is a mismatch between inflow and outflow, and with a loss of autoregulation.

As well as multiple potential causes of brain swelling there may also be varying degrees of susceptibility to the deleterious effects of cerebral sequestration amongst African children. For example, there is significant variation in the anatomy of paediatric cerebral venous drainage (Widjaja and Griffiths, 2004).

Patterns of damage in paediatric venous thrombosis correspond to drainage territories (Teksam *et al.*, 2008), and the absence of complementary pathways may put certain brain regions at higher risk of ischaemia secondary to venous congestion (MacCormick *et al.*, 2014). Although the brain is contained within the rigid skull, there is a certain degree of elastance in the cerebro-spinal system. This varies between individuals, and influences the relationship between increases in intracranial volume and corresponding changes in cerebrospinal fluid pressure. A given change in volume will lead to different magnitudes of increase in intracranial pressure, on a non-linear scale (Shapiro *et al.*, 1980).

My analyses of retinal signs suggested that, of the ophthalmoscopic findings, only orange vessels and very severe haemorrhage were related to death (Chapter 6). Of the angiographic features, punctate focal leak, and, to a lesser extent, large focal leak, were related to death (Chapter 7). The association between types of retinal leak and death, independent of IVFD (which may represent a similar process to orange vessels), suggested that breakdown of the blood-brain barrier might be the main reason for fatal brain swelling in paediatric CM. Although CNP and IVFD were not associated with death independent of retinal leakage, this does not prove that these signs are unimportant to CM pathogenesis—but only that they are not independent of leakage. They may have complex interactions with other variables that are not adequately represented by assumptions inherent in logistic regression modelling.

When I analysed data from the group of subjects who had both admission angiogram and MRI, associations between punctate focal leak and cerebrospinal fluid space (a measure of brain swelling) were not as strong as I anticipated. Similarly, in this sample associations between papilloedema and death, which should be considerable, were relatively weak. This phenomenon may be explained by other characteristics of the sample in comparison to subjects who did not have these investigations – in particular, it appeared that there was a lack of variation in disease severity in subjects who had MRI. This group tended to lack subjects who either woke up early (i.e. mild disease), or died early (i.e. severe disease).

Unfortunately, my analyses of retinal and MRI brain variables using the proportion of information gain were not able to confirm or refute my hypotheses about punctate and large focal leak being equivalent to brain swelling since the confidence intervals were extremely wide. I think this is consistent with the relative lack of spread in this particular sample of subjects, which tended not to include patients from the mild or severe end of the disease spectrum. Such sampling is difficult to avoid in conditions that progress rapidly to death or recovery.

Furthermore, the secondary analysis of retinal features against cerebrospinal fluid space indicated that arteriolar IVFD were independently associated with brain swelling, but punctate focal leak was not. This is surprising, since it is inconsistent with the results of Chapter 7. One possible explanation could be that punctate focal leak is related to death through a process that does not involve severe brain swelling. However, this seems unlikely given the strong association between severe brain swelling and death (Seydel *et al.*, 2015). More importantly, the clear issues with selection of patients from the middle rather than the tails of the disease spectrum in the sample of subjects who had both retinal and MRI imaging suggest strongly that these results should be interpreted with caution. Results from this analysis are unlikely to be generalisable.

Selection bias is a major threat to observational research generally. Unfortunately the acute nature of CM makes it very difficult to study subjects at the limits of disease severity. Furthermore, because CM is rapidly fatal, it is likely that a significant proportion of cases never even reach hospital. As far as we know, these cases might be radically different from hospitalised patients. Therefore, even if one could fully investigate 100% of admitted subjects this "ideal" study would still suffer from a particular kind of selection bias (known as "Neyman bias") (Grimes and Schulz, 2002). Such issues are difficult to resolve, and rarely discussed in the CM literature, or much observational research in general. But awareness of the problems at least gives researchers the opportunity to interpret published results with greater discernment, and also design future studies with these limitations in mind.

Future work on retina and brain in acute paediatric CM ought to involve analysis of admission angiographic and MRI features with reference to endpoints besides death. Although this variable (death) has the advantage of being completely unambiguous, with no measurement error, as a binary variable it contains a limited amount of information. Analysis with reference to a different "Z" variable (see Chapter 3) could give more useful results. One option would be to treat brain swelling itself as the ultimate disease outcome, and investigate retinal and other MRI changes against this. For example, high DWI signal in cortical grey matter (Seydel *et al.*, 2015). This analysis would assess relationships between focal DWI signal, retinal leakage, and brain swelling.

Future research should also target analysis of corresponding changes in retinal and MRI brain features over time during admission. And, as with all studies, the analyses described in Chapter 8 ought to be replicated in a different sample. If the number of CM cases in Blantyre continues to fall, this will only be possible once other countries with a high burden of CM obtain an MRI scanner, and all the necessary associated infrastructure to support this technology.

9.5 Conclusions and future work

In this thesis I set out to develop retinal signs as markers of cerebral disease in paediatric CM. This was an ambitious aim, and it has not yet been fully achieved. However, the process has led me to develop ideas about what it means for a retinal sign to reflect an analogous brain feature. This way of understanding retinal biomarkers is novel, and applicable to a range of neurological diseases currently being researched intensively. The comparison of retina and brain vasculature suggested an important role for haemorheological factors in addition to occlusion and local inflammation and coagulation. New associations between retinal features and clinical outcomes point to blood-brain barrier breakdown as a key mechanism linked to death and coma. The fluorescein grading scheme now allows these features to be studied in new cohorts.

Several questions remain to be targeted by future research on malarial retinopathy. Further development of retinal signs as markers of cerebral disease could allow them to be applied to at least three broad areas:

- Identification of subgroups within the general population of children with retinopathy positive CM. In this thesis I have discussed "retinopathy positive" as if it is a single group. However many differences exist within this group. For example, some children appear to have a predominantly haemorrhagic phenotype, while in others retinal whitening is the chief feature. Investigation of these groups may help to identify new factors that contribute to pathogenesis, such as the role of concomitant neurovascular infection.

- Identification of retinal markers of disease severity. Clearer assessment of disease severity could allow better characterisation of sample populations in interventional studies.

- Investigation of pathological mechanisms. This was the focus of my thesis. Much work remains to develop a clear picture of how visible retinal neurovascular changes (e.g. leakage) relate to brain swelling and death. One important step on this road will be to describe the natural history of retinopathy. I have presented a few figures suggesting that CNP resolves over a few days with associated venular leak, while retinal whitening persists. This type of temporal description may help to clarify which retinal features are most useful for assessing disease severity, and how these should be measured. For example, it may be that the absolute number of retinal haemorrhages is less important than whether or not the number of haemorrhages is actively *increasing* over a given period of time.

Beyond this, I hope that my general approach to retinal biomarkers will have a positive influence on research into other neurological diseases. The eyes may be a window to the soul, and even to the brain in some situations, but good science must place metaphor secondary to clear epistemology.

References

Abu Sayeed A, Maude RJ, Hasan MU, Mohammed N, Hoque MG, Dondorp AM, et al. Malarial retinopathy in Bangladeshi adults. Am J Trop Med Hyg 2011; 84: 141–7.

Agrawal A, McKibbin MA. Purtscher's and Purtscher-like retinopathies: a review. Surv Ophthalmol 2006; 51: 129–36.

Akima M. A morphological study on the microcirculation of the central nervous system. Selective vulnerability to hypoxia. Neuropathology 1993; 13: 99–112.

Albaum MN, Hill LC, Murphy M, Li YH, Fuhrman CR, Britton CA, et al. Interobserver reliability of the chest radiograph in community-acquired pneumonia. PORT Investigators. Chest 1996; 110: 343–50.

Alm A, Bill A. Ocular and optic nerve blood flow at normal and increased intraocular pressures in monkeys (Macaca irus): a study with radioactively labelled microspheres including flow determinations in brain and some other tissues. Exp Eye Res 1973; 15: 15–29.

Alonso A, Molenberghs G, Burzykowski T, Renard D, Geys H, Shkedy Z, et al. Prentice's approach and the meta-analytic paradigm: a reflection on the role of statistics in the evaluation of surrogate endpoints. Biometrics 2004; 60: 724–8.

Altman DG, Royston P. What do we mean by validating a prognostic model? Stat Med 2000; 19: 453–73.

An H, Lin W. Cerebral venous and arterial blood volumes can be estimated separately in humans using magnetic resonance imaging. Magn Reson Med 2002; 48: 583–8.

Anand-Apte B, Hollyfield JG. Developmental Anatomy of the Retinal and Choroidal Vasculature. In: Dartt DA, editor(s). Encyclopedia of the Eye. Oxford: Academic Press; 2010. p. 9–15.

Anderson B, Saltzman HA. Retinal oxygen utilization measured by hyperbaric blackout. Arch Ophthalmol 1964; 72: 792–5.

Anderson J. Analogical thoughts [Internet]. Blog 2015[cited 2015 May 29] Available from: http://www.proginosko.com/

Andeweg J. The anatomy of collateral venous flow from the brain and its value in aetiological interpretation of intracranial pathology. Neuroradiology 1996; 38: 621–628.

Andeweg J. Consequences of the anatomy of deep venous outflow from the brain. Neuroradiology 1999; 41: 233–41.

de Andrade C. Manifestacoes oculares nas doencas tropicais. Ar Clin Oftal 1937; 4: 17–64.

Archibald NK, Clarke MP, Mosimann UP, Burn DJ. The retina in Parkinson's disease. Brain 2009; 132: 1128–45.

Armah H, Dodoo AK, Wiredu EK, Stiles JK, Adjei AA, Gyasi RK, et al. High-level cerebellar expression of cytokines and adhesion molecules in fatal, paediatric, cerebral malaria. Ann Trop Med Parasitol 2005; 99: 629–47.

Bachmann J, Burté F, Pramana S, Conte I, Brown BJ, Orimadegun AE, et al. Affinity proteomics reveals elevated muscle proteins in plasma of children with cerebral malaria. PLoS Pathog 2014; 10: e1004038.

Barrera V, Hiscott PS, Craig AG, White VA, Milner DA, Beare NA V, et al. Severity of Retinopathy Parallels the Degree of Parasite Sequestration in Eye and Brain in Malawian Children with Fatal Cerebral Malaria. J Infect Dis 2015; 211: 1977–86.

Bartha P. Analogy and Analogical Reasoning [Internet]. Stanford Encycl Philos 2013[cited 2014 May 10] Available from: http://plato.stanford.edu/entries/reasoning-analogy/

Baskurt OK, Meiselman HJ. Blood rheology and hemodynamics. Semin Thromb Hemost 2003; 29: 435–50.

Beare N, Southern C, Kayira K, Taylor T, Harding S. Visual outcomes in children in Malawi following retinopathy of severe malaria. Br J Ophthalmol 2004; 88: 321–4.

Beare N, Southern C, Lochhead J, Molyneux M, Lewallen S, Harding S. Inter-observer concordance in grading retinopathy in cerebral malaria. Ann Trop Med Parasitol 2002; 96: 105–108.

Beare NA, Glover SJ, Lewallen S, Taylor TE, Harding SP, Molyneux ME. Prevalence of raised intracranial pressure in cerebral malaria detected by optic nerve sheath ultrasound. Am J Trop Med Hyg 2012; 87: 985–988.

Beare NA, Harding SP, Taylor TE, Lewallen S, Molyneux ME. Perfusion abnormalities in children with cerebral malaria and malarial retinopathy. J Infect Dis 2009; 199: 263–271.

Beare NA, Kampondeni S, Glover SJ, Molyneux E, Taylor TE, Harding SP, et al. Detection of raised intracranial pressure by ultrasound measurement of optic nerve sheath diameter in African children. Trop Med Int Heal 2008; 13: 1400–4.

Beare NA, Lewallen S, Taylor TE, Molyneux ME. Redefining cerebral malaria by including malaria retinopathy. Future Microbiol 2011; 6: 349–55.

Beare NA, Southern C, Chalira C, Taylor TE, Molyneux ME, Harding SP. Prognostic significance and course of retinopathy in children with severe malaria. Arch Ophthalmol 2004; 122: 1141–7.

Beare NA, Taylor TE, Harding SP, Lewallen S, Molyneux ME. Malarial retinopathy: a newly established diagnostic sign in severe malaria. Am J Trop Med Hyg 2006; 75: 790–7.

Beare NA. Malarial retinopathy: a window onto the brain. 2005

Bek T, Jensen PK. Three-dimensional structure of human retinal vessels studied by vascular casting. Acta Ophthalmol 1993; 71: 506–13.

Bell MA, Ball MJ. Laminar variation in the microvascular architecture of normal human visual cortex (area 17). Brain Res 1985; 335: 139–43.

Bell RW. Ophthalmologic findings in malaria. Ann Ophthalmol 1975; 7: 1439–42.

Belzung C, Lemoine M. Criteria of validity for animal models of psychiatric disorders: focus on anxiety disorders and depression. Biol Mood Anxiety Disord 2011; 1: 9.

Bennett A, Kazembe L, Mathanga DP, Kinyoki D, Ali D, Snow RW, et al. Mapping malaria transmission intensity in Malawi, 2000-2010. Am J Trop Med Hyg 2013; 89: 840–9.

Beran TN, Violato C. Structural equation modeling in medical research: a primer. BMC Res Notes 2010; 3: 267.

Van den Bergh R, Van der Eecken H. Anatomy and embryology of cerebral circulation. Prog Brain Res 1968; 30: 1–25.

Berntson GM. The Characterization of Topology: A Comparison of Four topological Indices for Rooted Binary Trees. J Theor Biol 1995; 177: 271–281.

Beyea J, Greenland S. The importance of specifying the underlying biologic model in estimating the probability of causation. Health Phys 1999; 76: 269–74.

Billig EMW, O'Meara WP, Riley EM, McKenzie FE. Developmental allometry and paediatric malaria. Malar J 2012; 11: 64.

Biomarkers Definitions Working Group. Biomarkers and surrogate endpoints: preferred definitions and conceptual framework. Clin Pharmacol Ther 2001; 69: 89–95.

Birbeck GL, Beare N, Lewallen S, Glover SJ, Molyneux ME, Kaplan PW, et al. Identification of malaria retinopathy improves the specificity of the clinical diagnosis of cerebral malaria: findings from a prospective cohort study. Am J Trop Med Hyg 2010; 82: 231–4.

Birbeck GL, Molyneux ME, Kaplan PW, Seydel KB, Chimalizeni YF, Kawaza K, et al. Blantyre Malaria Project Epilepsy Study (BMPES) of neurological outcomes in retinopathy-positive paediatric cerebral malaria survivors: a prospective cohort study. Lancet 2010; 9: 1173–1181.

Birol G, Wang S, Budzynski E, Wangsa-Wirawan ND, Linsenmeier RA. Oxygen distribution and consumption in the macaque retina. Am J Physiol Heart Circ Physiol 2007; 293: H1696–704.

Biswas J, Fogla R, Srinivasan P, Narayan S, Haranath K, Badrinath V. Ocular malaria. A clinical and histopathologic study. Ophthalmology 1996; 103: 1471–5.

Blatt N. Augenveränderungen bei malaria. Klin Monbl Augenheilkd 1928; 80: 468–478.

Bouwens EAM, Stavenuiter F, Mosnier LO. Mechanisms of anticoagulant and cytoprotective actions of the protein C pathway. J Thromb Haemost 2013; 11 Suppl 1: 242–53.

Box GEP, Draper NR. Empirical model-building and response surfaces. 1st ed. Chichester: Wiley; 1987.

Bradley DJ, Warrell, David A. Malaria. In: Warrell, David A, Cox TM, Firth JD, Benz EJ, editor(s). Oxford Textbook of Medicine. Oxford University Press; 2003. p. 1–68.

Bronzan RN, Taylor TE, Mwenechanya J, Tembo M, Kayira K, Bwanaisa L, et al. Bacteremia in Malawian children with severe malaria: prevalence, etiology, HIV coinfection, and outcome. J Infect Dis 2007; 195: 895–904.

Brown H, Hien TT, Day N, Mai NT, Chuong L V, Chau TT, et al. Evidence of blood-brain barrier dysfunction in human cerebral malaria. Neuropathol Appl Neurobiol 1999; 25: 331–40.

Brown H, Rogerson S, Taylor T, Tembo M, Mwenechanya J, Molyneux M, et al. Blood-brain barrier function in cerebral malaria in Malawian children. Am J Trop Med Hyg 2001; 64: 207–13.

Brown HC, Chau TT, Mai NT, Day NP, Sinh DX, White NJ, et al. Blood-brain barrier function in cerebral malaria and CNS infections in Vietnam. Neurology 2000; 55: 104–11.

Browning DJ. Patchy ischemic retinal whitening. Ophthalmology 2004; 111: 606–7; author reply 607.

Burton M, Nyong'o O, Burton K, John W, Inkoom E, Pinder M, et al. Retinopathy in Gambian children admitted to hospital with malaria. Trop Doct 2004; 34: 214–8.

Burzykowski T, Molenberghs G, Buyse M. The Evaluation of Surrogate Endpoints. 1st ed. New York: Springer; 2005.

Buxton RB, Griffeth VEM, Simon AB, Moradi F, Shmuel A. Variability of the coupling of blood flow and oxygen metabolism responses in the brain: a problem for interpreting BOLD studies but potentially a new window on the underlying neural activity. Front Neurosci 2014; 8: 139.

Buxton RB. Interpreting oxygenation-based neuroimaging signals: the importance and the challenge of understanding brain oxygen metabolism. Front Neuroenergetics 2010; 2: 8.

Buyse M, Molenberghs G. Criteria for the validation of surrogate endpoints in randomized experiments. Biometrics 1998; 54: 1014–29.

Buyse M, Sargent DJ, Grothey A, Matheson A, de Gramont A. Biomarkers and surrogate end points--the challenge of statistical validation. Nat Rev Clin Oncol 2010; 7: 309–17.

Carlotti. Troubles de l'appareil visuel attribuables au paludisme en macedoine. ann d'ocul 1918; 155: 478.

Carneiro I, Roca-Feltrer A, Griffin JT, Smith L, Tanner M, Schellenberg JA, et al. Age-patterns of malaria vary with severity, transmission intensity and seasonality in sub-Saharan Africa: a systematic review and pooled analysis. PLoS One 2010; 5: e8988.

Carraro MC, Rossetti L, Gerli GC. Prevalence of retinopathy in patients with anemia or thrombocytopenia. Eur J Haematol 2001; 67: 238–44.

Cassot F, Lauwers F, Fouard C, Prohaska S, Lauwers-Cances V. A novel three-dimensional computer-assisted method for a quantitative study of microvascular networks of the human cerebral cortex. Microcirculation 2006; 13: 1–18.

Cassot F, Lauwers F, Lorthois S, Puwanarajah P, Cances-Lauwers V, Duvernoy H. Branching patterns for arterioles and venules of the human cerebral cortex. Brain Res 2010; 1313: 62–78.

Chastang L. Les manifestations oculaires au cours du paludisme. Arch Med Nav 1918; 55: 241–267.

Cheung CY-L, Ong Y-T, Ikram MK, Chen C, Wong TY. Retinal microvasculature in Alzheimer's disease. J Alzheimers Dis 2014; 42: S339–52.

Cheung N, Islam FMA, Saw SM, Shankar A, de Haseth K, Mitchell P, et al. Distribution and associations of retinal vascular caliber with ethnicity, gender, and birth parameters in young children. Invest Ophthalmol Vis Sci 2007; 48: 1018–24.

Cho Y-I, Cho DJ. Hemorheology and microvascular disorders. Korean Circ J 2011; 41: 287–95.

Chotivanich K, Sritabal J, Udomsangpetch R, Newton P, Stepniewska KA, Ruangveerayuth R, et al. Platelet-induced autoagglutination of Plasmodium falciparum-infected red blood cells and disease severity in Thailand. J Infect Dis 2004; 189: 1052–5.

Chu EM-Y, Kolappan M, Barnes TRE, Joyce EM, Ron MA. A window into the brain: an in vivo study of the retina in schizophrenia using optical coherence tomography. Psychiatry Res 2012; 203: 89–94.

Chugani HT, Phelps ME, Mazziotta JC. Positron emission tomography study of human brain functional development. Ann Neurol 1987; 22: 487–97.

Chugani HT. A critical period of brain development: studies of cerebral glucose utilization with PET. Prev Med (Baltim) 1998; 27: 184–8.

Cogan DG, Kuwabara T. Comparison of retinal and cerebral vasculature in trypsin digest preparations. Br J Ophthalmol 1984; 68: 10–12.

Conroy AL, Glover SJ, Hawkes M, Erdman LK, Seydel KB, Taylor TE, et al. Angiopoietin-2 levels are associated with retinopathy and predict mortality in Malawian children with cerebral malaria: a retrospective case-control study*. Crit Care Med 2012; 40: 952–9.

Conroy AL, Phiri H, Hawkes M, Glover S, Mallewa M, Seydel KB, et al. Endothelium-based biomarkers are associated with cerebral malaria in Malawian children: a retrospective case-control study. PLoS One 2010; 5: e15291.

Craig A, Scherf A. Molecules on the surface of the Plasmodium falciparum infected erythrocyte and their role in malaria pathogenesis and immune evasion. Mol Biochem Parasitol 2001; 115: 129–43.

Craig AG, Grau GE, Janse C, Kazura JW, Milner D, Barnwell JW, et al. The Role of Animal Models for Research on Severe Malaria. PLoS Pathog 2012; 8: e1002401.

Crane IJ, Liversidge J. Mechanisms of leukocyte migration across the blood-retina barrier. Semin Immunopathol 2008; 30: 165–77.

Davis MW, Vaterlaws AL, Simes J, Torzillo P. Retinopathy in malaria. P N G Med J 1982; 25: 19–22.

Davis T. Malarial blindness with a report of six cases. New Orleans Med Surg J 1909; 61: 501–11.

Davis TM, Suputtamongkol Y, Spencer JL, Ford S, Chienkul N, Schulenburg WE, et al. Measures of capillary permeability in acute falciparum malaria: relation to severity of infection and treatment. Clin Infect Dis 1992; 15: 256–66.

Dedimos P. Les manifestations oculaires du paludisme. Arch d'opht 1932; 49: 166.

Dithmar S, Holz FG. Fluorescence angiography in ophthalmology: fluorescein angiography, indocyanine green angiography, fundus autofluorescence. Springer; 2008.

Dondorp AM, Angus BJ, Hardeman MR, Chotivanich KT, Silamut K, Ruangveerayuth R, et al. Prognostic significance of reduced red blood cell deformability in severe falciparum malaria. Am J Trop Med Hyg 1997; 57: 507–11.

Dondorp AM, Desakorn V, Pongtavornpinyo W, Sahassananda D, Silamut K, Chotivanich K, et al. Estimation of the total parasite biomass in acute falciparum malaria from plasma PfHRP2. PLoS Med 2005; 2: e204.

Dondorp AM, Omodeo-Salè F, Chotivanich K, Taramelli D, White NJ. Oxidative stress and rheology in severe malaria. Redox Rep 2003; 8: 292–4.

Dorner GT, Polska E, Garhöfer G, Zawinka C, Frank B, Schmetterer L. Calculation of the diameter of the central retinal artery from noninvasive measurements in humans. Curr Eye Res 2002; 25: 341–5.

Dorovini-Zis K, Schmidt K, Huynh H, Fu W, Whitten RO, Milner D, et al. The neuropathology of fatal cerebral malaria in malawian children. Am J Pathol 2011; 178: 2146–58.

Doubal FN, Hokke PE, Wardlaw JM. Retinal microvascular abnormalities and stroke: a systematic review. J Neurol Neurosurg Psychiatry 2009; 80: 158–65.

Doubal FN. Do retinal microvascular abnormalities shed light on the pathophysiology of lacunar stroke? 2010

Dowling JE. The retina: an approachable part of the brain. 2nd ed. Belknap Press; 2012.

Duane TD, Osher RH, Green WR. White centered hemorrhages: their significance. Ophthalmology 1980; 87: 66–9.

Duguid IG, Boyd AW, Mandel TE. Adhesion molecules are expressed in the human retina and choroid. Curr Eye Res 1992; 11 Suppl: 153–9.

Duvernoy HM, Delon S, Vannson JL. Cortical blood vessels of the human brain. Brain Res Bull 1981; 7: 519–79.

Early Treatment Diabetic Retinopathy Study research group. Photocoagulation for diabetic macular edema. Early Treatment Diabetic Retinopathy Study report number 1. Arch Ophthalmol 1985; 103: 1796–806.

Elliott RH. Tropical Ophthalmology. 1st ed. London: Hodder & Stoughton; 1920.

Essuman VA, Ntim-Amponsah CT, Astrup BS, Adjei GO, Kurtzhals JAL, Ndanu TA, et al. Retinopathy in severe malaria in Ghanaian children--overlap between fundus changes in cerebral and non-cerebral malaria. Malar J 2010; 9: 232.

Faraci FM. Protecting against vascular disease in brain. Am J Physiol Heart Circ Physiol 2011; 300: H1566–82.

Fedosov DA, Caswell B, Karniadakis GE. Wall shear stress-based model for adhesive dynamics of red blood cells in malaria. Biophys J 2011; 100: 2084–93.

Fedosov DA, Caswell B, Suresh S, Karniadakis GE. Quantifying the biophysical characteristics of Plasmodium-falciparum-parasitized red blood cells in microcirculation. Proc Natl Acad Sci U S A 2011; 108: 35–9.

Feke GT, Tagawa H, Deupree DM, Goger DG, Sebag J, Weiter JJ. Blood flow in the normal human retina. Invest Ophthalmol Vis Sci 1989; 30: 58–65.

Fialho A. Manifestacoes oculares do paludismo. Arch Bras Med 1927; 27: 162–167.

Finnoff WC. Dendritic Keratitis following Therapeutic Inoculation of Malaria. Trans Am Ophthalmol Soc 1929; 27: 72–5.

Fisher JH. Diseases of the retina. Trans Ophthalmol Soc United Kingdom 1921; 41: 235–238.

Fleming TR, DeMets DL. Surrogate end points in clinical trials: are we being misled? Ann Intern Med 1996; 125: 605–13.

Fox LL, Taylor TE, Pensulo P, Liomba A, Mpakiza A, Varela A, et al. Histidine-rich protein 2 plasma levels predict progression to cerebral malaria in Malawian children with Plasmodium falciparum infection. J Infect Dis 2013; 208: 500–3.

Freedman LS, Graubard BI, Schatzkin A. Statistical validation of intermediate endpoints for chronic diseases. Stat Med 1992; 11: 167–78.

Funatsu H, Yamashita H, Sakata K, Noma H, Mimura T, Suzuki M, et al. Vitreous levels of vascular endothelial growth factor and intercellular adhesion molecule 1 are related to diabetic macular edema. Ophthalmology 2005; 112: 806–16.

Ganesan P, He S, Xu H. Analysis of retinal circulation using an image-based network model of retinal vasculature. Microvasc Res 2010; 80: 99–109.

Geeraerts T, Devys J-M, Berges O, Dureau P, Plaud B. Sevoflurane effects on retrobulbar arteries blood flow in children. Br J Anaesth 2005; 94: 636–41.

Gitau EN, Kokwaro GO, Karanja H, Newton CRJC, Ward SA. Plasma And Cerebrospinal Proteomes Of Children With Cerebral Malaria Differ From Children With Other Encephalopathies. J Infect Dis 2013

Goldfeder A, Moldavskaya, Krichevkaya. Ocular complications in latent malaria and significance of melano-flocculation reaction for etiologic diagnostic. Vrach Delo 1935; 18: 717–718.

Green AJ, McQuaid S, Hauser SL, Allen I V, Lyness R. Ocular pathology in multiple sclerosis: retinal atrophy and inflammation irrespective of disease duration. Brain 2010; 133: 1591–601.

Greenland S, Pearl J, Robins JM. Causal diagrams for epidemiologic research. Epidemiology 1999; 10: 37–48.

Griffiths MJ, Ndungu F, Baird KL, Muller DP, Marsh K, Newton CR. Oxidative stress and erythrocyte damage in Kenyan children with severe Plasmodium falciparum malaria. Br J Haematol 2001; 113: 486–91.

Grimes DA, Schulz KF. Bias and causal associations in observational research. Lancet 2002; 359: 248–52.

Gubergrits A. Hemorrhage into retina during malaria. Vrach Delo 1934; 17: 603.

Guibert R, Fonta C, Plouraboué F. Cerebral blood flow modeling in primate cortex. J Cereb blood flow Metab 2010; 30: 1860–73.

Hall CN, Reynell C, Gesslein B, Hamilton NB, Mishra A, Sutherland BA, et al. Capillary pericytes regulate cerebral blood flow in health and disease. Nature 2014; 508: 55–60.

Hanson J, Lee SJ, Mohanty S, Faiz MA, Anstey NM, Charunwatthana P, et al. A simple score to predict the outcome of severe malaria in adults. Clin Infect Dis 2010; 50: 679–85.

Harding S, Lewallen S, Beare N, Smith A, Taylor T, Molyneux M. Classifying and grading retinal signs in severe malaria. Trop Doct 2006; 36 Suppl 1: 1–13.

Harris A. Atlas of Ocular Blood Flow: Vascular Anatomy, Pathophysiology, and Metabolism. 2nd ed. Butterworth-Heinemann; 2010.

Harris PA, Taylor R, Thielke R, Payne J, Gonzalez N, Conde JG. Research electronic data capture (REDCap)--a metadata-driven methodology and workflow process for providing translational research informatics support. J Biomed Inform 2009; 42: 377–81.

Haslett P. Retinal haemorrhages in Zambian children with cerebral malaria. J Trop Pediatr 1991; 37: 86–7.

Hassler O. Deep cerebral venous system in man. A microangiographic study on its areas of drainage and its anastomoses with the superficial cerebral veins. Neurology 1966; 16: 505–11.

Hawkes M, Elphinstone RE, Conroy AL, Kain KC. Contrasting pediatric and adult cerebral malaria The role of the endothelial barrier. Virulence 2013; 4: 543–555.

Hayreh SS. In vivo choroidal circulation and its watershed zones. Eye (Lond) 1990; 4 (Pt 2): 273–89.

Hayreh SS. Physiological Anatomy of the Choroidal Vasculature. In: Dartt DA, editor(s). Encyclopedia of the Eye. Elsevier; 2010. a. p. 418–430.

Hayreh SS. Physiological Anatomy of the Retinal Vasculature. In: Dartt DA, editor(s). Encyclopedia of the Eye. Elsevier; 2010. b. p. 431–438.

Helbok R, Kendjo E, Issifou S, Lackner P, Newton CR, Kombila M, et al. The Lambaréné Organ Dysfunction Score (LODS) is a simple clinical predictor of fatal malaria in African children. J Infect Dis 2009; 200: 1834–41.

Hemingway H, Croft P, Perel P, Hayden JA, Abrams K, Timmis A, et al. Prognosis research strategy (PROGRESS) 1: a framework for researching clinical outcomes. BMJ 2013; 346: e5595.

Hendriksen ICE, Mwanga-Amumpaire J, von Seidlein L, Mtove G, White LJ, Olaosebikan R, et al. Diagnosing severe falciparum malaria in parasitaemic African children: a prospective evaluation of plasma PfHRP2 measurement. PLoS Med 2012; 9: e1001297.

Hero M, Harding SP, Riva CE, Winstanley PA, Peshu N, Marsh K. Photographic and angiographic characterization of the retina of Kenyan children with severe malaria. Arch Ophthalmol 1997; 115: 997–1003.

van der Heyde HC, Nolan J, Combes V, Gramaglia I, Grau GE. A unified hypothesis for the genesis of cerebral malaria: sequestration, inflammation and hemostasis leading to microcirculatory dysfunction. Trends Parasitol 2006; 22: 503–8.

Hirsch S, Reichold J, Schneider M, Székely G, Weber B. Topology and hemodynamics of the cortical cerebrovascular system. J Cereb blood flow Metab 2012; 32: 952–67.

Hochman S, Kim K. The Impact of HIV Coinfection on Cerebral Malaria Pathogenesis. J Neuroparasitology 2012; 3

Holt JM, Gordon-Smith EC. Retinal abnormalities in diseases of the blood. Br J Ophthalmol 1969; 53: 145–60.

Hooshmand I, Rosenbaum AE, Stein RL. Radiographic anatomy of normal cerebral deep medullary veins: criteria for distinguishing them from their abnormal counterparts. Neuroradiology 1974; 7: 75–84.

Huang YP, Wolf BS. Veins of the white matter of the cerebral hemispheres (the medullary veins). Am J Roentgenol Radium Ther Nucl Med 1964; 92: 739–55.

Hudetz AG, Fehér G, Kampine JP. Heterogeneous autoregulation of cerebrocortical capillary flow: evidence for functional thoroughfare channels? Microvasc Res 1996; 51: 131–6.

Hughes AD, Wong TY, Witt N, Evans R, Thom SA, Klein BE, et al. Determinants of retinal microvascular architecture in normal subjects. Microcirculation 2009; 16: 159–66.

Ide K, Secher NH. Cerebral blood flow and metabolism during exercise. Prog Neurobiol 2000; 61: 397–414.

Ikoona E, Kalyesubula I, Kawuma M. Ocular manifestations in paediatric HIV/AIDS patients in Mulago Hospital, Uganda. Afr Health Sci 2003; 3: 83–6.

Iliff JJ, Wang M, Liao Y, Plogg BA, Peng W, Gundersen GA, et al. A paravascular pathway facilitates CSF flow through the brain parenchyma and the clearance of interstitial solutes, including amyloid β. Sci Transl Med 2012; 4: 147ra111.

International Conference on Harmonisation. ICH Topic E9 Statistical Principles for Clinical Trials. 1998.

Jallow M, Casals-Pascual C, Ackerman H, Walther B, Walther M, Pinder M, et al. Clinical features of severe malaria associated with death: a 13-year observational study in the Gambia. PLoS One 2012; 7: e45645.

Jean B, Seilnacht J, HJ T. Malaria tropica mit makulablutung. Ophthalmol 1987; 195: 141–144.

Jespersen SN, Ostergaard L. The roles of cerebral blood flow, capillary transit time heterogeneity, and oxygen tension in brain oxygenation and metabolism. J Cereb blood flow Metab 2011; 32: 264–77.

Jessen NA, Munk ASF, Lundgaard I, Nedergaard M. The Glymphatic System: A Beginner’s Guide. Neurochem Res 2015

Joffe MM, Greene T. Related causal frameworks for surrogate outcomes. Biometrics 2009; 65: 530–8.

Jonas JB, Schneider U, Naumann GO. Count and density of human retinal photoreceptors. Graefes Arch Clin Exp Ophthalmol 1992; 230: 505–10.

Kampondeni SD, Potchen MJ, Beare NA V, Seydel KB, Glover SJ, Taylor TE, et al. MRI findings in a cohort of brain injured survivors of pediatric cerebral malaria. Am J Trop Med Hyg 2013; 88: 542–6.

Kariuki SM, Gitau E, Gwer S, Karanja HK, Chengo E, Kazungu M, et al. Value of Plasmodium falciparum histidine-rich protein 2 level and malaria retinopathy in distinguishing cerebral malaria from other acute encephalopathies in Kenyan children. J Infect Dis 2014; 209: 600–9.

Kaul DK, Roth EF, Nagel RL, Howard RJ, Handunnetti SM. Rosetting of Plasmodium falciparum-infected red blood cells with uninfected red blood cells enhances microvascular obstruction under flow conditions. Blood 1991; 78: 812–9.

Kaur C, Foulds WS, Ling EA. Blood-retinal barrier in hypoxic ischaemic conditions: basic concepts, clinical features and management. Prog Retin Eye Res 2008; 27: 622–47.

Kee DB, Wood JH. Rheology of the cerebral circulation. Neurosurgery 1984; 15: 125–31.

Kennedy C, Sokoloff L. An adaptation of the nitrous oxide method to the study of the cerebral circulation in children; normal values for cerebral blood flow and cerebral metabolic rate in childhood. J Clin Invest 1957; 36: 1130–7.

Kestelyn P, Lepage P, Karita E, Van de Perre P. Ocular manifestations of infection with the human immunodeficiency virus in an African pediatric population. Ocul Immunol Inflamm 2000; 8: 263–73.

Kety SS, Schmidt CF. The nitrous oxide method for the quantitative determination of cerebral blood flow in man: theory, procedure and normal values. J Clin Invest 1948; 27: 476–83.

Kety SS. Blood flow and metabolism of the human brain in health and disease. Trans Stud Coll Physicians Phila 1950; 18: 103–8.

Kety SS. Human cerebral blood flow and oxygen consumption as related to ageing. J Chronic Dis 1956; 3: 478–86.

Kiep WH. Ocular complications occurring in malaria. Trans Ophthalmol Soc U K 1922; 42: 394.

Kim S-G, Ogawa S. Biophysical and physiological origins of blood oxygenation level-dependent fMRI signals. J Cereb Blood Flow Metab 2012; 32: 1188–206.

Kinnala A, Suhonen-Polvi H, Aärimaa T, Kero P, Korvenranta H, Ruotsalainen U, et al. Cerebral metabolic rate for glucose during the first six months of life: an FDG positron emission tomography study. Arch Dis Child Fetal Neonatal Ed 1996; 74: F153–7.

Kirk J. Malaria and diseases of the eye. BMJ 1918; 2: 110–111.

Klaassen I, Van Noorden CJF, Schlingemann RO. Molecular basis of the inner blood-retinal barrier and its breakdown in diabetic macular edema and other pathological conditions. Prog Retin Eye Res 2013; 34: 19–48.

Klatzo I. Pathophysiological aspects of brain edema. Acta Neuropathol 1987; 72: 236–239.

Kline RB. Principles and Practice of Structural Equation Modeling. 3rd ed. London: Guilford Press; 2011.

Kuhn TS. The Structure of Scientific Revolutions. 2nd ed. Chicago: University of Chicago Press; 1984.

Kuppusamy K, Lin W, Cizek GR, Haacke EM. In vivo regional cerebral blood volume: quantitative assessment with 3D T1-weighted pre- and postcontrast MR imaging. Radiology 1996; 201: 106–12.

Kur J, Newman EA, Chan-Ling T. Cellular and physiological mechanisms underlying blood Flow regulation in the Retina and Choroid in health and disease. Prog Retin Eye Res 2012; 31: 377–406.

Kuwabara T, Cogan DG. Studies of retinal vascular patterns. I. Normal architecture. Arch Ophthalmol 1960; 64: 904–11.

Lassere MN. The Biomarker-Surrogacy Evaluation Schema: a review of the biomarker-surrogate literature and a proposal for a criterion-based, quantitative, multidimensional hierarchical levels of evidence schema for evaluating the status of biomarkers as surrogate endp. Stat Methods Med Res 2007; 17: 303–40.

Lauwers F, Cassot F, Lauwers-Cances V, Puwanarajah P, Duvernoy H. Morphometry of the human cerebral cortex microcirculation: general characteristics and space-related profiles. Neuroimage 2008; 39: 936–48.

Lavagnac J. Contributions a l’étude de troubles oculaires paludiques en Macdeoine. 1920

Laveran. Deuxieme note relatif a un nonveau parasit trouve dans le sang des malades atteints de la fievre. Bull Acad med 1880; 9: 1346.

Lee KE, Klein BEK, Klein R, Knudtson MD. Familial aggregation of retinal vessel caliber in the beaver dam eye study. Invest Ophthalmol Vis Sci 2004; 45: 3929–33.

Leitgeb RA, Werkmeister RM, Blatter C, Schmetterer L. Doppler optical coherence tomography. Prog Retin Eye Res 2014; 41: 26–43.

Lewallen S, Bakker H, Taylor T, Wills B, Courtright P, Molyneux M. Retinal findings predictive of outcome in cerebral malaria. Trans R Soc Trop Med Hyg 1996; 90: 144–6.

Lewallen S, Bronzan RN, Beare NA, Harding SP, Molyneux ME, Taylor TE. Using malarial retinopathy to improve the classification of children with cerebral malaria. Trans R Soc Trop Med Hyg 2008; 102: 1089–94.

Lewallen S, Harding SP, Ajewole J, Schulenburg WE, Molyneux ME, Marsh K, et al. A review of the spectrum of clinical ocular fundus findings in P. falciparum malaria in African children with a proposed classification and grading system. Trans R Soc Trop Med Hyg 1999; 93: 619–22.

Lewallen S, Taylor TE, Molyneux ME, Wills BA, Courtright P. Ocular fundus findings in Malawian children with cerebral malaria. Ophthalmology 1993; 100: 857–861.

Lewallen S. Association Between Measures of Vitamin A and the Ocular Fundus Findings in Cerebral Malaria. Arch Ophthalmol 1998; 116: 293.

Lewallen SA, White VA, Whitten RO, Gardiner J, Hoar B, Lindley J, et al. Clinical-histopathological correlation of the abnormal retinal vessels in cerebral malaria. Arch Ophthalmol 2000; 118: 924–8.

Li L-J, Cheung CY-L, Liu Y, Chia A, Selvaraj P, Lin X-Y, et al. Influence of blood pressure on retinal vascular caliber in young children. Ophthalmology 2011; 118: 1459–65.

Ling R, James B. White-centred retinal haemorrhages (Roth spots). Postgrad Med J 1998; 74: 581–2.

Lipowsky HH. Microvascular rheology and hemodynamics. Microcirculation 2005; 12: 5–15.

Lochhead J, Movaffaghy A, Falsini B, Harding S, Riva C, Molyneux M. The effects of hypoxia on the ERG in paediatric cerebral malaria. Eye (Lond) 2010; 24: 259–64.

Lochhead J, Movaffaghy A, Falsini B, Winstanley PA, Mberu EK, Riva CE, et al. The effect of quinine on the electroretinograms of children with pediatric cerebral malaria. J Infect Dis 2003; 187: 1342–5.

Lombardo M. Ophthalmologic lesions encountered in the tropics, with special reference to the ocular manifestations of malaria. Am J Ophthalmol 1945; 28

London A, Benhar I, Schwartz M. The retina as a window to the brain-from eye research to CNS disorders. Nat Rev Neurol 2013; 9: 44–53.

Looareesuwan S, Warrell DA, White NJ, Chanthavanich P, Warrell MJ, Chantaratherakitti S, et al. Retinal hemorrhage, a common sign of prognostic significance in cerebral malaria. Am J Trop Med Hyg 1983; 32: 911–5.

Lorthois S, Cassot F. Fractal analysis of vascular networks: insights from morphogenesis. J Theor Biol 2010; 262: 614–33.

Lu M, Perez VL, Ma N, Miyamoto K, Peng HB, Liao JK, et al. VEGF increases retinal vascular ICAM-1 expression in vivo. Invest Ophthalmol Vis Sci 1999; 40: 1808–12.

Lucchi NW, Jain V, Wilson NO, Singh N, Udhayakumar V, Stiles JK. Potential serological biomarkers of cerebral malaria. Dis Markers 2011; 31: 327–35.

MacCormick I, Beare N, Taylor T, Barrera V, White V, Hiscott P, et al. Cerebral malaria in children: using the retina to study the brain. Brain 2014; 137: 2119–42.

MacGillivray TJ, Trucco E, Cameron JR, Dhillon B, Houston JG, van Beek EJR. Retinal imaging as a source of biomarkers for diagnosis, characterization and prognosis of chronic illness or long-term conditions. Br J Radiol 2014; 87: 20130832.

Mackenzie S. Retinal haemorrhages and melanaemia as symptoms of ague. Med times Gaz 1877; June 23: 663–5.

MacPherson GG, Warrell MJ, White NJ, Looareesuwan S, Warrell DA. Human cerebral malaria. A quantitative ultrastructural analysis of parasitized erythrocyte sequestration. Am J Pathol 1985; 119: 385–401.

Madsen PL, Holm S, Herning M, Lassen NA. Average blood flow and oxygen uptake in the human brain during resting wakefulness: a critical appraisal of the Kety-Schmidt technique. J Cereb blood flow Metab 1993; 13: 646–55.

Manson WH. Personal experiences of the ocular sequelae of malaria. Glasgow Med J 1920; 93: 127–129.

Marasini D, Quatto P, Ripamonti E. Assessing the inter-rater agreement for ordinal data through weighted indexes. Stat Methods Med Res 2014

Marsh K, Forster D, Waruiru C, Mwangi I, Winstanley M, Marsh V, et al. Indicators of life-threatening malaria in African children. N Engl J Med 1995; 332: 1399–404.

Mathanga DP, Walker ED, Wilson ML, Ali D, Taylor TE, Laufer MK. Malaria control in Malawi: current status and directions for the future. Acta Trop 2012; 121: 212–7.

Maude RJ, Beare NA V, Abu Sayeed A, Chang CC, Charunwatthana P, Faiz MA, et al. The spectrum of retinopathy in adults with Plasmodium falciparum malaria. Trans R Soc Trop Med Hyg 2009; 103: 665–71.

Maude RJ, Plewes K, Dimock J, Dondorp AM. Low-cost portable fluorescein angiography. Br J Ophthalmol 2011; 95: 1213–5.

Mckenna MC, Gruetter R, Sonnewald U, Waagepetersen HS, Schousboe A. Energy metabolism of the brain. In: Seigel GJ, Albers RW, Brady ST, Price DL, editor(s). Basic neurochemistry: molecular, cellular and medical aspects. Amsterdam, Boston: Elsevier; 2006. p. 535.

McLeod D. Krogh cylinders in retinal development, panretinal hypoperfusion and diabetic retinopathy. Acta Ophthalmol 2010; 88: 817–35.

Medana IM, Day NPJ, Sachanonta N, Mai NTH, Dondorp AM, Pongponratn E, et al. Coma in fatal adult human malaria is not caused by cerebral oedema. Malar J 2011; 10: 267.

Meder JF, Chiras J, Roland J, Guinet P, Bracard S, Bargy F. Venous territories of the brain. J Neuroradiol 1994; 21: 118–33.

Mendis KR, Balaratnasingam C, Yu P, Barry CJ, McAllister IL, Cringle SJ, et al. Correlation of histologic and clinical images to determine the diagnostic value of fluorescein angiography for studying retinal capillary detail. Invest Ophthalmol Vis Sci 2010; 51: 5864–9.

Migliorini S. Emorragie retiniche da infezione malarica. Morgagni 1917; 59: 69.

Miller LH, Ackerman HC, Su X-Z, Wellems TE. Malaria biology and disease pathogenesis: insights for new treatments. Nat Med 2013; 19: 156–67.

Milner D, Factor R, Whitten R, Carr RA, Kamiza S, Pinkus G, et al. Pulmonary pathology in pediatric cerebral malaria. Hum Pathol 2013

Milner DA, Dzamalala CP, Liomba NG, Molyneux ME, Taylor TE. Sampling of supraorbital brain tissue after death: improving on the clinical diagnosis of cerebral malaria. J Infect Dis 2005; 191: 805–8.

Milner DA, Lee JJ, Frantzreb C, Whitten RO, Kamiza S, Carr RA, et al. Quantitative Assessment of Multiorgan Tissue Sequestration in Fatal Pediatric Cerebral Malaria. J Infect Dis 2015

Milner DA, Vareta J, Valim C, Montgomery J, Daniels RF, Volkman SK, et al. Human cerebral malaria and Plasmodium falciparum genotypes in Malawi. Malar J 2012; 11: 35.

Milner DA, Whitten RO, Kamiza S, Carr R, Liomba G, Dzamalala C, et al. The systemic pathology of cerebral malaria in African children. Front Cell Infect Microbiol 2014; 4: 104.

Mishra SK, Panigrahi P, Mishra R, Mohanty S. Prediction of outcome in adults with severe falciparum malaria: a new scoring system. Malar J 2007; 6: 24.

Miyawaki E, Statland J. Cerebral Blood Vessels: Arteries. In: Aminoff MJ, Daroff RB, editor(s). Encyclopedia of the Neurological Sciences. New York: Academic Press; 2003. a. p. 584–591.

Miyawaki E, Statland J. Cerebral Blood Vessels: Veins and Venous Sinuses. In: Encyclopedia of the Neurological Sciences. New York: Academic Press; 2003. b. p. 591–594.

Miyawaki. Cerebral Blood Vessels : Veins and Venous Sinuses. 2003. p. 591–594.

Mohammed I, Ibrahim UY, Mukhtar M, Farouq Z, Obiagwu PN, Yashua AH. Malarial retinopathy in northern Nigerian children. Trop Doct 2010; 40: 50–2.

Molenberghs G, Geys H, Buyse M. Evaluation of surrogate endpoints in randomized experiments with mixed discrete and continuous outcomes. Stat Med 2001; 20: 3023–38.

Molyneux ME, Taylor TE, Wirima JJ, Borgstein A. Clinical features and prognostic indicators in paediatric cerebral malaria: a study of 131 comatose Malawian children. Q J Med 1989; 71: 441–59.

Montgomery J, Mphande FA, Berriman M, Pain A, Rogerson SJ, Taylor TE, et al. Differential var gene expression in the organs of patients dying of falciparum malaria. Mol Microbiol 2007; 65: 959–67.

Moody DM, Bell MA, Challa VR. Features of the cerebral vascular pattern that predict vulnerability to perfusion or oxygenation deficiency: an anatomic study. AJNR Am J Neuroradiol 1990; 11: 431–9.

Morano G. Contributo clinico allo studio delle affezioni oculare nella malaria. Ann di Ottalmol 1909; 38: 829–834.

Motegi A, Kan T, Ko S, Syu S. Ophthalmologische beobachtungen an 100 fällen von malaria-kranken. Klin Monbl Augenheilkd 1934; 92: 797–800.

Moxon CA, Chisala N V, Wassmer SC, Taylor TE, Seydel KB, Molyneux ME, et al. Persistent endothelial activation and inflammation after Plasmodium falciparum Infection in Malawian children. J Infect Dis 2014; 209: 610–5.

Moxon CA, Grau GE, Craig AG. Malaria: modification of the red blood cell and consequences in the human host. Br J Haematol 2011

Moxon CA, Heyderman RS, Wassmer SC. Dysregulation of coagulation in cerebral malaria. Mol Biochem Parasitol 2009; 166: 99–108.

Moxon CA, Wassmer SC, Milner DA, Chisala N V, Taylor TE, Seydel KB, et al. Loss of endothelial protein C receptors links coagulation and inflammation to parasite sequestration in cerebral malaria in African children. Blood 2013; 122: 842–51.

Mullins RF, Skeie JM, Malone EA, Kuehn MH. Macular and peripheral distribution of ICAM-1 in the human choriocapillaris and retina. Mol Vis 2006; 12: 224–35.

Murphy SC, Breman JG. Gaps in the childhood malaria burden in Africa: cerebral malaria, neurological sequelae, anemia, respiratory distress, hypoglycemia, and complications of pregnancy. Am J Trop Med Hyg 2001; 64: 57–67.

Nag S, Kapadia A, Stewart DJ. Review: molecular pathogenesis of blood-brain barrier breakdown in acute brain injury. Neuropathol Appl Neurobiol 2011; 37: 3–23.

Nag S, Manias JL, Stewart DJ. Pathology and new players in the pathogenesis of brain edema. Acta Neuropathol 2009; 118: 197–217.

Nag S. The Blood-Brain and Other Neural Barriers: reviews and protocols. Springer; 2011.

Nagai M, Terao S, Yilmaz G, Yilmaz CE, Esmon CT, Watanabe E, et al. Roles of inflammation and the activated protein C pathway in the brain edema associated with cerebral venous sinus thrombosis. Stroke 2010; 41: 147–52.

Nagaoka T, Sato E, Takahashi A, Sogawa K, Yokota H, Yoshida A. Effect of aging on retinal circulation in normotensive healthy subjects. Exp Eye Res 2009; 89: 887–891.

Nagaoka T, Yoshida A. Noninvasive evaluation of wall shear stress on retinal microcirculation in humans. Invest Ophthalmol Vis Sci 2006; 47: 1113–9.

Nagatake T, Hoang VT, Tegoshi T, Rabbege J, Ann TK, Aikawa M. Pathology of falciparum malaria in Vietnam. Am J Trop Med Hyg 1992; 47: 259–64.

Nakamura Y, Okudera T, Hashimoto T. Vascular architecture in white matter of neonates: its relationship to periventricular leukomalacia. J Neuropathol Exp Neurol 1994; 53: 582–9.

Narsaria N, Mohanty C, Das BK, Mishra SP, Prasad R. Oxidative Stress in Children with Severe Malaria. J Trop Pediatr 2011; 58: 147–150.

Nelson MD, Gonzalez-Gomez I, Gilles FH. Dyke Award. The search for human telencephalic ventriculofugal arteries. AJNR Am J Neuroradiol 1991; 12: 215–22.

Newton CR, Crawley J, Sowumni A, Waruiru C, Mwangi I, English M, et al. Intracranial hypertension in Africans with cerebral malaria. Arch Dis Child 1997; 76: 219–26.

Newton CR, Marsh K, Peshu N, Kirkham FJ. Perturbations of cerebral hemodynamics in Kenyans with cerebral malaria. Pediatr Neurol 1996; 15: 41–9.

Newton CR, Peshu N, Kendall B, Kirkham FJ, Sowunmi A, Waruiru C, et al. Brain swelling and ischaemia in Kenyans with cerebral malaria. Arch Dis Child 1994; 70: 281–7.

Newton CR, Winstanley PA, Marsh K. Retinal haemorrhages in falciparum malaria. Arch Dis Child 1991; 66: 753.

Newton CRJC, Kirkham FJ, Winstanley PA, Pasvol G, Peshu N, Warrell DA, et al. Intracranial pressure in African children with cerebral malaria. Lancet 1991; 337: 573–576.

Newton PN, Stepniewska K, Dondorp A, Silamut K, Chierakul W, Krishna S, et al. Prognostic indicators in adults hospitalized with falciparum malaria in Western Thailand. Malar J 2013; 12: 229.

Nguyen J, Nishimura N, Fetcho RN, Iadecola C, Schaffer CB. Occlusion of cortical ascending venules causes blood flow decreases, reversals in flow direction, and vessel dilation in upstream capillaries. J Cereb blood flow Metab 2011: 1–12.

Nishimura N, Rosidi NL, Iadecola C, Schaffer CB. Limitations of collateral flow after occlusion of a single cortical penetrating arteriole. J Cereb blood flow Metab 2010; 30: 1914–27.

Nonaka H, Akima M, Hatori T, Nagayama T, Zhang Z, Ihara F. The microvasculature of the cerebral white matter: arteries of the subcortical white matter. J Neuropathol Exp Neurol 2003a; 62: 154–61.

Nonaka H, Akima M, Hatori T, Nagayama T, Zhang Z, Ihara F. Microvasculature of the human cerebral white matter: arteries of the deep white matter. Neuropathology 2003b; 23: 111–8.

Nonaka H, Akima M, Nagayama T, Hatori T. The fundamental architecture of the microvasculature of the basal ganglia and changes in senility. Neuropathology 1998; 18: 47–54.

Van Noorden R. Insider view of cells scoops Nobel. Nature 2014; 514: 286.

Nowinski WL. Proposition of a new classification of the cerebral veins based on their termination. Surg Radiol Anat 2012; 34: 107–14.

Oka K, Rhoton AL, Barry M, Rodriguez R. Microsurgical anatomy of the superficial veins of the cerebrum. Neurosurgery 1985; 17: 711–48.

Okiro EA, Al-Taiar A, Reyburn H, Idro R, Berkley JA, Snow RW. Age patterns of severe paediatric malaria and their relationship to Plasmodium falciparum transmission intensity. Malar J 2009; 8: 4.

Olumese PE, Adeyemo AA, Gbadegesin RA, Walker O. Retinal haemorrhage in cerebral malaria. East Afr Med J 1997; 74: 285–7.

Oluwayemi OI, Brown BJ, Oyedeji OA, Adegoke SA, Adebami OJ, Oyedeji GA. Clinical and laboratory predictors of outcome in cerebral malaria in suburban Nigeria. J Infect Dev Ctries 2013; 7: 600–7.

Ong Y-T, Hilal S, Cheung CY-L, Xu X, Chen C, Venketasubramanian N, et al. Retinal vascular fractals and cognitive impairment. Dement Geriatr Cogn Dis Extra 2014; 4: 305–13.

Ong Y-T, De Silva DA, Cheung CY, Chang H-M, Chen CP, Wong MC, et al. Microvascular structure and network in the retina of patients with ischemic stroke. Stroke 2013; 44: 2121–7.

Ono M, Rhoton AL, Peace D, Rodriguez RJ. Microsurgical anatomy of the deep venous system of the brain. Neurosurgery 1984; 15: 621–57.

Oo MM, Aikawa M, Than T, Aye TM, Myint PT, Igarashi I, et al. Human cerebral malaria: a pathological study. J Neuropathol Exp Neurol 1987; 46: 223–31.

Pagliari G. L’infezione malarica in rapporto alle malattie dell'occhio (Malarial infection in relation to diseases of the eye). Gazz Int Med Chir 1933; 41: 18–20.

Pain A, Ferguson DJ, Kai O, Urban BC, Lowe B, Marsh K, et al. Platelet-mediated clumping of Plasmodium falciparum-infected erythrocytes is a common adhesive phenotype and is associated with severe malaria. Proc Natl Acad Sci U S A 2001; 98: 1805–10.

Pasvol G, Weatherall DJ, Wilson RJ. Effects of foetal haemoglobin on susceptibility of red cells to Plasmodium falciparum. Nature 1977; 270: 171–3.

Patton N, Aslam T, Macgillivray T, Pattie A, Deary IJ, Dhillon B. Retinal vascular image analysis as a potential screening tool for cerebrovascular disease: a rationale based on homology between cerebral and retinal microvasculatures. J Anat 2005; 206: 319–48.

Patton N, Aslam TM, MacGillivray T, Deary IJ, Dhillon B, Eikelboom RH, et al. Retinal image analysis: concepts, applications and potential. Prog Retin Eye Res 2006; 25: 99–127.

Pauers MJ. One fish, two fish, red fish, blue fish: geography, ecology, sympatry, and male coloration in the lake Malawi cichlid genus labeotropheus (perciformes: cichlidae). Int J Evol Biol 2011; 2011: 575469.

Penman A, Talbot JF, Chuang EL, Bird AC, Serjeant GR. Peripheral retinal vasculature in normal Jamaican children. Br J Ophthalmol 1994; 78: 615–7.

Pereyra G. Emorragie retiniche da malaria. Arch Di Ottal 1922; 29: 49.

Phiri HT, Bridges DJ, Glover SJ, van Mourik J a, de Laat B, M'baya B, et al. Elevated plasma von Willebrand factor and propeptide levels in malawian children with malaria. PLoS One 2011; 6: e25626.

Poncet F. De la retino-choroidite palustre. Ann d'Oculistique 1879; 79: 201–218.

Pongponratn E, Riganti M, Punpoowong B, Aikawa M. Microvascular sequestration of parasitized erythrocytes in human falciparum malaria: a pathological study. Am J Trop Med Hyg 1991; 44: 168–75.

Pongponratn E, Turner GDH, Day NPJ, Phu NH, Simpson JA, Stepniewska K, et al. An ultrastructural study of the brain in fatal Plasmodium falciparum malaria. Am J Trop Med Hyg 2003; 69: 345–59.

Ponsford MJ, Medana IM, Prapansilp P, Hien TT, Lee SJ, Dondorp AM, et al. Sequestration and microvascular congestion are associated with coma in human cerebral malaria. J Infect Dis 2012; 205: 663–71.

Popel AS, Johnson PC. Microcirculation and Hemorheology. Annu Rev Fluid Mech 2005; 37: 43–69.

Postels DG, Birbeck GL, Valim C, Mannor KM, Taylor TE. Seasonal Differences in Retinopathy-Negative versus Retinopathy-Positive Cerebral Malaria. Am J Trop Med Hyg 2012; 88: 315–318.

Postels DG, Li C, Birbeck GL, Taylor TE, Seydel KB, Kampondeni SD, et al. Brain MRI of Children with Retinopathy-Negative Cerebral Malaria. Am J Trop Med Hyg 2014; 91: 943–949.

Postels DG, Taylor TE, Molyneux M, Mannor K, Kaplan PW, Seydel KB, et al. Neurologic outcomes in retinopathy-negative cerebral malaria survivors. Neurology 2012; 79: 1268–72.

Potchen MJ, Kampondeni SD, Ibrahim K, Bonner J, Seydel KB, Taylor TE, et al. NeuroInterp: a method for facilitating neuroimaging research on cerebral malaria. Neurology 2013; 81: 585–8.

Potchen MJ, Kampondeni SD, Seydel KB, Birbeck GL, Hammond CA, Bradley WG, et al. Acute brain MRI findings in 120 Malawian children with cerebral malaria: new insights into an ancient disease. Am J Neuroradiol 2012; 33: 1740–6.

Pournaras CJ, Rungger-Brändle E, Riva CE, Hardarson SH, Stefansson E. Regulation of retinal blood flow in health and disease. Prog Retin Eye Res 2008; 27: 284–330.

Prentice RL. Surrogate endpoints in clinical trials: definition and operational criteria. Stat Med 1989; 8: 431–40.

Pries AR, Secomb TW, Gaehtgens P. The endothelial surface layer. Pflugers Arch 2000; 440: 653–66.

Pries AR, Secomb TW. Rheology of the microcirculation. Clin Hemorheol Microcirc 2003; 29: 143–8.

Pries AR, Secomb TW. Blood Flow in Microvascular Networks. In: Tuma RF, Duran WN, Ley K, editor(s). Handbook of Physiology: Microcirculation. London: Academic Press; 2008. p. 3–36.

Qu Y, Case M. Quantifying the effect of the surrogate marker by information gain. Biometrics 2007; 63: 958–62; author reply 962–3.

Rasalkar DD, Paunipagar BK, Sanghvi D, Sonawane BD, Loniker P. Magnetic resonance imaging in cerebral malaria: a report of four cases. Br J Radiol 2011; 84: 380–5.

Reina-de La Torre F, Rodriguez-baeza A, Sahuquillo-Barris J. Morphological Characteristics and Distribution Pattern of the Arterial Vessels in Human Cerebral Cortex : A Scanning Electron Microscope Study. Anat Rec 1998; 251: 87–96.

Reyburn H, Mbatia R, Drakeley C, Bruce J, Carneiro I, Olomi R, et al. Association of transmission intensity and age with clinical manifestations and case fatality of severe Plasmodium falciparum malaria. JAMA 2005; 293: 1461–70.

Reyburn H, Mbatia R, Drakeley C, Carneiro I, Mwakasungula E, Mwerinde O, et al. Overdiagnosis of malaria in patients with severe febrile illness in Tanzania: a prospective study. BMJ 2004; 329: 1212.

Ring CP, Pearson TC, Sanders MD, Wetherley-Mein G. Viscosity and retinal vein thrombosis. Br J Ophthalmol 1976; 60: 397–410.

Roca-Feltrer A, Carneiro I, Armstrong Schellenberg JRM. Estimates of the burden of malaria morbidity in Africa in children under the age of 5 years. Trop Med Int Health 2008; 13: 771–83.

Roca-Feltrer A, Carneiro I, Smith L, Schellenberg J, Greenwood B, Schellenberg D. The age patterns of severe malaria syndromes in sub-Saharan Africa across a range of transmission intensities and seasonality settings. Malar J 2010; 9: 282.

Roca-Feltrer A, Kwizombe CJ, Sanjoaquin MA, Sesay SSS, Faragher B, Harrison J, et al. Lack of decline in childhood malaria, Malawi, 2001-2010. Emerg Infect Dis 2012; 18: 272–8.

Rochtchina E, Wang JJ, Taylor B, Wong TY, Mitchell P. Ethnic variability in retinal vessel caliber: a potential source of measurement error from ocular pigmentation?--the Sydney Childhood Eye Study. Invest Ophthalmol Vis Sci 2008; 49: 1362–6.

Rowe JA, Claessens A, Corrigan RA, Arman M. Adhesion of Plasmodium falciparum-infected erythrocytes to human cells: molecular mechanisms and therapeutic implications. Expert Rev Mol Med 2009; 11: e16.

Sakai F, Nakazawa K, Tazaki Y, Ishii K, Hino H, Igarashi H, et al. Regional cerebral blood volume and hematocrit measured in normal human volunteers by single-photon emission computed tomography. J Cereb blood flow Metab 1985; 5: 207–13.

Sarda V, Nakashima K, Wolff B, Sahel J-A, Paques M. Topography of patchy retinal whitening during acute perfused retinal vein occlusion by optical coherence tomography and adaptive optics fundus imaging. Eur J Ophthalmol 2011; 21: 653–656.

Sarpeshkar R. Ultra low power bioelectronics: fundamentals, biomedical applications, and bio-inspired systems. Cambridge: Cambridge University press; 2010.

Schaller B. Physiology of cerebral venous blood flow: from experimental data in animals to normal function in humans. Brain Res Rev 2004; 46: 243–60.

Schémann JF, Doumbo O, Malvy D, Traore L, Kone A, Sidibe T, et al. Ocular lesions associated with malaria in children in Mali. Am J Trop Med Hyg 2002; 67: 61–3.

Schlosshauer B, Steuer H. Comparative Anatomy, Physiology and In Vitro Models of the Blood-Brain and Blood-Retina Barrier [Internet]. Curr Med Chem 2002: 175–186.Available from: http://connection.ebscohost.com/c/articles/11135040/comparative-anatomy-physiology-vitro-models-blood-brain-blood-retina-barrier

Schmid-Schönbein GW. Biomechanics of microcirculatory blood perfusion. Annu Rev Biomed Eng 1999; 1: 73–102.

Schmitt MMN, Megens RTA, Zernecke A, Bidzhekov K, van den Akker NM, Rademakers T, et al. Endothelial junctional adhesion molecule-a guides monocytes into flow-dependent predilection sites of atherosclerosis. Circulation 2014; 129: 66–76.

Sedan J. Cecite temporaire par angiospasme retinien d’origine paludique. Ann d’oculistque 1929; 166: 705.

von Seidlein L, Olaosebikan R, Hendriksen ICE, Lee SJ, Adedoyin OT, Agbenyega T, et al. Predicting the clinical outcome of severe falciparum malaria in african children: findings from a large randomized trial. Clin Infect Dis 2012; 54: 1080–90.

Seifert T, Secher NH. Sympathetic influence on cerebral blood flow and metabolism during exercise in humans. Prog Neurobiol 2011; 95: 406–26.

Sein KK, Maeno Y, Thuc H V, Anh TK, Aikawa M. Differential sequestration of parasitized erythrocytes in the cerebrum and cerebellum in human cerebral malaria. Am J Trop Med Hyg 1993; 48: 504–11.

Semmer AE, McLoon LK, Lee MS. Orbital vascular anatomy. In: Dartt DA, editor(s). Encyclopedia of the Eye. Elsevier; 2010. p. 241–251.

Seydel KB, Fox LL, Glover SJ, Reeves MJ, Pensulo P, Muiruri A, et al. Plasma Concentrations of Parasite Histidine-Rich Protein 2 Distinguish Between Retinopathy-Positive and Retinopathy-Negative Cerebral Malaria in Malawian Children. J Infect Dis 2012; 206: 309–18.

Seydel KB, Kampondeni SD, Valim C, Potchen MJ, Milner DA, Muwalo FW, et al. Brain Swelling and Death in Children with Cerebral Malaria. N Engl J Med 2015; 372: 1126–1137.

Seydel KB, Milner DA, Kamiza SB, Molyneux ME, Taylor TE. The Distribution and Intensity of Parasite Sequestration in Comatose Malawian Children. J Infect Dis 2006; 194: 208–205.

Shapiro K, Marmarou A, Shulman K. Characterization of clinical CSF dynamics and neural axis compliance using the pressure-volume index: I. The normal pressure-volume index. Ann Neurol 1980; 7: 508–14.

Silamut K, Phu NH, Whitty C, Turner GD, Louwrier K, Mai NT, et al. A quantitative analysis of the microvascular sequestration of malaria parasites in the human brain. Am J Pathol 1999; 155: 395–410.

Smith A, Beare NA, Musumba CO, Lochhead J, Newton CR, Harding SP. New classification of acute papilledema in children with severe malaria. J Pediatr Neurol 2009; 7: 381–388.

Smith JR, Choi D, Chipps TJ, Pan Y, Zamora DO, Davies MH, et al. Unique gene expression profiles of donor-matched human retinal and choroidal vascular endothelial cells. Invest Ophthalmol Vis Sci 2007; 48: 2676–84.

Snow RW, Bastos de Azevedo I, Lowe BS, Kabiru EW, Nevill CG, Mwankusye S, et al. Severe childhood malaria in two areas of markedly different falciparum transmission in east Africa. Acta Trop 1994; 57: 289–300.

Snow RW, Omumbo JA, Lowe B, Molyneux CS, Obiero JO, Palmer A, et al. Relation between severe malaria morbidity in children and level of Plasmodium falciparum transmission in Africa. Lancet 1997; 349: 1650–4.

Sokoloff L. Cerebral metabolism and blood flow. In: Encyclopedia of the Neurological Sciences. New York: Academic Press; 2003. p. 609–617.

Southern CL, Beare NA, Falsini B, Lochhead J, Molyneux ME, Taylor TE, et al. Delayed visual evoked potentials in children with Plasmodium falciparum malaria and reduced consciousness. J Pediatr Neurol 2008; 6: 17–24.

Sperber GO, Bill A. Blood flow and glucose consumption in the optic nerve, retina and brain: effects of high intraocular pressure. Exp Eye Res 1985; 41: 639–53.

Spitz S. The pathology of acute falciparum malaria. Mil Surg 1946; 99: 555–72.

Spitznas M, Bornfeld N. The architecture of the most peripheral retinal vessels. Albrecht Von Graefes Arch Klin Exp Ophthalmol 1977; 203: 217–29.

van der Staay FJ, Arndt SS, Nordquist RE. Evaluation of animal models of neurobehavioral disorders. Behav Brain Funct 2009; 5: 11.

Stefánsson E, Wilson CA, Lightman SL, Kuwabara T, Palestine AG, Wagner HG. Quantitative measurements of retinal edema by specific gravity determinations. Invest Ophthalmol Vis Sci 1987; 28: 1281–9.

Steuer H, Jaworski A, Elger B, Kaussmann M, Keldenich J, Schneider H, et al. Functional characterization and comparison of the outer blood-retina barrier and the blood-brain barrier. Invest Ophthalmol Vis Sci 2005; 46: 1047–53.

Steup M. Epistemology [Internet]. Stanford Encycl Philos 2005[cited 2015 Jul 26] Available from: http://plato.stanford.edu/entries/epistemology/

Stins MF, Pearce D, Di Cello F, Erdreich-Epstein A, Pardo CA, Sik Kim K. Induction of intercellular adhesion molecule-1 on human brain endothelial cells by HIV-1 gp120: role of CD4 and chemokine coreceptors. Lab Invest 2003; 83: 1787–98.

Sulzer D. Troubles de la vision dans l’impaludisme. Arch. D’opht. 1890: 193–203.

Sun C, Ponsonby A-L, Wong TY, Brown SA, Kearns LS, Cochrane J, et al. Effect of birth parameters on retinal vascular caliber: the Twins Eye Study in Tasmania. Hypertension 2009; 53: 487–93.

Suwanarusk R, Cooke BM, Dondorp AM, Silamut K, Sattabongkot J, White NJ, et al. The deformability of red blood cells parasitized by Plasmodium falciparum and P. vivax. J Infect Dis 2004; 189: 190–4.

Takahashi T, Shirane R, Sato S, Yoshimoto T. Developmental changes of cerebral blood flow and oxygen metabolism in children. AJNR Am J Neuroradiol 1999; 20: 917–22.

Tam J, Martin JA, Roorda A. Noninvasive visualization and analysis of parafoveal capillaries in humans. Invest Ophthalmol Vis Sci 2010; 51: 1691–8.

Tam J, Tiruveedhula P, Roorda A. Characterization of single-file flow through human retinal parafoveal capillaries using an adaptive optics scanning laser ophthalmoscope. Biomed Opt Express 2011; 2: 781–93.

Tapp RJ, Williams C, Witt N, Chaturvedi N, Evans R, Thom SA, et al. Impact of size at birth on the microvasculature: the Avon Longitudinal Study of Parents and Children. Pediatrics 2007; 120: e1225–8.

Taylor B, Rochtchina E, Wang JJ, Wong TY, Heikal S, Saw SM, et al. Body mass index and its effects on retinal vessel diameter in 6-year-old children. Int J Obes 2007; 31: 1527–33.

Taylor TE, Fu WJ, Carr RA, Whitten RO, Mueller JS, Fosiko NG, et al. Differentiating the pathologies of cerebral malaria by postmortem parasite counts. Nat Med 2004; 10: 143–5.

Taylor TE, Molyneux ME, Wirima JJ, Fletcher KA, Morris K. Blood glucose levels in Malawian children before and during the administration of intravenous quinine for severe falciparum malaria. N Engl J Med 1988; 319: 1040–7.

Taylor TE. Caring for children with cerebral malaria: insights gleaned from 20 years on a research ward in Malawi. Trans R Soc Trop Med Hyg 2009; 103 Suppl: S6–10.

Teksam M, Moharir M, Deveber G, Shroff M. Frequency and topographic distribution of brain lesions in pediatric cerebral venous thrombosis. AJNR Am J Neuroradiol 2008; 29: 1961–5.

Thanachartwet V, Desakorn V, Sahassananda D, Kyaw Win KKY, Supaporn T. Acute Renal Failure in Patients with Severe Falciparum Malaria: Using the WHO 2006 and RIFLE Criteria. Int J Nephrol 2013; 2013: 841518.

Timmons SD. Elevated intracranial pressure. In: Textbook of neurointensive care. 2013.

Toulant P. Complications oculaires du paludisme. Acta ophth Orient 1938; 1: 18–27.

Turner G. Cerebral malaria. Brain Pathol 1997; 7: 569–82.

Turner L, Lavstsen T, Berger SS, Wang CW, Petersen JE V., Avril M, et al. Severe malaria is associated with parasite binding to endothelial protein C receptor. Nature 2013; 498: 502–5.

Vandenbroucke JP, von Elm E, Altman DG, Gøtzsche PC, Mulrow CD, Pocock SJ, et al. Strengthening the Reporting of Observational Studies in Epidemiology (STROBE): explanation and elaboration. PLoS Med 2007; 4: e297.

VanderWeele TJ. Surrogate measures and consistent surrogates. Biometrics 2013; 69: 561–5.

Varela M, Groves AM, Arichi T, Hajnal J V. Mean cerebral blood flow measurements using phase contrast MRI in the first year of life. NMR Biomed 2012; 25: 1063–72.

Villard H. Les complications oculaires du paludisme. Arch. D'opht. 1930; 47: 200.

Vovenko E. Distribution of oxygen tension on the surface of arterioles, capillaries and venules of brain cortex and in tissue in normoxia: an experimental study on rats. Pflugers Arch 1999; 437: 617–23.

Vrabec TR. Posterior segment manifestations of HIV/AIDS. Surv Ophthalmol 2004; 49: 131–57.

Walker AS, Eyre DW, Wyllie DH, Dingle KE, Griffiths D, Shine B, et al. Relationship between bacterial strain type, host biomarkers, and mortality in Clostridium difficile infection. Clin Infect Dis 2013; 56: 1589–600.

Wang Q, Kocaoglu OP, Cense B, Bruestle J, Jonnal RS, Gao W, et al. Imaging retinal capillaries using ultrahigh-resolution optical coherence tomography and adaptive optics. Invest Ophthalmol Vis Sci 2011; 52: 6292–9.

Wardlaw JM. Blood-brain barrier and cerebral small vessel disease. J Neurol Sci 2010; 299: 66–71.

Warlomont. Analectes ophthalmologiques—Fievre larvee double quotidienne, forme amaurotique. Ann Ocul (Paris) 1866; 54: 317–318.

Weir CJ, Walley RJ. Statistical evaluation of biomarkers as surrogate endpoints: a literature review. Stat Med 2006; 25: 183–203.

Werner H. Uber Netzhautblutungen bei Malaria. Arch fur schiffs und tropen Hyg 1911; 15: 431–435.

White NJ, Turner GDH, Day NPJ, Dondorp AM. Lethal malaria: marchiafava and bignami were right. J Infect Dis 2013; 208: 192–8.

White VA, Lewallen S, Beare N, Kayira K, Carr RA, Taylor TE. Correlation of retinal haemorrhages with brain haemorrhages in children dying of cerebral malaria in Malawi. Trans R Soc Trop Med Hyg 2001; 95: 618–21.

White VA, Lewallen S, Beare NA, Molyneux ME, Taylor TE. Retinal pathology of pediatric cerebral malaria in Malawi. PLoS One 2009; 4: e4317.

Whitten R, Milner DA, Yeh MM, Kamiza S, Molyneux ME, Taylor TE. Liver pathology in Malawian children with fatal encephalopathy. Hum Pathol 2011; 42: 1230–9.

Widjaja E, Griffiths PD. Intracranial MR venography in children: normal anatomy and variations. AJNR Am J Neuroradiol 2004; 25: 1557–62.

Williamson TH, Harris A. Ocular blood flow measurement. Br J Ophthalmol 1994; 78: 939–45.

Willner P. Validation criteria for animal models of human mental disorders: Learned helplessness as a paradigm case. Prog Neuro-Psychopharmacology Biol Psychiatry 1986; 10: 677–690.

Wilson ML, Walker ED, Mzilahowa T, Mathanga DP, Taylor TE. Malaria elimination in Malawi: research needs in highly endemic, poverty-stricken contexts. Acta Trop 2012; 121: 218–26.

Wintermark M, Lepori D, Cotting J, Roulet E, van Melle G, Meuli R, et al. Brain perfusion in children: evolution with age assessed by quantitative perfusion computed tomography. Pediatrics 2004; 113: 1642–52.

Wolfram-Gabel R, Maillot C. Vascular networks of the nucleus lentiformis. Surg Radiol Anat 1994; 16: 373–77.

Wong-Riley M. Energy metabolism of the visual system. Eye Brain 2010; 2: 99–116.

World Health Organization. World Malaria Report [Internet]. 2014aAvailable from: http://apps.who.int/iris/bitstream/10665/144852/2/9789241564830_eng.pdf

World Health Organization. Severe malaria. Trop Med Int Heal 2014b; 19 Suppl 1: 7–131.

Wu Z, He P, Geng Z. Sufficient conditions for concluding surrogacy based on observed data. Stat Med 2011; 30: 2422–34.

Xu H, Manivannan A, Goatman KA, Liversidge J, Sharp PF, Forrester J V, et al. Improved leukocyte tracking in mouse retinal and choroidal circulation. Exp Eye Res 2002; 74: 403–10.

Yablonskiy DA, Sukstanskii AL, He X. Blood oxygenation level-dependent (BOLD)-based techniques for the quantification of brain hemodynamic and

metabolic properties - theoretical models and experimental approaches. NMR Biomed 2013; 26: 963–86.

Yachnis AT. Introduction to basic neuropathology. In: Layon AJ, Gabrielli A, Friedman WA, editor(s). Textbook of neuro-intensive care. Springer; 2013. p. 89–106.

Yadav P, Sharma R, Kumar S, Kumar U. Magnetic resonance features of cerebral malaria. Acta Radiol 2008; 49: 566–9.

Yospaiboon Y, Lawtiantong T, Chotibutr S. Clinical observations of ocular quinine intoxication. Jpn J Ophthalmol 1984; 28: 409–15.

Yu DY, Cringle SJ. Oxygen distribution and consumption within the retina in vascularised and avascular retinas and in animal models of retinal disease. Prog Retin Eye Res 2001; 20: 175–208.

Yu PK, Balaratnasingam C, Cringle SJ, McAllister IL, Provis J, Yu D-Y. Microstructure and network organization of the microvasculature in the human macula. Invest Ophthalmol Vis Sci 2010; 51: 6735–43.

Zehetner C, Bechrakis NE. White centered retinal hemorrhages in vitamin b(12) deficiency anemia. Case Rep Ophthalmol 2011; 2: 140–4.

Zhao Y, MacCormick IJ, Parry DG, Beare NA, Harding SP, Zheng Y. Automated Detection of Vessel Abnormalities on Fluorescein Angiogram in Malarial Retinopathy. Sci Rep 2015; 5: 11154.

Zhao Y, MacCormick IJ, Parry DG, Leach S, Beare NA, Harding SP, et al. Automated detection of leakage in fluorescein angiography images with application to malarial retinopathy. Sci Rep 2015; 5: 10425.

Zheng Y, Kwong MT, MacCormick IJ, Beare NA, Harding SP. A Comprehensive Texture Segmentation Framework for Segmentation of Capillary Non-Perfusion Regions in Fundus Fluorescein Angiograms. PLoS One 2014; 9: e93624.

CIA World Factbook | Malawi [Internet]. [cited 2015 May 27] Available from: https://www.cia.gov/library/publications/the-world-factbook/geos/mi.html

The World Bank | Data [Internet]. [cited 2015 May 27] Available from: http://data.worldbank.org/

UNdata | Malawi [Internet]. [cited 2015 May 27] Available from: http://data.un.org/CountryProfile.aspx?crName=malawi

UNAIDS | Malawi [Internet]. [cited 2015 May 27] Available from: http://www.unaids.org/en/regionscountries/countries/malawi

Transparency International [Internet]. [cited 2015 May 27] Available from: http://www.transparency.org/

Wikipedia | Blantyre [Internet]. Available from: http://en.wikipedia.org/wiki/Blantyre

Malaria atlas project [Internet]. [cited 2015 Jun 12] Available from: http://www.map.ox.ac.uk/

Appendix 1: Ophthalmoscopic grading form for malarial retinopathy

RETINAL STUDIES IN SEVERE MALARIA

Name: ID No:

Date of exam (DD/MM/YYYY): Time of exam (24 hour clock):

Examining doctor: DOB: Weight:

	Right eye	Left eye
Haemorrhages	0 1-5 5-20 20-50 50+ CG	0 1-5 5-20 20-50 50+ CG
% WC	None <50 50-75 >75 NA	None <50 50-75 >75 NA
Papilloedema	Y N CG If Y: mild mod sev	Y N CG If Y: mild mod sev
Hyperaemia	Y N CG	Y N CG
Macular whitening: (≤2.5DD fovea)	0 <1/3 1/3-1 >1 DA CG	0 <1/3 1/3-1 >1 DA CG
Foveal annulus: (500μm fovea)	0 <1/3 1/3-2/3 >2/3 CG	0 <1/3 1/3-2/3 >2/3 CG

Peripheral whitening (by quadrant):

	Right eye	Left eye
Temp	0 1+ 2+ 3+ NS	0 1+ 2+ 3+ NS
Sup	0 1+ 2+ 3+ NS	0 1+ 2+ 3+ NS
Inf	0 1+ 2+ 3+ NS	0 1+ 2+ 3+ NS
Nasal	0 1+ 2+ 3+ NS	0 1+ 2+ 3+ NS

Sum of quadrant scores _____ _____
Number of quadrants seen

Vessel changes (by quadrant):

	Right eye: Arterioles/venules	Right eye: Capillaries	Left eye: Arterioles/venules	Left eye: Capillaries
Temp	0 Or W	0 W NS	0 Or W	0 W NS
Sup	0 Or W	0 W NS	0 Or W	0 W NS
Inf	0 Or W	0 W NS	0 Or W	0 W NS
Nasal	0 Or W	0 W NS	0 Or W	0 W NS

Number of quadrants with vessel change _____ _____
Number of quadrants seen

Subjective overall severity score for child: 0 1+ 2+ 3+

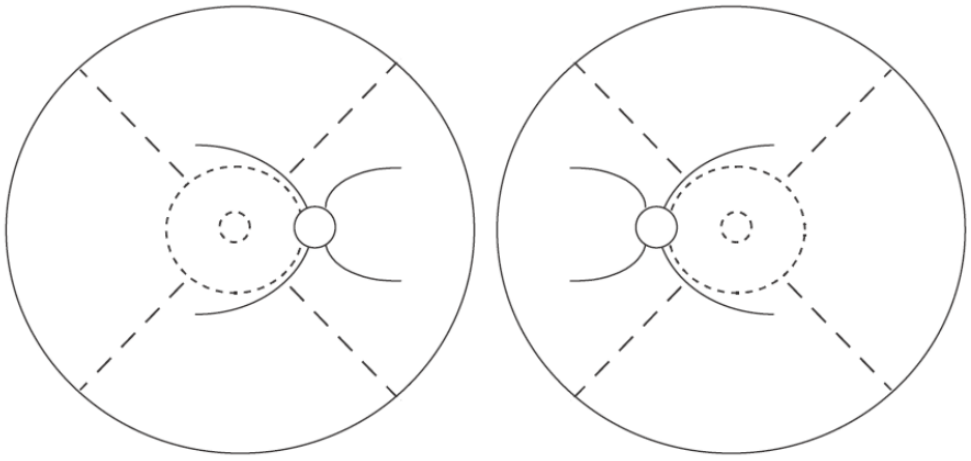

Appendix 2: Fluorescein angiography grading form for malarial retinopathy

Malarial Retinopathy Fluorescein Angiogram Grading Form

Study Eye	Right ☐ Left ☐	**Image Quality**	
		Good	☐
Participant ID	**Date of photographs**	Faiir	☐
		Poor Gradable	☐
Grader Initials	**Date of Grading**	Poor Ungradable	☐

	RETINAL AREA	Number options	SCORE
Area of retina visible			
Is the macula visible?	Macula	(No=0; Yes=1)	☐
What is the farthest peripheral zone visible for each quadrant?	Temporal	(none=0; Zone 1=1; Zone 2=2; Zone 3=3)	☐
	Superior	(none=0; Zone 1=1; Zone 2=2; Zone 3=3)	☐
	Inferior	(none=0; Zone 1=1; Zone 2=2; Zone 3=3)	☐
	Nasal	(none=0; Zone 1=1; Zone 2=2; Zone 3=3)	☐

	GRADE	Number options	SCORE
Capillary Non-Perfusion - CNP - Macula			
No evidence of capilary non-perfusion	Absent CNP	0	
A few small areas of capillary non-perfusion	Grade 1	1	
Total combined area of capillary non-perfusion < 1/3 disc area	Grade 2	2	
Total combined area of capillary non-perfusion 1/3 - 1 disc area	Grade 3	3	
Total combined area of capillary non-perfusion > 1 disc area	Grade 4	4	
Cannot grade	CG	.c	☐
Capillary Non-Perfusion - CNP - Periphery			
No evidence of capilary non-perfusion	Absent CNP	0	
Any capillary non-perfusion, areas each <1/3 disc area	Grade 1	1	
Areas of capillary non-perfusion are each 1/3-1 disc area	Grade 2	2	
One or more large bays, each >1 disc area	Grade 3	3	
One or more bays extend into zone 1 (temporal, superior, inferior quadrants) or zone 2 (nasal quadrant)	Grade 4	4	
cannot grade	CG	.c	☐
Large Focal Leak - LFL			
Number of sites	Count of LFL	write number of sites; write ".c" for CG	☐
Punctate Focal Leak - PFL			
No evidence of punctate focal leak	Absent PFL	0	
1-5 sites of punctate focal leak	Grade 1	1	
6-20 sites of punctate focal leak	Grade 2	2	
21-50 sites of punctate focal leak	Grade 3	3	
>50 sites of punctate focal leak	Grade 4	4	
Cannot grade	CG	.c	☐
Disc Leak - DL			
No evidence of disc leak	Absent DL	0	
Definite disc leak	Definite DL	1	
Disc not visible	NA	.d	
Cannot grade (disc visble but ungradeable)	CG	.c	☐
Post-capillary Venule Complex Leak - PCVL			
No evidence of Post-Capillary Venule Complex leak	Absent PCVL	0	
1-5 sites of Post-Capillary Venule Complex leak	Grade 1	1	
6-20 sites of Post-Capillary Venule Complex leak	Grade 2	2	
21-50 sites Post-Capillary Venule Complex leak	Grade 3	3	
>50 sites of Post-Capillary Venule Complex leak	Grade 4	4	
Cannot grade	CG	.c	☐
Large/small Venule Leak - LVL			
No evidence of large/small venule leak	Absent LVL	0	
<1/3 of all vessel segments display leak	Grade 1	1	
1/3-2/3 of all vessel segments display leak	Grade 2	2	
>2/3 of all vessel segments display leak	Grade 3	3	
Cannot grade	CG	.c	☐

Intra-Vascular Filling Defects - IVFD

Capilary intra-vascular filling defects	(Absent=0; Present=1; Can't grade=.c)	
Post-capillary venule unit intra-vascular filling defects	(Absent=0; Present=1; Can't grade=.c)	
Pre-capillary arteriole unit intra-vascular filling defects	(Absent=0; Present=1; Can't grade=.c)	
Small venule intra-vascular filling defects	(Absent=0; Present=1; Can't grade=.c)	
Small arteriole intra-vascular filling defects	(Absent=0; Present=1; Can't grade=.c)	
Large venule intra-vascular filling defects	(Absent=0; Present=1; Can't grade=.c)	
Large arteriole intra-vascular filling defects	(Absent=0; Present=1; Can't grade=.c)	

Other features - OF

Any other features seen	(No=0; Yes=1; Can't grade=.c)	
Small arteriolar leak	(No=0; Yes=1; Can't grade=.c)	
Large arteriolar leak	(No=0; Yes=1; Can't grade=.c)	
Cystoid macular oedema	(No=0; Yes=1; Can't grade=.c)	
Any other feature not previously described (if yes describe under 'comments', below)	(No=0; Yes=1; Can't grade=.c)	

Comments

Appendix 3: Published papers directly resulting from this thesis

The full text of all papers resulting from this thesis is freely available online. Title pages and abstracts are provided here.

doi:10.1093/brain/awu001 Brain 2014: Page 1 of 24 | 1

BRAIN
A JOURNAL OF NEUROLOGY

REVIEW ARTICLE

Cerebral malaria in children: using the retina to study the brain

Ian J. C. MacCormick,[1,2] Nicholas A. V. Beare,[2,3] Terrie E. Taylor,[5,6] Valentina Barrera,[2] Valerie A. White,[7] Paul Hiscott,[2] Malcolm E. Molyneux,[1,4,8] Baljean Dhillon[9,10] and Simon P. Harding[2,3]

1 Malawi-Liverpool-Wellcome Trust Clinical Research Programme, PO Box 30096, Chichiri, Blantyre 3, Malawi
2 University of Liverpool, Department of Eye and Vision Science, Faculty of Health & Life Sciences, University of Liverpool Room 356, 4th Floor, UCD Building, Daulby Street, Liverpool L69 3GA, UK
3 Royal Liverpool University Hospital, St. Paul's Eye Unit, Prescot St, Liverpool, Merseyside L7 8XP, UK
4 University of Malawi College of Medicine, College of Medicine, P/Bag 360 Chichiri, Blantyre 3 Malawi
5 Blantyre Malaria Project, Blantyre, Malawi
6 Michigan State University, Department of Osteopathic Medical Specialities, West Fee Hall, 909 Fee Road, Room B305, East Lansing, MI 48824, USA
7 Vancouver General Hospital, Department of Pathology and Laboratory Medicine, Vancouver, B.C. V5Z1M9, Canada
8 Liverpool School of Tropical Medicine, Liverpool School of Tropical Medicine, Pembroke Place , Liverpool, L3 5QA , UK
9 University of Edinburgh, Department of Ophthalmology, Edinburgh, UK
10 Princess Alexandra Eye Pavilion, Edinburgh, UK

Correspondence to: Ian J.C. MacCormick,
Malawi-Liverpool-Wellcome Trust Clinical Research Programme,
PO Box 30096, Chichiri,
Blantyre 3, Malawi
E-mail: ian.maccormick@gmail.com

Cerebral malaria is a dangerous complication of *Plasmodium falciparum* infection, which takes a devastating toll on children in sub-Saharan Africa. Although autopsy studies have improved understanding of cerebral malaria pathology in fatal cases, information about *in vivo* neurovascular pathogenesis is scarce because brain tissue is inaccessible in life. Surrogate markers may provide insight into pathogenesis and thereby facilitate clinical studies with the ultimate aim of improving the treatment and prognosis of cerebral malaria. The retina is an attractive source of potential surrogate markers for paediatric cerebral malaria because, in this condition, the retina seems to sustain microvascular damage similar to that of the brain. In paediatric cerebral malaria a combination of retinal signs correlates, in fatal cases, with the severity of brain pathology, and has diagnostic and prognostic significance. Unlike the brain, the retina is accessible to high-resolution, non-invasive imaging. We aimed to determine the extent to which paediatric malarial retinopathy reflects cerebrovascular damage by reviewing the literature to compare retinal and cerebral manifestations of retinopathy-positive paediatric cerebral malaria. We then compared retina and brain in terms of anatomical and physiological features that could help to account for similarities and differences in vascular pathology. These comparisons address the question of whether it is biologically plausible to draw conclusions about unseen cerebral vascular pathogenesis from the visible retinal vasculature in retinopathy-positive paediatric cerebral malaria. Our work addresses an important cause of death and neurodisability in sub-Saharan Africa. We critically appraise evidence for associations between retina and brain neurovasculature in health and disease, and in the process we develop new hypotheses about why these vascular beds are susceptible to sequestration of parasitized erythrocytes.

Keywords: cerebral malaria; cerebral microvasculature; retinal microvasculature; haemorheology; surrogate marker

Received May 27, 2013. Revised October 16, 2013. Accepted November 17, 2013.

doi:10.1093/brain/awu146 Brain 2014: 137; 1–2 | e299

BRAIN
A JOURNAL OF NEUROLOGY

LETTER TO THE EDITOR

Reply: Retinopathy, histidine-rich protein-2 and perfusion pressure in cerebral malaria

Ian J. C. MacCormick,[1,2] Nicholas A. V. Beare,[2,3] Terrie E. Taylor,[4,5,6] Valentina Barrera,[2] Valerie A. White,[7] Paul Hiscott,[2] Malcolm E. Molyneux,[1,4,8] Baljean Dhillon[9,10] and Simon P. Harding[2,3]

1 Malawi-Liverpool-Wellcome Trust Clinical Research Programme, Blantyre, Malawi
2 Department of Eye and Vision Science, University of Liverpool, UK
3 St. Paul's Eye Unit, Royal Liverpool University Hospital, Liverpool, UK
4 College of Medicine, University of Malawi, Blantyre, Malawi
5 Blantyre Malaria Project, Blantyre, Malawi
6 Department of Osteopathic Medical Specialities, Michigan State University, Michigan, USA
7 Department of Pathology and Laboratory Medicine, Vancouver General Hospital, British Columbia, Canada
8 Liverpool School of Tropical Medicine, Liverpool, UK
9 Department of Ophthalmology, University of Edinburgh, Edinburgh, UK
10 Princess Alexandra Eye Pavilion, Edinburgh, UK

Correspondence to: Ian J. C. MacCormick,
Malawi-Liverpool-Wellcome Trust Clinical Research Programme,
PO Box 30096, Chichiri,
Blantyre 3, Malawi
E-mail: ian.maccormick@gmail.com

Sir, We thank Kariuki and Newton for their letter which raises several interesting points. We value their contributions to this discussion.

Failure of cerebral autoregulation may be an important step in the cerebral malaria disease process. Ideally our review would have not only included comparisons of autoregulatory function in retinal and cerebral vessels, but also other important subjects such as the nature of the blood-tissue barriers, distribution of endothelial receptors, and vessel ultrastructure in retina and brain. Comparing and contrasting the retina with other areas of the CNS in terms of these and other features could well provide valuable insights, not just into cerebral malaria, but for a whole range of neurovascular diseases. We hope our paper will help to stimulate individual reviews on these topics.

The utility of *Plasmodium falciparum* histidine-rich protein 2 (*pf*HRP2) as a biomarker in severe malaria has recently been reviewed (Manning and Davis, 2013). In African children with severe malaria, high *pf*HRP2 has been associated with anaemia, coma and death (Hendriksen *et al*., 2012), and distinguishes presence/absence of cerebral sequestration or malarial retinopathy in separate derivation and validation cohorts (Seydel *et al*., 2012). *pf*HRP2 shows clear promise as an important indicator of *P. falciparum* pathogenesis, and further evaluation as a biomarker of disease severity seems warranted. However, as with any prospective biomarker, evaluation must consider the biological context (Buyse *et al*., 2010). For example, some strains of *P. falciparum* do not produce *pf*HRP2 (Gamboa *et al*., 2010). Estimates of total body parasite load may provide useful information at a population level, but subject level variance in important biological parameters leads to improbable values for individual patients (Hendriksen *et al*., 2012).

Biological context is equally important when considering retinal features as potential markers of cerebral damage. This concern motivated our review. The available evidence suggests that malarial retinopathy, in the context of clinically defined paediatric cerebral malaria (Newton *et al*., 1998), does indeed reflect similar disease processes in the brain. Although empirical associations between retinopathy and cerebral histopathology necessarily come from limited populations, similarities between retina and brain in terms of anatomy and physiology imply that these associations are also likely to exist more broadly. This biological context suggests inference of several distinct pathological processes from the retina

Advance Access publication June 11, 2014

Perspective

For reprint orders, please contact: reprints@futuremedicine.com

Biomarkers in Medicine

Developing retinal biomarkers of neurological disease: an analytical perspective

The inaccessibility of the brain poses a problem for neuroscience. Scientists have traditionally responded by developing biomarkers for brain physiology and disease. The retina is an attractive source of biomarkers since it shares many features with the brain. Some even describe the retina as a 'window' to the brain, implying that retinal signs are analogous to brain disease features. However, new analytical methods are needed to show whether or not retinal signs really are equivalent to brain abnormalities, since this requires greater evidence than direct associations between retina and brain. We, therefore propose a new way to think about, and test, how clearly one might see the brain through the retinal window, using cerebral malaria as a case study.

Keywords: biomarker • brain • cerebral malaria • proxy marker • retina • surrogate end point

Ian JC MacCormick*[1,2,3], Gabriela Czanner[1,4] & Brian Faragher[5]

[1]Department of Eye & Vision Science, University of Liverpool, Liverpool, UK
[2]Malawi-Liverpool-Wellcome Trust Clinical Research Programme, Blantyre, Malawi
[3]Centre for Clinical Brain Sciences, University of Edinburgh, Edinburgh, UK
[4]Department of Biostatistics, University of Liverpool, Liverpool, United Kingdom
[5]Liverpool School of Tropical Medicine, Liverpool, UK
*Author for correspondence: ian.maccormick@gmail.com

Background

The appeal of the retina as a research tool

There is a great temptation to describe the retina as a 'window to the brain'. For example, a recent review of neurological conditions was titled 'The retina as a window to the brain – from eye research to CNS disorders' [1]. A popular textbook on retinal anatomy and physiology is called: 'The retina – an approachable part of the brain' [2]. Similar language and concepts are present in recent literature on Alzheimer's disease [3], schizophrenia [4] and stroke [5].

The appeal of the retina as a neuroscientific research tool arises from three points: first, it is difficult to directly observe the brain in living patients. This limits the amount and type of information that can be collected about the CNS in health and disease. Second, the retina is thought to be similar to the brain [6,7]. Although important differences exist (e.g., photoreceptor and neuron metabolism) [2], the retina is part of the central nervous system (CNS) and has similar embryological origins, anatomy and physiology to other CNS regions. This leads to a related idea that retinal disease manifestations ought to be associated with brain disease manifestations – at least for certain conditions, where both organs are exposed to the same insults. Finally, unlike the brain, direct observation of the retina is relatively simple. Several noninvasive high resolution techniques to measure retinal structure and/or function are available [8], and technological advances are likely to increase the range and power of such modalities.

Given these points, it is not surprising that the retina has been the subject of a significant amount of biomarker research, leading to many reports of associations between retina and brain. Prominent associations include relationships between retinal parameters and outcomes from several neurological conditions, including stroke [9], cognitive impairment [3,10], multiple sclerosis [11] and others (reviewed in [1,8]).

It is clear that associations between retina and brain exist for a range of neurological and neurovascular conditions of varying etiologies. This is consistent with the hypothesis that the retina and brain are similar,

Future Medicine part of fsg

MacCormick *et al. Malar J (2015) 14:367*
DOI 10.1186/s12936-015-0897-7

MALARIA JOURNAL

METHODOLOGY Open Access

Grading fluorescein angiograms in malarial retinopathy

Ian J. C. MacCormick[1,2,3*], Richard J. Maude[4,5,6], Nicholas A. V. Beare[1,7], Shyamanga Borooah[3,8,9], Simon Glover[10], David Parry[11], Sophie Leach[11], Malcolm E. Molyneux[2,12], Baljean Dhillon[3,8,9], Susan Lewallen[13] and Simon P. Harding[1,7]

Abstract

Background: Malarial retinopathy is an important finding in *Plasmodium falciparum* cerebral malaria, since it strengthens diagnostic accuracy, predicts clinical outcome and appears to parallel cerebral disease processes. Several angiographic features of malarial retinopathy have been described, but observations in different populations can only be reliably compared if consistent methodology is used to capture and grade retinal images. Currently no grading scheme exists for fluorescein angiographic features of malarial retinopathy.

Methods: A grading scheme for fluorescein angiographic images was devised based on consensus opinion of clinicians and researchers experienced in malarial retinopathy in children and adults. Dual grading were performed with adjudication of admission fluorescein images from a large cohort of children with cerebral malaria.

Results: A grading scheme is described and standard images are provided to facilitate future grading studies. Inter-grader agreement was >70 % for most variables. Intravascular filling defects are difficult to grade and tended to have lower inter-grader agreement (>57 %) compared to other features.

Conclusions: This grading scheme provides a consistent way to describe retinal vascular damage in paediatric cerebral malaria, and can facilitate comparisons of angiographic features of malarial retinopathy between different patient groups, and analysis against clinical outcomes. Inter-grader agreement is reasonable for the majority of angiographic signs. Dual grading with expert adjudication should be used to maximize accuracy.

Keywords: Severe malaria, Malarial retinopathy, Fluorescein angiography, Grading, Inter-grader agreement

Background

Malarial retinopathy in severe malaria

The clinical syndrome of cerebral malaria (CM) is a major cause of death and disability, yet the pathogenesis remains unclear [1]. Improvements in diagnosis, treatment, and prognosis are likely to be possible only through an improved understanding of the disease process. The neurovasculature of the retina has attracted interest as a potential model of unseen cerebrovascular damage, both in CM [2] and other neurological conditions, including stroke [3], cerebral small vessel disease [4], and others [5, 6].

A system to classify and grade malarial retinopathy from ophthalmoscopy [7, 8] and colour photographs has been widely used, in both children [9, 10] and adults [11, 12]. This has led to an awareness that malarial retinopathy in paediatric CM is a sensitive and specific indicator of cerebral sequestration [13], and that the severity of retinopathy correlates with the severity of retinal and cerebral sequestration [14], the intensity of cerebral haemorrhages [15], and the likelihood of a fatal outcome [10]. Retinopathy in adults with CM appears to involve fewer features than paediatric cases, but is also associated with death and other clinical markers of disease severity [11, 12].

Fundus fluorescein angiograms (FA) have been performed on children [16, 17] and adults with CM [18]. This procedure involves injection of a fluorescent solution (fluorescein sodium) into a peripheral vein, and

*Correspondence: ian.maccormick@gmail.com
[1] Department of Eye and Vision Science, University of Liverpool, Liverpool, UK
Full list of author information is available at the end of the article